Flexibility options in a sustainable power system

- Approaches from different power system perspectives -

Zur Erlangung des akademischen Grades eines

Doktors der Wirtschaftswissenschaften
(Dr. rer. pol.)

von der KIT-Fakultät für Wirtschaftswissenschaften
des Karlsruher Instituts für Technologie (KIT)

genehmigte

DISSERTATION

von

Alexandra Ilg, M.Sc.
(geb. Märtz)

Tag der mündlichen Prüfung:	20. Dezember 2023
Referent:	Prof. Dr. Wolf Fichtner
Korreferent:	Prof. Dr. Stefan Nickel

Acknowledgements

This dissertation was written during my time as a research associate at the Chair of Energy Economics at the Institute for Industrial Production (IIP) at Karlsruhe Institute of Technology (KIT). During this time, I have received support from many sides, for which I would like to express my sincere appreciation.

First and foremost, I would like to thank my doctoral supervisor Prof. Dr. Wolf Fichtner for his support and guidance throughout the entire dissertation process. His valuable feedback and encouragement were of great value for the realisation of this dissertation. Moreover, I am grateful to Prof. Dr. Stefan Nickel, who kindly took over the role as co-reviewer, and Prof. Dr. Christof Weinhardt as well as Prof. Dr. Frank Schultmann for serving as committee members.

To my friends and colleagues from IIP who have supported me along this journey, I am deeply thankful. The resulting motivation, support and shared experiences have made this academic journey much more enjoyable.

My sincere thanks go to my family for their encouragement and understanding during this journey. Their unwavering belief in me has been a constant source of strength and motivation.

I am especially grateful to my husband, who has given me unconditional support, love and understanding. His patience and encouragement have strengthened me in the most difficult moments.

Karlsruhe, Dezember 2023

Alexandra Ilg

Kurzfassung

Die Energiesysteme befinden sich in einem grundlegenden strukturellen und regulatorischen Wandel, um den Herausforderungen des Klimawandels zu begegnen. Der Begriff "Energiewende" bezeichnet den Wandel des Energiesystems von der konventionellen Stromerzeugung aus fossilen Energieträgern hin zur Stromerzeugung aus erneuerbaren Energien. Mit dem steigenden Anteil der Stromerzeugung aus wetterabhängigen erneuerbaren Energiequellen sind Schwankungen in der Einspeisung in das Stromnetz zu erwarten. Diese Volatilität der Stromerzeugung durch die Integration erneuerbarer Energiequellen stellt das gesamte Stromsystem vor neue Herausforderungen. Um Schwankungen in der Stromeinspeisung auszugleichen, müssen Flexibilitätsoptionen in das Stromsystem integriert werden, um Netzstabilität und Versorgungssicherheit zu gewährleisten.

Im Rahmen der vorliegenden Dissertation werden Flexibilitätsoptionen im nachhaltigen Stromsystem sowohl aus theoretischer Sicht als auch hinsichtlich ihrer politischen Implikationen untersucht. Vor dem Hintergrund der Integration eines steigenden Anteils an erneuerbaren Energien im Stromsektor erfolgt dabei eine differenzierte Betrachtung aus Gesamtsystemsicht sowie aus Perspektive des lokalen Stromsystems.

Aus Gesamtsystemsicht werden angebots- und nachfrageseitige Flexibilitätsoptionen sowie die Flexibilität durch den Einsatz von Speichern und den Ausbau der Netzinfrastruktur im Hinblick auf das Gesamtstromsystem untersucht. Ausgangspunkt ist dabei eine Modellierung des komplexen Zusammenwirkens von regulierten Ebenen und wettbewerblichen Prozessen, wobei die Interessen der verschiedenen Akteure und ihrer wechselseitigen Beziehungen berücksichtigt werden. Dazu wird der Strommarkt durch mehrstufige mathematische Optimierungsmodelle abgebildet, die mit Ansätzen aus der Spieltheorie kombiniert werden.

Aus Sicht des lokalen Stromsystems werden Elektrofahrzeuge als Flexibilitätsoptionen betrachtet. Nachdem die Bedeutung von Elektrofahrzeugen für die Emissionsreduktion und somit für die Erreichung der Klimaziele mittels einer reduzierten Lebens-

zyklusanalyse dargelegt worden ist, werden darauf aufbauend mögliche Einflussfaktoren für eine effiziente Integration von Elektrofahrzeugen in das lokale Stromsystem umfassend analysiert. Dabei werden statistische Analysen und ein zweistufiger Clusteransatz angewendet sowie ein Simulationstool entwickelt und eingesetzt.

Als wesentliches Ergebnis ist festzuhalten, dass bei der Gestaltung eines nachhaltigen Strommarktdesigns die Berücksichtigung von Flexibilitätsoptionen von entscheidender Bedeutung ist. Neben den Wechselwirkungen von verschiedenen Flexibilitätsoptionen ist insbesondere auch die individuelle Risikobereitschaft der zentralen Akteure im Stromsystem zu berücksichtigen, um so gezielte marktwirtschaftliche Anreize in (Flexibilitäts-)Investitionen zu schaffen. Es wird gezeigt, dass Investitionen in Stromspeicher durch privatwirtschaftliche Marktteilnehmer maßgeblich die Entscheidungen des staatlich regulierten Netzbetreibers hinsichtlich Ort und Höhe von Netzinvestitionen beeinflussen. Darüber hinaus wird ebenfalls aufgezeigt, dass verschiedene Risikoeinstellungen privater und öffentlicher Investoren zu unterschiedlichen Investitionen in Flexibilitätsoptionen führen können. In Bezug auf die Integration von Elektrofahrzeugen als Flexibilitätsoption in das lokale Stromsystem wird durch die Analysen die Bedeutung des individuellen Ladeverhaltens und der damit verbundenen Gleichzeitigkeitsfaktoren als zentrale Schlüsselfaktoren für politische Entscheidungen hervorgehoben. Die Ergebnisse der Arbeit liefern somit politische Handlungsempfehlungen für die Gestaltung des Strommarktdesigns, um Flexibilitätsoptionen erfolgreich in das deutsche Stromsystem zu integrieren und eine nachhaltige Energieversorgung zu gewährleisten.

Abstract

Energy systems are undergoing fundamental structural and regulatory change to meet the challenges of climate change. The term "Energiewende" refers to the change in the energy system from conventional electricity generation from fossil fuels to electricity generation from renewable energy sources. With the increasing share of electricity generation from weather-dependent renewable energy sources, fluctuations in the feed-in to the electricity grid are to be expected. This volatility in electricity generation due to the integration of renewable energy sources poses new challenges for the entire electricity system. In order to compensate for fluctuations in electricity feed-in, flexibility options must be integrated into the electricity system to ensure grid stability and security of supply.

In the scope of this dissertation, flexibility options in the sustainable electricity system are examined both from a theoretical perspective and with regard to their political implications. Against the background of the integration of an increasing share of renewable energies in the electricity sector, a differentiated view is taken from a holistic power system perspective as well as from a local power system perspective.

From a holistic power system perspective, supply-side and demand-side flexibility options as well as flexibility through the use of storage and the expansion of the grid infrastructure are examined. The starting point is a modeling of the complex interaction of regulated levels and competitive processes, taking into account the interests of the different market actors and their mutual relationships. For this purpose, the electricity market is modeled using multi-level mathematical optimization models, which are combined with approaches from game theory.

From the perspective of the local power system, electric vehicles are considered as flexible options. After the importance of electric vehicles for the reduction of emissions and thus for the achievement of climate targets has been presented by means of a reduced life cycle analysis, possible influencing factors for an efficient integration of electric vehicles

into the local power system are comprehensively analyzed. Statistical analyses and a two-stage cluster approach will be applied, and a simulation tool will be developed and applied.

As a key result, it can be noted that the consideration of flexibility options is of crucial importance in the design of a sustainable electricity market. In addition to the interactions of different flexibility options, the individual risk attitude of the central actors in the power system must also be taken into account in particular in order to create targeted market-based incentives for (flexibility) investments. It is shown that investments in electricity storage by private market participants have a decisive influence on the decisions of the state-regulated grid operator regarding the location and amount of grid investments. Furthermore, it is also shown that the different risk attitudes of private and public investors can lead to different investments in flexibility options. With regard to the integration of electric vehicles as a flexibility options in the local power system, the analyses highlight the importance of individual charging behavior and the associated simultaneity factors as central key factors for political decisions. The results of the work thus provide policy implications for the electricity market design in order to successfully integrate flexibility options into the German power system and ensure a sustainable energy supply.

Contents

List of Figures

List of Tables

Abbreviations

ATC	Available transfer capacity
BEV	Battery electric vehicle
BNetzA	Federal network agency/Bundesnetzagentur
CO_2	Carbon dioxide
DER	Distributed energy resources
DC	Direct current
DSM	Demandside-management
DSO	Distribution system operator
EEG	Renewable energy act/Erneuerbare-Energien-Gesetz
EVs	Electric vehicles
GHG	Greenhouse gas
GMM	Gaussian mixture model
ICEV	Internal combustion engine vehicles
IEA	International energy agency
IRENA	International renewable energy agency
KSG	Federal climate protection act/Bundes-Klimaschutzgesetz
KKT	Karush-Kuhn-Tucker
kWh	Kilowatt-hour
LCA	Life cycle assessment

MPEC	Mathematical programs with equilibrium constraints
NPS	New policy scenario
PCA	Principal component analysis
PEV	Plug-in electric vehicles
PHEV	Plug-in hybrid electric vehicles
PV	Photovoltaic
RES	Renewable energy sources
SDS	Sustainable development scenario
TSO	Transmission system operator
TWh	Terawatt-hour
VRE	Variable renewable energy
V2G	Vehicle-to-grid

List of appended research papers

Paper A
Weibelzahl, M., Märtz, A. (2020), Optimal storage and transmission investments in a bilevel electricity market model, *Annals of Operations Research*, 287, 911-940, doi:10.1007/s10479-018-2815-1.

Paper B
Coniglio, S., Halbrügge, S., Märtz, A., Weibelzahl, M. (forth.), The flexibility puzzle in liberalized electricity markets: Understanding flexibility investments under different risk attitudes, submitted to a scientific journal.

Paper C
Märtz, A., Plötz, P., Jochem, P. (2021), Global perspective on CO_2 emissions of electric vehicles, *Environmental Research Letters*, 16 (5), doi:10.1088/1748-9326/abf8e1.

Paper D
Märtz, A., Langenmayr, U., Ried, S., Seddig, K., Jochem, P. (2022), Charging behavior of electric vehicles: Temporal clustering based on real-world data, *Energies*, 15(18), doi:10.3390/en15186575.

Paper E
Märtz, A., Held, L., Jochem, P., Fichtner, W., Suriyah, M., Leibfried, T. (2019), Development of a tool for the determination of simultaneity factors in PEV charging processes, *3rd E-Mobility Integration Symposium*, Dublin, Ireland.

Part I

Overview

1 Introduction

Energy systems are undergoing a fundamental structural and regulatory transformation to address the challenges of climate change. The term ”Energiewende” refers to the transformation of the energy system from one primarily based on fossil fuels to a more sustainable energy system primarily relying on renewable energy sources. This involves the transition of energy generation, transportation, and usage throughout the entire energy system. The electricity system, which is a part of the energy system, specifically pertains to the generation, transmission, distribution, and consumption of electric power. It encompasses the different types of power plants that generate electrical energy, the transmission grids that transport electricity from generation sites to consumers, and the distribution networks that deliver electricity to end users.

1.1 Motivation

With regard to achieving climate goals, Germany faces significant challenges in shaping its energy system. The paradigm shift in German energy policy involves considering renewable energies as a central component. The goal is to reduce dependence on fossil fuels, lower greenhouse gas emissions, and ensure a sustainable energy supply. Concerning the electricity system, the expansion of renewable energies has led to a changed supply and demand structure and a substantial increase in decentralized energy sources. Electricity generation increasingly relies on renewable sources such as photovoltaic and wind power installations, while electricity demand includes integral components such as electric vehicles and heat pumps in the German electricity system. In this context, the electricity system has fundamentally transformed from a unidirectional centralized system to a bidirectional decentralized system. The integration of renewable energies into the electricity system, along with resulting structural changes, introduces more frequent fluctuations in electricity generation and consumption. The surplus or deficit of volatile renewable electricity generation increases the need for flexibility in the electricity system in order to balance the growing temporal and regional discrepancy between electricity supply and demand (Brunner, 2014).

Fundamental flexibility options in the electricity system include not only electricity generation and consumption but also electricity storage, the electricity grid, and sector coupling (Heider et al., 2021). In a sustainable electricity system with a high share of renewable energies, a mix of various flexibility measures is required to compensate for the divergence between electricity generation and consumption (Brunner, 2014). This necessitates analyzing both structural changes and associated regulatory framework conditions concerning the integration of flexibility options into the existing electricity system and incorporating them into the electricity market design.

1.2 Scope and research objective

This work examines flexibility options in the context of the entire German electricity power system as well as local electricity power systems, against the background of an increasing share of renewable energies. In this context, the relevance of flexibility options in the electricity power system for policy measures and future electricity market design is also discussed. From a scientific perspective, the fundamental question is whether and to what extent flexibility options can be used to ensure an efficient, sustainable, and stable electricity supply. The following energy economics research questions are central to this dissertation:

- How can the flexibility gap associated with a growing share of renewable energies be reduced from a holistic power system perspective and from a local power system perspective?
- How can the use of the optimal combination of flexibility options be fostered from a holistic system perspective in order to support the integration of renewable energy sources and ensure a stable power supply?
- From the local power system point of view, what are the decisive factors for integrating electric vehicles as flexibility resources into the electricity power system?
- What role do flexibility options play in the further design of the electricity market, i.e., how should the regulatory framework be structured to ensure a system-optimal deployment (both from a system-wide and a local perspective) of these options?

1.3 Structure of the thesis

The present cumulative dissertation consists of two parts, whose structure is illustrated in Figure 1. The first part begins with this introduction (Chapter 1) that addresses the motivation, research objective, and structure of the work. Based on the objectives of the energy transition in Germany, the structural framework of sustainable power systems and the related future challenges for the electricity system arising from the increased utilization of renewable energies are examined (Chapter 2).

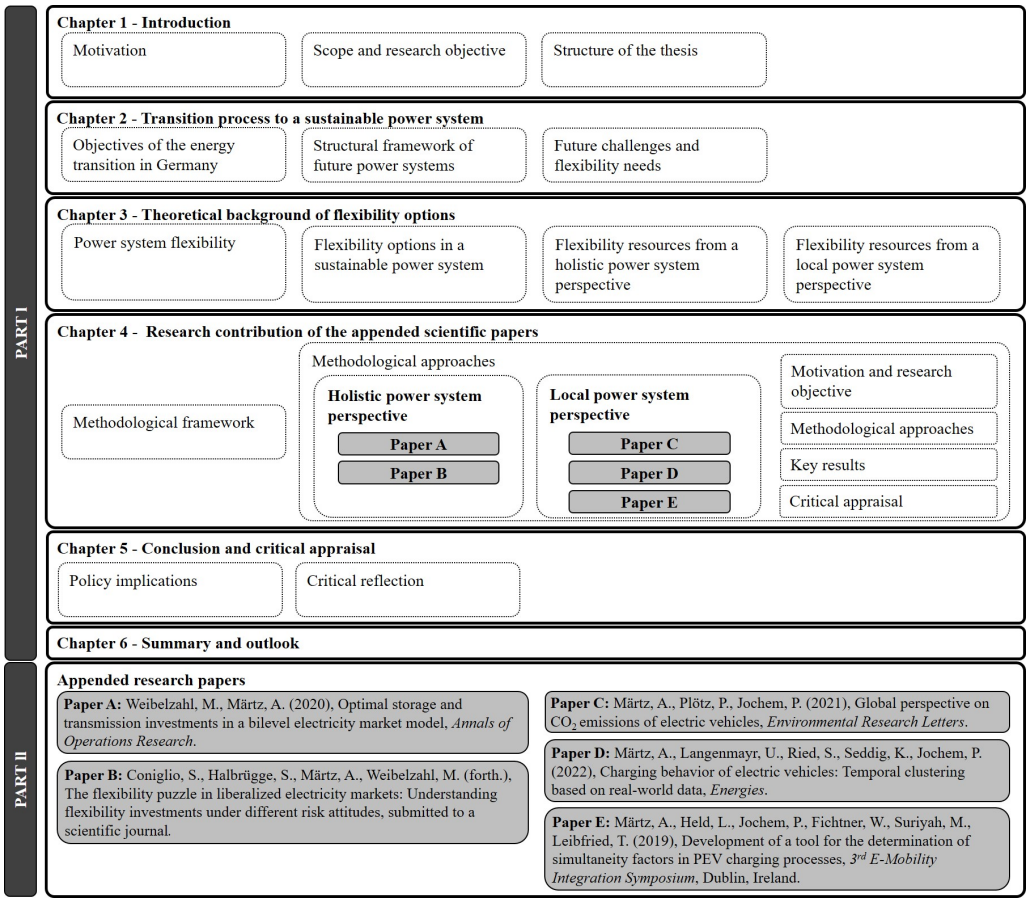

Figure 1: Structure of this thesis.

Subsequently, the central significance of flexibility options in the electricity system, which are available in various forms, is emphasized, and the flexibility resources are examined from different power system perspectives (Chapter 3). From a methodological point of view, the analysis of flexibility options differentiates between the holistic power system perspective and a local power system perspective (Chapter 4). In this context, the underlying publications, including the methodologies, are presented and the obtained key results are summarized. A critical assessment is provided for each publication. Based on this foundation, policy implications for a reform of the electricity market design in Germany with regard to the integration of flexibility options are derived (Chapter 5). A brief summary and an outlook form the end of this thesis (Chapter 6).

The second part of the thesis includes the interconnected scientific papers A-E:

Paper A This paper analyzes the interplay of transmission and storage investments in a multistage game that accounts for a hierarchical decision structure. In the multistage game, on the first stage, a transmission operator chooses optimal line investments and a corresponding optimal network fee. On the second stage, competitive firms trade energy on a zonal market with limited transmission capacities and decide on their optimal storage facility investments. The main solution strategy for the the multistage game and the corresponding bilevel optimization model is presented. The paper is published in the journal Annals of Operations Research (2020).

Paper B The underlying paper deals with the effects of different risk attitudes of public and private decision-makers on long-term flexibility options under uncertainty. The proposed four-stage Stackelberg game is translated into a four-level (equilibrium-finding) optimization problem. It accounts for public line investments made by a Transmission System Operator (TSO) in anticipation of private investments in storage and conventional backup generation facilities (first level). These private investments take place on the second level based on expected spot-market profits, which are determined within a zonal spot market on the third level. The fourth level accounts for the redispatch actions of a TSO in the case where contracted spot market quantities cannot be transmitted through the electricity network. From the four-level optimization problem, an equivalent single-level reformulation is derived, which is then solved to global optimality with a state-of-the-art spatial branch-and-bound solver. The article is submitted to a scientific journal (forth.).

Paper C This scientific contribution investigates the interdependencies of a dynamic decrease in carbon emissions from electricity provision and electric vehicle (EV) diffusion. A reduced life-cycle assessment approach is applied, including well-to-wheel emissions of EVs and taking into account future changes in the electricity mix. Based on the comparison of future global energy scenarios, they are combined with EV diffusion scenarios. The paper is published in the journal Environmental Research Letters (2021).

Paper D The paper deals with the investigation of the energy demand and flexibility potential of EVs for different user groups based on their temporal charging behavior. The contribution is based on a comprehensive data set of 2.6 million empirical charging processes and investigates the possibility of identifying different user groups based on their temporal charging behavior. For this, a Gaussian mixture model as well as a k-means clustering approach are applied, and the results are validated against synthetic load profiles and the original data. The article is published in the journal Energies (2022).

Paper E In this proceeding article, an open-source tool for the calculation of simultaneity factors of EVs (i.e. battery electric vehicles and plug-in hybrid electric vehicles) charging processes is presented. In addition, the peak loads of EVs and households can also be displayed, taking into account the EV and household-specific simultaneities. This paper was presented at the 3rd E-Mobility Integration Symposium in 2019 and published in the Symposium's proceedings.

2 Transition process to a sustainable power system

The energy transition aims to generate electricity from renewable sources (e.g., solar, wind, water), thereby replacing conventional fossil fuel-based power generation. Beyond the traditional energy policy goals of security of supply and economic efficiency, climate goals are particularly pressing.

Based on the paradigm shift in German energy policy, there are fundamental changes in the underlying principles, objectives, and strategies concerning electricity generation, distribution, and consumption. This involves a transition from conventional centralized power generation to decentralized renewable power generation while simultaneously integrating new components and players into the power system.

Renewable electricity generation faces the central challenge of weather-related fluctuations preventing a consistent and secure supply, as compared to electricity generation from conventional fossil-fueled power plants. In this context, both the holistic electricity system and the local electricity systems face an increasing need for flexibility in designing a sustainable power system.

2.1 Objectives of the energy transition in Germany

Under the Federal Climate Protection Act (KSG), numerous national measures have been adopted to support the Paris Climate Agreement goals (Bundesministerium für Wirtschaft und Klimaschutz (BMWK), 2023). The overarching climate goal of the German government is to achieve "climate neutrality", meaning the avoidance or offsetting of greenhouse gas emissions (Prognos, Öko-Institut, Wuppertal-Institut, 2021). In this context, effective and comprehensive policy measures are necessary to decarbonize the energy system.

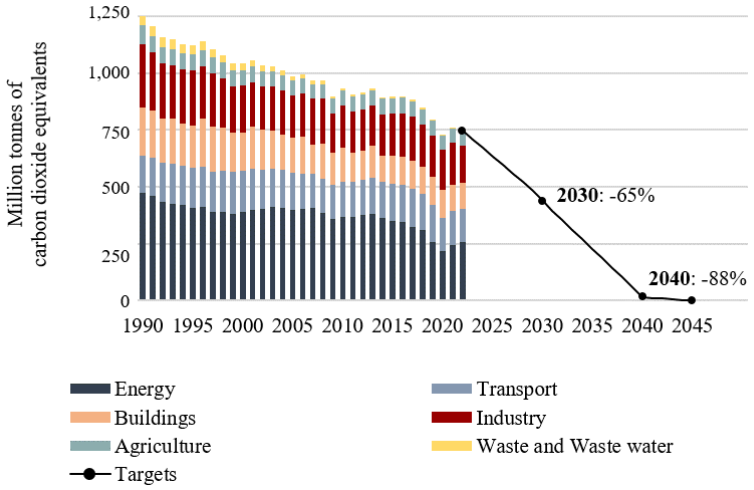

Figure 2: Greenhouse gas emissions by sector in Germany from 1990 to 2022 and the adjusted targets for 2030 and 2045 according to the revision of the Federal Climate Protection Act (KSG) (Own illustration based on Umweltbundesamt (2023)).

Figure 2 illustrates the development of greenhouse gas emissions (by sectors) in Germany since 1990, along with the German government's emission reduction targets for the period up to 2045. The greenhouse gas emission reduction goals encompass the sectors of energy, industry, transport, buildings, agriculture, and waste management (Umweltbundesamt, 2023). By 2030, greenhouse gas emissions are to be reduced by at least 65% (compared to 1990). By 2040, emissions are targeted to be reduced by 88%, with a binding target of achieving climate neutrality in Germany by 2045 (Bundesministerium für Wirtschaft und Klimaschutz (BMWK), 2023). To achieve these goals, a sustainable transformation of the energy sector is necessary, implying a redesign of the power sector towards a climate-friendly, decentralized, and renewable energy supply.

The central prerequisite for achieving climate neutrality across all sectors by 2045 is that the power sector must already be largely climate neutral by 2035 (Agora Energiewende et al., 2022). Hence, renewable sources must come to account for most power generation, and greenhouse gas emissions from electricity generation must be significantly reduced. Therefore, the further expansion of renewable energy sources is intended to shape the sustainable transformation of the power sector.

According to the Renewable Energy Sources Act (EEG) and the German government's Climate Protection Plan 2050, an increase in the share of renewable energy in gross electricity consumption to at least 80% by 2030 is envisaged (Bundesministerium für Wirtschaft und Klimaschutz (BMWK), 2023).

Figure 3 illustrates the share of renewable energy sources in gross electricity consumption in Germany. Their share has been rising sharply recently. In 2022, the share of renewable energies was around 46%. However, this share would have to almost double by 2030 to achieve the political objective.

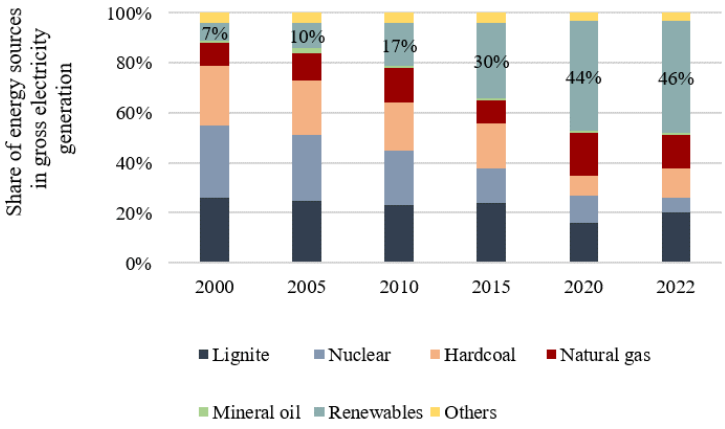

Figure 3: Share of energy sources in gross electricity generation in Germany from 2000 to 2022 (Own illustration based on Umweltbundesamt (2023)).

Due to the increasing cross-sector electrification (e.g., transportation and industry), the power sector is decisive in the energy transition. A climate-neutral power system grounds the decarbonization of other sectors such as transportation, industry, and buildings. Based on the expanded use of renewable energy sources in the power sector, cross-sector electrification also incentivizes the adoption of climate-friendly technologies in other sectors.

In this context, the massive expansion of renewable energy sources is also central to the framework of sector coupling (Bundesministerium für Wirtschaft und Klimaschutz, 2023). Sector coupling involves linking various sectors within the energy system: particularly the electricity sector, the heat and cooling sector, and the transportation sector. Sector coupling creates synergies and enables renewable energy sources to be applied efficiently across all

sectors.

In the transportation sector, the German government aims to have at least 15 million electric vehicles registered in Germany by 2030 to achieve climate goals. Figure 4 shows the development of the electric vehicle fleet in Germany.

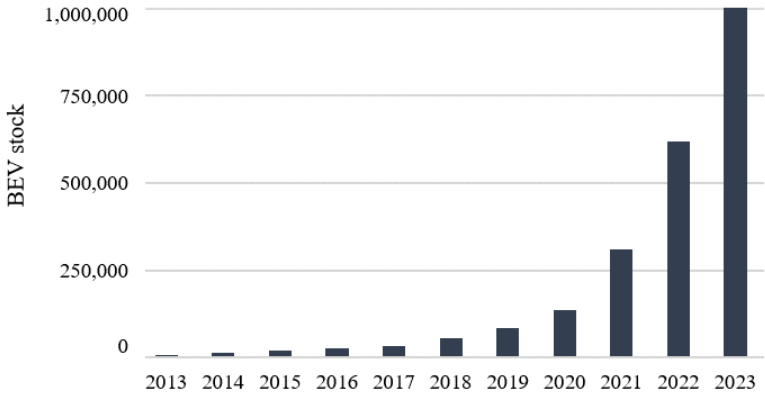

Figure 4: Share of energy sources in gross electricity generation from 2000 to 2022 (own illustration based on Umweltbundesamt (2023)).

Recently, a significant increase in the registration of battery electric vehicles in absolute numbers has been recorded. To achieve the goals of the German government, the number of battery electric vehicles in Germany must continue to grow substantially (Prognos, Öko-Institut, Wuppertal-Institut, 2021). Therefore, the government commits to further improving the policy framework conditions for electromobility and accelerating the transition to low-emissions and climate-friendly transportation.

2.2 Structural framework of future power systems

The power system is undergoing a structural and regulatory paradigm change in response to a rapidly evolving energy landscape. This transformation is driven by the need to address critical challenges, including the integration of renewable energy sources and the reduction of carbon emissions.

2.2.1 Transformation to a sustainable bidirectional power system

In the structural framework of the German electricity sector, multiple market players with their own economic objectives interact in a very complex way. The liberalization of the German electricity market in 1998 marked a paradigm shift. Until then, the electricity market had been organized vertically integrated, such that the respective energy suppliers were responsible in their grid areas for the generation, transport, and supply of electricity to the consumers located in those grid areas.

A key element of liberalization is the creation of a wholesale electricity market in which supply and demand meet. Ergo, any energy supplier can supply electricity to any consumer anywhere in the country. Conversely, each customer is free to choose their own electricity supplier, not tied to a regional supplier. Another key feature of liberalized electricity markets is the legal and organizational unbundling of grid operation and electricity trading; that is, in principle, no electricity supplier may also be an electricity grid operator. This unbundling ensures that any electricity supplier can supply its customers with electricity from other networks without suffering any disadvantages. The liberalized electricity market can, thus, be divided into regulated and market-based market areas.

With regard to the value chain, the liberalized electricity market can be represented by electricity generation, transmission, and distribution, as well as electricity consumption (see Figure 5). In the traditional, mainly centralized power system based on conventional power generation, electricity is produced in large power plants fired mainly by fossil fuels. These have different cost structures and compete with each other.

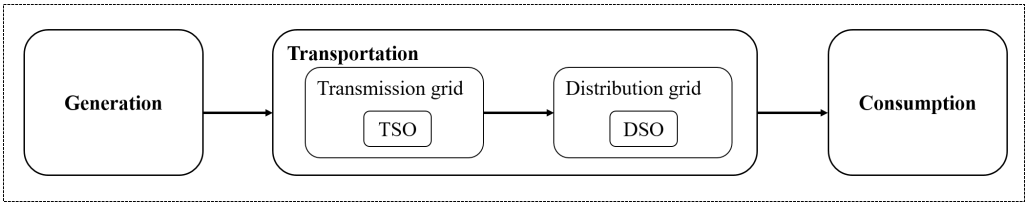

Figure 5: Traditional unidirectional power system.

Electricity flows unidirectionally from these power plants through the transmission and distribution grids to consumers (Heider et al., 2021). Various grid operators control and operate the electricity grid, which is subject to supervision by the state, primarily the Federal

Grid Agency. The responsibility for the transmission grids lies with the Transmission System Operators (TSO), who are in charge of the operational management, maintenance, and adequate sizing. Simultaneously, they must ensure non-discriminatory access to these grids for electricity traders and suppliers. The distribution grid connected to the transmission grid is operated by Distribution System Operators (DSOs), whose scope includes ensuring a secure, stable network operation and providing a reliable supply to end customers.

In general, end customers are connected to the low-voltage level of the distribution grid. Individual large consumers (e.g., energy-intensive industries), may also be directly connected to the transmission grid. Electricity demand is characterized by many factors, including strong daily and seasonal fluctuations, and reacts inelastically to prices in the short term.

The increased integration of renewable energy sources into electricity generation has precipitated a decline in electricity generation from coal and gas power plants. Electricity generation is no longer exclusively confined to centralized fossil-fueled large power plants, but is increasingly decentralized through renewable energy sources such as photovoltaic (PV) systems, wind farms, and biomass installations. Therefore, the resulting transformation of the power system leads to an altered generation and demand structure in the sustainable electricity system (see Figure 6).

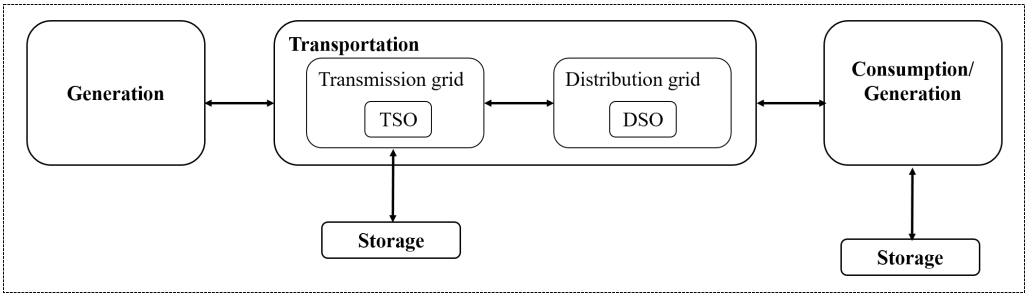

Figure 6: Sustainable bidirectional power system.

Given the increasing share of renewable energy sources on the supply-side, the future power system will need to emphasize energy storage technologies (such as batteries, pumped storage and thermal storage), which are gaining importance in the future power system, as they can significantly contribute to mitigating the volatility in energy generation from renewable energy sources. Electricity storage can house the surplus energy generated during periods

of high production for the market to consume during times of high demand or limited availability of renewable energy.

Also marked by an increasing deployment of distributed energy resources (DER) at the local level, the structural transformation of the power system equally implies a consumer-side change. DER refers to decentralized electricity-generating resources or controllable loads, particularly those integrated into the local power system. Examples include rooftop PV systems, electric vehicles, heat pumps, and battery storage (Badanjak and Pandžić, 2021).

As decentralized electricity generation at the consumer level through renewables grows, the flow of electricity in the grid becomes bidirectional (see Figure 6). While in the traditional fossil fuel-based system, electricity flows from central power plants to end consumers, the use of local decentralized generation sources (e.g., rooftop PV, rural wind turbines) also enables reverse power flow into the grid.

Consequently, due to the multitude of decentralized energy sources based on renewable resources, the sustainable power system exhibits a significantly dezentralized character compared to the traditional power system (Koch et al., 2021). Against this backdrop, the energy transition entails a fundamental transformation of the German power system from a unidirectional centralized model to a bidirectional decentralized one. The shift from the conventional centralized electricity system to a more decentralized and renewable energy-based system stands as one of the key components for the success of the energy transition.

2.2.2 Holistic and local power system perspectives

The analysis of power systems is essential to understand and optimize the complex dynamics of modern electricity systems, and both holistic and local perspectives can be applied in such an examination. These complementary perspectives provide a comprehensive understanding of the way electricity is generated, distributed, and consumed, and they feature in the evolution of energy environments.

While the holistic power system perspective encompasses the entire power system and its integration into the national and international energy infrastructure, the local view focuses on specific regional or municipal matters. Both perspectives contribute to the development of a sustainable, efficient, and resilient power system.

The holistic system view enables an analysis of the performance and stability of the entire power system. Aspects such as generation, grid capacity, national and international energy trade, and the integration of renewable energy sources are taken into account. The consideration of the entire electricity system thus includes the generation, transport, and consumption of electricity at a high level. The transmission grid is the principal grid end under consideration (see Figure 7).

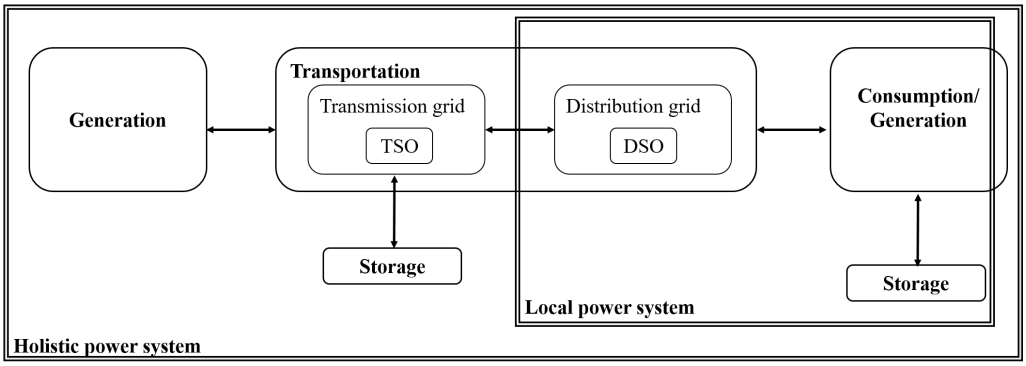

Figure 7: Holistic and local power system perspective.

In the local power system view, the focus is tighter and concentrates on the distribution network and the consumption or generation at the household level of the end consumers (see Figure 7). In this context, the integration of decentralized energy generation, the development of microgrids, or the promotion of electric mobility in cities can be investigated.

Considering the power system from a perspective both holistic and local is essential to comprehensively understanding the challenges and opportunities in the energy sector. Furthermore, the connection between the overall system view and the local view is crucial, since local measures can influence the system as a whole. For example, the increased use of electric vehicles in a city can have an impact on electricity demand and the need for transmission grid expansion.

2.3 Future challenges and flexibility needs

The success of the energy transition depends largely on how effectively and to what extent the electricity sector can adapt to the changes induced by the integration of renewable resources into the power system. To manage anticipated and unforeseen fluctuations in generation and demand, a structural adaptation of the power system is crucial to the success of the energy transition, considering flexible forms of adjustment. Hence, the new challenges in the electricity sector, accompanied by an increasing share of fluctuating renewable energies in electricity generation and a decreasing contribution from (flexible) conventional generators, pose new challenges to future power systems and amplify the need for flexibility.

In the recent power system, flexible generation capacities have traditionally been utilized to manage both unforeseen and anticipated changes in demand, as well as generation unit failures. The two primary functions of the power plant have been to respond to demand fluctuations (variability) and to ensure system balance in the event of a sudden generation unit outage (stability) (Papaefthymiou et al., 2014). However, the future variable and intermittent generation fluctuations are greater than those caused by the operation of previous conventional generators and the variability of demand in the existing power system (Babatunde et al., 2020; Bhuiyan et al., 2022; Cruz et al., 2018; Kaushik et al., 2022; Mohandes et al., 2019; Papaefthymiou and Dragoon, 2016).

In addition, due to the structural changes in the sustainable power system, multiple uncertainties and challenges arise, further intensifying the need for flexibility (Arboleya et al., 2022; Sinsel et al., 2020). These changes include, on the one hand, the electrification of various end-use sectors, the widespread integration of DER, and the associated demand-side load uncertainty (Babatunde et al., 2020; Badanjak and Pandžić, 2021; Bhuiyan et al., 2022; Corinaldesi et al., 2019; Emmanuel et al., 2020; Hall and Geissler, 2021; Li and Mulder, 2021). On the other hand, price volatility, negative prices, and fuel uncertainty add to the complexity (Babatunde et al., 2020; Bhuiyan et al., 2022; Emmanuel et al., 2020; Kaushik et al., 2022).

The emergence of decentralized energy sources such as distributed generation, energy storage, and flexible loads like electric vehicles also has significant implications for the operation of the distribution grid (Eid et al., 2016). In this context, DER can pose challenges to network stability and reliability due to resulting congestion and voltage issues, primarily affecting the distribution grid (Knezovic et al., 2015).

To meet the challenges of the decarbonized power system, the flexibility of the power system must be increased. The necessary level of flexibility can be demonstrated by the concept of residual load (Zöphel, 2022), referring to the total grid load minus the uncontrollable fluctuating generation that must be covered by conventional power plants or other flexible technologies. The fluctuation in future electricity generation leads to stronger and more frequent fluctuations in the residual load (Ela et al., 2016) and, increasing demand for flexibility in the power system.

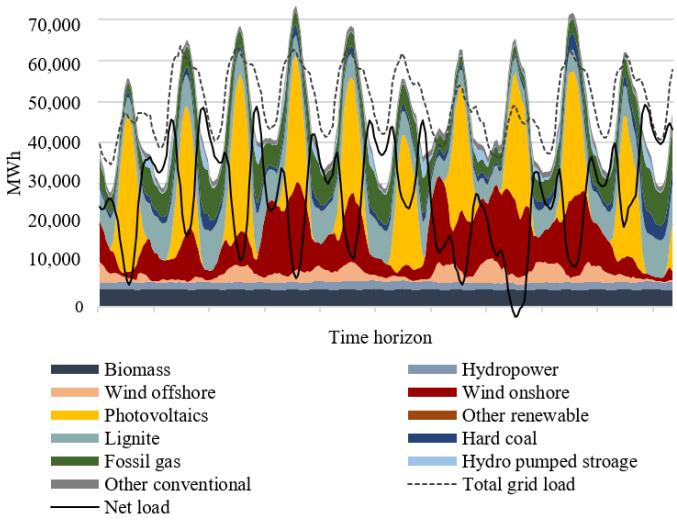

Figure 8: Electricity generation, total grid load, and net load in Germany from 9th July to 18th July 2023 (Own illustration, source: Bundesnetzagentur - SMARD (2023)).

Figure 8 shows the electricity generation per energy source and the total grid load. In addition, it depicts the daily fluctuation range of the residual load in relation to the contribution of renewable energy generation. At the same time, the variable and intermittent generation fluctuations are evident. Demonstrably, the higher the feed-in from PV and wind power plants, the lower the residual load necessary to cover. When the residual load is zero, the electricity demand is completely covered by renewable energy production. If the residual load becomes negative, the electricity generation from renewable energies exceeds the amount demanded.

As a result, the flexibility need is necessary to address both holistic and local concerns. More specifically, flexible electricity generation, distribution, storage, and demand are crucial to

mitigate fluctuations in renewable energy generation, to ensure reliable power supply, and to facilitate the efficient integration of renewable energy sources. Flexibility needs within the power system must be understood to identify and select the most suitable flexibility solutions and the means of realizing them.

In this context, the central challenge in the decarbonized power system lies in ensuring sufficient flexibility in the power system to respond to the volatile and intermittent electricity generation from renewable energies and the challenges posed by the sustainable electricity system.

3 Theoretical background of flexibility options in future power systems

The fundamental requirement of achieving a high share of variable renewable energies is the integration of flexibility options into the power system to manage temporal and spatial fluctuations in electricity supply and demand (Lund et al., 2015; Ma et al., 2013). In this context, the topics of power system flexibility and the intelligent coordination of different flexibility options will become increasingly important.

3.1 Power system flexibility

The flexibility of the power system is regarded as a key factor in addressing the challenges posed by future sustainable power systems. There exists a broad range of definitions of power system flexibility (Degefa et al., 2021; Eurelectric, 2014; International Energy Agency, 2014). Generally, flexibility refers to the ability of the electricity system to manage both unforeseen and anticipated changes (Ela et al., 2016; Zöphel et al., 2018).

Previously, flexibility in power systems was defined as the ability of electricity generators to respond to unexpected changes in load or system components. However, in the context of high shares of variable renewable energy (VRE) in power systems, the definition has evolved. The International Renewable Energy Agency (IRENA) extends this definition to emphasize the need for rapid adaptability of the power system to address the volatility of renewable energies in electricity supply and fluctuations in electricity demand. According to IRENA, "Flexibility is the capability of a power system to cope with the variability and uncertainty that VRE generation introduces into the system in different time scales, from the very short to the long term, avoiding curtailment of VRE and reliably supplying all the demanded energy to customers" (International Renewable Energy Agency, 2018, p. 92).

The coordination of flexibility options at various levels of the power system are of paramount importance. Congestion in distribution grids can be avoided by providing local flexibility, in turn impacting the transmission grid. Efficient management of local decentralized flexibility can reduce strain on the transmission grid and better utilize overall system resources.

Specifically, from a holistic power system perspective, power system flexibility pertains to the capability of the transmission grid and its control mechanisms to adjust to fluctuations in power generation and demand, ensuring secure, stable, and efficient power transmission. In the context of the local power system perspective, flexibility mainly corresponds to the ability to change the power pattern of a unit within a time interval. Thus, local flexibility aims to reduce peak loads, avoid distribution network bottlenecks, regulate network voltage, optimize the integration of decentralized renewable energies, and optimize network utilization. Hence, the flexibility requirements and types of flexibility options may vary based on the specific tasks and responsibilities of different market players and the perspective of the power system.

3.2 Flexibility options in a sustainable power system

Flexibility must be created both systemically and locally (International Smart Grid Action Network, 2019). Therefore, flexibility options are crucial to providing flexibility and shaping a sustainable and efficient electricity system.

There are various approaches to characterizing and classifying flexibility options (Akrami et al., 2019; Alexopoulos et al., 2021; Alizadeh et al., 2016; Chatzivasileiadis et al., 2023; Deng et al., 2022; Kara et al., 2022; Lund et al., 2015). Flexibility options within the power grid can be characterized by multiple dimensions to understand their capabilities and contributions to the power system's flexibility. These dimensions provide insights into the potential of different flexibility options and their suitability for specific applications.

Numerous scientific contributions address various assessment characteristics, considering multiple dimensions including specific flexibility resource location, capacity, the duration and timing of flexibility provision, ramp rate, direction, and response time (Akrami et al., 2019; Bhuiyan et al., 2022; Degefa et al., 2021; Eid et al., 2016; Ela et al., 2016; Lannoye et al., 2012b; Salman et al., 2022; Villar et al., 2018). More recent studies have identified four dimensions for characterizing a flexibility product or service: time, spatiality, resource type

(technology), and risk (Del Granado et al., 2023; Kara et al., 2022).

Flexibility options have been examined in the scientific literature from various perspectives, including renewable energy integration (Alizadeh et al., 2016; Cruz et al., 2018; Lund et al., 2015), Distributed Energy Resources (Eid et al., 2016; Villar et al., 2018), new technologies (Cruz et al., 2018; Lund et al., 2015), ancillary services (Degefa et al., 2021; Saele et al., 2020), markets (Eid et al., 2016), power system needs (Badanjak and Pandžić, 2021; International Smart Grid Action Network, 2019), and security of electricity supply (Santos et al., 2022; Sperstad et al., 2020).

Among others, the main flexibility options can be differentiated in terms of transmission, storage, generation, and demand. In this context, a distinction is made between temporal and spatial flexibility. Temporal flexibility is the ability to change the timing of electricity generation or consumption, and its resources for flexibility pertain to generation, demand, and storage. Spatial flexibility is the ability to balance supply and demand geographically and is particularly supported by grid-side flexibility options (Heider et al., 2021). Sector coupling enables the linkage of temporal and spatial flexibility.

Successful integration and utilization of flexibility resources require coordinated planning and cooperation for various flexibility deployments. Holistically, flexibility options can be used to support the power system's ability to adjust its generation or consumption in response to sudden, anticipated, or unanticipated changes (Minniti et al., 2018). Locally, flexibility options are often deployed to effect changes in consumption or generation patterns due to direct or indirect signals (Minniti et al., 2018). Therefore, when assessing flexibility resources from different power system perspectives, the spatial granularity and aggregation level of individual flexibility options are pivotal.

3.3 Flexibility resources from a holistic power system perspective

From a holistic power system perspective, flexibility resources can be broadly categorized into demand-side, supply-side, grid expansion, and storage flexibility potentials. Flexibility resources here refer to flexible assets that are located near central power generation plants or within the national or regional power grid. These resources typically have larger capacities

and greater potential to provide flexibility. Figure 9 presents the flexibility resources related to the holistic power system (highlighted in gray).

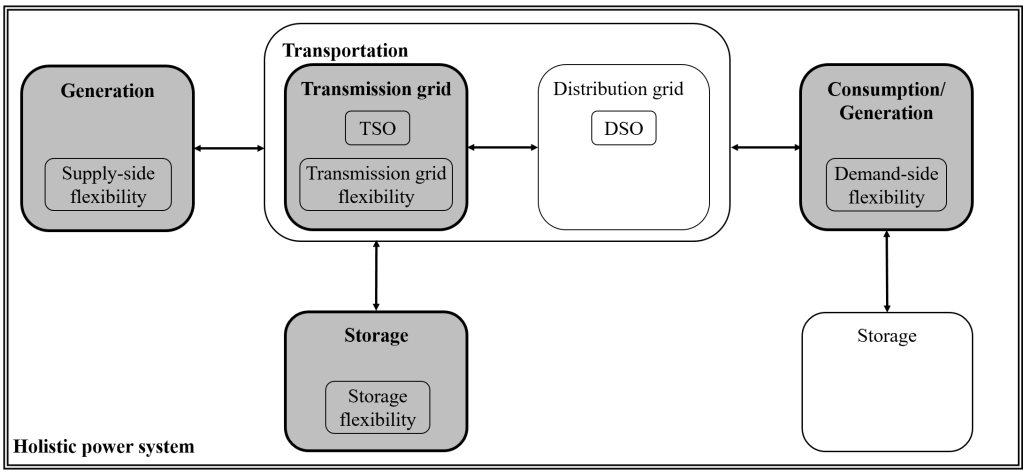

Figure 9: Flexibility resources from a holistic power system perspective.

With respect to holistic power system, flexibility resources on the supply-side can involve centralized solutions such as natural gas-fired power plants and large-scale energy storage systems to align electricity generation with demand. Supply-side flexibility involves adjusting the output of conventional power plants, renewable energy sources, and even flexible industrial processes to balance supply and demand. Therefore, supply-side flexibility helps to mitigate fluctuations in generation, ensuring power system reliability and reducing the need for costly backup capacities.

With regard to demand-side flexibility, the potential flexibility may include engaging consumers as active participants in the energy system. The goal is to collaborate with consumers to optimize energy consumption patterns and adjust them to match the available electricity generation. In overview, this can be achieved particularly through centralized demand-response programs to create incentives for consumers to reduce their electricity consumption during peak load periods, alleviating stress on the grid and enhancing its stability.

One further flexible resource to increase the flexibility of the power system from an overall point of view are energy storages. Battery storage, pumped hydro storage, compressed

air energy storage, and other storage technologies allow excess energy generated during periods of high production to be stored and released during periods of high demand. Hence, storages can help to bridge the gap between electricity generation and consumption, bolstering power system stability. In this context, such technologies are significant in the overall optimization of the power system and can store or provide a substantial amount of energy, capable of responding to fluctuations in both electricity generation and demand across the entire grid.

Likewise, another source of flexibility exists with regard to the transmission grid. The grid has significant flexibility potential, involving the expansion and reinforcement of grid infrastructure to accommodate the integration of renewable energy sources and utilizing smart grid technologies to efficiently control and monitor grid operations.

To sum up, from an overall system perspective, flexibility provision refers to the ability to maintain a balance between electricity generation and demand across the entire grid. This includes the coordination of flexibility provision by various stakeholders, including flexible generation resources, energy storage, and demand response measures, to balance fluctuations in electricity generation and demand and ensure grid stability. Flexibility provision at the holistic system level aims to avoid congestion in the transmission grid, maintain grid frequency stability, and facilitate the integration of renewable energy sources (Lannoye et al., 2012a; Ma et al., 2013; Zeng et al., 2022; Zhao et al., 2016).

3.4 Flexibility resources from a local power system perspective

In general, from a local power system perspective, flexibility resources refer to decentralized flexible assets positioned at the local or regional level, closer to consumers. These resources are typically smaller in scale and have lower capacity compared to flexible resources from a holistic power system point of view. Decentralized flexibility options pertain to the potential of small and distributed resources to contribute to the flexibility of the power system.

Similar to central flexibility resources, from a local power system level, flexibility potentials encompass a spectrum of demand-side, supply-side, grid, and storage resources collectively contributing to a resilient and adaptable power system (see Figure 10, highlighted in gray). From a local perspective, both demand and generation flexibilities are located on the end-consumer side.

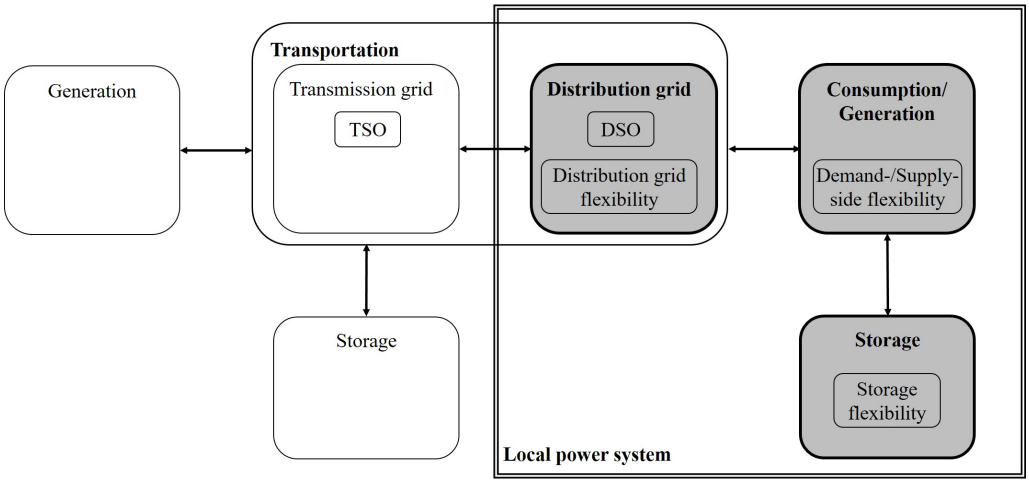

Figure 10: Flexibility resources from a local power system perspective.

Traditionally, the distribution grid has been considered a passive conduit for the delivery of electricity from the transmission grid to end-users. However, the increasing penetration of renewable energy sources, distributed generation, and energy storage systems has endowed the distribution grid with newfound capabilities to offer flexibility services.

In addition, supply-side flexibility resources in a decentralized context include local renewable energy sources such as rooftop solar panels, small wind turbines, or micro-hydropower plants. These resources can be utilized to feed into the local area or to feed excess energy back into the grid.

With regard to the decentralized storage flexibility resources, storages integrated into the local power system offer valuable flexibility. These can encompass batteries or other energy storage systems located in households, businesses, or community buildings. Hence, storages can be employed to store surplus energy from renewable sources and utilize it during periods of high demand or low renewable energy generation, so it can stabilize the grid during demand peaks or generation shortfalls.

In this local context, resources for demand-side flexibility in a decentralized context might involve the use of smart home devices or energy management systems to adjust energy consumption patterns based on real-time energy prices or grid conditions. In particular, electric vehicles can be utilized for demand response, making them a valuable flexibility

service provider.

Hence, locally, flexibility provision regards the adaption of electricity generation and consumption within a local distribution network. It can be used to manage voltage levels, mitigate congestion, and ensure efficient power flow. Flexibility resources can enhance local reliability and contribute to overall grid stability. In this context, DERs enable flexibility and represent flexibility resources, from the demand- and supply-side, alongside storage flexibility. Apart from intensifying grid-related issues, DERs can also offer a potential solution due to their inherent controllability. Many DER units can change their generation and consumption patterns with limited impact on their primary energy service. The flexibility potential that DERs offer is substantial and suitable to address location-specific issues, such as congestion, but also, when properly aggregated, to support flexibility sources at the transmission level. This contribution can help to avoid bottlenecks in the local distribution grid, support network stability, and promote decentralized renewable energy supply.

4 Research contribution of the appended scientific papers

This section provides an overview of the five research papers appended in this dissertation with regard to their motivations and research objectives, highlighting the contribution of each paper in the context of the methodology used. The key results and a critical appraisal are also presented for each paper. Regarding the approaches for analyzing the impacts of flexible resources in the power system, two power system perspectives are differentiated. From a holistic power system perspective, the flexibility resources consisting of storage capacities, grid expansion, and demand-side and generation-side flexibility options are considered. With regard to the flexibility resources at the local level, EVs are the focus of the scientific contributions.

4.1 Methodological framework

The methodological framework for analyzing the impact of flexibility options can vary depending on the perspective and the related points of interest. In the following, a differentiation is made between the holistic and the local power system perspective. In this context, the geographical scope, spatial granularity, and aggregation level of individual flexibility resources play a significant role. Table 1 illustrates the key differences between these to perspectives within this dissertation and associates them with the related methodological approach and the corresponding scientific publications.

Table 1: Methodological framework within this thesis.

	Holistic power system perspective	Local power system perspective
Grid level	• Transmission grid	• Distribution grid
Aggregation level	• High aggregation level (low spatial granularity)	• Low aggregation level (high spatial granularity)
Flexible resources considered	• Demand-side flexibility • Supply-side flexibility • Storage flexibility • Grid-side flexibility	• Electric vehicles
Points of interest	• Incentives to flexibility investments • Risk attitudes of public and private decision makers • Congestion management • Interdependencies of different flexibility options	• Market penetrations of EVs • Individual charging behavior and related flexibility potential • Simultaneity factors of EV charging processes
Methodological approaches	• Game theoretical approaches combined with implementing stylized models of liberalized electricity markets • Robust/Stochastic optimization	• Reduced LCA approach • Statistical analysis • Clustering approaches • Simulation

Table 4.1:Methodological framework within this thesis (cont.).

	Holistic power system perspective	Local power system perspective
Related publications	• **Paper A:** Weibelzahl, M., Märtz, A. (2020), Optimal storage and transmission investments in a bilevel electricity market model, *Annals of Operations Research*. • **Paper B:** Coniglio, S., Halbrügge, S., Märtz, A., Weibelzahl, M. (forth.), The flexibility puzzle in liberalized electricity markets: Understanding flexibility investments under different risk attitudes, submitted to a scientific journal.	• **Paper C:** Märtz, A., Plötz, P., Jochem, P. (2021), Global perspective on CO_2 emissions of electric vehicles, *Environmental Research Letters*. • **Paper D:** Märtz, A., Langenmayr, U., Ried, S., Seddig, K., Jochem, P. (2022), Charging behavior of electric vehicles: Temporal clustering based on real-world data, *Energies*. • **Paper E:** Märtz, A., Held, L., Jochem, P., Fichtner, W., Suriyah, M., Leibfried, T. (2019), Development of a tool for the determination of simultaneity factors in PEV charging processes, *Proceedings of the 3rd E-Mobility Integration Symposium*.

From the holistic power system perspective, the focus lies on examining the entire power system. The goal is to identify flexibility resources available at the aggregated level of the overall power system and explore how they can contribute to renewable energy integration and ensure supply security. This perspective involves consideration of large geographical areas, typically encompassing the transmission grid. Consequently, this perspective implies a coarse granularity and a high level of analytic aggregation. From a holistic perspective, grid-side, demand-side, generation-side, and storage-side flexibility resources are considered in

particular. The central focus of the analysis lies on the analysis of incentives for investing in flexibility options, considering the individual risk attitude of private and public actors with regard to (flexibility) investments, different congestion management regimes, and the interplay between different flexibility resources.

From the local power system perspective, flexibility options are examined at a much smaller and more localized level. The emphasis is on utilizing flexible resources, particularly within the distribution network. From a local viewpoint, specific technologies are investigated to identify technology-specific flexibility potential. Simultaneously, the load profiles of individual consumers and installations are analyzed to understand how flexibility can be used to adjust electricity demand to fluctuating generation and to reduce peak loads. Analyses at the distribution network level are conducted on smaller geographical scales, focusing on local or even individual units. From the local power system perspective, the spatial granularity is much finer, and the aggregation level is very small, as individual units and specific locations are detailed. EVs are under central analysis in this thesis. For flexibility provision locally, the market ramp-up of EVs, individual charging behavior, available flexibility potential, and simultaneity of the charging processes are decisive features.

4.2 Methodological approaches from a holistic power system perspective

To examine flexibility options holistically, this study translates electricity market models into multistage mathematical optimization models. To account for various stakeholders and their interdependent relationships, these models are coupled with approaches from game theory. Specifically, the methodology introduced within this thesis considers

- the multistage Stackelberg game and
- stylized models of liberalized electricity markets.

The starting point of this consideration is a modeling of the complex interaction of regulated levels and competitive processes in the electricity market, considering the interest of the different market players and their mutual relationships. This interaction rests on the interdependencies between optimal grid investments by the regulated network operator and optimal investments in storage and generation capacities by private actors. From a game-theoretical perspective, this constellation corresponds to a multistage Stackelberg game, in

which the mutual reactions of individual market players are analyzed. In this context, market participants act interdependently and respond to the decisions of other market players. Each market player optimizes their own actions while considering the decisions of the other players.

For the methodological approaches in this dissertation, the liberalized electricity market is represented by multilevel mathematical optimization models, which are combined with game-theoretical approaches. Depending on the research objective and its level of complexity, a bilevel electricity market model (Chapter 4.2.1) and a four-level electricity market model (Chapter 4.2.2) are implemented.

4.2.1 A bilevel market model (Paper A)

4.2.1.1 Motivation and research objective

Modern electricity markets are typically characterized by spatial or regional divergence of energy supply and demand. This trend also typifies the German electricity market, with significant wind production in the north and high consumption in the south (Bucksteeg et al., 2015). In addition to the regional divergence of supply and demand, intermittent renewable energy injection also leads to a temporal divergence between generated and consumed energy. The regional and temporal dimensions of divergence are closely interrelated.

As a direct consequence of the regional divergence between supply and demand, situations often arise in which transmission constraints limit electricity flows between nodes due to technical limitations (Dijk and Willems, 2011; Neuhoff et al., 2013). To address the spatial divergence, long-term transmission investments and the implementation of various short-term congestion management measures were discussed as potential solutions to network congestion (Grimm et al., 2016a; Grimm et al., 2016b; Jenabi et al., 2013; Zambrano and Olaya, 2017). Simultaneously, energy storage technologies play a crucial role. On one hand, storage facilities that typically smooth out intertemporal demand peaks also have the potential to reduce the need for large network investments. On the other hand, an expanded interregional network can improve the adaptation of the intertemporal divergence between demand and intermittent supply (Steinke et al., 2013).

This research paper investigates the interdependencies between storage and network investments by different players under various congestion management regimes in a multistage game translated into a two-level market model. The study also analyzes whether the chosen congestion management mechanism can significantly impact on long-term investments in both transmission lines and storage facilities.

4.2.1.2 Methodological approach

This contribution centers on a game-theoretic perspective utilizing a multistage Stackelberg game framework, translated into a two-level mathematical optimization problem. In this hierarchical game, the TSO acts as the leader, making the initial optimal investment decision in network capacities. Competing firms then act as followers, optimally responding to the leader's investment decision. This structure is consistent with extensive literature such as Baringo and Conejo (2012), Fan et al. (2009), Gil et al. (2002), Grimm et al. (2016a), Jenabi et al. (2013), and Sauma and Oren (2006), which also consider multistage games with the TSO serving as the leader. The TSO anticipates the market outcomes of the second stage, where competitive firms engage in energy trading and invest in storage facilities once the network expansion by the TSO has been realized. Following the sequential investment decisions of the TSO and the firms, trading occurs across multiple zonal spot markets. This trading reflects the profitability and efficiency of respective investment decisions while directly considering potentially constrained network capacities, which may lead to a regionally differentiated price structure.

The temporal timeframe of the modeled relationships and the underlying Stackelberg game is depicted in Figure 11.

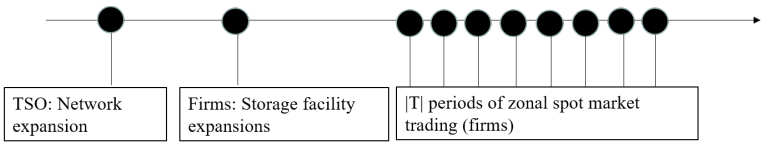

Figure 11: Timing of the underlying multistage Stackelberg game of the bilevel market model (based on Weibelzahl and Märtz (2020)).

It is assumed that, in each phase, all (investment) decisions from the preceding stage(s) can be observed by rational actors, enabling accurate expectation formation (Sauma and Oren, 2006).

The mathematical modeling thus results in a bilevel optimization model, corresponding to an equilibrium model of the electricity market. In this model, a central planner (e.g., the regulated grid operator) anticipates the location and production decisions of private-generation companies when making network expansion decisions (investments in network capacities). The bilevel optimization problem is illustrated schematically in Figure 12.

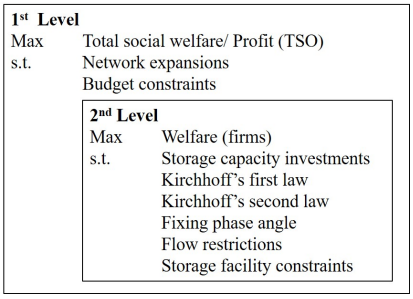

Figure 12: Schematic representation of the bilevel optimization problem.

Being non-convex and non-differentiable, bilevel models are known to be NP-hard, implying that this class of optimization problem is in general very challenging and hard to solve (Jeroslow, 1985; Pozo et al., 2017; Sariddichainunta and Inuiguchi, 2017; Zare et al., 2017). In the underlying contribution, the bilevel optimization model was reformulated to a single-level problem by using a linear reformulation. In addition, given that the second problem is a convex (concave) and continuous optimization problem with only linear constraints, Karush-Kuhn-Tucker (KKT) reformulation including complementary constraints can be used to replace the bilevel problem with a single-level problem (Colson et al., 2007; Dempe, 2002).

Accounting for various zonal congestion management regimes, the model was applied using a commonly used six-node example in the literature (Chao and Peck, 1996), and the numerical results were interpreted.

4.2.1.3 Key results

Within the scope of this research contribution, both the absolute capacity of investments and the locations of corresponding storage facilities and grid investments were evaluated, considering different congestion management regimes.

It was observed that appropriate storage investments by private firms can generally reduce TSO transmission investments. However, investments in a (zonal) market environment can yield suboptimal outcomes compared to an integrated planning solution (nodal pricing). Moreover, invested storage facilities may affect inter-regional price and demand structures, requiring a reconfiguration of optimal zonal boundaries; that is, in the case of storage facilities, the welfare-maximizing zone configuration may change, as compared to the no-storage case.

In overview, in the long-term, investments from private market participants in energy storage significantly influences decisions made by the state-regulated grid operator concerning the level of network fees set by the TSO, the location and extent of transmission investments, the configuration of optimal price zones, and social welfare. Hence, policy recommendations should be based on economic analyses encompassing storage capacities and interactions with grid expansion.

4.2.1.4 Critical appraisal

For the purposes of the paper, only two time periods were examined as part of the case study. This can be justified due to the complexity of the model. This temporal frame contains the smallest number of time periods to be able to represent storage facility effects. Nevertheless, in contrast to simple two-period models (see e.g. (Sioshansi, 2010; Sioshansi, 2014)), the implemented model is, however, generally able to capture more than two time periods. Ultimately, this may help to increase the accuracy of the proposed model and should be considered in future research.

With regard to the case study, the six-node model used represents a highly generalized case study. However, it is widely accepted and used in a broad scientific community (Jenabi et al., 2013; Grimm et al., 2016a; Ambrosius et al., 2022). Due to the complexity of the model, the six-node model is a suitable to validate modeling approaches. Notably, the presented optimization model is also appropriate for highly complex case studies.

4.2.2 A four-level market model (Paper B)

4.2.2.1 Motivation and research objective

With the increasing penetration of renewable energy sources, supply-side variability and its inherent uncertainty pose new challenges to balance supply and demand. In particular, the loss of generation flexibility due to the growing dominance of renewable energy production leads to a phenomenon known as the flexibility gap. To address this gap, new forms of flexibility are required. In this context, the challenge of selecting the "right" mix of flexibility options, akin to a flexibility puzzle, becomes pivotal.

Simultaneously, the degree of risk aversion exhibited by numerous stakeholder groups in the electricity market can significantly impact the location and quantity of flexibility assets that these stakeholders are willing to invest in. Properly modeling the flexibility investment behavior of diverse market participants necessitates accurately and realistically incorporating the level of risk tolerance of involved parties into energy market models (Ambrosius et al., 2020; Ambrosius et al., 2022; Grimm et al., 2019; Grimm et al., 2021).

This research analyzes the emerging flexibility challenge and, consequently, covers an appropriate mix of flexibility options while considering the individual risk attitudes of different stakeholders. To this end, a game-theoretical approach to a multistage investment game is proposed, accounting for uncertainties, and is then translated into a four-level mathematical market model.

4.2.2.2 Methodological approach

The contribution examines the flexibility puzzle in a liberalized electricity market under uncertainty as an investment game. This can be interpreted as a multistage Stackelberg game in which different players with varying risk attitudes make decisions under uncertainty. It is assumed that the involved players form rational expectations about the optimal responses of players who make decisions after them.

The temporal framework underlying the multistage game-theoretical approach is illustrated in Figure 13. The first stage considers public transmission investments by the TSO, made anticipating private investments in storage and conventional backup generation facilities.

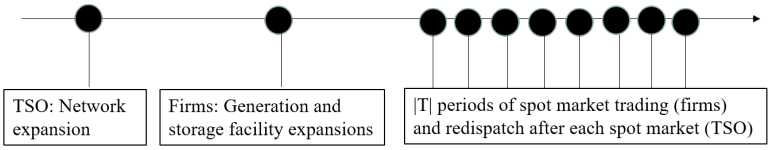

Figure 13: Timing of the underlying multistage Stackelberg game of the four-level market model (based on Weibelzahl and Märtz (2020)).

These private investments are made in the second stage based on expected spot market profits, which are determined in the third stage on a zonal spot market. The fourth stage considers TSO's redispatch measures in case the contracted spot market quantities cannot be transmitted through the power grid.

While investment decisions are made only once, trading on the spot market and the redispatch performed by the TSO for all modeled time periods follow. This modeling is also based on an equilibrium model of the electricity market, where a central planner (e.g., the regulated grid operator) anticipates private investment decisions by generation companies in storage and backup generators to determine network expansion (investment in network capacities). Electricity trading occurs through a central power exchange, neglecting possible network restrictions, following the merit order principle.

In the fourth stage, if a non-transportable spot market outcome occurs, a cost-based redispatch is conducted. In this process, the TSO utilizes power plants and consumers in the most cost-effective way possible to ensures permissible flows. To achieve this, the TSO may require some generators to shut down or ramp up their plants, or may ask consumers to change their demand. Plants that are shut down must pay their variable costs saved through the shutdown to the TSO, while newly ramped-up plants receive their variable costs.

The multistage Stackelberg game developed in the paper is translated into a four-level optimization problem (see Figure 14) and transformed through reformulation into an equivalent single-level optimization model. This model is then solved using a spatial branch-and-bound method to achieve global optimality.

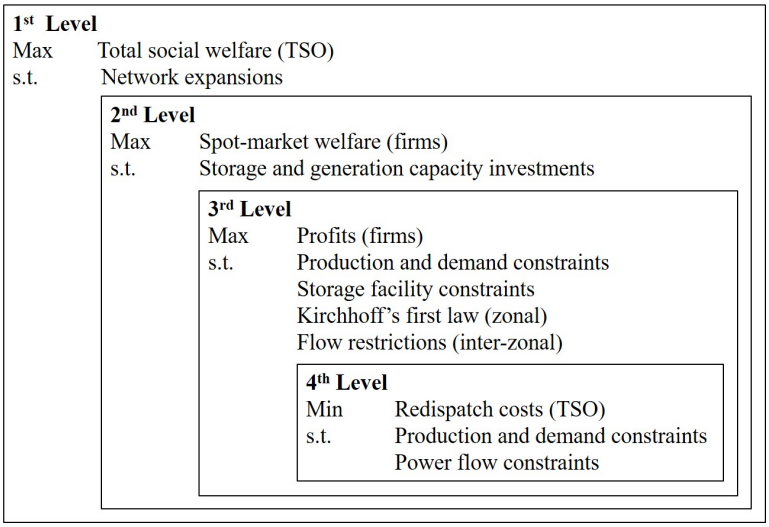

Figure 14: Schematic representation of the four-level optimization problem.

Using a well-established academic case study, the model is applied to analyze the effects of the varying risk preferences of private and public decision-makers on long-term investments in the considered flexibility options. One key feature of the study involves simulating investments in an uncertain environment. The uncertainties are reflected in variables such as CO_2 prices, levels of renewable energy injection, and demand levels.

4.2.2.3 Key results

Through the modeling and analysis of various types of risk preferences and with the help of a comprehensive case study, this contribution has demonstrated that the lower risk aversion of a public investor leads to higher investments and greater welfare, even if the private investor's risk attitude remains risk-averse. When comparing uniform and zonal market designs, the results indicate that a zonal market design, thanks to the consideration of inter-zonal transmission lines, can require less network expansion and can consequently lead to increased regional investments in generation capacity and storage.

The computational results of the case study also highlight that, due to the urgent need for adequate investments in flexibility, it is important to consider not only the market design but also the risk behavior inherent in different market designs. It has been observed that differing risk preferences among private and public investors (e.g., companies and grid operators)

result in distinct investments that are more or less desirable from a system perspective. To create targeted incentives for (flexible) investments it becomes crucial understanding how policymakers can address varying risk preferences.

4.2.2.4 Critical appraisal

The model could be expanded in various directions, such as incorporating different forms of demand flexibility (including demand shifting) or storage, market-based redispatch, and investments in electrification (e.g., EVs or heat pumps), which could help policymakers to pave the way towards a flexible, climate-neutral electricity system.

As already critically noted in the bilevel market model, the applied six-node model represents a highly generalized case study. Nevertheless, it is accepted and applied by a broad scientific community. For reasons of complexity, it is a suitable option for validating model approaches. In general, the established model is also appropriate for highly complex case studies.

It is worth mentioning critically that the model assumes an ATC-based market coupling. In this setup, companies belonging to a given zonal spot market receive price signals that encourage them to consider inter-zonal network capacity. Intra-zonal transmission limits and phase angles are completely ignored during the spot market clearing. Such a commonly applied market coupling approach can, depending on the structure of the transmission network and associated capacities, lead to post-optimization in redispatch.

4.3 Methodological approaches from a local power system perspective

From the local perspective, market penetration of distributed energy sources and technologies, individual behavior (demand and generation), and spatial granularity regionalization play a role with regard to decentralized flexibility options.

In the context of this dissertation, the focus lies on EVs as decentralized flexibility resources. To address the future challenges and opportunities associated with the introduction of EVs,

it is essential to quantify the impacts on the local power system. In this context, the methodology used within this thesis provides

- a reduced LCA approach,
- statistical analysis,
- clustering approaches, and
- a simulation approach.

There is a broad consensus that the critical factor for a system integration of EVs is not the additional energy demand but the potential load peaks resulting from many simultaneous charging processes. Therefore, accurate predictions of the new additional load caused by EV charging are necessary. As is common today, synthetic load profiles or empirical data from field tests are used as input for energy system models. Current knowledge of the characteristics of load profiles of EVs in local areas is limited (Helmus et al., 2020; Noussan and Neirotti, 2020). More informed insights into charging habits, the amount of energy charged, and charging power can empower to harness the flexibility potential of electric vehicle charging, for instance, to mitigate peak loads.

Therefore, from a local power system perspective, the market penetration and the CO_2 mitigation potential of EVs (Chapter 4.3.1), informed knowledge about individual charging behavior (Chapter 4.3.2), and the simultaneities of charging processes (Chapter 4.3.3) are analyzed in this dissertation.

4.3.1 Market penetration of electric vehicles and related greenhouse gas mitigation potential (Paper C)

4.3.1.1 Motivation and research objective

The transportation sector is responsible for approximately a quarter of global energy-related greenhouse gas emissions and is the only energy-related sector that continues to exhibit increasing emissions compared to 1990. EVs are viewed as a promising option to reduce greenhouse gas emissions in the transportation sector, particularly due to the growing share of renewable energy in electricity generation.

Numerous studies have already examined the life-cycle greenhouse gas emissions of plug-in electric vehicles (PEVs) compared to internal combustion engine vehicles (ICEVs). These studies demonstrate that PEV emissions depend heavily on the assumed electricity mix, driving behavior, and environmental conditions, leading to regional variability (Cox et al., 2018; Gómez Vilchez and Jochem, 2020).

The increasing proportion of renewable energy in electricity generation also affects battery production and the charging of EVs. However, most studies still assume a fixed carbon content for electricity in the environmental assessment of PEVs, and the rapid evolution of the generation mix has yet to be examined on a global scale. Furthermore, the inclusion of upstream emissions remains an open policy issue. The overall reduction of greenhouse gas emissions through PEVs is primarily determined primarily by the evolution of the vehicle fleet and the specific emissions of electricity generation.

This study combine two PEV market scenarios with an electricity generation scenario and investigate the mutual influence of the electricity mix development on the potential for CO_2 emissions reduction through EVs.

4.3.1.2 Methodological approaches

This paper employs a reduced Life Cycle Assessment (LCA) approach, with a focus on the usage phase, while additionally incorporating emission factors from the literature stemming from battery and vehicle production.

The assessment is conducted by combining scenarios for the future PEV fleet in key automotive markets with values from the literature concerning their life cycle greenhouse gas balances, along with the impacts of decreasing the carbon intensity of electricity over time.

In this process, a forthcoming energy scenario is examined for various global markets (China, Europe, Japan, United States, and India) characterized by high passenger car sales and connected with two distinct PEV market diffusion models. An evaluation is performed to evaluate the potential impact of the combined consideration of electricity generation mix and PEV market diffusion in Europe, China, Japan, the United States, and India.

4.3.1.3 Key results

The results obtained through the reduced LCA indicate that PEVs can lead to the necessary reduction, but it is crucial for the entire vehicle fleet to be operated nearly emission-free. The greenhouse gas emissions of PEVs exhibit significant temporal variation in many countries due to the decarbonization of the grid. The common assumption in many studies of a fixed carbon intensity in the grid significantly underestimates this change. If PEVs are chosen as a key option for reducing GHG emissions from passenger cars, the market diffusion of PEVs should not be delayed, as improvements in the carbon intensity of the electricity grid can immediately increase the remaining carbon budget. Our findings demonstrate that postponing PEV market diffusion negatively impacts the remaining carbon budgets.

The central result shows, that the remaining carbon budget is best utilized with early PEV market diffusion. Waiting for cleaner PEV battery production cannot compensate for the lost carbon budget associated with the use of internal combustion engine vehicles.

4.3.1.4 Critical appraisal

Within the scope of the underlying paper, no low-carbon or carbon-free fuels were considered. The article focused exclusively on the indirect emissions of PEVs and the changes related to the energy transition in electricity generation, specifically the reduced greenhouse gas emissions from battery production and lower upstream emissions from electricity generation that affect the vehicle use phase of all current PEVs (Cox et al., 2018; Kim et al., 2016). In addition, due to limited experience with PEV disposal, emissions from vehicle disposal were not considered.

Notably, the results are subject to uncertainty, as future parameters may evolve differently than anticipated. The scenarios and greenhouse gas reduction potentials are based on a set of assumptions. However, all relevant electricity scenarios assume future decarbonization of electricity generation, but at different rates. Therefore, the observed impact on the carbon budget remains robust across variations in the chosen scenario, although the extent of the impact may vary.

4.3.2 Individual charging behavior and flexibility potential (Paper D)

4.3.2.1 Motivation and research objective

With the increasing penetration of BEVs, understanding the driving and charging patterns of BEV users becomes of paramount importance to comprehend their charging behaviors and the associated flexibility potential. Gaining insight into the complexity of spatial and temporal charging behavior is immensely significant for future sizing and flexibility assessment of local charging infrastructure or leveraging BEV flexibility for renewable energy integration. Therefore, comprehensive knowledge of charging behavior and the resulting load profiles is essential for a successful and thoughtful integration of EVs into the energy system.

The goal is to investigate the insights that can be gained from the individually timed charging behavior of BEV users. To achieve this, a two-stage cluster algorithm approach was employed to identify user groups and derive a standard charging pattern for each group. The BEV user groups were subsequently validated and associated with charging locations such as home, workplace, and public areas, supported by synthetic load profiles. Furthermore, this paper also wants to provide statistical parameters for the replication and reuse of the underlying real-world dataset.

4.3.2.2 Methodological approaches

In the context of the paper, statistical analyses and a two-stage cluster algorithm approach were employed to investigate the insights that can be derived from the temporal charging behavior of BEV users, identify user groups, and derive a standard charging pattern for each group.

Through the statistical analyses, real-world insights into charging behavior were provided based on a comprehensive dataset of 2.6 million charging sessions in 2019. This analysis focused particularly on the charging process, including charging behavior, utilized charging power, and plug-in times, which represent the corresponding charging flexibility potential.

Subsequently, a two-stage clustering approach was applied. Before the determination of the final number of clusters, the clustering approach was executed with several different cluster numbers, and the Akaike Information Criterion and Bayesian Information Criterion (Schwarz, 1978) were calculated. Both criteria helped assess the fit of the developed model

and avoid overfitting the data. Based on the analysis of these criteria, Gaussian Mixture Model (GMM) clustering with seven clusters was performed.

The total number of charging activities during each of the derived temporal charging clusters was counted, and the proportion of charging activities for each cluster was calculated for each user. These proportions for each user formed the basis for the next clustering step. The unsupervised k-Means clustering approach was utilized to derive different temporal behavioral clusters (Lloyd, 1982). K-Means is a simple and commonly used clustering method for behavioral analysis. Examples of applying k-Means for analyzing driving patterns are Fugiglando et al. (2019) and Dardas et al. (2020).

To assess whether all these dimensions were necessary for the k-Means clustering, the dimensions were normalized, and the number of dimensions was reduced through a subsequent Principal Component Analysis (PCA) (Fugiglando et al., 2019). The final number of clusters was determined by applying the elbow method to different numbers of clusters (Syakur et al., 2018).

Finally, the BEV user groups were validated and mapped to charging locations such as home, workplace, and public areas, supported by synthetic load profiles.

4.3.2.3 Key results

The results obtained from the underlying paper allow for insights into real charging behavior. Applying a GMM to a real dataset reveals seven distinct charging clusters. Building upon this, five BEV user groups are identified through k-means clustering. These user groups are then mapped to charging locations, with validation using synthetic load profiles. This paper further provides the statistical parameters necessary to replicate and reuse the underlying real dataset. Thus, the paper not only offers insights into real charging behavior but also the opportunity to replicate the dataset, thereby reducing data scarcity. This replication can greatly assist current energy system modelers in examining the load flexibility of BEVs in much finer detail.

Based on the results of cluster analysis, an investigation was conducted into how homogeneous the charging behavior of BEV users was. Evidently, BEV users did not behave homogeneously, charging their vehicles at similar times and for similar durations. This insight contradicted the categorization of BEV users into fixed user groups.

In conclusion, the results demonstrate that insights into user groups of battery electric vehicles and associated charging patterns and flexible (shiftable) loads can be drawn from the exclusive examination of individual temporal charging data. Two main findings can be highlighted: in this early market phase, the analysis identified a surprisingly high number of opportunistic chargers during the day and the shifting of users between charging clusters. Furthermore, an estimation of charging locations is possible. Derived load profiles have been created, which can be used in energy system models to more accurately consider the load shifting potential of BEVs.

4.3.2.4 Critical appraisal

Due to certain limiting factors, the Gaussian Mixture Model (GMM) clustering was employed. The high data concentration serves as a general indicator for the application of density-based approaches, and in addition, the clustering approach must perform well in terms of computation time and storage constraints when dealing with large datasets.

While the underlying dataset was extensive compared to other currently available BEV data, the chosen approach relied solely on technical data, with user-specific data unavailable. Additionally, all data originated from a specific BEV model, the BMW i3, and all charging events occurred during an early phase of BEV market adoption. Nevertheless, the dataset provides valuable insights for the current literature.

For future research, in addition to temporal aspects, further charging process factors should be taken into account, including charging power, amount of energy charged, and charging frequency. Furthermore, spatial distribution should be considered in future studies.

4.3.3 Simultaneity factors of EV charging processes (Paper E)

4.3.3.1 Motivation and research objective

One challenge associated with the integration of EVs into the power system is their relatively high additional load compared to other household appliances, which can impact the power grid. One crucial factor that has often been neglected in previous analyses is the simultaneity factor of charging processes. Previous studies have typically assumed that all EVs are

charged simultaneously at a constant rate throughout the entire charging process. Nevertheless, this assumption does not align with the real-world behavior of EV users.

An analysis of the simultaneity factor of charging processes of EVs requires one to distinguish between two different aspects of simultaneity. Firstly, there is the simultaneity factor, which describes the percentage of EVs being charged on the same day. This factor recognizes the fact that not all EV owners necessarily charge their vehicles on a daily basis. Secondly, there is the simultaneity factor related to the timing of charging processes within a single day. This aspect considers the variation in when EVs are plugged in for charging throughout the day.

The objective of this tool is to understand the simultaneity factor, crucial to accurately assess the impact of EV charging on the power grid. It involves recognizing that not all EVs are charged daily, as well as that the timing of charging events within a day can vary significantly. These considerations are essential for effective grid management and planning to accommodate the growing adoption of EVs.

4.3.3.2 Methodological approaches

With regard to the simultaneity factor of the charging processes taking place within one day, an open-source tool was developed. The tool calculates the simultaneity of the charging processes within one day, considering several key factors, including the number of EVs, their arrival and departure times, different vehicle classes, various charging rates, and State of Charge (SoC) at arrival as well as the desired SoC at departure.

Users of the tool have the flexibility to choose between using pre-included data or inputting their own customized data, allowing for consideration of future trends in EV charging behavior and infrastructure. The tool is also particularly valuable when assessing the resulting impacts on the power grid, as it enables the incorporation of household loads with specific simultaneity patterns in combination with the associated simultaneities of EV charging, significantly influencing grid dynamics.

An additional feature of the tool is its ability to differentiate between balanced and unbalanced charging. Ergo, it accounts for scenarios in which EVs are unevenly distributed across the three phases of a three-phase electrical system, as commonly found in Germany and other countries. Accordingly, the tool can effectively model cases in which individual

EVs are connected in an unbalanced manner across these three phases.

The tool not only provides a comprehensive framework by which to assess the simultaneity of EV charging processes but also considers factors such as household loads, phase imbalances, and future trends in EV adoption. Additionally, the tool includes a sensitivity analysis to enhance its robustness and practical utility.

4.3.3.3 Key results

The results of this study and the tool presented are pivotal in understanding the interplay between EV charging behavior and household load dynamics and the related simultaneity factors.

The simultaneity of charging processes features in the analysis of the network effects of EVs. However, it is crucial to differentiate between whether the EVs are evenly distributed across the three phases of the electrical system or whether there is an uneven distribution. In any scenario, it is important to note that the simultaneity factor is consistently lower than the often assumed but empirically unrealistic factor of 1.

The results show occasional peaks in the match of about 0.8, although with a very low probability when 10 EVs are considered. Since the total peak load is a critical factor in grid analyses, it is essential to consider household loads in addition to EV loads. Since the peak load of households and that of EVs usually differ in time, this temporal discrepancy should also be considered when calculating the total peak load. This adjustment consideres the fact that the peak load is less than the sum of the individual peak loads due to the time discrepancy.

4.3.3.4 Critical appraisal

The default data set provided is sourced from various references, allowing user modifications for each value. However, when utilizing the tool and interpreting the resulting simultaneity or peak load values, it is important to be aware that extreme values may occasionally arise empirically by chance.

In the tool, it is assumed that individual EVs are unevenly distributed across the three phases of the electrical system. However, due to the lack of available data, household loads are considered to be symmetrically distributed across these three phases.

As demonstrated, both the charging power and the number of EVs under consideration significantly influence the simultaneity factors. These variables must be carefully analyzed to better understand the simultaneity of EV charging processes and their implications for the grid.

5 Conclusion and critical appraisal

The creation of an efficient and sustainable power system is a factor central to the success of the energy transition and the realization of climate goals. The aim is to create an efficient, flexible, and stable electricity market supporting the integration of renewable energies and the use of flexibility options. In this context, the structural paradigm shift in the electricity environment requires adaptations in regulatory structures and market mechanisms to foster the integration of renewable energy sources and to harness the benefits of decentralization and bidirectional power flow within a future sustainable power infrastructure.

Given these circumstances, a comprehensive revision of the electricity market design emerges as imperative to support the assimilation of renewable energy sources and, consequently, the introduction of flexibility options into the power system. At the same time, it becomes essential to introduce incentives for stakeholders involved in the electricity sector to contribute to the efficient integration of renewable energy sources and targeted investments in flexibility options.

Beyond the policy implications derived from the key results of this dissertation, the limitations of the work are critically appraised.

5.1 Policy implications

Flexibility options enable the further design of the electricity market, as they are essential for increasing the integration of renewable energy sources, ensuring grid reliability and enabling a more sustainable and efficient energy system. Consequently, electricity market regulation and the corresponding market design must promote upcoming long-term investments in flexibility and, thus, support the integration of flexibility options in the electricity system.

This redesign of the market structure applies to both the holistic and local power systems

and requires a careful assessment of specific needs and framework conditions. Simultaneously, the complex interdependencies and interactions between different flexibility options must be considered. This need for scrutiny pertains to the characteristics of individual flexibility resources and the interplay across different grid levels and market players.

Policy recommendations for political decision-makers may derive from the central results of this dissertation. These results underline the necessity of adapting the future market design in the electricity market. In this context, the creation of a competitive market environment for renewable energies is particularly important. Simultaneously, due to the urgent need for appropriate flexibility investments, not only should targeted incentives for (flexibility) investments be created, but also the risk tolerance of the different market participants should also be comprehensively recognized. With regard to the appropriate design of the market, policymakers must also consider the interdependencies between the different flexibility options.

5.1.1 Market integration of renewable energies

The market design and institutional framework of the electricity power market should be carefully designed to promote the integration of renewables into the German power system. In achieving a sustainable and environmentally friendly energy power supply, the integration of renewable energies into the energy sector is a central objective. However, the growing prominence of renewable energy sources such as wind and solar power also challenges the electricity market design.

To ensure a smooth integration of renewable energies into the power system, certain policy implications are of paramount importance. Policymakers need to establish incentives facilitating the expansion of renewable energy sources, thereby augmenting their contribution to the energy mix. Various instruments like feed-in tariffs, quota systems, or auction methods can be deployed to encourage investments in renewables.

In this context, fostering competitive market dynamics for renewable energies is immensely significant. A powerful instrument for transitioning the electricity sector from fossil fuel dependency to renewable sources lies in the prudent incorporation of social and environmental costs into electricity pricing.

The electricity market design should incorporate the internalized environmental costs associated with fossil fuels, thereby ensuring fair competition between diverse energy sources and achieving precision in the accounting of social costs. In a market-driven economy, prices serve as key signals and control mechanisms, encouraging efficient behavior among market participants and incentivizing investments in innovative business models.

Currently, fossil fuels are subsidized compared to renewable energies, and thus the costs stemming from CO_2-induced air pollution remain inadequately reflected in electricity prices. As the cost of CO_2 emissions from fossil fuels escalates due to the internalization of external social costs, the attractiveness of renewable energy sources within the electricity market will increase. Furthermore, the consistent pricing of CO_2 incentivizes investment in technologies that significantly curtail CO_2 emissions throughout the value chain. Consequently, market-based pricing may be more influential than legislative mandates and prohibitions, given that relative prices between fossil and renewable energy sources stimulate incentives for innovation and investments within the electricity market.

5.1.2 Efficient long-term investments in flexibility

Policy implications to incentivize investments in flexibility options centrally facilitate the integration of renewables, increasing grid stability, and strengthening the overall flexibility of the power system. Given the paramount importance of carefully assembling the optimal mix of flexibility options in modern power systems, policymakers have a key role to play in creating strong incentives to effectively promote the deployment of novel flexibility options.

The results presented in this dissertation underline the crucial importance of carefully designing the market structure to ensure efficient investment incentives for different market participants. Thus, it importantly contributes to the evaluation of effective market architectures providing appropriate long-term investment incentives with regard to the flexibility puzzle in terms of demand-side, supply-side, storage, and grid-side flexibility resources.

With regard to appropriate investment incentives, the risk attitude of private and public investors is also critical to the decision on investments in flexibility options. Given the rapid and extensive transformation of energy systems, individual market participants are confronted with various uncertainties, ranging from the progress of decarbonization to the speed and extent of electrification.

The results of this thesis show that to encourage investments in flexibility options, policymakers must consider the implications between the risk attitudes of public and private investors in combination with different market framework conditions. To create targeted incentives for investments, especially in flexible resources, it is necessary to understand how policymakers can address different risk attitudes. This understanding enables to target investments in flexibility that are consistent with overall climate goals.

5.1.3 Integration of electric vehicles as flexibility resources in the power system

The rapid uptake of EVs holds great potential to transform the power system, as they can serve not only as a means of transport but also as valuable components of a dynamic and flexible energy system. The results underline the potential role of EVs in achieving the required emission reductions. However, the realization of this potential depends on the entire vehicle fleet being operated with almost zero emissions. Demonstrably, policies must be developed to ensure that by 2050 either the entire vehicle fleet is electric or the remaining fuel for combustion engine vehicles is carbon neutral.

Consequently, policies must simultaneously address both dimensions of this challenge: the widespread introduction of EVs and the introduction of low-carbon fuels. Effective policies to address these issues include the implementation of CO_2 fleet targets and EV mandates to address the first dimension, while the introduction of low-carbon fuel standards can address the second.

As EVs represent a relevant flexibility resource, their integration into the local power system needs to be promoted by decision-makers. In particular, the individual charging behavior, its considerable variability and its importance in combination with the resulting flexibility potential must be considered in the future electricity market design. The simultaneous charging of numerous EVs at peak times can lead to grid congestion and, thus, can damage the power system. The promotion of controlled charging behavior that favors off-peak charging can help to distribute the grid load more evenly and reduce congestion. Thus, promoting flexible charging behavior, where EV users adapt their charging times to the availability of cheap electricity or renewable energy, can reduce charging costs and can support the integration of renewable energy.

5.1.4 Interdependencies of different flexibility options

Policymakers must understand the complicated interactions between different flexibility options and solve the resulting flexibility puzzle to find a robust bundle of flexibility solutions for the future. Market regulations can provide incentives to encourage the transfer of flexibility across different grid levels.

The key findings of this work underline the need to consider the complex interaction of different flexibility options in upcoming, cost-intensive (flexibility) investments. While the expansion of transmission lines is subject to certain regulatory framework conditions, investments in storage are shaped by the profit expectations of the firms and the associated (zonal) market constellations. This complex market environment must also be examined, as it can significantly influence the investment decisions of individual market players.

Thus, the interplay of flexibility options between local and higher-level power systems can help to balance energy supply and demand in different regions and ensure the overall stability and reliability of the power grid. The development and implementation of effective flexibility options tailored to the specific needs and characteristics of both local and higher-level power systems require coordination and cooperation between different power system actors, including local utilities, grid operators and, policymakers.

5.2 Critical reflection

Within this thesis, flexibility options were investigated both from an overall system perspective and from a local perspective. Based on the results, policy implications were derived for the design of the future electricity market, taking flexibility options into account. The adaptation of the market design to include flexibility options can be done from both the overall system perspective and the local perspective. However, these are based on certain limitations that need to be critically appraised.

The underlying analyses rely primarily on the available flexibility resources from different perspectives. However, notably, the concrete provision of flexibility and the use of flexibility by the various market players were not considered. The market-, grid-, and system-oriented usage of flexibility in the power system involves various actors with different interests and

objectives. Moreover, in addition to long-term investments in flexibility options, it is imperative to incentivize the efficient short-term use of flexibility options.

Given the liberalization of the electricity market and the coexistence of market-based and regulated processes, it is essential to emphasize that not all stakeholders can readily access and harness the available flexibility resources. Therefore, the legal framework also plays a significant role. Hence, each market actor faces distinct responsibilities and challenges within the electricity system, necessitating tailored adjustments to adequately account for flexibility options. In this context, the analysis could benefit from a more comprehensive examination of how these actors can interact with and leverage flexibility resources in the power system.

Regarding the flexibility of EVs, the dissertation focuses primarily on their role within the local power system. However, it is important to note that EVs can provide flexibility at various power system levels, such as aggregated contribution from an overall system perspective or through sector coupling. Numerous influencing factors determine the integration of EVs into the local power system. Thus, future scientific approaches should extend beyond individual charging behavior. By aligning the short-term use of EVs with grid demand through these incentives, the full potential of EVs as dynamic flexibility resources can be realized, ultimately contributing to a more stable, sustainable, and cost-effective electricity system.

In addition, the link between the overall system perspective and the local perspective is crucial, as local measures can impact the overall power system. For example, an increased adoption of EVs in a city can influence regional electricity demand and the need for broader grid expansion. Consequently, coordination and communication between local authorities, utilities, and higher-level regulators are paramount. Therefore, future analyses should prominently address the interaction between different levels of the power system.

In sum, it is essential that the use of flexibility options be tailored to the unique characteristics and needs of the grid. Factors such as grid size, geographical location, and the extent of renewable energy penetration must all be considered. Moreover, the ideal mix of flexibility options may change over time, as technologies evolve and as grid demands change. This fluidity underlines the significance of adaptability and continuous investment in flexible resources to ensure a stable and reliable electricity supply.

6 Summary and outlook

The fundamental paradigm shift in German energy policy means a transition from conventional fossil fuel-based power generation to the use of renewable energy sources. Hence, the paradigm shift in the electricity sector, accompanied by an increasing share of fluctuating renewable energies in electricity generation and a decreasing contribution from (flexible) conventional generators, poses new challenges to future power systems and amplifies a growing need for flexibility.

To successfully advance the energy transition, it is essential to establish economic and political framework conditions to promote the further expansion of renewable energies and their integration into the electricity grid. In this context, a basic prerequisite for the effective use of an increasing share of fluctuating renewable energies (e.g., wind, solar) is the integration of flexibility options into the power system to balance temporal and spatial fluctuations in energy supply and demand. In line with the transformation of the energy sector, decision-makers and stakeholders are faced with the task of dealing with the future design of a sustainable electricity market incorporating flexibility options.

This dissertation investigated different flexibility options from both a holistic power system perspective and from the perspective of a local power system. From the conceptual dimension of power system flexibility to different definitions and measures of flexibility options in terms of dimensions such as the temporal, the spatial, and the operational, the theoretical background showed the associated complexities and the central importance of flexibility resources in the future power system. An overview of flexibility resources related to the holistic and local power system perspectives was given.

From a holistic power system perspective, supply-side and demand-side flexibility options, along with the role of flexibility through the use of storage and the expansion of the grid infrastructure, were analyzed. To represent the electricity market and account for the complex interactions between regulated entities and competitive processes, this thesis employed

multi-level mathematical optimization models combined with approaches from game theory. Game-theoretically, this constellation corresponds to a multistage Stackelberg game in which the mutual reactions of individual market players are analyzed. In this context, market participants act interdependently and respond to the decisions of other market players. Each market player optimizes their own actions while considering the decisions of the other players.

This dissertation showed that, in addition to the interactions of different flexibility options, the individual risk attitude of the central stakeholders, in particular, must be factored into the design of the future electricity market in order to create targeted market-based incentives for (flexibility) investments. The research revealed interdependencies between investments in electricity storage by private firms and the decisions of the state-regulated grid operator in grid expansion. It also demonstrated that the varying risk attitudes of private and public investors can lead to different investments in flexibility options.

Examining the local power system, EVs were primarily considered flexibility resources. The research underlined the importance of EVs for emissions reduction and conducted a comprehensive analysis of potential factors influencing an efficient integration of EVs into the local power system. A central conclusion was that EVs represent a significant flexible resource in the local power system, and accounting for individual charging behavior in defining future regulatory conditions can support a fast and successful integration into the power system.

In relation to the research questions posed within the framework of the dissertation, the following findings can be summarized. To alleviate the flexibility gap caused by the growing share of renewable energies, it is vital to consider both a holistic power system perspective and a local power system perspective. On a holistic level, a comprehensive approach involves diversifying flexibility options, including supply-side, demand-side, storage, and grid-side resources. These options should be strategically integrated to address temporal and spatial fluctuations in renewable energy supply and ensure grid stability. From a local power system perspective, integrating EVs as flexibility resources plays a significant role. Factors like individual charging behavior, bidirectional charging capabilities, and the development of supportive regulatory frameworks are key considerations.

To encourage the use of the optimal combination of flexibility options, particularly from a holistic system perspective, various measures can be adopted. In this context, such encouragement can stem from the targeted incentives for investments in flexibility options, considering the interactions between different flexibility options and the risk behavior of stakeholders. From a local power system perspective, it is crucial to consider individual mobility and charging behavior when considering the integration of EVs as flexibility resources.

With regard to the role of flexibility options in future electricity market design, a well-structured regulatory framework can help to ensure the optimal use of flexibility resources. First, adapting the electricity market design to encourage and facilitate the use of flexibility options. In addition, market-based incentives to encourage investment in flexibility resources must be formulated, recognizing that flexibility options work at both holistic and local levels and ensuring their coordinated deployment. At the same time, the interactions between flexibility options and stakeholder behavior must also be taken into account.

In summary, bridging the flexibility gap created by a growing share of renewable energies is a crucial challenge for the future power system to confront. Therefore, the regulatory framework for the electricity market should be designed to encourage the use of flexibility options. By restructuring electricity markets and the associated electricity market design, policymakers can ensure that flexibility resources are used optimally, leading to a more reliable, sustainable, and responsive power system at both the system-wide and local level. Integrating flexibility options requires the simultaneous evolution of the existing electricity market framework that not only incentivizes investments in flexibility resources, but also formulates strategies for their strategic deployment across all levels of the power system.

Hence, this dissertation demonstrated the importance of flexibility options for the transformation of the electricity sector and their essential role in the successful implementation of the energy transition in Germany. The future consideration of flexibility options in sustainable electricity market design will be crucial. However, the successful transformation of the power sector is a complex and multidimensional process requiring the cooperation of all relevant actors in the electricity market.

References

Agora Energiewende, Prognos, and Consentec, eds. (2022). *Klimaneutrales Stromsystem 2035. Wie der deutsche Stromsektor bis zum Jahr 2035 klimaneutral werden kann.*

Akrami, A., M. Doostizadeh, and F. Aminifar (2019). "Power system flexibility: an overview of emergence to evolution". In: *Journal of Modern Power Systems and Clean Energy* 7.5, pp. 987–1007. ISSN: 2196-5625. DOI: 10.1007/s40565-019-0527-4.

Alexopoulos, D. K., A. G. Anastasiadis, G. A. Vokas, S. D. Kaminaris, and C. S. Psomopoulos (2021). "A review of flexibility options for high RES penetration in power systems — Focusing the Greek case". In: *Energy Reports* 7, pp. 33–50. ISSN: 23524847. DOI: 10.1016/j.egyr.2021.09.050.

Alizadeh, M. I., M. P. Moghaddam, N. Amjady, P. Siano, and M. K. Sheikh-El-Eslami (2016). "Flexibility in future power systems with high renewable penetration: A review". In: *Renewable and Sustainable Energy Reviews* 57, pp. 1186–1193.

Ambrosius, M., J. Egerer, V. Grimm, and A. van der Weijde (2022). "Risk aversion in multilevel electricity market models with different congestion pricing regimes". In: *Energy Economics* 105.

Ambrosius, M., V. Grimm, T. Kleinert, F. Liers, M. Schmidt, and G. Zöttl (2020). "Endogenous price zones and investment incentives in electricity markets: An application of multilevel optimization with graph partiioning". In: *Energy Economics* 92.

Arboleya, P., M. A. Kippke, and S. Kerscher (2022). "Flexibility management in low-voltage distribution grid as a tool in the process of decarbonization through electrification". In: *Energy Reports* 8, pp. 248–256. ISSN: 23524847.

Babatunde, O. M., J. L. Munda, and Y. Hamam (2020). "Power system flexibility: A review". In: *Energy Reports* 6, pp. 101–106. ISSN: 23524847. DOI: 10.1016/j.egyr.2019.11.048.

Badanjak, D. and H. Pandžić (2021). "Distribution-Level Flexibility Markets—A Review of Trends, Research Projects, Key Stakeholders and Open Questions". In: *Energies* 14.20, p. 6622. DOI: 10.3390/en14206622.

Baringo, L. and A. J. Conejo (2012). “Transmission and Wind Power Investment”. In: *IEEE Transactions on Power Systems* 27.2, pp. 885–893. ISSN: 0885-8950. DOI: 10.1109/TPWRS.2011.2170441.

Bhuiyan, R., J. Weissflog, M. Schoepf, and G. Fridgen (2022). “Indicators for assessing the necessity of power system flexibility: a systematic review and literature meta-analysis”. In: *18th International Conference*, pp. 1–7. DOI: 10.1109/EEM54602.2022.9921149.

Brunner, C. (2014). “Berücksichtigung von Flexibilität im zukünftigen Strommarktdesign”. In: *Energiewirtschaftliche Tagesfragen* 64.4.

Bucksteeg, M., K. Trepper, and C. Weber (2015). “Impacts of RES-generation and demand pattern on net transfer capacity: Implications for effectiveness of market splitting in Germany”. In: *Generation Transmission and Distribution* 9.9, pp. 1510–1518.

Bundesministerium für Wirtschaft und Klimaschutz, ed. (2023). *Wohlstand klimaneutral erneuern: Werkstattbericht des Bundesministerium für Wirtschaft und Klimaschutz (BMWK)*.

Bundesministerium für Wirtschaft und Klimaschutz (BMWK) (2023). *Referentenentwurf des Bundesministeriums für Wirtschaft und Klimaschutz*. URL: https://www.bmwk.de/Redaktion/DE/Downloads/klimaschutz/entwurf-eines-zweiten-gesetzes-zur-aenderung-des-bundes-klimaschutzgesetzes.pdf?__blob=publicationFile&v=6 (Retrieved 08/01/2023).

Bundesnetzagentur - SMARD, ed. (2023). *SMARD - Strommarktdaten*. URL: www.smard.de (Retrieved 08/01/2023).

Chao, H.-P. and S. Peck (1996). “A market mechanism for electric power transmission”. In: *Journal of Regulatory Economics* 10.1, pp. 25–59.

Chatzivasileiadis, S., P. Aristidou, I. Dassios, T. Dragicevic, D. Gebbran, F. Milano, C. Rahmann, and D. Ramasubramanian (2023). “Micro-flexibility: Challenges for power system modeling and control”. In: *Electric Power Systems Research* 216, p. 109002. ISSN: 03787796. DOI: 10.1016/j.epsr.2022.109002.

Colson, B., P. Marcotte, and G. Savard (2007). “An overview of bilevel optimization”. In: *Annals of Operations Research* 153.1, pp. 235–256.

Corinaldesi, C., A. Fleischhacker, L. Lang, J. Radl, D. Schwabeneder, and G. Lettner (2019). “European Case Studies for Impact of Market-driven Flexibility Management in Distribution Systems”. In: *European Case Study for Impact of Market-driven Flexibility Management in Distribution Systems*. IEEE, pp. 1–6. ISBN: 978-1-5386-8099-5. DOI: 10.1109/SmartGridComm.2019.8909689.

Cox, B., C. L. Mutel, C. Bauer, A. Mendoza Beltran, and D. P. van Vuuren (2018). "Uncertain environmental footprint of current and future battery electric vehicles". In: *Environmental Science & Technology* 52.8, pp. 4989–4995.

Cruz, M. R., D. Z. Fitiwi, S. F. Santos, and J. P. Catalão (2018). "A comprehensive survey of flexibility options for supporting the low-carbon energy future". In: *Renewable and Sustainable Energy Reviews* 97, pp. 338–353. ISSN: 13640321. DOI: 10.1016/j.rser.2018.08.028.

Dardas, A. Z., A. Williams, and D. Scott (2020). "Carer-employees' travel behaviour: Assisted-transport in time and space". In: *Journal Transp. Geogr.* 82.

Degefa, M. Z., I. B. Sperstad, and H. Sæle (2021). "Comprehensive classifications and characterizations of power system flexibility resources". In: *Electric Power Systems Research* 194. ISSN: 03787796. DOI: 10.1016/j.epsr.2021.107022.

Del Granado, P. C., J. Rajasekharan, S. V. Pandiyan, A. Tomasgard, G. Kara, H. Farahmand, and S. Jaehnert (2023). "Flexibility Characterization, Aggregation, and Market Design Trends with a High Share of Renewables: a Review". In: *Current Sustainable/Renewable Energy Reports* 10.1, pp. 12–21. DOI: 10.1007/s40518-022-00205-y.

Dempe, S. (2002). *Foundations of bilevel programming*. Ed. by Springer.

Deng, X., T. Lv, X. Hou, J. Xu, D. Pi, F. Liu, and N. Li (2022). "Regional disparity of flexibility options for integrating variable renewable energy". In: *Renewable Energy* 192, pp. 641–654. ISSN: 09601481. DOI: 10.1016/j.renene.2022.04.135.

Dijk, J. and B. Willems (2011). "The effect of counter-trading on competition in electricity markets". In: *Energy Policy* 39.3, pp. 1764–1773. ISSN: 03014215.

Eid, C., P. Codani, Y. Perez, J. Reneses, and R. Hakvoort (2016). "Managing electric flexibility from Distributed Energy Resources: A review of incentives for market design". In: *Renewable and Sustainable Energy Reviews* 64, pp. 237–247. ISSN: 13640321. DOI: 10.1016/j.rser.2016.06.008.

Ela, E., M. Milligan, A. Bloom, A. Botterud, A. Townsend, T. Levin, and B. A. Frew (2016). "Wholesale electricity market design with increasing levels of renewable generation: Incentivizing flexibility in system operations". In: *The Electricity Journal* 29.4, pp. 51–60. ISSN: 10406190. DOI: 10.1016/j.tej.2016.05.001.

Emmanuel, M., K. Doubleday, B. Cakir, M. Markovic, and Hodge B. (2020). "A review of power system planning and operational models for flexibility assessment in high solar energy penetration scenarios". In: *Solar Energy*.

Eurelectric, ed. (2014). *Flexibility and Aggregation: Requirements for their interaction in the market*. Brussels.

Fan, H., H. Cheng, and L. Yao (2009). "A bi-level programming model for multistage transmission network xpansion planning in competitive electricity market". In: *Power and energy engineering conference*. Ed. by APPEEC 2009. Asia-Pacific.

Fugiglando, U., E. Massaro, P. Santi, S. Milardo, K. Abida, R. Stahlmann, F. Netter, and C. Ratti (2019). "Driving behavior analysis through CAN bus data in an uncontrolled environment". In: *IEEE Trans. Intell. Transp. Syst.* 20, pp. 737–748.

Gil, H. A., E. L. Da Silva, and F. D. Galiana (2002). "Modeling competition in transmission expansion". In: *IEEE Transactions on Power Systems* 17.4, pp. 1043–1049.

Gómez Vilchez, J. J. and P. Jochem (2020). "Powertrain technologies and their impact on greenhouse gas emissions in key car markets". In: *Transportation Research Part D: Transport and Environment* 80, p. 102214.

Grimm, V., B. Rückel, C. Sölch, and G. Zöttl (2019). "Regionally differentiated network fees to affect incentives for generation investment". In: *Energy* 177, pp. 487–502. ISSN: 03605442.

Grimm, V., A. Martin, M. Schmidt, M. Weibelzahl, and G. Zöttl (2016a). "Transmission and generation investment in electricity markets: The effects of market splitting and network fee regimes". In: *European Journal of Operational Research* 254.2, pp. 493–509.

Grimm, V., A. Martin, M. Weibelzahl, and G. Zöttl (2016b). "On the long run effects of market splitting: Why more price zones might decrease welfare". In: *Energy Policy* 94, pp. 453–467.

Grimm, V., B. Rückel, C. Sölch, and G. Zöttl (2021). "The impact of market design on transmission and generation investment in electricity markets". In: *Energy Economics* 93, p. 104934.

Hall, M. and A. Geissler (2021). "Comparison of Flexibility Factors and Introduction of A Flexibility Classification Using Advanced Heat Pump Control". In: *Energies* 14.24, p. 8391. DOI: 10.3390/en14248391.

Heider, A., R. Reibsch, P. Blechinger, A. Linke, and G. Hug (2021). "Flexibility options and their representation in open energy modelling tools". In: *Energy Strategy Reviews* 38, p. 100737. ISSN: 2211467X. DOI: 10.1016/j.esr.2021.100737.

Helmus, J. R., M. H. Lees, and R. van den Hoed (2020). "A data driven typology of electric vehicle user types and charging sessions". In: *Transportation Research Part C: Emerging Technologies* 115, p. 102637. ISSN: 0968090X. DOI: 10.1016/j.trc.2020.102637.

International Energy Agency, ed. (2014). *The power of transformation: Wind, sun and the economics of flexible power systems*. Paris, France.

International Renewable Energy Agency, ed. (2018). *Power system flexibility for the energy transition: Part 1: Overview for policy makers*. Abu Dhabi.

International Smart Grid Action Network, ed. (2019). *Power Transmission & Distribution Systems: Flexibility need in the future power system*.

Jenabi, M., S. Ghomi, and Y. Smeers (2013). "Bi-level approaches for coordination of generation and tranmission expansion planning within a market environment". In: *IEEE Transactions on Power Systems* 28.3, pp. 2639–2650.

Jeroslow, R. G. (1985). "The polynomial hierarchy and a simple model for competitive analysis". In: *Mathematical Programming* 32.2, pp. 146–164. ISSN: 0025-5610. DOI: 10.1007/BF01586088.

Kara, G., A. Tomasgard, and H. Farahmand (2022). "Characterizing flexibility in power markets and systems". In: *Utilities Policy* 75, p. 101349. ISSN: 09571787. DOI: 10.1016/j.jup.2022.101349.

Kaushik, E., V. Prakash, O. P. Mahela, B. Khan, A. El-Shahat, and A. Y. Abdelaziz (2022). "Comprehensive Overview of Power System Flexibility during the Scenario of High Penetration of Renewable Energy in Utility Grid". In: *Energies* 15.2, p. 516. DOI: 10.3390/en15020516.

Kim, H. C., T. J. Wallington, R. Arsenault, C. Bae, S. Ahn, and J. Lee (2016). "Cradle-to-gate emissions from a commercial electric vehicle Li-ion battery: a comparative analysis". In: *Environmental science & technology* 50.14, pp. 7715–7722.

Knezovic, K., M. Marinelli, P. Codani, and Y. Perez (2015). "Distribution grid services and flexibility provision by electric vehicles: A review of options". In: *50th International Universities Power Engineering Conference (UPEC)*. IEEE, pp. 1–6. ISBN: 978-1-4673-9682-0. DOI: 10.1109/UPEC.2015.7339931.

Koch, M., M. Vogel, C. Heinemann, T. Hesse, D. Bauknecht, M. Wingenbach, E. Tröster, D. Masendorf, S. Hempel, L. Hülsmann, P.-P. Schierhorn, M. Kahles, A. Halbig, and M. Wimmer (2021). *Pilotprojekt Dezentralisierung: Stärkere Dezentralisierung des bundesdetuschen Strom-Wärme-Systems: Rechtliche und organisatoriche Rahmenbedingungen sowie infrastrukturelle Folgen*. Ed. by Öko-Institut e.V.

Lannoye, E., D. Flynn, and M. O'Malley (2012a). "Power system flexibility assessment — State of the art". In: *IEEE Power and Energy*, pp. 1–6. DOI: 10.1109/PESGM.2012.6345375.

Lannoye, E., D. Flynn, and M. O'Malley (2012b). "Evaluation of Power System Flexibility". In: *IEEE Transactions on Power Systems* 27.2, pp. 922–931. ISSN: 0885-8950. DOI: 10.1109/TPWRS.2011.2177280.

Li, X. and M. Mulder (2021). "Value of power-to-gas as a flexibility option in integrated electricity and hydrogen markets". In: *Applied Energy* 304, p. 117863. ISSN: 03062619. DOI: 10.1016/j.apenergy.2021.117863.

Lloyd, S. (1982). "Least squares quantization in PCM". In: *IEEE Transactions on Information Theory* 28.2, pp. 129–137.

Lund, P. D., J. Lindgren, J. Mikkola, and J. Salpakari (2015). "Review of energy system flexibility measures to enable high levels of variable renewable electricity". In: *Renewable and Sustainable Energy Reviews* 45, pp. 785–807. ISSN: 13640321. DOI: 10.1016/j.rser.2015.01.057.

Ma, J., V. Silva, R. Belhomme, D. S. Kirschen, and L. F. Ochoa (2013). "Evaluating and planning flexibility in sustainable power systems". In: *2013 IEEE Power & Energy Society General Meeting*. IEEE, pp. 1–11. ISBN: 978-1-4799-1303-9. DOI: 10.1109/PESMG.2013.6672221.

Minniti, S., N. Haque, P. Nguyen, and G. Pemen (2018). "Local Markets for Flexibility Trading: Key Stages and Enablers". In: *Energies* 11.11, p. 3074. DOI: 10.3390/en11113074.

Mohandes, B., M. S. E. Moursi, N. Hatziargyriou, and S. E. Khatib (2019). "A Review of Power System Flexibility With High Penetration of Renewables". In: *IEEE Transactions on Power Systems* 34.4, pp. 3140–3155. ISSN: 0885-8950. DOI: 10.1109/TPWRS.2019.2897727.

Neuhoff, K., J. Barquin, J. W. Bialek, R. Boyd, C. J. Dent, and F. Echavarren (2013). "Renewable electric energy integration: Quantifying the value of design of markets for international transmission capacity". In: *Energy Economics* 40, pp. 760–772.

Noussan, M. and F. Neirotti (2020). "Cross-Country Comparison of Hourly Electricity Mixes for EV Charging Profiles". In: *Energies* 13.10, p. 2527. DOI: 10.3390/en13102527.

Papaefthymiou, G. and K. Dragoon (2016). "Towards 100% renewable energy systems: Uncapping power system flexibility". In: *Energy Policy* 92, pp. 69–82. ISSN: 03014215. DOI: 10.1016/j.enpol.2016.01.025.

Papaefthymiou, G., K. Grave, and K. Dragoon (2014). "Flexibility options in electricity systems". In: *Project number: POWDE14426, Ecofys*.

Pozo, D., E. Sauma, and J. Contreras (2017). “Basic theoretical foundations and insights on bilevel models and their applications to power systems”. In: *Annals of Operations Research* 254.1-2, pp. 303–334.

Prognos, Öko-Institut, Wuppertal-Institut, ed. (2021). *Klimaneutrales Deutschland 2045: Wie Deutschland seine Klimaziele schon vor 2050 erreich kann: Zusammenfassung im Auftrag von Stiftung Klimaneutralität, Agora Energiewende und Agora Verkehrswende*.

Saele, H., A. Morch, and M. Z. Degefa (2020). “Assessment of flexibility in different ancillary services for the power system”. In: *17th International Conference on the European Energy Market (EEM)*. DOI: 10.1109/EEM49802.2020. URL: https://ieeexplore.ieee.org/servlet/opac?punumber=9217568.

Salman, U. T., S. Shafiq, F. S. Al-Ismail, and M. Khalid (2022). “A Review of Improvements in Power System Flexibility: Implementation, Operation and Economics”. In: *Electronics* 11.4, p. 581. DOI: 10.3390/electronics11040581.

Santos, S. F., M. Gough, D. Z. Fitiwi, A. F. P. Silva, M. Shafie-Khah, and J. P. S. Catalao (2022). “Influence of Battery Energy Storage Systems on Transmission Grid Operation With a Significant Share of Variable Renewable Energy Sources”. In: *IEEE Systems Journal* 16.1, pp. 1508–1519. ISSN: 1932-8184. DOI: 10.1109/JSYST.2021.3055118.

Sariddichainunta, P. and M. Inuiguchi (2017). “Global optimality test for maximin solution of bilevel linear programming with ambiguous lower-level objective function”. In: *Annals of Operations Research* 256.2, pp. 285–304.

Sauma, E. E. and S. S. Oren (2006). “Proactive planning and valuation of transmission investments in restructured electricity markets”. In: *Journal of Regulatory Economics* 30.3, pp. 261–290. DOI: 10.1007/s11149-006-9012-x.

Schwarz, G. (1978). “Estimating the dimension of a model”. In: *The Annals of Statistics*, pp. 461–464.

Sinsel, S. R., R. L. Riemke, and V. H. Hoffmann (2020). “Challenges and solution technologies for the integration of variable renewable energy sources—a review”. In: *renewable energy* 145, pp. 2271–2285. DOI: 10.3929/ETHZ-B-000373407.

Sioshansi, R. (2010). “Welfare impacts of electricity storage and the implications of ownership structure”. In: *The Energy Journal*, pp. 173–198.

Sioshansi, R. (2014). “When energy storage reduces social welfare”. In: *Energy Economics* 41, pp. 106–116.

Sperstad, I. B., M. Z. Degefa, and G. Kjølle (2020). “The impact of flexible resources in distribution systems on the security of electricity supply: A literature review”. In: *Electric Power Systems Research* 188, p. 106532. ISSN: 03787796. DOI: 10.1016/j.epsr.2020.106532.

Steinke, F., P. Wolfrum, and C. Hoffmann (2013). “Grid vs. storage in a 100% renewable europe”. In: *Renewable Energy* 50, pp. 826–832. ISSN: 09601481.

Syakur, M. A., B. K. Khotimah, E. Rochman, and B. D. Satoto (2018). “Integration k-means clustering method and elbow method for identification of the best customer profile cluster”. In: *IOP Conf. Series Mater. Sci. Eng.* 336.

Umweltbundesamt, ed. (2023). *National Greenhouse Gas Inventory 1990 to 2021*. URL: https://www.umweltbundesamt.de/en/data/environmental-indicators/indicator-greenhouse-gas-emissions#at-a-glance (Retrieved 08/01/2023).

Villar, J., R. Bessa, and M. Matos (2018). “Flexibility products and markets: Literature review”. In: *Electric Power Systems Research* 154, pp. 329–340. ISSN: 03787796.

Weibelzahl, M. and A. Märtz (2020). “Optimal storage and transmission investments in a bilevel electricity market model”. In: *Annals of Operations Research* 287, pp. 911–940. DOI: 10.1007/s10479-018-2815-1.

Zambrano, C. and Y. Olaya (2017). “An agent-based simulation approach to congestion management for the Colombian electricity market”. In: *Annals of Operations Research* 258, pp. 217–236.

Zare, M. H., J. S. Borreroo, B. Zeng, and O. A. Prokopyev (2017). “A note on linearized reformulations for a class of bilevel linear integer problems”. In: *Annals of Operations Research*, pp. 1–19.

Zeng, X., G. Chen, S. Luo, Y. Teng, Z. Zhang, and T. Zhu (2022). “Renewable transition in the power and transport sectors under the goal of carbon-neutral in Sichuan, China”. In: *Energy Reports* 8, pp. 738–748. ISSN: 23524847. DOI: 10.1016/j.egyr.2022.02.213.

Zhao, J., T. Zheng, and E. Litvinov (2016). “A Unified Framework for Defining and Measuring Flexibility in Power System”. In: *IEEE Transactions on Power Systems* 31.1, pp. 339–347. ISSN: 0885-8950. DOI: 10.1109/TPWRS.2015.2390038.

Zöphel, C. (2022). “Flexibility options in energy systems: The influence of Wind - PV rations and sector coupling on optimal combinations of flexible technologies in a European electricity system”. PhD thesis. Dresden.

Zöphel, C., S. Schreiber, T. Müller, and D. Möst (2018). “Which Flexibility Options Facilitate the Integration of Intermittent Renewable Energy Sources in Electricity Systems?” In: *Current Sustainable/Renewable Energy Reports* 5.1, pp. 37–44. DOI: 10.1007/s40518-018-0092-x.

Part II

Research papers

A Optimal storage and transmission investments in a bilevel electricity market model

Martin Weibelzahl[a,b], Alexandra Märtz[c]

[a] FIM Research Center, Wittelsbacherring 10, 95444 Bayreuth, Germany.

[b] University of Bayreuth, Wittelsbacherring 10, 95444 Bayreuth, Germany.

[c] Karlsruhe Institute of Technology (KIT), Institute for Industrial Production (IIP), Chair of Energy Economics, Hertzstraße 16, 76187 Karlsruhe, Germany.

Published in:
Annals of Operations Research (2020), 287, 911-940, doi:10.1007/s10479-018-2815-1.

Abstract

This paper analyzes the interplay of transmission and storage investments in a multistage game that we translate into a bilevel market model. In particular, on the first level we assume that a transmission system operator chooses optimal line investments and a cor- responding optimal network fee. On the second level we model competitive firms that trade energy on a zonal market with limited transmission capacities and decide on their optimal storage facility investments. To the best of our knowledge, we are the first to analyze interdependent transmission and storage facility investments in a zonal market environment that accounts for the described hierarchical decision structure. As a first best benchmark, we also present an integrated, single-level problem that may be interpreted as a long-run nodal pricing model. Our numerical results show that adequate storage facility investments of firms may in general have the potential to reduce the amount of line investments of the transmission system operator. However, our bilevel zonal pricing model may yield inefficient investments in storages, which may be accompanied by suboptimal network facility extensions as compared to the nodal pricing benchmark. In this context, the chosen zonal configuration of the network will highly influence the equilibrium investment outcomes including the size and location of the newly invested facilities. As zonal pricing is used for instance in Australia or Europe, our models may be seen as valuable tools for evaluating different regulatory policy options in the context of long-run investments in storage and network facilities.

A.1 Introduction

Modern electricity markets are typically characterized by a spatial or regional divergence of energy supply and demand. One example is the German electricity market with substantial wind production in the north and a high consumption in the south; see Bucksteeg et al. (2015). Given transmission capacity shortages, as a direct result of the regional divergence of demand and supply, corresponding network congestion arises in many situations, where power flows between nodes are restricted by binding technical constraints; see also Dijk and Willems (2011) or Neuhoff et al. (2013). In this context, long-run transmission investments and the implementation of different short-run congestion management regimes are frequently discussed as possible solutions to network congestion; see for instance Jenabi et al. (2013), Grimm et al. (2016a), Grimm et al. (2016b), and Zambrano and Olaya (2017). Besides the described regional divergence of supply and demand, intermittent renewable energy

supply additionally yields a temporal divergence of the produced and consumed energy. In general, such an intermittent renewable energy production calls for additional transmission capacities in order to being able to accommodate arising peak flows. Obviously, both the regional and temporal dimension are highly interdependent. On the one side, storage facilities that typically smoothen inter-temporal demand spikes may simultaneously have the potential to lower the necessity for large network investments. On the other side, an extended inter-regional network may simultaneously contribute to a better adjustment of the described inter-temporal divergence of demand and intermittent supply; see also Steinke et al. (2013).

To the best of our knowledge, we are the first to analyze such interdependencies of storage and network investments under different congestion management regimes in a multi-stage game that we translate into a bilevel market model. As we will demonstrate, in such a framework the chosen congestion management mechanism will highly influence long-run investments in both transmission lines and storage facilities.

In particular, this paper assumes a transmission system operator (TSO) that decides on optimal line investments as well as on a corresponding network fee on the first level. The TSO anticipates market outcomes of the second level, where competitive firms trade energy and invest in storage facilities given the realized network extensions of the TSO. Energy trading on the second level directly accounts for possibly scare network capacities that may result in a regionally differentiated price structure. Within our model, we also study the effects of different zonal designs. In this context we will evaluate both absolute investment levels and the locations of the corresponding facility investments. Given that zonal pricing is applied in European countries as well as in Australia (see for instance (Bjørndal et al., 2003; Glachant and Pignon, 2005; Dijk and Willems, 2011)), our analyses may directly contribute to the current policy discussion on the design of efficient market structures that account for adequate long-run investment incentives in both storage facilities and network lines. In addition, in times of growing importance of storage facilities, the proposed models may also be seen as tools for a meaningful evaluation of the need for huge network extension plans that typically involve billions of euros like in Germany; for more details see German Transmission System Operators (2017).

As our numerical results show, both under nodal and zonal pricing storage investments may in general have the potential to reduce network extensions as compared to the no-storage

case. However, our bilevel, zonal-pricing market may yield inefficient storage facility investments that may be accompanied by suboptimal line investments as compared to a nodal pricing model. Moreover, invested storage facilities may affect inter-regional price and demand structures in a way that requires a reconfiguration of optimal zonal boundaries, i.e., in the case of storage facilities the welfare-maximizing zone configuration may change as compared to the no-storage case.

Our work directly contributes to various strands of the energy market literature. In particular, we elaborate on different congestion management regimes. In the context of congestion management, nodal prices are known to yield a first-best outcome, as they simultaneously reflect all relevant economic and technical restrictions between the different nodes of the network; see Bohn et al. (1984), Hogan (1992), and Chao and Peck (1996). In contrast, zonal pricing assumes identical prices within zonal boundaries, which gives a simplified price structure; see Bjørndal et al. (2014). Even though, zonal pricing may in general be accompanied by a welfare loss as compared to a system of nodal prices, zonal pricing is sometimes seen as being more attractive from an administrative and political point of view. For this reason, in the past various studies have focused on properties of zonal pricing systems that ensure a comparatively small welfare loss. Such properties relate for instance to the number of price zones and their respective boundaries; see Bjørndal and Jørnsten (2001), Ehrenmann and Smeers (2005), and Oggioni and Smeers (2013).

In addition, with this paper we also contribute to the increasing literature on transmission investments. Traditionally, reference investment solutions were derived for integrated, single-level optimization problems as in Gallego et al. (1998), Hirst and Kirby (2001), and Alguacil et al. (2003). In recent years transmission investments were also analyzed in multistage games and corresponding multilevel optimization problems; see for instance Sauma and Oren (2006), Fan et al. (2009), Garcés et al. (2009), Baringo and Conejo (2012), and Jenabi et al. (2013). As pointed out by Grimm et al. (2016a), in such games the market environment and the chosen congestion management regime will highly influence optimal transmission expansions of the TSO. In particular, hierarchical market models may yield suboptimal line investments as compared to an integrated network expansion plan.

Finally, we link the two above stands of congestion management and transmission investment literature to existing studies on price and welfare effects of storage facilities. Most of the latter studies including Sioshansi et al. (2009), Sioshansi (2010), Gast et al. (2013), and

Sioshansi (2014) mainly abstracted from transmission constraints and the network management regime. Only recently, Weibelzahl and Märtz (2018) study storage facilities and their effects in a zonal electricity market. However, the authors only consider the short-run perspective, where both the transmission network and storage facilities are given. It is the aim of the present paper to analyze the interplay of transmission and storage facility investments in a multilevel market environment from a long-run perspective.

This paper is organized as follows. Our model framework is introduced in Sect. A.2. Then, Sects. A.3 and A.4 present our investment benchmark models and the bilevel zonal pricing model with storage, respectively. The main solution strategy for our multistage game and for the corresponding bilevel optimization model is then discussed in Sect. A.5. Numerical results of our long-run investment analysis regarding storage facility investments and network extensions are presented in Sect. A.6. Finally, Sect. A.7 concludes and highlights main policy implications.

A.2 Notation and economic quantities

This section introduces the main model framework that is used in our paper. All sets, parameters, and variables are summarized in Tables A.4, A.5, and A.6 in the Appendix.

A.2.1 Electricity network and time horizon

In this paper we assume a finite time-period set T.[1] In addition, we are given a connected and directed graph $\mathcal{G} = (N, L)$, which is defined on a set of network nodes N and a set of transmission lines L. Each transmission line $l \in L$ is characterized by different technical properties such as the maximal transmission capacity $\overline{f}_l$ or the susceptance B_l. Corresponding lossless DC power flows on a line $l \in L$ will be denoted by $f_{l,t}$ for any given time period $t \in T$. In addition, we consider the case where different candidate transmission lines may be built by the TSO. Therefore, we assume a subset of lines L^{inv} that can be invested in.

[1] In contrast to simple two-period models [see, e.g., Sioshansi (2010) or Sioshansi (2014)] our model is able to capture more than two time periods. Ultimately, this may help to increase the accuracy of the proposed storage model.

In order to being able to model the building of new (lumpy) lines and not only a simple increase in the thermal capacity of existing lines, we let the binary variable $w_l \in \{0,1\}$ describe whether candidate line l is built by the TSO. Line investment cost are denoted by i_l.

Additionally, in this paper we assume that the node set N is partitioned into r connected price zones. We consider the case where a fixed zonal configuration $Z = \{Z_1, \ldots, Z_r\}$ is exante specified:

$$\varnothing \notin Z, \tag{A.1}$$

$$\bigcup_{i \in \{1,\ldots,r\}} Z_i = N, \tag{A.2}$$

$$Z_i \in Z, Z_j \in Z \text{ with } i \neq j \Rightarrow Z_i \cap Z_j = \varnothing. \tag{A.3}$$

Note that in its two limit cases, the above definition comprises both a single zone as well as a nodal pricing configuration, i.e., $r = 1$ and $r = |N|$.

A.2.2 Electricity demand

We further assume a set of demand nodes $D \subset N$ where consumers are located at. We denote by $x_{d,t}$ the endogenous consumption variable of d in period t. To model price-sensitive demand behaviour that is node- and time-dependent, for each demand node $d \in D$ and time period $t \in T$ we are given a continuous and strictly decreasing inverse demand function $p_{d,t}(x_{d,t})$ that depend on the respective consumption quantity $x_{d,t}$, i.e., plugging a given consumption quantity $x_{d,t}$ into the inverse demand function $p_{d,t}(x_{d,t})$ gives the node-specific price in the considered time period; see for instance the vaste literature using elastic demand including Chao and Peck (1996), Bjørndal and Jørnsten (2001), Bjørndal et al. (2003), Ehrenmann and Smeers (2005), and Bjørndal and Jørnsten (2007). Finally, we refer to

$$\sum_{t \in T} \sum_{d \in D} \int_0^{x_{d,t}} p_{d,t}(u) \mathrm{d}u$$

as the gross consumer surplus that is aggregated over all demand nodes and time periods. This gross consumer surplus measures the sum of all monetary consumer benefits.

A.2.3 Electricity generation

Throughout this paper, we will denote by G the set of all ex-ante given generation facilities. $G_n \subset G$ describes the generators, which are located at a node n. In addition, we denote production of a generator g in a time period t by $y_{g,t}$. Production is further described by a continuous and strictly increasing marginal cost function $V_{g,t}(y_{g,t})$ that gives the respective variable production costs of a generator implied by a production level $y_{g,t}$, i.e., variable production costs $V_{g,t}$ depend on the argument $y_{g,t}$; see also Chao and Peck (1998), Bjørndal and Jørnsten (2001), Ehrenmann and Smeers (2005), and Oggioni and Smeers (2013).

We will assume that all firms act in a perfectly competitive environment as price takes. Such an assumption has been established as a standard in order to keep complex electricity market models computationally tractable, see, e.g. Boucher and Smeers (2001), Daxhelet and Smeers (2007), and Grimm et al. (2016a), or Weibelzahl (2017). We further note that perfect competition may also serve as a benchmark for evaluating deviations or abuses of market power; see Bunn and Oliveira (2003).

A.2.4 Storage facilities

We assume a set of storage facilities S that may be invested in. The non-storage scenario is captured by the limit case $S = \varnothing$. As above, by $S_n \subset S$ we denote the subset of storage facilities that are located at node n. Storage facilities are described by their (roundtrip) storage efficiency $e_s \in [0,1]$, which may significantly vary in reality between different storage technologies, e.g., 60% for a hydrogen storage and 90% for a battery storage; see Kuznia et al. (2013) or Sioshansi et al. (2013). Storage investment costs are given by a continuous and strictly increasing function $I_s(\bar{z}_s)$, with the argument $\bar{z}_s$ denoting the invested storage capacity. An example is an affine investment cost function with a positive slope.[2] Further note that our framework allows to explicitly analyze both the size and location of storage facility investment within the electricity network $\mathscr{G}$. For each storage facility we additionally introduce the variables $z^+_{s,t}$ and $z^-_{s,t}$ that describe the amount of electricity that is stored or discharged in the different periods, respectively. The latter two variables are obviously limited by the invested storage capacity $\bar{z}_s$. Finally, we introduce the variable $z_{s,t}$ that gives the current storage level and we assume that the initial storage level is zero.

[2] Observe that for an infinitely small slope, such an affine investment cost function will converge to a constant investment cost function.

A.3 Investment benchmark models

A.3.1 Single-level nodal pricing & integrated planning with storage facilities as an overall investment optimum

As a first benchmark, we present an integrated planning model. We add storage facility investments to this standard model in order to derive welfare-maximizing line and storage capacities while accounting for all relevant technical and economic restrictions. Using a single-level optimization problem, these constraints relate to electricity production, constrained transportation, price-sensitive consumption, and inter-temporal storage. Note that given such an integrated single-level model, optimal investments will be determined (out of the given discrete line investment options), as the whole industry is planned in a benevolent and welfare-maximizing manner. In particular, such an integrated view implies that line investments are not constrained by budget restrictions, but the benevolent planner can make lump-sum transfers in the case of a loss-making TSO. Using a more economic point of view, the integrated planner model is also equivalent to an electricity market under perfect competition and therefore maximizes total welfare. In this context, our benchmark may be interpreted as a long-run nodal pricing model with discrete line extensions similar to Jenabi et al. (2013), Grimm et al. (2016a), and Grimm et al. (2016b). Ultimately, the corresponding reference investments can be used to assess and evaluate inefficiencies of our bilevel market model in Sect. A.4, where investments are made in a complex hierarchical environment based on the expectations of the optimal decision response of other market players.

In line with Sect. A.2, we assume fully competitive firms that have no market power. This assumption directly implies that nodal pricing may be modeled as a welfare maximization problem:

$$W^i := \sum_{t\in T}\left(\sum_{d\in D}\int_0^{x_{d,t}} p_{d,t}(u)\,\mathrm{d}u - \sum_{n\in N}\sum_{g\in G_n}\int_0^{y_{g,t}} V_{g,t}(u)\,\mathrm{d}u\right) - \sum_{s\in S}\int_0^{\bar{z}_s} I_s(u)\,\mathrm{d}u - \sum_{l\in L^{\mathrm{inv}}} i_l\, w_l. \tag{A.4}$$

Denoting by $\delta_n^{\mathrm{in}}(L)$ and $\delta_n^{\mathrm{out}}(L)$ the set of in- and outgoing lines of node $n \in N$, Kirchhoff's First Law ensures power balance at every node and in each of the two time periods, i.e.,

demand, generation, charging and decharging activities as well as power flows in and out of a given node are balanced:

$$x_{n,t} = \sum_{g \in G_n} y_{g,t} + \sum_{l \in \delta_n^{\text{in}}(L)} f_{l,t} - \sum_{l \in \delta_n^{\text{out}}(L)} f_{l,t} + \sum_{s \in S_n} z_{s,t}^{-} - \sum_{s \in S_n} z_{s,t}^{+} \qquad \forall\, n \in N,\ t \in T. \tag{A.5}$$

For all lines, the following set of constraints ensures that no transmission capacities are exceeded:

$$-\overline{f}_l \leqslant \quad f_{l,t} \leqslant \quad \overline{f}_l \qquad \forall\, l \in L \setminus L^{\text{inv}},\ t \in T. \tag{A.6}$$

$$-\overline{f}_l\, w_l \leqslant \quad f_{l,t} \leqslant \quad \overline{f}_l\, w_l \qquad \forall\, l \in L^{\text{inv}},\ t \in T. \tag{A.7}$$

Power flows $f_{l,t}$ on each line $l = (n,m)$ are further characterized by Kirchhoff's Second Law, which links line flows to the corresponding phase angles $\Theta_{n,t}$ and $\Theta_{m,t}$. While for already existing transmission lines Kirchhoff's Second Law can be written as

$$f_{l,t} = B_l\,(\Theta_{n,t} - \Theta_{m,t}) \qquad \forall\, l = (n,m) \in L \setminus L^{\text{inv}},\ t \in T, \tag{A.8}$$

for all candidate transmission lines Kirchhoff's Second Law is given by

$$-M(1-w_l) \leqslant f_{l,t} - B_l(\Theta_{n,t} - \Theta_{m,t}) \leqslant M(1-w_l) \qquad \forall\, l = (n,m) \in L^{\text{inv}},\ t \in T, \tag{A.9}$$

with M denoting a large constant. We additionally set the phase angle of the reference node 1 to zero, which will ensure unique phase angle values:

$$\Theta_{1,t} = 0 \qquad \forall\, t \in T. \tag{A.10}$$

For each storage facility $s \in S$, the storage level in period t is described by

$$z_{s,t} = \sum_{i=1}^{t} e_s\, z_{s,i}^{+} - \sum_{i=1}^{t} z_{s,i}^{-} \qquad \forall\, s \in S,\ t \in T. \tag{A.11}$$

Moreover, we assume that storage investment is nonnegative

$$0 \leqslant \bar{z}_s \qquad \forall\, s \in S, \tag{A.12}$$

and that all charging variables and discharging variables, and the storage level variable will not violate their lower nonnegativity bounds as well as their upper storage capacity investment bounds, respectively:

$$0 \leqslant z^{+}_{s,t} \leqslant \bar{z}_s, \quad 0 \leqslant z^{-}_{s,t} \leqslant \bar{z}_s, \quad 0 \leqslant z_{s,t} \leqslant \bar{z}_s \qquad \forall\, s \in S,\ t \in T. \tag{A.13}$$

At the same time, the discharging variable is restricted by the storage level through

$$z^{-}_{s,t} \leqslant z_{s,t-1} \qquad \forall\, s \in S,\ t \in T \backslash \{1\}, \tag{A.14}$$

and

$$z^{-}_{s,1} = 0 \qquad \forall\, s \in S. \tag{A.15}$$

In analogy, demand and generation are restricted by the following nonnegativity constraints:

$$0 \leqslant \quad x_{d,t} \quad \forall\, d \in D,\ t \in T. \tag{A.16}$$

$$0 \leqslant \quad y_{g,t} \quad \forall\, n \in N,\ g \in G_n,\ t \in T. \tag{A.17}$$

Finally, line investment is assumed to be discrete:

$$w_l \in \{0,1\} \qquad \forall\, l \in L^{\text{inv}}. \tag{A.18}$$

Thus, the complete nodal-pricing problem can be stated as:

$$\begin{aligned}
\max \quad & \text{Welfare}: \text{(A.4)}, && \text{(A.19a)}\\
\text{s.t.} \quad & \text{Kirchoff's First Law: (A.5)}, && \text{(A.19b)}\\
& \text{Flow Restrictions: (A.6), (A.7)}, && \text{(A.19c)}\\
& \text{Kirchhoffs Second Law: (A.8), (A.9)}, && \text{(A.19d)}\\
& \text{Reference Phase Angle: (A.10)}, && \text{(A.19e)}\\
& \text{Storage Level Constraints: (A.11), (A.14), (A.15)}, && \text{(A.19f)}\\
& \text{Variable Restrictions: (A.12), (A.13), (A.16), (A.17), (A.18)}. && \text{(A.19g)}
\end{aligned}$$

Let us conclude this section with an observation: The well-known concept of congestion cost measure the welfare loss of the network-constrained model (A.19) as compared to a non-network model, where transmission constraints and corresponding power flows do not play a relevant role. It is obvious that maximizing welfare coincides with a minimization of congestion costs, i.e., a minimization of the difference between welfare under unlimited transmission and welfare under the actual transmission-limiting conditions:

Observation 1 *The nodal pricing model* (A.19) *does not only maximize welfare, but also minimizes congestion cost.*

A.3.2 Single-level zonal pricing with storage facilities

In the previous section we introduced an integrated single-level benchmark model that resembles a long-run nodal pricing system. While such a benchmark is commonly used in the literature, it may be difficult to discern whether sub-optimality of our bilevel zonal pricing model (Sect. A.4) is primarily due to the zonal market structure or due to the strategic interaction. For this reason, in this section we discuss a single-level zonal market as a second benchmark model.

As in Sect. A.2, we consider a given zonal configuration Z, which satisfies the connectivity conditions (A.1) - (A.3). We will use the zonal pricing formulation introduced by Bjørndal and Jørnsten (2001), which requires that prices at network nodes that belong to a given zone $Z_i \in Z$ must be equal for every time period $t \in T$.[3] Assuming elastic, inverse demand functions, this price equality can be formulated as follows

$$p_{n,t}\left(x_{n,t}\right) = p_{m,t}\left(x_{m,t}\right) \qquad \forall\, i \in \{1,...,r\}, \{(n,m) : n,m \in Z_i,\ n < m\},\ t \in T, \tag{A.20}$$

where the right- or left-hand inverse demand functions may be replaced by corresponding supply functions in order to link consumer prices to producer prices. Note that in the case $r = 1$, all nodes will have an identical price, which implies a uniform pricing system. In its other extreme, $r = |N|$ yields a nodal pricing system, where all prices may possibly differ. In addition, a system with $2 \leqslant r$ price zones is a relaxion of a zonal system with $r-1$ zones, if the new zone is constructed by splitting one of the existing zones. Ultimately, this implies

[3] For applications of this zonal pricing formulation, see for instance Bjørndal et al. (2003), Ehrenmann and Smeers (2005), Bjørndal and Jørnsten (2007), Weibelzahl and Märtz (2018), and Weibelzahl (2017).

that our nodal pricing model ($r = |N|$) introduced in the previous section is a relaxation of the following zonal pricing model ($r < |N|$) that again accounts for all production, transportation, generation, and consumption restrictions:

$$\begin{aligned}
\max \quad & \text{Welfare}: \text{(A.4)}, && \text{(A.21a)}\\
\text{s.t.} \quad & \text{Kirchoff's First Law: (A.5)}, && \text{(A.21b)}\\
& \text{Flow Restrictions: (A.6), (A.7)}, && \text{(A.21c)}\\
& \text{Kirchhoffs Second Law: (A.8), (A.9)}, && \text{(A.21d)}\\
& \text{Reference Phase Angle: (A.10)}, && \text{(A.21e)}\\
& \text{Storage Level Constraints: (A.11), (A.14), (A.15)}, && \text{(A.21f)}\\
& \text{Zonal-Pricing Constraints: (A.20)}, && \text{(A.21g)}\\
& \text{Variable Restrictions: (A.12), (A.13), (A.16), (A.17), (A.18)}. && \text{(A.21h)}
\end{aligned}$$

A.4 Bilevel zonal pricing model with storage

A.4.1 Structure of the hierarchical game and the corresponding bilevel optimization problem

Assuming price-sensitive demand, an integrated nodal pricing system ensures welfare maximizing investments out of the set of candidate transmission and storage facilities, as investments are always decided on from an overall welfare perspective by taking all scarce capacity constraints (stemming from production, transmission, and storage) into account. Nevertheless, such a first-best and integrated mechanism is not a realistic policy option for different countries and regions including for instance Europe; see Oggioni and Smeers (2013) and Bucksteeg et al. (2015).

In contrast, in liberalized electricity markets decisions of independent market players are typically made in a highly complex market environment, which often uses a system of zonal prices. In such an interdependent market structure, the extent of optimal line investment of the TSO highly depends on optimal storage facility investments and vice versa. While transmission line extensions base on the respective regulatory structures, investments in storage facilities are driven by future profits of firms and corresponding structures of the (zonal) market. As we will see in our numerical results that are presented in Sect. A.6, such a complex market environment will yield a quite different equilibrium investment solution

as compared to our integrated benchmark models.

In this section we assume that the TSO decides on an optimal transmission expansion and on a corresponding network fee before firms invest in their storage facilities. In this hierarchical game the TSO is the leader that is the first to make an optimal investment decision with competitive firms reacting as followers in an optimal way to the leader's investment choice; see also the vast literature including Gil et al. (2002), Sauma and Oren (2006), Fan et al. (2009), Garcés et al. (2009), Baringo and Conejo (2012), Jenabi et al. (2013), and Grimm et al. (2016b) that also consider multistage games with the TSO acting as the leader. Our game directly relates to the classical problem of Von Stackelberg (2010), where a leader and different followers interact in an anticipative environment.

Note that in our setting the sequential investment decisions of the TSO and of the firms are followed by trading on several zonal spot markets, which determine the profitability and efficiency of the respective investment decisions; see also Fig. A.1.

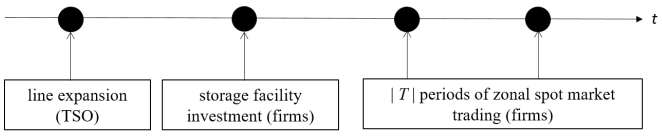

Figure A.1: Timing of the underlying multistage game.

As in Sauma and Oren (2006), we assume that at each stage all (investment) decisions of the previous stage(s) can be observed by the rational players, which allows a correct expectation formation. Therefore, our game can be translated into a bilevel programming problem with a network-extending TSO on the first level that anticipates storage investments and competitive market outcomes on the second level. Observe that storage investment and spot

market trading may be analyzed jointly on the second level, as we assume a competitive market.[4] The following two sections will describe the two problem levels in more detail.

A.4.2 First level problem: network extension

On the first level, we assume that the TSO chooses a line expansion plan, i.e., the TSO decides, which line to build. Such a long-term network development of the grid is a very challenging task, as in principle the TSO should eliminate the transmission capacity shortages that are welfare diminishing; see also Hornnes et al. (2000), David and Wen (2001), and Rious et al. (2008). In this paper we assume that the TSO maximizes social welfare, which can be stated as:

$$W^f := \sum_{t\in T}\left(\sum_{d\in D}\int_0^{x_{d,t}} p_{d,t}(u)\,\mathrm{d}u - \sum_{n\in N}\sum_{g\in G_n}\int_0^{y_{g,t}} V_{g,t}(u)\,\mathrm{d}u\right) - \sum_{s\in S}\int_0^{\bar{z}_s} I_s(u)\,\mathrm{d}u - \sum_{l\in L^{\mathrm{inv}}} i_l\, w_l. \tag{A.22}$$

In order to recover network investment cost, the TSO charges a network fee. In particular, as in the US market, we consider the case of a flow-based fee that is paid for each unit of transported electricity. As a main characteristic, such a fee bases on the actual usage of the network and is therefore not paid for pure power output; see also Galiana et al. (2003) and Jenabi et al. (2013). The corresponding fee variable is denoted by φ^{TSO}. Income I^{TSO} of the TSO is given by

$$I^{\mathrm{TSO}} = \sum_{t\in T}\sum_{l\in L}\varphi^{\mathrm{TSO}}|f_{l,t}|, \tag{A.23}$$

[4] We note that the time to build new transmission lines will in general be much larger than the time to build (battery) storage facilities. In turn, investments in storage facilities will have a larger time horizon than the market clearing interval. From this point of view, our bilevel model may be (re)interpreted as some kind of trilevel problem. On the first level, again the TSO chooses an optimal line extension plan with a corresponding network fee. The TSO anticipates optimal storage investments of perfectly competitive firms on the second level and competitive market outcomes of a zonal market on the third level. Assuming perfectly competitive firms, the objective functions of the second level and of the third level will be affine-equivalent as described in Grimm et al. (2016a). In particular, the objective of the second level will correspond to the aggregated difference between consumer surplus, variable generation cost, network charges, and storage investment cost. On the opposite, on the third level the spot market welfare objective can be expressed as the difference between consumer surplus, network fees, and variable production cost. From a mathematical point of view, we can equivalently subtract storage investment costs from the objective function of the third level without changing the optimal solution. This implies that the discussed hierarchical trilevel model may be reformulated and solved as the bilevel maximization problem introduced in this section. On the other hand, our proposed bilevel model may be reinterpreted using three levels that correspond to long-term line investment, medium-term storage investment, and short-term market clearing.

where $|f_{l,t}|$ is the absolute flow value on line l in time period t.

Analogously, expenses of the TSO in form of line investments can be written as

$$E^{\text{TSO}} = \sum_{l \in L^{\text{inv}}} i_l \; w_l. \tag{A.24}$$

Then, the following budget constrain ensures that investment costs of the TSO are covered by its income in form of network fees:

$$\sum_{t \in T} \sum_{l \in L} \varphi^{\text{TSO}} \, |f_{l,t}| \geqslant \sum_{l \in L^{\text{inv}}} i_l \; w_l. \tag{A.25}$$

To sum up, on the first level the TSO decides on both an optimal transmission fee φ^{TSO} and on adequate line investments w_l as to maximize welfare. Therefore, the first-level problem can be written as

$$\begin{aligned}
\max \quad & \text{Objective: (A.22)}, && \text{(A.26a)}\\
\text{s.t.} \quad & \text{Budget Constraint: (A.25)}, && \text{(A.26b)}\\
& \text{Investment Variable Restrictions: (A.18)}, && \text{(A.26c)}\\
& \text{s.t.} \quad \text{Second Level Problem: (A.28)}, && \text{(A.26d)}
\end{aligned}$$

where the TSO anticipates optimal spot market outcomes and storage investment decisions that are determined on the second level. Thus, the second-level problem is embedded in the constraint set of the first level problem, i.e., spot market outcomes and storage investment decisions are chosen as the argmax of the lower level problem (A.28). Note that even though the TSO cannot explicitly enforce certain private storage investments on the second level, optimal second-level variables will be influenced by optimal first-level decisions, which are treated as parameters on the second level; see also the following section.

Table A.1: Problem levels and corresponding decision variables.

Level	Variables							
First level	φ^{TSO}	w						
Second level	x	y	z^+	z^-	$\bar{z}$	z	f	Θ

For the ease of improved clarity, the decision variables of the two levels are summarized in Table A.1, where variables without an index denote the vector of corresponding decision variables.

A.4.3 Second level problem: storage investment and energy trading

On the second level firms invest in new storage technologies and trade energy on a competitive market. Note that the decision behaviour of the firms on the second level is part of the constraint set of the TSO on the first level.

As in Jenabi et al. (2013), the assumption of perfect competition allows to model profit-maximization behaviour of firms as a welfare maximization problem, where costs in form of the transmission fee φ^{TSO} are directly taken into account:

$$W^{\mathrm{s}} := \sum_{t\in T}\left(\sum_{d\in D}\int_0^{x_{d,t}} p_{d,t}(u)\,\mathrm{d}u - \sum_{n\in N}\sum_{g\in G_n}\int_0^{y_{g,t}} V_{g,t}(u)\,\mathrm{d}u - \sum_{l\in L}\varphi^{\mathrm{TSO}}\,|f_{l,t}|\right) - \sum_{s\in S}\int_0^{\bar{z}_s} I_s(u)\,\mathrm{d}u. \tag{A.27}$$

Again, we assume price equality within a given zone as modelled in Eq. (A.20). As all equilibrium quantities must be both technically and economically feasible, on the second level all power flow, production, storage, and market clearing constraints are taken into account. In this context we again note that the second-level problem is not an independent problem, but the second-level problem determines equilibrium spot market and storage investment outcomes given an optimal transmission fee φ^{TSO} and corresponding first-level line investments w_l of the TSO; see Table A.1.

Ultimately, the second-level problem – that is embedded in the first level by the argmax operator – writes for a fixed transmission fee φ^{TSO} and parameterized first-level line investments w_l as:

$$
\begin{aligned}
\max \quad & \text{Welfare}: \text{(A.27)}, && \text{(A.28a)}\\
\text{s.t.} \quad & \text{Kirchoff's First Law: (A.5)}, && \text{(A.28b)}\\
& \text{Flow Restrictions: (A.6), (A.7)}, && \text{(A.28c)}\\
& \text{Kirchhoffs Second Law: (A.8), (A.9)}, && \text{(A.28d)}\\
& \text{Reference Phase Angle: (A.10)}, && \text{(A.28e)}\\
& \text{Storage Level Constraints: (A.11), (A.14), (A.15)}, && \text{(A.28f)}\\
& \text{Zonal-Pricing Constraints: (A.20)}, && \text{(A.28g)}\\
& \text{Variable Restrictions: (A.12), (A.13), (A.16), (A.17)}. && \text{(A.28h)}
\end{aligned}
$$

Let us conclude this section with the following trivial, but important observation, which states that welfare under the integrated planning model (A.19) yields an upper bound for the bilevel model (A.26) and (A.28):

Observation 2: *The optimal welfare level of the bilevel model* (A.26) *and* (A.28) *can not exceed welfare of the integrated planning model in* (A.19)*, i.e., welfare of the integrated model is at least as high as welfare of the bilevel model.*

A.5 Solution strategy and problem reformulation

Our market model introduced in the previous section can be seen as a special instance of a general bilevel model. Being non-convex and non-differentiable, bilevel models are known to be NP hard, which implies that this class of optimization problem is in general very challenging and hard to solve; see for instance Jeroslow (1985), Ishizuka and Aiyoshi (1992), Campêlo and Scheimberg (2005), Dempe and Zemkoho (2012), Pozo et al. (2017), Sariddichainunta and Inuiguchi (2017), and Zare et al. (2017). In this section we present a single-level problem reformulation and discuss our main solution strategy.

A.5.1 Linear Reformulation of the absolute value of transmission flows

Similar to Jenabi et al. (2013) and Kirschen and Strbac (2004), we first linearize the absolute value of transmission flows. For this reason, we introduce the continuous variables $f^+_{l,t} \geqslant 0$ and $f^-_{l,t} \geqslant 0$ for all lines $l \in L$ and time periods $t \in T$. Then, the absolute flow value can be rewritten as

$$|f_{l,t}| = f^+_{l,t} + f^-_{l,t} \qquad \forall\, l \in L,\ t \in T, \tag{A.29}$$

where line flows are given by:

$$f_{l,t} = f^+_{l,t} - f^-_{l,t} \qquad \forall\, l \in L,\ t \in T. \tag{A.30}$$

Ultimately, this allows to rewrite

$$\sum_{t \in T} \sum_{l \in L} \varphi^{\mathrm{TSO}} |f_{l,t}| \tag{A.31}$$

as

$$\sum_{t \in T} \sum_{l \in L} \varphi^{\mathrm{TSO}} \left(f^+_{l,t} + f^-_{l,t} \right). \tag{A.32}$$

A.5.2 Linear reformulation of the non-convex flow product

In a second step, we linearize the non-convex flow product in the second-level objective (A.27). Let us assume a set K of discretized fee values, e.g., K may comprise fees measured in cent. We introduce the binary variables $\varphi^{\mathrm{TSO}} \in \{0,1\}$ indicating whether fee k is chosen. Obviously, exactly one fee must be implemented by the TSO:

$$\sum_{k \in K} \varphi^{\mathrm{TSO}}_k = 1. \tag{A.33}$$

This allows to further rewrite (A.32) as

$$\sum_{t \in T} \sum_{l \in L} \sum_{k \in K} k\, \varphi^{\mathrm{TSO}}_k \left(f^+_{l,t} + f^-_{l,t} \right). \tag{A.34}$$

In a next step, we introduce the continuous variable $f^{\text{abs}}_{l,t,k}$ that measures the absolute flow value on line l in period t under fee regime k. Obviously, $f^{\text{abs}}_{l,t,k}$ must satisfy the following constraints:

$$0 \leqslant f^{\text{abs}}_{l,t,k} \leqslant \bar{f}_l \, \varphi^{\text{TSO}}_k \qquad \forall\, l \in L,\ t \in T,\ k \in K. \tag{A.35}$$

$$\sum_{k \in K} f^{\text{abs}}_{l,t,k} = f^{+}_{l,t} + f^{-}_{l,t} \qquad \forall\, l \in L,\ t \in T. \tag{A.36}$$

Then, we can finally rewrite (A.32) linear as

$$\sum_{t \in T} \sum_{l \in L} \sum_{k \in K} k \, f^{\text{abs}}_{l,t,k}. \tag{A.37}$$

A.5.3 KKT reformulation & (non-)uniqueness issues

Given that the second level is a convex (concave) and continuous optimization problem with only linear constraints, we can use a Karush–Kuhn–Tucker (KKT) reformulation including complementarity constraints[5] in order to replace the bilevel problem by a single-level problem; see for instance Dempe (2002), Boyd and Vandenberghe (2004), and Colson et al. (2007). From a mathematical point of view, such a reformulation strategy yields a mathematical program under equilibrium constraints (MPEC); see Huppmann and Egerer (2015).

Applying a KKT reformulation, caution must be taken whenever the second-level problem has a non-unique optimal solution. In particular, in the case of non-uniqueness of lower-level optimal solutions, without additional assumptions the TSO cannot anticipate the optimal out- comes on the lower level. Therefore, ignoring multiplicity of optimal lower level solutions may make it hard (or even impossible) to assess the value of an optimal transmission expansion on the first level; for details and further discussions see, e.g., Dempe (2003) or Zugno et al. (2013). From a policy perspective, such ambiguities will also make it difficult to compare and quantitatively analyze the (in)efficiency of different policy regulations and market designs, as it is unclear which equilibrium will be realized; see also Hu and Ralph (2007). Ultimately, (non-)uniqueness of lower level solutions is therefore an important aspect, both from a theoretical and a practical point of view. Being a prerequisite for meaningful bilevel policy analyses, we first prove uniqueness of the optimal solution of the

[5] An alternative approach would be to use an explicit formulation of the strong duality equality; see, e.g., Garcés et al. (2009).

second-level problem with respect to all production variables $y_{g,t}$, consumption variables $x_{d,t}$, and storage investment variables $\bar{z}_s$.

Theorem 1 *The second level problem* (A.28) *has a unique optimal solution in all production variables $y_{g,t}$, consumption variables $x_{d,t}$, and storage investment variables $\bar{z}_s$.*

Proof By assumption, all inverse demand functions $p_{d,t}$ are continuous and strictly decreasing. In addition, both the variable cost functions $V_{g,t}$ and the storage investment functions I_s are continuous and strictly increasing. As a direct consequence, the second-stage objective is strictly concave in all demand, production, and storage investment variables, with

$$\frac{\partial^2 W^S}{\partial x_{d,t}^2} = p_{d,t}^{'} \quad \forall\, d \in D,\ t \in T, \qquad \frac{\partial^2 W^S}{\partial y_{g,t}^2} = -V_{g,t}^{'} \quad \forall\, n \in N,\ g \in G_n, t \in T,$$

$$\frac{\partial^2 W^S}{\partial \bar{z}_s^2} = -I_s^{'} \quad \forall\, n \in N,\ s \in S_n.$$

The strict concavity directly implies uniqueness of these variable, see Mangasarian (1988).

We next show that for only two time periods, additionally the operational storage variables $z_{s,t}^+$ and $z_{s,t}^-$ that are used for charging and discharging are unique. In direct consequence, in this case power flows $f_{l,t}$ are also uniquely determined:

Theorem 2 *Assume a planning horizon of only two time periods with an initial- and end-storage level of zero. Then, the optimal solution of the second-level problem* (A.28) *is unique in all second-level variables.*

Proof We first show that for each storage facility s, the amount of stored-in electricity $z_{s,1}^+$ in period 1 equals the uniquely determined storage capacity $\bar{z}_s$. To see this, assume the contrary, i.e., consider the case $z_{s,1}^+ < \bar{z}_s$. Obviously, $\bar{z}_s^* := z_{s,1}^+$ is also a feasible investment solution. However, as $\bar{z}_s^*$ yields a welfare increase as compared to $\bar{z}_s$, with $\Delta W = W(\cdot, \bar{z}_s^*) - W(\cdot, \bar{z}_s) = \int_{\bar{z}_s^*}^{\bar{z}_s} I_s(u)\mathrm{d}u > 0$, the original investment level $\bar{z}_s$ cannot be optimal. This observation directly yields a contradiction.

Using an optimal end of horizon inventory, the amount of discharged electricity in period 2 is uniquely determined by Constraint (A.11), Constraint (A.14), and Constraint (A.15), which readily imply

$$z_{s,2}^- = e_s\ z_{s,1}^+. \tag{A.38}$$

To show uniqueness of power flows, we finally consider Kirchhoff's First Law (A.5) for period 1 and period 2:

$$x_{n,1} = \sum_{g \in G_n} y_{g,1} + \sum_{l \in \delta_n^{\text{in}}(L)} f_{l,1} - \sum_{l \in \delta_n^{\text{out}}(L)} f_{l,1} - \sum_{s \in S_n} z^+_{s,1} \qquad \forall n \in N. \tag{A.39}$$

$$x_{n,2} = \sum_{g \in G_n} y_{g,2} + \sum_{l \in \delta_n^{\text{in}}(L)} f_{l,2} - \sum_{l \in \delta_n^{\text{out}}(L)} f_{l,2} + \sum_{s \in S_n} z^-_{s,2} \qquad \forall n \in N. \tag{A.40}$$

Note that for a given line expansion plan on the first level, we can treat newly constructed lines as already existing lines. In addition, not constructed candidate lines can be removed from the network. For all nodes $n \in N$ we set

$$F_{n,1} := x_{n,1} - \sum_{g \in G_n} y_{g,1} + \sum_{s \in S_n} z^+_{s,1}, \tag{A.41}$$

$$F_{n,2} := x_{n,2} - \sum_{g \in G_n} y_{g,2} - \sum_{s \in S_n} z^-_{s,2}, \tag{A.42}$$

and rewrite Constraints (A.39) and (A.40) for both periods $t \in \{t_1, t_2\}$ as:

$$F_{n,t} = \sum_{l=(m,n) \in \delta_n^{\text{in}}(L)} B_l \left(\Theta_{m,t} - \Theta_{n,t}\right) - \sum_{l=(n,m) \in \delta_n^{\text{out}}(L)} B_l \left(\Theta_{n,t} - \Theta_{m,t}\right). \tag{A.43}$$

Using (A.43) and Theorem 1, we see that for the unique optimal demand, production, and storage variable values captured in $F_{n,t}$, all phase angles are determined by a system of linear equations. The latter can equivalently be stated by using the following matrix representation

$$F_t = B\,\Theta_t \quad \forall\, t \in T, \tag{A.44}$$

where Θ_t denotes the vector of phase angles in period t, F_t is the vector of optimal nodal net injections in period t, and B is the corresponding matrix of (aggregated) susceptances. As $\sum_{n \in N} F_{n,t} = 0$ holds for all time periods t, it directly follows that B is singular. However, in Constraint (A.10) we have set the phase angle value of the (arbitrarily chosen) reference node to zero, which yields non-singularity. Ultimately, optimal phase angles will be uniquely determined. By using the relation between phase angles and power flows given in Constraint (A.8), in each of the two periods and on each transmission line optimal power flows will also be unique.

Despite the fact that the optimal lower-level solution is unique for the case of two time periods, assuming a general planning horizon with $|T| \geqslant 3$, operational storage variables

will not always be unique. Thus, uniqueness does not hold in the general case. This ambiguity directly translates into optimal transmission flows $f_{l,t}$. To see this non-uniqueness, consider the following simple three-period counter example that is depicted in Fig. A.2.

We assume three network nodes that are connected by two limited transmission lines with a transmission capacity of 4 units each. Note that our counter example does not require the assumption of loop flows, which shows that non-uniqueness can already be observed in very simple networks. In addition to transmission facilities, we are given a single generator that is located at node 1 with a strictly increasing variable production cost function of $V(y) = y$.

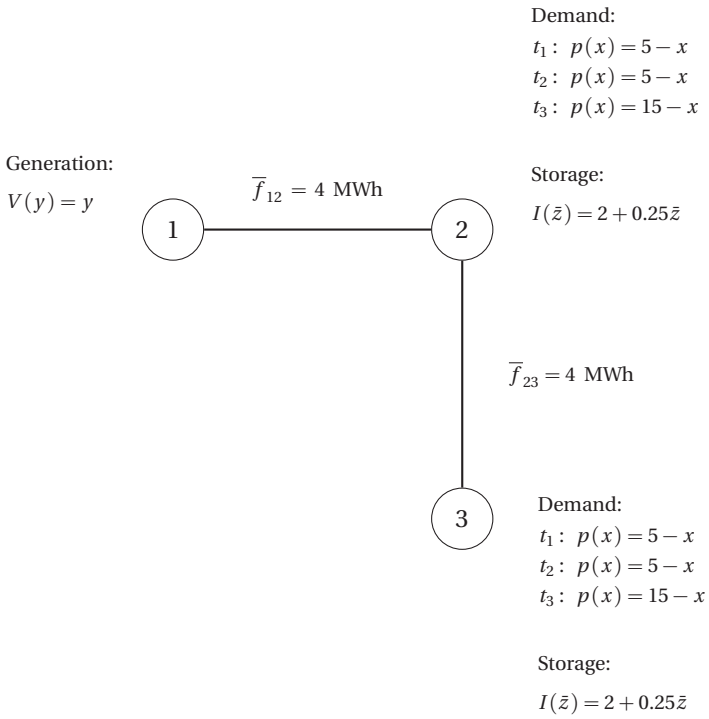

Figure A.2: Counter example: Three-node network.

The electricity network is complemented by two consumers, which are located at node 2 and node 3. To keep our example as simple as possible, the two demand nodes 2 and 3 have identical inverse demand functions of $p(x) = 5 - x$ in the two off-peak periods 1 and 2, respectively. In the on-peak period 3, the two demand nodes are characterized by an

inverse demand function of $p(x) = 15 - x$. We also assume that storage investment can take place at the two demand nodes with a strictly increasing investment cost function of $I(\bar{z}) = 2 + 0.25\bar{z}$. For ease of presentation, we neglect storage losses that could easily be included in the counter example. Finally, the TSO charges a transmission fee of 1 for using the given network facilities.

Obviously, the limited northern transmission line (1, 2) determines the maximal production that can be supplied in each of the three time periods. Therefore, total production aggregated over the entire planning horizon cannot exceed $4 \cdot 3 = 12$ units. In order to being able to increase peak demand in period 3 in contrast to a no-storage scenario with a total consumption of 4, from an overall welfare perspective it is optimal to install 4 units of storage capacity at node 2 and at node 3, respectively. As the off-peak demand is too low in order to being efficiently served, in our stylized example both in period 1 and in period 2 the produced electricity in the amount of 4 units is completely stored at the two nodes 2 and 3. However, note that respecting the flow bound on link (2, 3), in period 1 we can arbitrarily distribute the produced electricity of 4 units among the two storage facilities, i.e., we can choose $\xi \in [0,1]$ and charge an amount of 4ξ at node 2 as well as an amount of $4(1-\xi)$ at node 3. Obviously, this directly implies that in period 2 the two storage facilities charge additional electricity amounting to $4(1-\xi)$ and 4ξ, respectively. Ultimately, this allows to discharge 4 units at the two nodes in period 3. Together with the production in period 3, a demand of 6 units can be served both at node 2 and at node 3; see also Fig. A.3.

Most important, the non-uniqueness of storage activities in periods 1 and 2 translates in corresponding ambiguous north-south transmission flows. In particular, the choice $\xi = 0$ implies in period 1 a flow on line (2, 3) in the amount of 4 units. In periods 2 and 3 the corresponding north-south flows are given by 0 and 2, respectively. However, if a solution with $\xi = 0.5$ is realized, line (2, 3) is characterized by flows amounting to 2 in each of the three periods. Note that under the latter solution north-south flows aggregated over the three periods are again 6. In view of congested networks and possibly needed transmission facility investments, a solution with $\xi = 0.5$ may somehow indicate a reduced need for grid extensions on the first level as opposed to a lower-level solution relating to $\xi = 0$. Finally, observe that in line with Theorem 2, a deletion of the first time period would result in unique charging and discharging quantities in the corresponding two-period model. In particular, in the resulting two-period model storage facility investments would amount to 2 at node 2 and node 3, respectively. The two storage facilities would be charged in the off-peak period and discharged in the on-peak period, which does not yield the problem of multiplicity of

solutions.

Given the above discussion on multiplicity of solutions, in the following we will assume the optimistic bilevel case, where for non-unique optimal lower level solutions the solution that maximizes the first-level objective will be realized on the second level. From our point of view such an assumption seems appropriate, as competitive firms should in general not have any incentives that leads them to choose a solution out of their indifference set with a welfare-diminishing effect.

Therefore, we can now equivalently describe the second-level problem by its KKT formulation[6], which comprises primal and dual feasibility as well as complementary slackness.

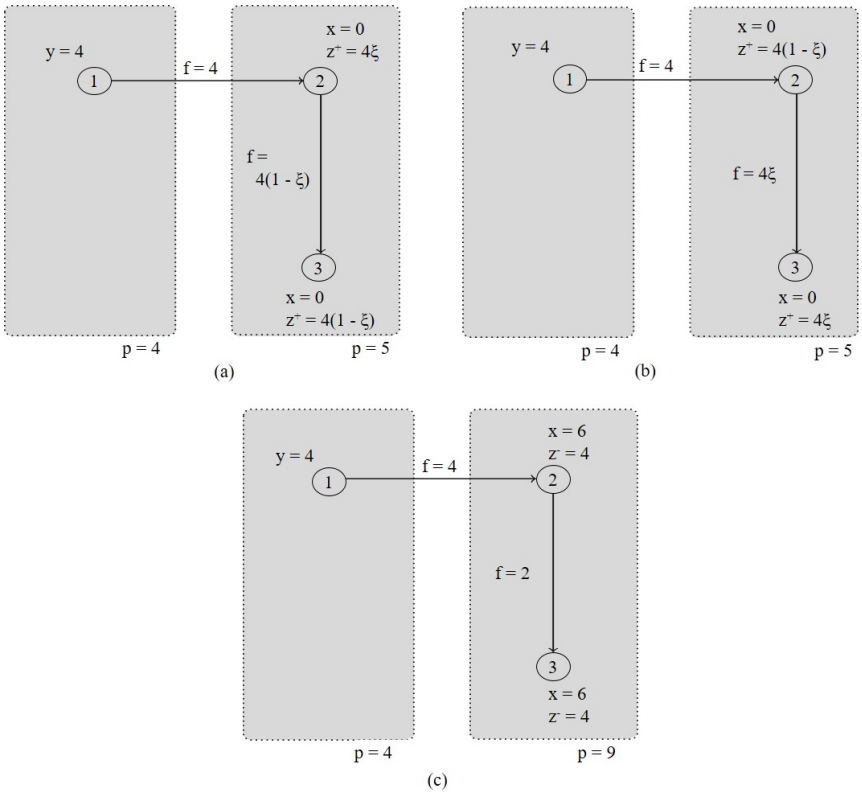

Figure A.3: East-west zonal pricing system: non-unique optimal solution with $\xi \in [0,1]$. (a) Period 1, (b) Period 2, (c) Period 3.

[6] Note that for the case of presentation, we neglect supply functions in Eq. (A.20).

We first state the corresponding primal-dual pairs of complementarity, where the symbol $\perp$ denotes orthogonality:

$$0 \leqslant f_{l,t} + \overline{f}_l \perp \delta^{\text{low}}_{l,t} \geqslant 0 \qquad \forall\, l \in L \setminus L^{\text{inv}},\ t \in T, \tag{A.45}$$

$$0 \leqslant -f_{l,t} + \overline{f}_l \perp \delta^{\text{up}}_{l,t} \geqslant 0 \qquad \forall\, l \in L \setminus L^{\text{inv}},\ t \in T, \tag{A.46}$$

$$0 \leqslant f_{l,t} + (\overline{f}_l\ w_l) \perp \epsilon^{\text{low}}_{l,t} \geqslant 0 \qquad \forall\, l \in L^{\text{inv}},\ t \in T, \tag{A.47}$$

$$0 \leqslant -f_{l,t} + (\overline{f}_l\ w_l) \perp \epsilon^{\text{up}}_{l,t} \geqslant 0 \qquad \forall\, l \in L^{\text{inv}},\ t \in T, \tag{A.48}$$

$$0 \leqslant f_{l,t} - B_l\,(\Theta_{n,t} - \Theta_{m,t}) + M(1-w_l) \perp \varpi^{\text{low}}_{l,t} \geqslant 0 \qquad \forall\, l = (n,m) \in L^{\text{inv}},\ t \in T, \tag{A.49}$$

$$0 \leqslant M(1-w_l) - (f_{l,t} - B_l(\Theta_{n,t} - \Theta_{m,t})) \perp \varpi^{\text{up}}_{l,t} \geqslant 0 \qquad \forall\, l = (n,m) \in L^{\text{inv}},\ t \in T, \tag{A.50}$$

$$0 \leqslant f^{+}_{l,t} \perp \Delta_{l,t} \geqslant 0 \qquad \forall\, l \in L,\ t \in T, \tag{A.51}$$

$$0 \leqslant f^{-}_{l,t} \perp \Upsilon_{l,t} \geqslant 0 \qquad \forall\, l \in L,\ t \in T, \tag{A.52}$$

$$0 \leqslant f^{\text{abs}}_{l,t,k} \perp \Lambda_{l,t,k} \geqslant 0 \qquad \forall\, k \in K,\ l \in L,\ t \in T, \tag{A.53}$$

$$0 \leqslant \bar{f}_l \varphi^{\text{TSO}}_k - f^{\text{abs}}_{l,t,k} \perp \phi_{l,t,k} \geqslant 0 \qquad \forall\, k \in K,\ l \in L,\ t \in T, \tag{A.54}$$

$$0 \leqslant \bar{z}_s \perp \chi_s \geqslant 0 \qquad \forall\, n \in N,\ s \in S_n, \tag{A.55}$$

$$0 \leqslant z^{+}_{s,t} \perp \rho_{s,t} \geqslant 0 \qquad \forall\, n \in N,\ s \in S_n,\ t \in T, \tag{A.56}$$

$$0 \leqslant z^{-}_{s,t} \perp \varphi_{s,t} \geqslant 0 \qquad \forall\, n \in N,\ s \in S_n,\ t \in T, \tag{A.57}$$

$$0 \leqslant z_{s,t} \perp \tau_{s,t} \geqslant 0 \qquad \forall\, n \in N,\ s \in S_n,\ t \in T, \tag{A.58}$$

$$0 \leqslant -z^{+}_{s,t} + \bar{z}_s \perp \zeta_{s,t} \geqslant 0 \qquad \forall\, n \in N,\ s \in S_n,\ t \in T, \tag{A.59}$$

$$0 \leqslant -z^{-}_{s,t} + \bar{z}_s \perp \eta_{s,t} \geqslant 0 \qquad \forall\, n \in N,\ s \in S_n,\ t \in T, \tag{A.60}$$

$$0 \leqslant -z_{s,t} + \bar{z}_s \perp \varepsilon_{s,t} \geqslant 0 \qquad \forall\, n \in N,\ s \in S_n,\ t \in T, \tag{A.61}$$

$$0 \leqslant z_{s,t-1} - z^{-}_{s,t} \perp \mu_{s,t} \geqslant 0 \qquad \forall\, n \in N,\ s \in S_n,\ t \in T : t \geqslant 2, \tag{A.62}$$

$$0 \leqslant x_{d,t} \perp \upsilon_{d,t} \geqslant 0 \qquad \forall\, d \in D,\ t \in T, \tag{A.63}$$

$$0 \leqslant y_{g,t} \perp \nu_{g,t} \geqslant 0 \qquad \forall\, n \in N,\ g \in G_n,\ t \in T. \tag{A.64}$$

Note that these complementarity pairs correspond exclusively to inequalities of the primal problem, while primal equality constraints are only equipped with unrestricted dual variables:

$$0 = \sum_{g \in G_n} y_{g,t} + \sum_{l \in \delta_n^{\text{in}}(L)} f_{l,t} - \sum_{l \in \delta_n^{\text{out}}(L)} f_{l,t} + \sum_{s \in S_n} z_{s,t}^- - \sum_{s \in S_n} z_{s,t}^+ - x_{n,t}$$

$$\text{and} \quad \alpha_{n,t} \in \mathbb{R} \quad \forall\, n \in N,\ t \in T, \tag{A.65}$$

$$0 = B_l\,(\Theta_{n,t} - \Theta_{m,t}) - f_{l,t} \quad \text{and} \quad \beta_{l,t} \in \mathbb{R} \quad \forall\, l \in L \setminus L^{\text{inv}},\ t \in T, \tag{A.66}$$

$$0 = f_{l,t}^+ + f_{l,t}^- - \sum_{k \in K} f_{l,t,k}^{\text{abs}} \quad \text{and} \quad \omega_{l,t} \in \mathbb{R} \quad \forall\, l \in L,\ t \in T, \tag{A.67}$$

$$0 = f_{l,t}^+ - f_{l,t}^- - f_{l,t} \quad \text{and} \quad \varrho_{l,t} \in \mathbb{R} \quad \forall\, l \in L,\ t \in T, \tag{A.68}$$

$$0 = \Theta_{1,t} \quad \text{and} \quad \gamma_t \in \mathbb{R} \quad \forall\, t \in T, \tag{A.69}$$

$$0 = \sum_{i=1}^{t} e_s\ z_{s,i}^+ - \sum_{i=1}^{t} z_{s,i}^- - z_{s,t} \quad \text{and} \quad \iota_{s,t} \in \mathbb{R} \quad \forall\, n \in N,\ s \in S_n,\ t \in T, \tag{A.70}$$

$$0 = z_{s,1}^- \quad \text{and} \quad \kappa_s \in \mathbb{R} \quad \forall\, n \in N,\ s \in S_n, \tag{A.71}$$

$$0 = p_{n,t}(x_{n,t}) - p_{m,t}(x_{m,t}) \quad \text{and} \quad \omega_{t,n,m} \in \mathbb{R}$$
$$\forall\, t \in T, i \in \{1,\ \ldots, r\}, \{(n,\ \ m) : n, m \in Z_i,\ n < m\}. \tag{A.72}$$

We complement the KKT system with the set of dual feasibility requirements that correspond to the partial derivates with respect to the primal variables:

$$-\delta_{l,t}^{\text{low}} + \delta_{l,t}^{\text{up}} + \sum_{n \in N:\ l \in \delta_n^{\text{in}}(L)} \alpha_{n,t} - \sum_{n \in N:\ l \in \delta_n^{\text{out}}(L)} \alpha_{n,t} - \beta_{l,t} - \varrho_{l,t} = 0$$
$$\forall\, l \in L \setminus L^{\text{inv}},\ t \in T, \tag{A.73}$$

$$-\epsilon_{l,t}^{\text{low}} + \epsilon_{l,t}^{\text{up}} - \varpi_{l,t}^{\text{low}} + \varpi_{l,t}^{\text{up}} + \sum_{n \in N:\ l \in \delta_n^{\text{in}}(L)} \alpha_{n,t} - \sum_{n \in N:\ l \in \delta_n^{\text{out}}(L)} \alpha_{n,t} - \varrho_{l,t} = 0$$
$$\forall\, l \in L^{\text{inv}},\ t \in T, \tag{A.74}$$

$$k - \Lambda_{l,t,k} + \phi_{l,t,k} - \omega_{l,t} = 0 \qquad \forall\, k \in K,\ l \in L,\ t \in T, \tag{A.75}$$

$$-\Delta_{l,t} + \omega_{l,t} + \varrho_{l,t} = 0 \qquad \forall\, l \in L,\ t \in T, \tag{A.76}$$

$$-\Upsilon_{l,t} + \omega_{l,t} - \varrho_{l,t} = 0 \qquad \forall\, l \in L,\ t \in T, \tag{A.77}$$

$$\sum_{l\in\delta_1^{\text{out}}(L^{\text{inv}})} B_l\varpi_{l,t}^{\text{low}} - \sum_{l\in\delta_1^{\text{in}}(L^{\text{inv}})} B_l\varpi_{l,t}^{\text{low}} - \sum_{l\in\delta_1^{\text{out}}(L^{\text{inv}})} B_l\varpi_{l,t}^{\text{up}} + \sum_{l\in\delta_1^{\text{in}}(L^{\text{inv}})} B_l\varpi_{l,t}^{\text{up}}$$

$$+ \sum_{l\in\delta_1^{\text{out}}(L\setminus L^{\text{inv}})} B_l\beta_{l,t} - \sum_{l\in\delta_1^{\text{in}}(L\setminus L^{\text{inv}})} B_l\beta_{l,t} + \gamma_t = 0 \qquad \forall\ t\in T, \tag{A.78}$$

$$\sum_{l\in\delta_n^{\text{out}}(L^{\text{inv}})} B_l\varpi_{l,t}^{\text{low}} - \sum_{l\in\delta_n^{\text{in}}(L^{\text{inv}})} B_l\varpi_{l,t}^{\text{low}} - \sum_{l\in\delta_n^{\text{out}}(L^{\text{inv}})} B_l\varpi_{l,t}^{\text{up}} + \sum_{l\in\delta_n^{\text{in}}(L^{\text{inv}})} B_l\varpi_{l,t}^{\text{up}}$$

$$+ \sum_{l\in\delta_n^{\text{out}}(L\setminus L^{\text{inv}})} B_l\beta_{l,t} - \sum_{l\in\delta_n^{\text{in}}(L\setminus L^{\text{inv}})} B_l\beta_{l,t} = 0$$

$$\forall\ n\in N:\ n\geqslant 2,\ t\in T, \tag{A.79}$$

$$-\rho_{s,t} + \zeta_{s,t} - \alpha_{n(s),t} + \sum_{i=1}^{t} e_s\iota_{s,i} = 0 \qquad \forall\ s\in S,\ t\in T, \tag{A.80}$$

$$-\varphi_{s,1} + \eta_{s,1} + \alpha_{n(s),1} - \iota_{s,1} + \kappa_s = 0 \qquad \forall\ s\in S, \tag{A.81}$$

$$-\varphi_{s,t} + \eta_{s,t} + \mu_{s,t} + \alpha_{n(s),t} - \sum_{i=1}^{t}\iota_{s,i} = 0 \qquad \forall\ s\in S, t\in T:\ t\geqslant 2, \tag{A.82}$$

$$-\tau_{s,t} + \varepsilon_{s,t} - \mu_{s,t+1} - \iota_{s,t} = 0 \qquad \forall s\in S,\ t\in T:\ t\leqslant 23, \tag{A.83}$$

$$-\tau_{s,24} + \varepsilon_{s,24} - \iota_{s,24} = 0 \qquad \forall\ s\in S, \tag{A.84}$$

$$I_s - \chi_s - \zeta_{,t} - \eta_{s,t} - \varepsilon_{s,t} = 0 \qquad \forall\ s\in S,\ t\in T, \tag{A.85}$$

$$-p_{d,t}(x_{d,t}) - \upsilon_{d,t} - \alpha_{d,t} + \sum_{\{Z_i\in Z:\ d\in Z_i\}}\ \sum_{\{m\in Z_i:\ d<m\}} \frac{\partial p_{d,t}(x_{d,t})}{\partial x_{d,t}}\omega_{t,d,m}$$

$$- \sum_{\{Z_i\in Z:\ d\in Z_i\}}\ \sum_{\{n\in Z_i:\ n<d\}} \frac{\partial p_{d,t}(x_{d,t})}{\partial x_{d,t}}\omega_{t,n,d} = 0 \qquad \forall\ d\in D,\ t\in T, \tag{A.86}$$

$$V_{g,t}(y_{g,t}) - \nu_{g,t} + \alpha_{n(g),t} = 0 \qquad \forall\ n\in N,\ g\in G_n,\ t\in T. \tag{A.87}$$

A.5.4 Linearization of complementary slackness conditions and final single-level problem reformulation

In the above KKT reformulation, all constraints except from the complementary slackness conditions are linear. Exploiting the disjunctive structure of these complementary slackness conditions, in this section we use a Fortuny-Amat-like linearization to handle these non-convexities in Eqs. (A.45)-(A.64); see Fortuny-Amat and McCarl (1981). For example, KKT condition (A.63) can be linearized as

$$0 \leqslant x_{d,t} \leqslant \overline{\boldsymbol{M}}_{d,t} m_{d,t} \qquad \forall d \in D,\ t \in T, \tag{A.88}$$

$$0 \leqslant \upsilon_{d,t} \leqslant \underline{\boldsymbol{M}}_{d,t} (1 - m_{d,t}) \qquad \forall d \in D,\ t \in T, \tag{A.89}$$

where $m_{d,t} \in \{0,1\}$ is a binary auxiliary variable and $\overline{\boldsymbol{M}}_{d,t}$, $\underline{\boldsymbol{M}}_{d,t}$ are sufficiently large constants denoted as "big-M". Note that from a computational point of view it is important to choose adequate big-M parameters that are as large as necessary but as small as possible. For instance, in the above example we could set $\overline{\boldsymbol{M}}_{d,t} = p_{d,t}(0)$, which gives the maximum consumption possible at demand node d in period t. In an analogous way we also linearize and reformulate all complementarity constraints in (A.45) - (A.64), which yields a more tractable problem formulation. Applying the results of the present and the previous section, the single-level reformulation of our bilevel model is given by the first-level objective that is subject to

(1) the original first-level constraints,
(2) the primal constraints of the second-level problem,
(3) the linearization constraints for the absolute flow value and the non-convex flow product,
(4) the linearized complementary slackness conditions, and
(5) the dual feasibility constraints.

We implemented this single-level mixed-integer program in Zimpl [see Koch (2004)] and used CPLEX [see CPLEX (2013)] as a solver.

A.6 On the effects of storage facilities on optimal pricing: A case study based on Chao and Peck (1998)

A.6.1 Six-node network

In this section we analyze the economic interdependencies between transmission and storage facility investments under different market environments including variants of our bilevel market model. We consider the standard six-node example of Chao and Peck (1998) that has frequently been used for various policy-related analysis including Ehrenmann and Smeers (2005) and Oggioni and Smeers (2013), or Grimm et al. (2016a). To this standard example we add storage as well as transmission facility investments in order to elaborate on these two investment dimensions.

As can be seen in Fig. A.4, the network consists of three demand nodes (node 3, node 5, and node 6) and three production nodes (node 1, node 2, and node 4) that are interconnected by 8 existing transmission lines. Storage facilities with constant losses of 10% may be built at the three demand nodes, respectively. Only the two lines that interconnect the north with the south have a limited capacity of 200 and 250 MWh, respectively. As the three nodes in the north (node 1 to node 3) are characterized by relatively low generation cost and a low demand, with the south (node 4 to node 6) having the opposite characteristics, trade will naturally take place from the north to the south. Therefore, we assume that each of the 2 constrained north-south transmission corridors can be strengthened by 4 new candidate lines with a capacity of 200, 220, 240, and 260 MWh, respectively. Corresponding investment cost amount to 17,500, 19,057.5, 20,580, and 22,067.5 $. In line with our theoretical framework introduced in the previous sections, we consider 24 periods that resemble fluctuations of a typically day. All relevant demand and production input data that characterizes the respective market participants is given in Fig. A.4.

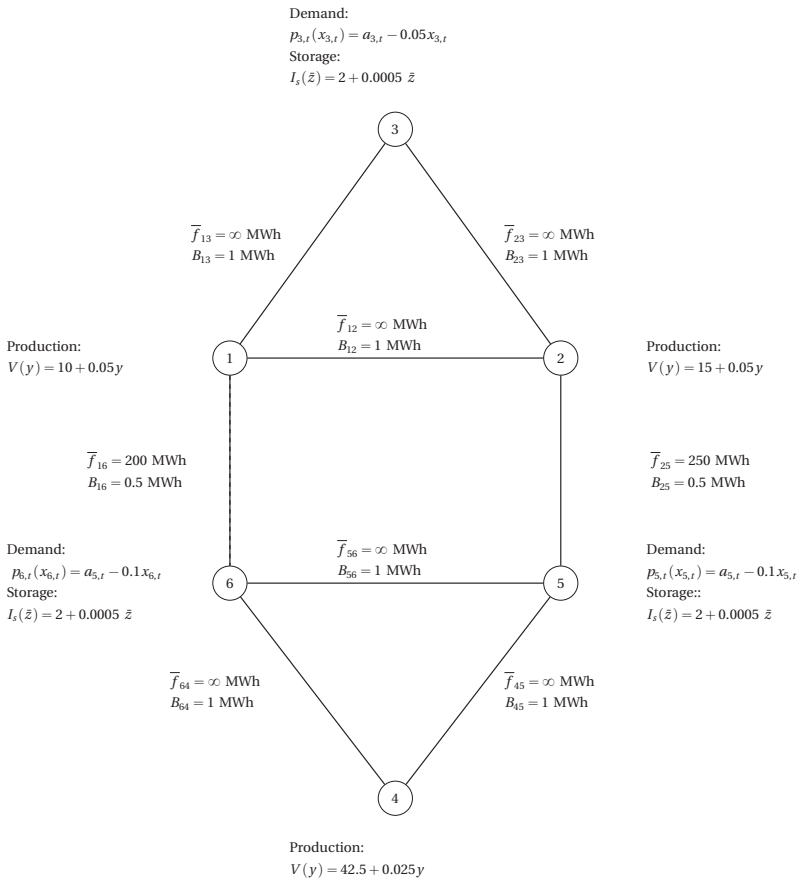

Figure A.4: Six-node network of Chao and Peck (1998) (demand fluctuations are modeled using location- and time-varying intercepts).

In particular, in this section we identify the optimal long-term combination of storage- and transmission-facility investments as to maximize welfare of an electricity system. In this context, we will evaluate

- the single-level nodal-pricing model (first benchmark),
- the single-level zonal pricing model (second benchmark), and
- the bilevel zonal pricing model

for the two cases of a traditional no-storage world as well as a world with endogenous storage facility investments, respectively. In the zonal pricing models, we will consider different zonal configurations and their effects on long-run investment behaviour.

A.6.2 Benchmark results

Integrated planning and nodal pricing
Let us first consider the nodal pricing, reference solution; see also Table A.2. In the no-storage case, the TSO invests in 4 out of the 8 candidate transmission lines. Welfare amounts to 2,373,564.93$. In the case where storage facility investments are possible, storages are built at all three nodes. Storage capacity investments at node 3 amount to 918.96 MWh, while at node 5 storage facility investments of 1590.42 MWh take place. At node 6 we observe storage investments of 1928.46 MWh. Thus, most storage capacities are installed in the consumption-intense south. Ultimately, these high storage facility investments in the south reduce line extensions as compared to the no-storage case, i.e., both the number of constructed transmission lines and their capacity reduces. Observe that these findings are in line with the results found in Conejo et al. (2017).

Table A.2: Solutions of the investment benchmark models.

	Nodal		Z^{3-3}	
Storages	No	Yes	No	Yes
Welfare	2,373,564.93	2,419,114.32	2,370,417.08	2,415,994.50
Line investment (1,6)				
Capacity 200 MWh	Yes	Yes	Yes	Yes
Capacity 220 MWh	Yes	Yes	Yes	Yes
Capacity 240 MWh	Yes	No	Yes	No
Capacity 260 MWh	No	No	No	No
Line investment (2,5)				
Capacity 200 MWh	No	No	No	No
Capacity 220 MWh	No	No	No	Yes
Capacity 240 MWh	No	Yes	No	No
Capacity 260 MWh	Yes	No	Yes	No
Storage investment				
Node 3	-	918.96	-	470.69
Node 5	-	1590.42	-	1751.21
Node 6	-	1928.46	-	1750.01

	Z^{4-2}	
Storages	No	Yes
Welfare	2,370,924.24	2,407,291.61
Line investment (1,6)		
Capacity 200 MWh	Yes	Yes
Capacity 220 MWh	Yes	Yes
Capacity 240 MWh	Yes	Yes
Capacity 260 MWh	No	No
Line investment (2,5)		
Capacity 200 MWh	No	No
Capacity 220 MWh	No	No
Capacity 240 MWh	No	Yes
Capacity 260 MWh	Yes	No
Storage investment		
Node 3	-	321.81
Node 5	-	1732.96
Node 6	-	1105.91

Ultimately, we note that under storage facilities welfare rises to 2,419,114.32 $. As expected, Fig. A.5 shows that the inclusion of storage facilities yields a smoothened inter-temporal price development at all three demand nodes.

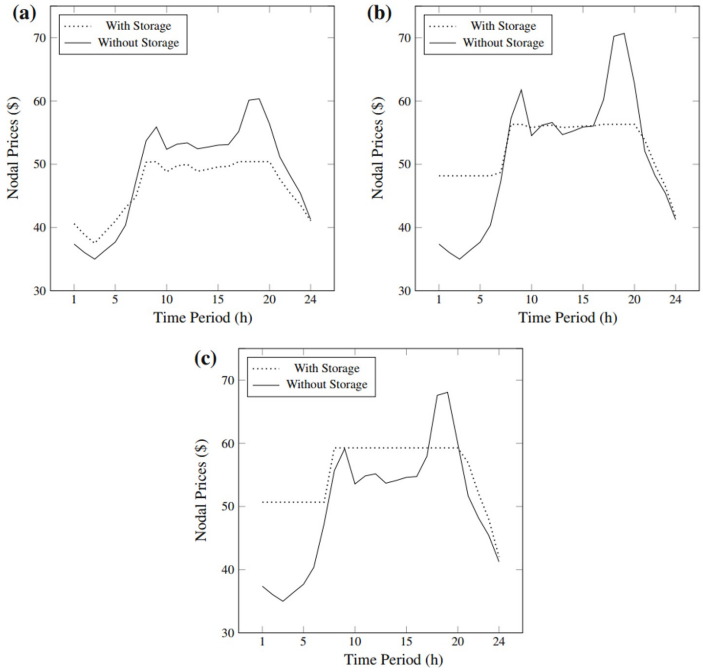

Figure A.5: Effects of storage facilities on nodal prices. (a) Node 3, (b) Node 5, (c) Node 6.

This reduction in the price volatility is mainly driven by the efficient use of the available storage facilities that are charged and discharged throughout the planning horizon as shown in Fig. A.6.

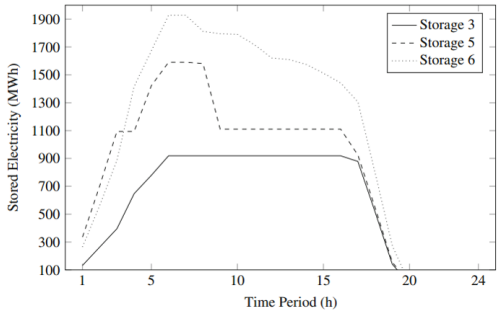

Figure A.6: Stored electricity (nodal pricing).

Therefore, storage facilities can serve as a prosumer to meet time-varying demand / generation and thus reduce high-peak period prices.

Single-level zonal pricing

In the case of our single-level zonal market model, similar to Oggioni and Smeers (2013), we evaluate both a 3-3 and 4-2 configuration, i.e., we consider the two cases of $Z^{3-3} = \{\{1,2,3\},\{4,5,6\}\}$ and $Z^{4-2} = \{\{1,2,3,6\},\{4,5\}\}$. Note that under the two zonal designs at least one inter-zonal line has a limited transmission capacity, which directly yields a regionally differentiated demand and generation structure; see also the thick lines in Fig. A.7.

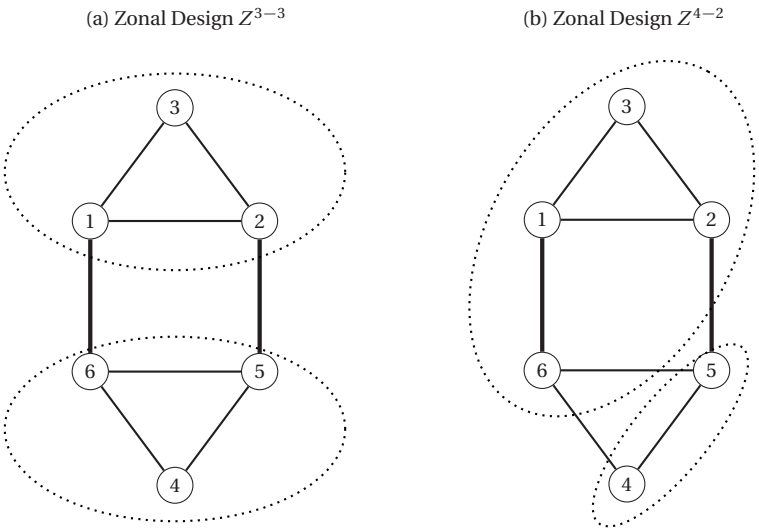

Figure A.7: Zonal design taken from Oggioni and Smeers (2013). (a) Zonal design Z^{3-3}, (b) Zonal design Z^{4-2}.

Like in the case of nodal pricing, in our single-level zonal pricing models storage facility investments allow for a welfare increase as compared to the case where no storage facilities are available. This holds for both zonal designs. Given the two zonal choices, in the no storage case the 4-2 zonal configuration is welfare maximizing. In contrast, in the case of storage facility investments, the 3-3 zonal design yields a higher welfare level as compared to the 4-2 configuration.

As can further be seen, zonal pricing disturbs optimal storage facility investment behaviour

of firms. In particular, in the north we observe an underinvestment in storage facilities, while at the southern nodes 5 and 6 we have both an over- and underinvestment in storage capacity, respectively. Ultimately, these inefficient storage facility investments are accompanied by inefficient transmission line investments. However, despite being inefficient, line investments tend to decrease in the presence of storages.

Table A.3: Solutions of the bilevel zonal pricing model.

	Z^{3-3}		Z^{4-2}	
Storages	No	Yes	No	Yes
Welfare	2,069,757.71	2,414,564.02	2,370,854.89	2,407,165.54
Network fee	0.84	0.89	1	0.46
TSO revenues	47,066.43	716,951.16	82,612.56	567,532.36
TSO expenses	17,500	57,137.50	79,205	79,205
TSO profits	29,566.43	659,813.66	3407.56	488,327.36
Line investment (1,6)				
Capacity 200 MWh	Yes	Yes	Yes	Yes
Capacity 220 MWh	No	Yes	Yes	Yes
Capacity 240 MWh	No	No	Yes	Yes
Capacity 260 MWh	No	No	No	No
Line investment (2,5)				
Capacity 200 MWh	No	No	No	No
Capacity 220 MWh	No	No	No	No
Capacity 240 MWh	No	Yes	No	No
Capacity 260 MWh	No	No	Yes	Yes
Storage investment				
Node 3	-	0	-	599.07
Node 5	-	2020.89	-	1476.41
Node 6	-	1698.21	-	989.16

A.6.3 Bilevel zonal market model

As in our reference models, under both zonal configurations storage facilities allow for a welfare increase as compared to the no-storage case; see also Table A.3. However, in the 3-3 zonal design no storage facility investments take place in the north. At the southern node 5 overinvestment in storage capacity increases to 2020.89 MWh. In direct consequence, the TSO increases his line investments as compared to the bilevel, no-storage case in order to being able to efficiently use the southern storage. Thus, storage facility investments may

also imply increased transmission facility investments. Accordingly, transmission fees increase in the case of storage facilities. Note that even though the constructed transmission lines are identical to nodal pricing line extensions, we observe inefficient private storage facility investments. Therefore, investment efficiency of one party does not ensure efficient investments of the other party.

If we consider the 4-2 configuration, storage facility investments now take place at all three nodes. However, storage facility investments are again inefficient as compared to the benchmarks. Interestingly, line investments are identical for the storage and for the no-storage case.

Again, as in the single-level zonal pricing model, the optimal zonal design changes with the introduction of storages. In the no-storage case the 4-2 zonal configuration is welfare maximizing over the two zonal choices. In contrast, in the case of storage facility investments the 3-3 zonal design yields a higher welfare level as compared to the 4-2 configuration. Thus, with the introduction of storage, the 3-3 zonal design becomes the welfare-maximizing configuration. This underlies that markets with increased storage facility investments may require an adjustment and reconfiguration of the current zonal design in order to ensure and maintain efficient market structures.

A.7 Conclusion and policy implications

Since storage and transmission facility investments can both potentially help to serve peak loads in times of a low-carbon transformation of the energy system, these two investment dimensions are highly interdependent. Therefore, in this paper we are the first to analyze the interplay of network extensions and storage facility investments in a multistage game. We translate the investment game into a mathematical bilevel model. In particular, on the first level we assume a transmission system operator (TSO) that decides on optimal network extensions and on a corresponding optimal network fee. On the second level we consider competitive firms that trade energy on zonal spot markets and invest in new storage facilities.

As we show, adequate storage investments of firms may in general have the potential to reduce line investments of the TSO. However, investments in a (zonal) market environment

may yield suboptimal results as compared to an integrated planning (nodal pricing) solution. As zonal pricing is currently applied in different regions and countries all around the world (see, e.g., Australia or Europe), these results call for a careful design of market structures that ensure efficient investment incentives of the different market players. In addition, in order to avoid inefficiently large grid investment, cost-intense network extension plans that are currently developed in various countries including Germany should take the interdependencies of line and storage facility investments into account.

Appendix: Sets, parameters, and variables

Tables A.4, A.5, and A.6 summarize the main sets, parameters, and variables used in this paper.

Table A.4: Sets.

Symbol	Description
$\mathscr{G}$	Electricity network
N	Set of network nodes
D	Set of demand nodes
L	Set of all transmission lines
L^{inv}	Set of candidate transmission lines
T	Set of time periods
Z	Price zone configuration
G	Set of generators
$G_n \subset G$	Set of generators located at node n
S	Set of storage facilities
$S_n \subset S$	Set of storage facilities located at node n
K	Set of network fees

Table A.5: Parameters.

Symbol	Description	Unit
$a_{n,t}$	Intercept of inverse demand function $p_{n,t}$	\$/MWh
e_s	Storage efficiency of facility s	%
$\overline{f}_l$	Transmission capacity of line l	MWh
B_l	Susceptance of line l	MWh
r	Number of price zones	1
i_l	Line investment cost for $l \in L^{\text{new}}$	\$

Table A.6: Variables and Derived Quantities.

Symbol	Description	Unit
$x_{n,t}$	Electricity demand at n in period t	MWh
$p_{n,t}$	Electricity price at n in period t	\$/MWh
$y_{g,t}$	Electricity generation of g in period t	MWh
$z^+_{s,t}$	Amount of electricity stored in at s in period t	MWh
$z^-_{s,t}$	Amount of electricity stored out at s in period t	MWh
$\bar{z}_s$	Invested storage capacity of facility s	MWh
$z_{s,t}$	Amount of stored electricity in s in period t	MWh
$f_{l,t}$	Power flow on line l in period t	MWh
$\lvert f_{l,t} \rvert$	Absolute flow value on line l in period t	MWh
$\Theta_{n,t}$	Phase angle value at node n in period t	rad
w_l	Decision variable for candidate line $l \in L^{\text{inv}}$	1
φ^{TSO}	Network fee	1
I^{TSO}	Income of TSO	\$
E^{TSO}	Expenses of TSO	\$
P^{TSO}	Profits of TSO	\$
I_s	Storage investment cost function	\$/MWh
$V_{g,t}$	Marginal generation cost function	\$/MWh
W	Aggregated welfare	\$

References

Alguacil, N., A. L. Motto, and A. J. Conejo (2003). "Transmission expansion planning: A mixed-integer LP approach". In: *IEEE Transactions on Power Systems* 18.3, pp. 1070–1077. DOI: 10.1109/TPWRS.2003.814891.

Baringo, L. and A. J. Conejo (2012). "Transmission and Wind Power Investment". In: *IEEE Transactions on Power Systems* 27.2, pp. 885–893. ISSN: 0885-8950. DOI: 10.1109/TPWRS.2011.2170441.

Bjørndal, E., M. Bjørndal, and H. Cai (2014). "Nodal pricing in a coupled electricity market". In: *European Energy Market (EEM), 2014 11th International Conference on the*. IEEE, pp. 1–6.

Bjørndal, M. and K. Jørnsten (2001). "Zonal pricing in a deregulated electricity market". In: *The Energy Journal*, pp. 51–73.

Bjørndal, M. and K. Jørnsten (2007). "Benefits from coordinating congestion management: The Nordic power market". In: *Energy Policy* 35.3, pp. 1978–1991.

Bjørndal, M., K. Jørnsten, and V. Pignon (2003). "Congestion management in the Nordic power market: Counter purchasers and zonal pricing". In: *Journal of Network Industries* 4.3, pp. 271–292.

Bohn, R. E., M. C. Caramanis, and F. C. Schweppe (1984). "Optimal pricing in electrical networks over space and time". In: *The Rand Journal of Economics*, pp. 360–376. JSTOR: 2555444.

Boucher, J. and Y. Smeers (2001). "Alternative models of restructured electricity systems, part 1: No market power". In: *Operations Research* 49.6, pp. 821–838. ISSN: 0030364X. DOI: 10.1287/opre.49.6.821.10017.

Boyd, S. and L. Vandenberghe (2004). *Convex optimization*. Cambridge: Cambridge University Press. ISBN: 0-521-83378-7.

Bucksteeg, M., K. Trepper, and C. Weber (2015). "Impacts of RES-generation and demand pattern on net transfer capacity: Implications for effectiveness of market splitting in Germany". In: *Generation Transmission and Distribution* 9.9, pp. 1510–1518.

Bunn, D. W. and F. S. Oliveira (2003). "Evaluating individual market power in electricity markets via agent-based simulation". In: *Annals of Operations Research* 121, pp. 57–77.

Campêlo, M. and S. Scheimberg (2005). “A simplex approach for finding local solutions of a linear bilevel program by equilibrium points”. In: *Annals of Operations Research* 138, pp. 143–157.

Chao, H.-P. and S. C. Peck (1996). “A market mechanism for electric power transmission”. In: *Journal of Regulatory Economics* 10.1, pp. 25–59.

Chao, H.-P. and S. C. Peck (1998). “Reliability management in competitive elctricity markets”. In: *Journal of Regulatory Economics* 14.2, pp. 189–200. DOI: 10.1023/A:1008061319181.

Colson, B., P. Marcotte, and G. Savard (2007). “An overview of bilevel optimization”. In: *Annals of Operations Research* 153.1, pp. 235–256.

Conejo, A. J., Y. Cheng, N. Zhang, and C. Kang (2017). “Long-term coordination of transmission and storage to integrate wind power”. In: *CSEE Journal of Power and Energy Systems* 3.1, pp. 36–43.

CPLEX (2013). *User’s Manual for CPLEX*. 12.6. IBM Corporation. Armonk, USA.

David, A. and F. Wen (2001). “Transmission planning and investment under competitive electricity market environment”. In: *Power Engineering Society Summer Meeting, 2001*. Vol. 3. IEEE, pp. 1725–1730.

Daxhelet, O. and Y. Smeers (2007). “The EU regulation on cross-border trade of electricity: A two-stage equilibrium model”. In: *European Journal of Operational Research* 181.3, pp. 1396–1412. ISSN: 0377-2217. DOI: 10.1016/j.ejor.2005.12.040.

Dempe, S. (2002). *Foundations of bilevel programming*. Springer.

Dempe, S. (2003). “Annotated bibliography on bilevel programming and mathematical programs with equilibrium constraints”. In: *Optimization* 52.3, pp. 333–359.

Dempe, S. and A. B. Zemkoho (2012). “Bilevel road pricing: theoretical analysis and optimality conditions”. In: *Annals of Operations Research* 196, pp. 223–240.

Dijk, J. and B. Willems (2011). “The effect of counter-trading on competition in electricity markets”. In: *Energy Policy* 39.3, pp. 1764–1773. ISSN: 03014215.

Ehrenmann, A. and Y. Smeers (2005). “Inefficiencies in European congestion management proposals”. In: *Utilities Policy* 13.2, pp. 135–152. DOI: 10.1016/j.jup.2004.12.007.

Fan, H., H. Cheng, and L. Yao (2009). “A bi-level programming model for multistage transmission network xpansion planning in competitive electricity market”. In: *Power and energy engineering conference*. Ed. by APPEEC 2009. Asia-Pacific.

Fortuny-Amat, J. and B. McCarl (1981). “A representation and economic interpretation of a two-level programming problem”. In: *Journal of the Operational Research Society* 32, pp. 783–792.

Galiana, F. D., A. J. Conejo, and H. A. Gil (2003). “Transmission network cost allocation based on equivalent bilateral exchanges”. In: *IEEE Transactions on Power Systems* 18.4, pp. 1425–1431.

Gallego, R. A., A. Monticelli, and R. Romero (1998). “Transmission system expansion planning by an extended genetic algorithm”. In: *IEEE Proceedings – Generation, Transmission and Distribution* 145.3, pp. 329–335. DOI: 10.1049/ip-gtd:19981895.

Garcés, L. P., A. J. Conejo, R. García-Bertrand, and R. Romero (2009). “A bilevel approach to transmission expansion planning within a market environment”. In: *Power Systems, IEEE Transactions on* 24.3, pp. 1513–1522.

Gast, N., J.-Y. Le Boudec, A. Proutière, and D.-C. Tomozei (2013). “Impact of storage on the efficiency and prices in real-time electricity markets”. In: *Proceedings of the 4th international conference on future energy systems*. ACM, pp. 15–26.

German Transmission System Operators (2017). *Grid development plan electricity 2030*. URL: https://%20www.netzentwicklungsplan.de/sites/default/files/paragraphs-files/NEP_2030_1_Entwurf_Teil1.pdf (Retrieved 03/2017).

Gil, H. A., E. L. Da Silva, and F. D. Galiana (2002). “Modeling competition in transmission expansion”. In: *IEEE Transactions on Power Systems* 17.4, pp. 1043–1049.

Glachant, J.-M. and V. Pignon (2005). “Nordic congestion’s arrangement as a model for Europe? Physical constraints vs. economic incentives”. In: *Utilities Policy* 13.2, pp. 153–162.

Grimm, V., A. Martin, M. Schmidt, M. Weibelzahl, and G. Zöttl (2016a). “Transmission and generation investment in electricity markets: The effects of market splitting and network fee regimes”. In: *European Journal of Operational Research* 254.2, pp. 493–509.

Grimm, V., A. Martin, M. Weibelzahl, and G. Zöttl (2016b). “On the long run effects of market splitting: Why more price zones might decrease welfare”. In: *Energy Policy* 94, pp. 453–467.

Hirst, E. and B. Kirby (2001). “Key transmission planning issues”. In: *The Electricity Journal* 14.8, pp. 59–70.

Hogan, W. (1992). “Contract networks for electric power transmission”. In: *Journal of Regulatory Economics* 4.3, pp. 211–242.

Hornnes, K. S., O. S. Grande, and B. H. Bakken (2000). "Main grid development planning in a deregulated market regime". In: *Power Engineering Society Winter Meeting, 2000. IEEE*. Vol. 2. IEEE, pp. 845–849.

Hu, X. and D. Ralph (2007). "Using EPECs to model bilevel games in restructured electricity markets with locational prices". In: *Operations Research* 55.5, pp. 809–827. DOI: 10.1287/opre.1070.0431.

Huppmann, D. and J. Egerer (2015). "National-strategic investment in European power transmission capacity". In: *European Journal of Operational Research* 247.1, pp. 191–203. DOI: 10.1016/j.ejor.2015.05.056.

Ishizuka, Y. and E. Aiyoshi (1992). "Double penalty method for bilevel optimization problems". In: *Annals of Operations Research* 34.1, pp. 73–88.

Jenabi, M., S. M. T. F. Ghomi, and Y. Smeers (2013). "Bi-level game approaches for coordination of generation and transmission expansion planning within a market environment". In: *IEEE Transactions on Power Systems* 28.3, pp. 2639–2650. DOI: 10.1109/TPWRS.2012.2236110.

Jeroslow, R. G. (1985). "The polynomial hierarchy and a simple model for competitive analysis". In: *Mathematical Programming* 32.2, pp. 146–164. DOI: 10.1007/BF01586088.

Kirschen, D. and G. Strbac (2004). "Transmission networks and electricity markets". In: *Fundamentals of Power System Economics*, pp. 141–204.

Koch, T. (2004). "Rapid mathematical programming". PhD thesis. Technische Universität Berlin. URL: http://opus.kobv.de/zib/volltexte/2005/834/.

Kuznia, L., B. Zeng, G. Centeno, and Z. Miao (2013). "Stochastic optimization for power system configuration with renewable energy in remote areas". In: *Annals of Operations Research* 210, pp. 411–432.

Mangasarian, O. L. (1988). "A simple characterization of solution sets of convex programs". In: *Operations Research Letters* 7.1, pp. 21–26.

Neuhoff, K., J. Barquin, J. W. Bialek, R. Boyd, C. J. Dent, and F. Echavarren (2013). "Renewable electric energy integration: Quantifying the value of design of markets for international transmission capacity". In: *Energy Economics* 40, pp. 760–772.

Oggioni, G. and Y. Smeers (2013). "Market failures of market coupling and counter-trading in Europe: An illustrative model based discussion". In: *Energy Economics* 35, pp. 74–87. DOI: 10.1016/j.eneco.2011.11.018.

Pozo, D., E. Sauma, and J. Contreras (2017). “Basic theoretical foundations and insights on bilevel models and their applications to power systems”. In: *Annals of Operations Research* 254.1-2, pp. 303–334.

Rious, V., J.-M. Glachant, Y. Perez, and P. Dessante (2008). “The diversity of design of TSOs”. In: *Energy Policy* 36.9, pp. 3323–3332.

Sariddichainunta, P. and M. Inuiguchi (2017). “Global optimality test for maximin solution of bilevel linear programming with ambiguous lower-level objective function”. In: *Annals of Operations Research* 256.2, pp. 285–304.

Sauma, E. E. and S. S. Oren (2006). “Proactive planning and valuation of transmission investments in restructured electricity markets”. In: *Journal of Regulatory Economics* 30.3, pp. 261–290. DOI: 10.1007/s11149-006-9012-x.

Sioshansi, R. (2010). “Welfare impacts of electricity storage and the implications of ownership structure”. In: *The Energy Journal*, pp. 173–198.

Sioshansi, R. (2014). “When energy storage reduces social welfare”. In: *Energy Economics* 41, pp. 106–116.

Sioshansi, R., P. Denholm, T. Jenkin, and J. Weiss (2009). “Estimating the value of electricity storage in PJM: Arbitrage and some welfare effects”. In: *Energy Economics* 31.2, pp. 269–277.

Sioshansi, R., S. H. Madaeni, and P. Denholm (2013). “A dynamic programming approach to estimate the capacity value of energy storage”. In: *IEEE Transactions on Power Systems* 29.1, pp. 395–403.

Steinke, F., P. Wolfrum, and C. Hoffmann (2013). “Grid vs. storage in a 100% renewable europe”. In: *Renewable Energy* 50, pp. 826–832. ISSN: 09601481.

Von Stackelberg, H. (2010). *Market structure and equilibrium*. Springer Science & Business Media.

Weibelzahl, M. (2017). “Nodal, zonal, or uniform electricity pricing: how to deal with network congestion”. In: *Frontiers in Energy* 11, pp. 210–232.

Weibelzahl, M. and A. Märtz (2018). “On the effects of storage facilities on optimal zonal pricing in electricity markets”. In: *Energy Policy* 113, pp. 778–794.

Zambrano, C. and Y. Olaya (2017). “An agent-based simulation approach to congestion management for the Colombian electricity market”. In: *Annals of Operations Research* 258, pp. 217–236.

Zare, M. H., J. S. Borreroo, B. Zeng, and O. A. Prokopyev (2017). “A note on linearized reformulations for a class of bilevel linear integer problems”. In: *Annals of Operations Research*, pp. 1–19.

Zugno, M., J. M. Morales, P. Pinson, and H. Madsen (2013). “A bilevel model for electricity retailers’ participation in a demand response market environment”. In: *Energy Economics* 36, pp. 182–197.

B The flexibility puzzle in liberalized electricity markets: Understanding flexibility investments under different risk attitudes

Stefano Coniglio[a], Stephanie Halbrügge[b], Alexandra Märtz[c], Martin Weibelzahl[d]

[a] Department of Economics, University of Bergamo, Via Dei Caniana 2, 35238 Bergamo, Lombardy, Italy.

[b] FIM Research Center for Information Management, University of Bayreuth, Branch Business & Informations Systems Engineering of the Fraunhofer FIT, Alter Postweg 101, 86159 Augsburg, Bavaria, Germany.

[c] Karlsruhe Institute of Technology (KIT), Institute for Industrial Production (IIP), Chair of Energy Economics, Hertzstraße 16, 76187 Karlsruhe, Germany.

[d] FIM Research Center for Information Management, University of Applied Sciences Augsburg, Branch Business & Informations Systems Engineering of the Fraunhofer FIT, Alter Postweg 101, 86159 Augsburg, Bavaria, Germany.

This paper is submitted to a scientific journal.

Abstract

In the past, the load-following operation of conventional power plants was a key characteristic of electricity systems and a main ingredient for system stability. In recent times, however, the steady growth of the share of highly-variable renewable energy sources has lead to a loss in electricity-production flexibility. To compensate for such a loss and ensure a successful low-carbon transformation with a secure electricity supply, electricity systems face a *flexibility puzzle* of deciding how to invest in (and exploit) alternative flexibility options in a highly uncertain environment, with uncertainties stemming from, e.g., unknown CO_2 prices. Among other, the main flexibility options in such a puzzle include: (i) transmission flexibility, (ii) storage flexibility, (iii) generation flexibility, and (iv) demand flexibility. In this paper, we address the flexibility puzzle by proposing a multi-stage Stackelberg game in which different players with different risk attitudes operate under uncertainty. Stage I accounts for public line investments made by a transmission system operator (TSO) in anticipation of private investments in storage and conventional backup generation facilities. These private investments take place at stage II and are based on expected spot-market profits, which are determined within a zonal spot market at stage III. Finally, stage IV accounts for the redispatch actions the TSO undertakes in the case he contracted spot market quantities can not be feasibly transmitted through the electricity network. We translate our proposed four-stage Stackelberg game into a four-level (equilibrium-finding) optimization problem and, from it, derive an equivalent single-level reformulation which we then solve to global optimality with a state-of-the-art spatial branch-and-bound solver. By means of a widely-adopted case study, we use our model to analyze the effects of different risk attitudes of public and private decision makers on long-run investments in the flexibility options we considered. Our work highlights the importance of taking uncertainties into account when making private flexibility investment decisions as well as within public policy making to ensure sufficient flexibility with an adequate mix of different flexibility options.

B.1 Introduction

Modern electricity systems are changing rapidly. While, in the past, the number of flexibly adjustable conventional power plants was sufficient to adapt electricity production to a time-varying consumer demand, the ongoing decarbonization of energy systems is leading to an increased share of volatile renewable energy sources. Despite their contribution to cleaner energy production with reduced carbon emissions, renewable sources are hardly

controllable and their production is not always available in the required quantity, at the needed place, and at the right time. For instance, the wind does not always blow with the predicted intensity and the sun does not always shine bright enough to satisfy the demand of electricity. Ultimately, the adoption of renewable sources leads to a loss of flexibility on the electricity-production side. Its mitigation requires finding future sources of flexibility to bridge the *flexibility gap* that an increasing share of renewables – together with a simultaneous phase-out of conventional power plants and the increased policy focus on energy independence – is causing.

In general terms, flexibility is defined as the capability of handling uncertainty and variability on the electricity demand or on the supply side (Ma et al., 2013; Lund et al., 2015). There are different options to increase the degree of flexibility in modern electricity systems. They typically ascribe to four categories: (i) transmission flexibility, (ii) storage flexibility, (iii) generation flexibility, and (iv) demand flexibility.

As for transmission flexibility, traditionally electricity grids were designed to connect a few large conventional power plants to the centralized high-voltage grid. In contrast to such traditional network structures, the emergence of many small-scale renewable sources has increased the need for a decentralised transportation system and for identifying new transmission corridors to supply new consumers and accommodate the additional (possibly bidirectional if storage is considered) energy flows that are due to the increased share of renewables. Transmission investments are, thus, needed to meet the requirements of modern electricity systems, and discussions around their development are ongoing in many countries worldwide (ENTSO-E, 2023). In Germany, for instance, north-south grid extensions are planned in order to allow for an increased transportation of a large portion of the electricity produced by Northern Germany wind farms to be delivered to Southern Germany consumption centres (German Transmission System Operators, 2017).

Large network expansion projects are inherently very cost-intensive. Besides this, expansion plans are often met with skepticism by the general public (often due to fear of a negative impact on the general population's health), which can lead to severe delays in carrying out network-expansion works (Komendantova and Battaglini, 2016). On the contrary, privately-invested, decentralized storage facilities can be utilized to supply additional flexibility to the system by better balancing consumer demand with an intermittent supply without expanding its transmission capacity. In particular, by allowing for shifting the production and demand of energy between different time periods, storage facilities can partially decouple

demand and supply in cases where the two cannot be matched in one point in time (Weitemeyer et al., 2016; Wogrin and Gayme, 2014). Despite significant technological progress in the past years, however, storages are currently quite expensive, limiting their market penetration.

Crucially, even in an optimal mix of storage and transmission flexibility, conventional generators may still be needed to guarantee some (flexibly-adjustable) conventional production as a form of backup to mitigate the variability of the renewable sources. Such conventional-production flexibility can be offered, for instance, by fast-responding technologies such as gas power plants, which can rapidly compensate for quick variations in power supply (Stolten et al., 2013).

Switching perspectives from generation to demand, a flexible demand can naturally follow an intermittent generation in a much better way than a completely inelastic one. As a consequence, an increased demand flexibility could directly improve the balancing of demand and supply within a preexisting electricity network. The role of demand-side management shows great promise, and it is indeed gaining a growing relevance in the current times of low-carbon transition (Fridgen et al., 2016; Fridgen et al., 2022; Heffron et al., 2020). Demand-side management can be helpful in both spot and redispatch markets. In spot markets, a flexible load allows for either shaving peaks of demand or for increasing the demand in periods with a low electricity price and a high supply of renewables (Keller et al., 2020). In redispatch markets, demand-side flexibility allows for altering the consumers' consumption profile whenever the spot market outcomes result in infeasible transmission flows. Although, in many countries, Transmission System Operators (TSOs) are still only implementing redispatch on the supply side (Grimm et al., 2021), demand flexibility has an enormous potential for a more efficient congestion management. Against this backdrop, demand-side flexibility will play a key role in the electricity systems of the future, especially for redispatch.

Given the high importance of choosing the right mix of flexibility options in modern electricity systems, policy makers must actively incentivize the efficient integration of new flexibility. Electricity-market regulation and the corresponding market design should, therefore, ensure an efficient short-run use of existing flexibility and support new long-run flexibility investments. The latter is of special relevance, as high investments will be needed to build and activate new flexible assets in near future. For example, in its annual report 2022, the

German Council of Economic Experts explicitly highlighted the need for flexibility investments [1], which was also stressed by the recent Report on Security of Supply of the German Network Agency [2]. The German Federal Government also announced that in its "Climate-neutral electricity-system" platform, the expansion and integration of flexibility options will be one of four key policy-relevant topics. At the European level, for example, the European Network of Transmission System Operators for Electricity (ENTSO-E) or the Agency for the Cooperation for Energy Regulators (ACER) regularly stress the importance of following a road-map to unlock sufficient flexibility potentials within the European energy transition and ensure corresponding investments [3] Here, policy makers must take the complex interdependencies between the different flexibility options into account and solve the corresponding **flexibility puzzle** in order to find a future-proof flexibility mix. In this paper, we call flexibility puzzle the problem of choosing the ”right” mix of flexibility options, which each have their own characteristics are described above.

As energy systems undergo fast and far-reaching transformations, they face many uncertainties regarding, e.g., the actual path to decarbonization or the speed and scale of electrification. For private investors, their risk attitude plays a major role in deciding on future flexibility investments. The role of risk was recently also stressed by the EU in its proposal to improve the Union's electricity market design.[4] Indeed, the level of risk aversion of the many players involved in the electricity market can drastically affect the number and location of flexibility assets that the players are actually willing to invest in. In such an investment context, a model that is purely risk-averse may not always be appropriate, as some private investors accept facing a certain level of risk to increase their profits. On the contrary, a *risk-seeking* attitude could cause excessive investments that, due to their risk nature, may not always be "robust". In order to appropriately model the flexibility-investment behavior of different market players, it is, therefore, crucial to incorporate the level of risk aversion of the involved players into energy-market models in an accurate and realistic manner (Ambrosius et al., 2022; Grimm et al., 2021; Grimm et al., 2019; Ambrosius et al., 2020).

In this paper. we analyze the flexibility puzzle in a liberalized electricity market under uncertainty as an investment game. In particular, we assume that the involved players form

[1] https://www.sachverstaendigenrat-wirtschaft.de/en/annualreport-2022.html
[2] https://www.bmwk.de/Redaktion/DE/Downloads/V/versorgungssicherheitsbericht-strom.pdf?__blob=publicationFile&v=4
[3] https://acer.europa.eu/Official_documents/Acts_of_the_Agency/Framework_Guidelines/FrameworkGuidelines/FG_DemandResponse.pdf
[4] https://eur-lex.europa.eu/legal-content/EN/TXT/HTML/?uri=CELEX:52023PC0148

rational expectations on the optimal response made by the players who make decisions after them in the form of a multi-stage Stackelberg game. This yields a multi-stage Stackelberg game in which the different players with different risk attitudes make decisions under uncertainty. It accounts for public line investments made by a TSO in anticipation of private investments in storage and conventional backup generation facilities (first stage). These private investments take place in the second stage based on expected spot-market profits, which are determined within a zonal spot market in the third stage. The fourth stage accounts for redispatch actions of a TSO in the case where contracted spot market quantities can not be transmitted through the electricity network.

We formulate the problem of computing an equilibrium in our four-stage Stackelberg game as a four-level optimization problem, which we then reformulate and solve to global optimality via a spatial branch-and-bound method. By relying on a well-known case study from the literature, we utilize our model to study the impact of the different options of flexibility investments under different risk attitudes and quantify possible inefficiencies.

The paper is organized as follows. Our modeling framework is introduced in Section B.2. Section B.3 presents our four-stage game. Section B.4 illustrates our approach for solving the equilibrium-finding problem. Section B.5 elaborates on different modeling approaches to account for the risk attitude of the players. The main results of our analysis are illustrated in Section B.6. Section B.7 concludes the paper and highlights its main policy implications.

B.2 Notation and economic quantities

This section introduces the main sets, parameters, and variables that are used throughout the paper. For the reader's convenience, a summary is provided in the Appendix in Tables B.4, B.5, and B.6.

We denote by $T = \{1,\dots,|T|\}$ the finite planning horizon under consideration. Ω denotes a discrete set of scenarios, each of which may for example be given by discrete CO_2 paths, development in renewables capacity expansions, or the degree of electrification. $p_\omega > 0$ is the probability that scenario $\omega \in \Omega$ realizes. In the following, we will assume that the realization of a scenario is completely known to each player at time $t = 1$.

Throughout the paper, decision variables reported without subscripts are assumed to be

vectors. For vectors of variables or constants that pertain to a specific scenario $\omega \in \Omega$, the scenario ω they belong to is denoted by the subscript ω. For instance, the post-redispatch consumption of customer c under scenario ω in period t is denoted by $\mathbf{d}_{ct\omega}$, and it may be either smaller, equal, or larger that the corresponding pre-redispatch consumption $d_{ct\omega}$. For convenience, the scenario set Ω is used as a subscript to denote the collection containing a vector per scenario.

B.2.1 Electricity network and network expansion

We consider an electricity network $\mathcal{G} = (N, L)$ consisting of a set N of network nodes (or buses) linked by different transmission lines L. In the context of zonal pricing, which is widely used in different regions such as Europe or Australia, we further assume that the node set N is partitioned into k connected and nonempty price zones $Z_1, \ldots, Z_k$ with indices in $\mathcal{Z} = \{1, \ldots, k\}$. The uniform pricing system with a uniform electricity price is obtained when $k = 1$.

We assume that each transmission line $\ell \in L$ be completely characterized by its maximal transmission capacity $\bar{f}_\ell \in \mathbb{R}_+$ and by its susceptance $B_\ell \in \mathbb{R}_+$. By $L^{\text{new}} \subset L$ we denote the set of new transmission lines that can be installed by the TSO via a suitable investment. $L^{\text{ex}} = L \setminus L^{\text{new}}$ denotes the complementary set of pre-existing lines.

In order to account for the large fixed costs associated with line expansion, we consider discrete line investment decisions modeled by a binary variable $k_\ell \in \{0, 1\}$, which is equal to 1 if and only if line $\ell \in L^{\text{new}}$ is built. The corresponding line investment costs are denoted by $i_\ell \in \mathbb{R}_+$.

B.2.2 Flexible electricity demand

We denote by $C \subseteq N$ the set of nodes where the consumers are located at. In line with the vast literature on energy market modeling, which includes, among others, Chao and Peck (1996), Bjørndal and Jørnsten (2001), Bjørndal et al. (2003), Ehrenmann and Smeers (2005), Bjørndal and Jørnsten (2007), Pechan (2017), and Weibelzahl and Märtz (2020), we assume

an *elastic long-term demand*. As such, for each time period t and demand Node $c \in C$, we introduce the following decreasing linear *inverse demand function*:

$$\pi_{ct\omega}(d_{ct\omega}) = a_{ct} - b_c d_{ct\omega},$$

where $d_{ct\omega}$ denotes the endogenous demand of consumer c in period t under scenario $\omega \in \Omega$. We note that changes in the demand behaviour between different time periods are exclusively modeled by the intercept $a_{ct} \geqslant 0$. In contrast, the slope $b_c \geqslant 0$ is assumed to be constant over time (it only varies between different demand nodes c) – this is a standard assumption in literature; see, e.g., Grimm et al. (2016) and Ambrosius et al. (2020). For notational convenience, we introduce a variable $d_{nt\omega}$ for each $n \in N$ even if $n \notin C$. For all such variables, we assume a demand function with intercept $a_{ct} = 0$.

For each scenario $\omega \in \Omega$, we express the *gross consumer surplus* as the total monetary consumer benefit aggregated over all demand nodes $c \in C$ and time periods $t \in T$:

$$\sum_{t\in T}\sum_{c\in C}\int_0^{d_{ct\omega}} \pi_{ct\omega}(h)\mathrm{d}h = \sum_{t\in T}\sum_{c\in C}\left(a_{ct} - \frac{b_c}{2} d_{ct\omega}\right).$$

As one can see, such function is concave and it achieves its (unique) maximum at $d_{ct\omega} = \frac{a_{ct}}{b_c}$.

B.2.3 Electricity generation and storage

Inelastic generation of renewable energy sources

We denote by R the set of carbon-neutral, renewable power generators that are available throughout the grid. For all $n \in N$, the subset R_n describes the renewable generators which are located at Node n. We denote the maximum power output in each time period $t \in T$ and for each scenario $\omega \in \Omega$ of the renewable generator of index $r \in R$ by $\bar{x}_{rt\omega}$. We assume that such a value is subject to the conditions captured by the scenario ω. The actual power output is modeled by the continuous variable $x_{rt\omega} \geqslant 0$. As usually done in the literature, we assume that renewable energy is produced at a zero variable cost.

Flexible generation of conventional (backup) facilities

We denote the set of conventional generation facilities by G. Such facilities act as a backup to compensate for the intermittent renewable energy production. For all $n \in N$, we denote by $G_n \subseteq G$ the subset of conventional generators located at Node n.

We characterize the production of each generator $g \in G$ by the variable production cost $v_g > 0$. For each generator $g \in G$, the amount of conventionally-produced electricity in period $t \in T$ under scenario $\omega \in \Omega$ is modeled by the continuous variable $y_{gt\omega} \in \mathbb{R}_+$.

We further partition the set of generation facilities G in two sets, with $G = G^{\text{ex}} \cup G^{\text{new}}$, where G^{ex} is the set of pre-existing generators and G^{new} the set of candidate generators in whose construction the private investors can invest. For each candidate generator $g \in G^{\text{new}}$, we assume an investment cost of i_g per unit of installed generation capacity $\bar{y}_g$.

Storage facilities

We denote by $S = S^{\text{ex}} \cup S^{\text{new}}$ the set of storage facilities, where S^{ex} is the set of pre-existing facilities and S^{new} is the set of candidate facilities which can be build via private investment. For a given Node $n \in N$, $S_n \subseteq S$ denotes the set of storage facilities located at n.

From a technical point of view, each storage facility is completely described by its roundtrip storage efficiency $e_s \in [0,1]$ as well as by a pair of upper and lower bounds $\hat{z}_s \in \mathbb{R}^+$ and $\check{z}_s \in \mathbb{R}^+$ on the amount of electricity that can be charged into or discharged from the facility during a single time period.

Throughout the paper, we consider four types of storage-related variables. For each $s \in S$, $\bar{z}_s \in \mathbb{R}_+$ denotes the newly invested storage capacity. For each $s \in S$, $t \in T$, and $\omega \in \Omega$, $\hat{z}_{st\omega} \in [0, \bar{z}_s]$ and $\check{z}_{st\omega} \in [0, \bar{z}_s]$ denote the amount of electricity discharged or charged from/to the storage facility s in period t under scenario ω. For each $s \in S$, $t \in T$, and $\omega \in \Omega$, $z_{st\omega} \in \mathbb{R}_+$ denotes the storage level at the end of period t under scenario ω.

For each non pre-existing storage facility $s \in S^{\text{new}}$, its construction requires an investment cost of i_s per unit of installed storage capacity $\bar{z}_s$.

B.2.4 Zonal spot market dispatch

We assume a *available transfer-capacity-based (ATC-based) market coupling*, in which the firms that belong to one of the given zonal spot markets $Z_1, \ldots, Z_k$ receive price signals that incentivize them to account for the inter-zonal network capacity in such a way that the inter-zonal transfer capacities are satisfied. Intra-zonal transmission bounds and phase angles are completely ignored when the spot market clears. Such a commonly applied market coupling – see, e.g., Grimm et al. (2016) – translates into a set of spot-market power-flow variables $f_{\ell t \omega} \in \mathbb{R}_+$ defined for all lines $\ell \in L$ that interconnect two nodes belonging to different zones Z_i and Z_j, $i \neq j$. For the ease of notation, we define L^{inter} as the set of inter-zone transmission lines, either pre-existing or subject to investment.

As both intra-zonal capacities and phase angles are ignored at the market clearing phase, the spot market outcome does not guarantee that the network will be balanced and, as a consequence, a subsequent redispatch phase may be required.

B.2.5 Redispatch

On the redispatch market, the TSO adjusts all the contractually agreed spot market volumes to ensure a feasible electricity flow that minimizes the arising redispatch costs. Post-redispatch volumes may either be smaller, equal, or larger than the corresponding pre-redispatch ones.

Throughout the paper, boldface variables describe quantities whose value is determined after redispatch: the post-redispatch power flow for line $\ell \in L$, time period $t \in T$, and scenario $\omega \in \Omega$ is denoted by $\boldsymbol{f}_{\ell t \omega}$; the post-redispatch phase angle of a Node $n \in N$ in time period $t \in T$ and scenario $\omega \in \Omega$ is denoted by $\boldsymbol{\Theta}_{nt\omega}$; the post-redispatch renewable and conventional production as well as demand at Node $n \in N$ at time $t \in T$ under scenario $\omega \in \Omega$ are denoted by $\boldsymbol{x}_{nt\omega}$, $\boldsymbol{y}_{nt\omega}$, and $\boldsymbol{\Theta}_{nt\omega}$, respectively.

As it is the case in, for instance, Germany, we assume a cost-based redispatch which is, by design, profit neutral for both firms and consumers. For this reason, no player can make profits on it.

B.3 A four-level market model with zonal pricing

With the liberalization of electricity markets, private firms have become free to decide on their own (flexibility) investments and to freely trade electricity on the market.

In this section, we introduce a four-stage investment game of Stackelberg type, which captures the interdependent and sequential nature of the decision-making structure of real-world electricity markets. While complex, a model of such nature is necessary since, as argued in the literature Grimm et al. (2016), a single-stage formulation that accounts for the simultaneous decision on line, storage, and backup generation investments with a single decision maker cannot capture the nature of the different investment dimensions.

At Stage I, a benevolent decision maker (the TSO) decides on a set of network extensions with the aim of maximizing the expected welfare. The TSO forms rational (in the game-theoretic sense) expectations on how the other players (private firms and consumers) will make their decisions in reaction to the chosen network extension plan so as to be able to quantify its impact on welfare. In doing so, the TSO directly influences the expected future returns on the investment in storage and backup generation facilities that are made by the private investors at Stage II as well as, indirectly, the outcome of the two markets at Stages III and IV. The monetary returns on the private firms' investments made at Stage II are determined as a consequence of the result of the competitive zonal spot market, which is modeled to explicitly take into account the inter-regional line extensions made by the TSO at Stage I. Such a market is cleared at Stage III. If the spot market volumes that were determined at the market-clearing stage are technically infeasible (i.e., electricity cannot be feasibly transmitted through the network as doing so would violate one or more transmission capacities), the TSO undertakes a cost-based redispatch action to balance supply and demand in such a way that the network constraints are satisfied and the network is balanced. The redispatch that the TSO organizes to do so is modeled at Stage IV.

The sequential decision-making structure of the four-stage Stackelberg game we propose is summarized as follows:

- Stage I: The TSO decides on a network extension plan by which new transmission lines are added.
- Stage II: Private firms make investment decisions w.r.t. their storage and backup generation capacity.

- Stage III: For each scenario in Ω and time period $t \in T$, the electricity-production and electricity-storage firms trade electricity on the corresponding spot market.
- Stage IV: For each scenario in Ω and time period $t \in T$, redispatch takes place.

We consider two options for modeling the risk attitude of the decision makers involved in the game: risk-neutrality, which we model via stochastic optimization techniques, and risk-aversion, which we model via robust optimization techniques. For a in-depth overview of these techniques, we refer the reader to Shapiro et al. (2021). For the relationship between robust/stochastic optimization and multi-stage/multi-level problems, see the survey Bolusani et al. (2020).

B.3.1 Stage I: public line investments

For a given scenario $\omega \in \Omega$, at Stage I the benevolent TSO chooses a line expansion plan that maximizes the following scenario-dependent *post-redispatch welfare function*:

$$\phi^1_\omega(k, \bar{y}, \bar{z}, \mathbf{y}_\omega, \mathbf{d}_\omega) = \underbrace{\sum_{t \in T} \left(\sum_{c \in C} \int_0^{\mathbf{d}_{ct\omega}} \pi_{ct\omega}(h) \mathrm{d}h - \sum_{g \in G} v_g \mathbf{y}_{gt\omega} \right)}_{q_\omega(\boldsymbol{y}_\omega, \boldsymbol{d}_\omega)} \underbrace{- \sum_{\ell \in L^{\text{new}}} i_\ell k_\ell}_{h(k)} \underbrace{- \sum_{g \in G^{\text{new}}} i_g \bar{y}_g - \sum_{s \in S^{\text{new}}} i_s \bar{z}_s}_{g(\bar{y}, \bar{z})}.$$

The function consists of three terms: the post-redispatch *endogenous gross consumer benefit* $q_\omega(\boldsymbol{y}_\omega, \boldsymbol{d}_\omega)$, which depends on the consumer demand variables $\boldsymbol{d}_\omega$ and the (variable) post-redispatch production cost $\boldsymbol{y}_\omega$, the *fixed costs* $h(k)$ associated with the public line expansions, and the *private investment costs* $g(\bar{y}, \bar{z})$ in generation (y) and storage (z).

The k variables (which are the only variables that are directly controlled by the TSO at Stage I) are constrained to satisfy a set of integrality constraints by belonging to the following feasible region:

$$\mathscr{F}_1 = \{k_\ell \in \{0,1\}, \ell \in L^{\text{new}}\}.$$

We remark that, for each scenario $\omega \in \Omega$, the first-level utility function ϕ^1_ω does not depend just on the k variables, but also on those variables whose value is set by the decision makers

that control the subsequent levels of the four-stage Stackelberg game, e.g., the variables $\bar{y}$, $\bar{z}$, $\mathbf{y}_\omega$, and $\mathbf{d}_\omega$.

B.3.2 Stage II: private storage and generation investments

The second stage accounts for the flexibility investments that are made by the private firms. In line with Boucher and Smeers (2001), Daxhelet and Smeers (2007), Grimm et al. (2016), and Weibelzahl (2017), we assume that every firm acts in a *perfectly competitive environment* as a price taker, which implies that none of them can strategically affect the prices. This assumption is realistic as the energy transition comes with a large number of new active players on electricity markets, and has been established as an economic standard to keep complex electricity market models computationally tractable and assess possible deviations from the perfect competition benchmark (Jenabi et al., 2013; Grimm et al., 2016).

As the cost-based redispatch that we will model at Stage IV is, by design, profit neutral for both firms and consumers, all the private investment decisions that are made at Stage II are independent of the redispatch action. It follows that, besides the first-stage investments in generation and storage, only the anticipation of the spot market profits (determined at Stage III) will have an impact on the decisions taken at Stage II by the private firms.

For a given scenario $\omega \in \Omega$, the decision-making problem collectively faced by the private firms at Stage II calls for maximizing the following *spot-market welfare function*:

$$\phi^2_\omega(\bar{y},\bar{z},y_\omega,d_\omega) = \underbrace{\sum_{t\in T}\left(\sum_{c\in C}\int_0^{d_{ct\omega}}\pi_{ct\omega}(h)\mathrm{d}h - \sum_{g\in G} v_g\, y_{gt\omega}\right)}_{q_\omega(y_\omega,d_\omega)} \underbrace{- \sum_{g\in G^{\text{new}}} i_g\,\bar{y}_g - \sum_{s\in S^{\text{new}}} i_s\,\bar{z}_s}_{g(\bar{y},\bar{z})}.$$

In contrast to the Stage I post-redispatch welfare function ϕ^1_ω, the spot-market welfare function ϕ^2_ω depends via the endogenous gross consumer benefit function q_ω on the spot-market volumes rather than on the post-redispatch ones (i.e., on y_ω, d_ω rather than on $\mathbf{d}_\omega, \mathbf{y}_\omega$) and it ignores the line expansion costs (which, from the perspective of the Stage II decision makers, are sunken). The dependence on the investment costs via the function g is retained. Notice that ϕ^2_ω depends on the y_ω and d_ω variables, whose value is determined

at the next stage and which, in turn, is affected by $\bar{y}$ and $\bar{z}$.

The investment variables $\bar{y}, \bar{z}$ are constrained to take nonnegative values by belonging in the following feasible region:

$$\mathscr{F}_2 = \left\{ \begin{array}{lll} (\bar{y}, \bar{z}) \in \mathbb{R}^{|G^{\text{new}}|} \times \mathbb{R}^{|S^{\text{new}}|} : & \bar{y}_g \geqslant 0 & g \in G^{\text{new}} \\ & \bar{z}_s \geqslant 0 & s \in S^{\text{new}} \end{array} \right\}.$$

B.3.3 Stage III: spot market trade

At Stage III, competitive spot market trade takes place for each time period $t \in T$ and scenario $\omega \in \Omega$. The market quantities that are revenue-relevant at this stage and whose value is determined at this stage are y_ω and d_ω, together with the corresponding storage quantities $z_\omega, \hat{z}_\omega, \check{z}_\omega$ and the inter-zonal spot-market flow variables f_ω.

As already mentioned, we assume that the scenario reveals itself completely at time $t = 0$ to each player. As such, we assume that the bids made by the private companies for each time period are all collected before the market-clearing phase starts. Due to this assumption, we assume w.l.o.g. that a single market-clearing problem which encompasses the whole time horizon is solved. Other assumptions of considering, for instance, a rolling-horizon model where the market is cleared at each time $t \in T$ with a discounted penalty on the future states $t+1, \ldots, |T|$ could clearly be taken into account (albeit at the cost of complicating the model).

As it is standard in the literature Hasan et al. (2008) and Sensfuß et al. (2008), we assume a *merit order ranking*. According to it, the spot-market outcomes of each scenario are determined by the market by maximizing the difference between the gross consumer benefit and the variable costs of power production. This coincides with maximizing for each scenario $\omega \in \Omega$ the following *spot-market welfare function*:

$$\phi^3_\omega(y_\omega, d_\omega) = \underbrace{\sum_{t \in T} \left(\sum_{c \in C} \int_0^{d_{ct\omega}} \pi_{ct\omega}(h) \mathrm{d}h - \sum_{g \in G} v_g y_{gt\omega} \right)}_{q_\omega(y_\omega, d_\omega)}.$$

We remark that, for a given scenario $\omega \in \Omega$, such a function also coincides with the spot-market welfare function ϕ^2_ω that is maximized at level two after dropping the sunken generation and storage investment costs.

As the scenarios in Ω are independent at this stage, we have $|\Omega|$ individual and independent problems, one per scenario, each of which is parametric in the first- and second-stage variables.

Since, as mentioned before, the cost-based redispatch at Stage IV is assumed to be profit neutral for both firms and consumers, the decisions made at Stage III are independent from it and, thus, no Stage IV variables appear at this stage.

The spot-market trading variables must belong in the following feasible region, which is parametric in k, $\bar{y}$ and $\bar{z}$, and also dependent on the scenario ω due to featuring the scenario-dependent constant term $\bar{x}_{rt\omega}$:

$$
\begin{aligned}
&\mathscr{F}^3_\omega(k,\bar{y},\bar{z}) = \\
&\Bigg\{(x_\omega, y_\omega, d_\omega, f_\omega, z_\omega, \hat{z}_\omega, \check{z}_\omega) \in \mathbb{R}^{|G^{\text{new}}|}\times\mathbb{R}^{|G^{\text{ren}}|}\times\mathbb{R}^{|G^{\text{con}}|}\times\mathbb{R}^{|S|}\times\mathbb{R}^{|S|}\times\mathbb{R}^{|C|} : \\
&\sum_{n\in Z_i}\Bigg(\sum_{r\in R_n} x_{rt\omega} + \sum_{g\in G_n} y_{gt\omega} + \sum_{s\in S_n}\check{z}_{st\omega} - \sum_{s\in S_n}\hat{z}_{st\omega}\Bigg) = \\
&\qquad = \sum_{n\in Z_i} d_{nt\omega} - \sum_{\ell\in\delta^{\text{out}}_{Z_i}(L)} f_{\ell t\omega} + \sum_{\ell\in\delta^{\text{in}}_{Z_i}(L)} f_{\ell t\omega} \qquad i\in\mathscr{Z}, t\in T, \qquad \text{(B.1)}\\
&z_{st\omega} = \sum_{i=1}^{t} e_s\hat{z}_{si\omega} - \sum_{i=1}^{t}\check{z}_{si\omega} \qquad s\in S, t\in T, \qquad \text{(B.2)}\\
&\check{z}_{st\omega} \leqslant z_{s,t-1,\omega} \qquad s\in S, t\in T, \qquad \text{(B.3)}\\
&z_{s0\omega} = 0 \qquad s\in S, \qquad \text{(B.4)}\\
&-\overline{f}_\ell \leqslant f_{\ell t\omega} \leqslant \overline{f}_\ell \qquad \ell\in L^{\text{ex}}\cap L^{\text{inter}}, t\in T, \qquad \text{(B.5)}\\
&-\overline{f}_\ell k_\ell \leqslant f_{\ell t\omega} \leqslant \overline{f}_\ell k_\ell \qquad \ell\in L^{\text{new}}\cap L^{\text{inter}}, t\in T, \qquad \text{(B.6)}\\
&0 \leqslant x_{rt\omega} \leqslant \bar{x}_{rt\omega} \qquad r\in R, t\in T, \qquad \text{(B.7)}\\
&0 \leqslant y_{gt\omega} \leqslant \bar{y}_g \qquad n\in N, g\in G_n, t\in T, \qquad \text{(B.8)}\\
&0 \leqslant z_{st\omega} \leqslant \bar{z}_s \qquad s\in S, t\in T\Bigg\}. \qquad \text{(B.9)}
\end{aligned}
$$

Constraints (B.2)–(B.4) are the storage constraints. Constraints (B.5)–(B.9) impose suitable bounds on the spot market demand, generation, storage, and inter-zonal flow variables. *Zonal balance* is modeled by introducing a balance equation for each zone of the network via Constraints (B.1). These constraints involve the consumer demand, the electricity generated by both renewable and conventional sources, the electricity which is charged and discharged in each zone, and the inter-zonal power flows. We note that, while the $z_{st\omega}$ variable can be dropped by backward substitution, doing so would make the formulation denser, leading, according to our preliminary experiments, to a harder to solve problem.

Since, as mentioned before, intra-zonal power flows and phase angles are ignored at this stage, an ex-post redispatch may be necessary.

B.3.4 Stage IV: redispatch

At Stage IV, the TSO undertakes a minimum-cost redispatch activity for each scenario $\omega \in \Omega$:

$$\sum_{t\in T}\left(\sum_{c\in C}\int_{d_{ct\omega}}^{\mathbf{d}_{ct\omega}}\pi_{ct\omega}(h)\mathrm{d}h-\sum_{g\in G}v_g(\mathbf{y}_{gt\omega}-y_{gt\omega})\right).$$

For each point in time $t \in T$ and consumer $c \in C$, the term $\int_{\mathbf{d}_{ct\omega}}^{d_{ct\omega}}\pi_{ct\omega}(h)$ accounts for the loss of gross consumer benefit if $\mathbf{d}_{ct\omega} \leqslant d_{ct\omega}$ or for its increment if $\mathbf{d}_{ct\omega} \geqslant d_{ct\omega}$ caused by the redispatch adjustment. In addition, each term $v_g(\mathbf{y}_{gt\omega} - y_{gt\omega})$ takes into account the additional variable production costs of the firms that are called on the redispatch market if $\mathbf{y}_{gt\omega} \geqslant y_{gt\omega}$ or the associated production-cost reduction if $\mathbf{y}_{gt\omega} \leqslant y_{gt\omega}$.

Since minimizing the above redispatch cost is equal to maximizing its opposite, we define the following Stage-IV utility function:

$$\phi^4_\omega(y_\omega,d_\omega,\mathbf{y}_\omega,\mathbf{d}_\omega)=\underbrace{\sum_{t\in T}\left(\sum_{c\in C}\int_{d_{ct\omega}}^{\mathbf{d}_{ct\omega}}\pi_{ct\omega}(h)\mathrm{d}h-\sum_{g\in G}v_g(\mathbf{y}_{gt\omega}-y_{gt\omega})\right)}_{q_\omega(\boldsymbol{y}_\omega,\boldsymbol{d}_\omega)-q_\omega(y_\omega,d_\omega)},$$

which, by nature, coincides with the difference between $q_\omega(\boldsymbol{y}_\omega,\boldsymbol{d}_\omega)$ and $q_\omega(y_\omega,d_\omega)$.

Assuming the widely adopted Direct Current (DC) power flow formulation, for each scenario $\omega \in \Omega$ the Stage IV feasible region reads:

$$
\begin{aligned}
&\mathscr{F}^4_\omega(k, \bar{y}, \hat{z}_\omega, \check{z}_\omega) = \\
&\Big\{ (\boldsymbol{x}_\omega, \boldsymbol{y}_\omega, \boldsymbol{d}_\omega, \boldsymbol{f}_\omega, \boldsymbol{\Theta}_\omega) \in \mathbb{R}^{|G^{\text{con}}|} \times \mathbb{R}^{|C|} \times \mathbb{R}^{|L|} \times \mathbb{R}^{|N|} : \\
&\boldsymbol{d}_{nt\omega} = \sum_{r \in R_n} \bar{x}_{rt\omega} + \sum_{g \in G_n} \boldsymbol{y}_{gt\omega} + \sum_{s \in S_n} (\check{z}_{st\omega} - \hat{z}_{st\omega}) + \\
&\qquad + \sum_{\ell \in \delta^{\text{in}}_n(L)} \boldsymbol{f}_{\ell t\omega} - \sum_{\ell \in \delta^{\text{out}}_n(L)} \boldsymbol{f}_{\ell t\omega} && n \in N, t \in T, && \text{(B.10)} \\
&-\overline{f}_\ell \leqslant \boldsymbol{f}_{\ell t\omega} \leqslant \overline{f}_\ell && \ell \in L^{\text{ex}}, t \in T, && \text{(B.11)} \\
&-\overline{f}_\ell k_\ell \leqslant \boldsymbol{f}_{\ell t\omega} \leqslant \overline{f}_\ell k_\ell && \ell \in L^{\text{new}}, t \in T, && \text{(B.12)} \\
&\boldsymbol{f}_{\ell t\omega} = B_\ell(\boldsymbol{\Theta}_{nt\omega} - \boldsymbol{\Theta}_{mt\omega}) && \ell = (n,m) \in L^{\text{ex}}, t \in T, && \text{(B.13)} \\
&-M^-_\ell(1-k_\ell) \leqslant \boldsymbol{f}_{\ell t\omega} - B_\ell(\boldsymbol{\Theta}_{nt\omega} - \boldsymbol{\Theta}_{mt\omega}) \leqslant M^+_\ell(1-k_\ell) \\
&\qquad && \ell = (n,m) \in L^{\text{new}}, t \in T, && \text{(B.14)} \\
&\boldsymbol{\Theta}_{1t\omega} = 0 && t \in T, && \text{(B.15)} \\
&0 \leqslant \boldsymbol{\Theta}_{nt\omega} \leqslant 2\pi && n \in N, t \in T, && \text{(B.16)} \\
&0 \leqslant \boldsymbol{x}_{rt\omega} \leqslant \bar{x}_{rt\omega} && r \in R, t \in T, && \text{(B.17)} \\
&0 \leqslant \boldsymbol{y}_{gt\omega} \leqslant \bar{y}_g && n \in N, g \in G_n, t \in T, && \text{(B.18)} \\
&\boldsymbol{d}_{ct\omega} \geqslant 0 && c \in C, t \in T, && \text{(B.19)} \\
&\boldsymbol{d}_{nt\omega} = 0 && n \in N \backslash C, t \in T \Big\}. && \text{(B.20)}
\end{aligned}
$$

Constraints (B.11) and (B.12) guarantee that the power flow $\boldsymbol{f}_{\ell t\omega}$ on each line $\ell \in L$ does not exceed the line's transmission capacity (also accounting for any potential transmission extensions). Constraints (B.13) and (B.14) rely on Kirchhoff's Second Law to determine the value of the power flow for each line $\ell = (n,m)$ via the corresponding phase angle variables $\boldsymbol{\Theta}_{nt\omega}$ and $\boldsymbol{\Theta}_{mt\omega}$. In Constraints (B.14), M^+_ℓ and M^-_ℓ are two "big M" parameters large enough to guarantee that the constraints corresponding to the lines $\ell \in L^{\text{new}}$ are inactive whenever $w_\ell = 0$. Both are set to tight values. Indeed, we set $M^+_\ell := \overline{f}_\ell$ (which is an upper bound on $\boldsymbol{f}_{\ell t\omega} - B_\ell(\boldsymbol{\Theta}_{nt\omega} - \boldsymbol{\Theta}_{mt\omega})$ attained at $\boldsymbol{f}_{\ell t\omega} = \overline{f}_\ell$ and $\boldsymbol{\Theta}_{nt\omega} - \boldsymbol{\Theta}_{mt\omega} = 0$) and $M^-_\ell := -\overline{f}_\ell - B_\ell 2\pi$ (which is a lower bound on $\boldsymbol{f}_{\ell t\omega} - B_\ell(\boldsymbol{\Theta}_{nt\omega} - \boldsymbol{\Theta}_{mt\omega})$ attained at $\boldsymbol{f}_{\ell t\omega} = -\overline{f}_\ell$, $\boldsymbol{\Theta}_{nt\omega} = 2\pi$, and $\boldsymbol{\Theta}_{mt\omega} = 0$). In order to ensure that the power flows are unique, Constraints (B.15) set to 0 the phase angle of Node 1, which is an arbitrary node chosen w.l.og. as reference. According to Kirchhoff's First Law, Constraints (B.10) model the power balance at every node, explicitly

accounting for nodal injections and withdrawals. In such constraints, $\delta_n^{\text{in}}(L)$ and $\delta_n^{\text{out}}(L)$ are the sets of, respectively, ingoing and outgoing lines from each Node $n \in N$.

We remark that, in line with many real-world markets, our formulation does not encompass the post-redispatch adjustment of the storage values.

B.4 Problem formulation under different risk attitudes

We assume that the risk attitude of each player is public so that, when anticipating a player's decision, every other player knows it.

The role of the decisions taken at Stages III and IV is to assign a return on investment to the Stage-I and Stage-II investment variables, scenario by scenario. In this sense, Stages III and IV are only instrumental insomuch as they allow the decision makers of the game (the TSO and the firms) to predict the outcome of the spot and redispatch markets in each scenario as a function of the strategic decisions they make at Stages I and II. Therefore, rather than considering an instance of the Stage-III and Stage-IV problems for each scenario $\omega \in \Omega$, we can w.l.o.g. consider the only scenarios that are relevant to match the player's Stage-I and Stage-II risk attitude. In particular, the risk attitude of Stage III and Stage IV will match the risk attitudes of, respectively, the Stage I and Stage II.

We introduce the the following generalized formulation of our four-stage game:

$$
k \in \operatorname{argmax}\left\{
\begin{array}{l}
\mathscr{A}^{I}\left(\{q_\omega(\boldsymbol{y}_\omega, \boldsymbol{d}_\omega)\}_{\omega\in\Omega}\right) + h(k) + g(\bar{y}, \bar{z}) \\
\text{s.t. } k \in \mathscr{F}^1 \\
(\bar{y}, \bar{z}) \in \operatorname{argmax}\left\{
\begin{array}{l}
\mathscr{A}^{II}\left(\{q_\omega(y_\omega, d_\omega)\}_{\omega\in\Omega}\right) + g(\bar{y}, \bar{z}) \\
\text{s.t. } (\bar{y}, \bar{z}) \in \mathscr{F}^2 \\
\begin{pmatrix} x_\omega, y_\omega, \\ z_\omega, \hat{z}_\omega, \\ \check{z}_\omega, d_\omega \end{pmatrix} \in \operatorname{argmax}\left\{
\begin{array}{l}
q_\omega(y_\omega, d_\omega) \\
\text{s.t. } (x_\omega, y_\omega, z_\omega, \hat{z}_\omega, \check{z}_\omega, \boldsymbol{d}_\omega) \in \mathscr{F}^3_\omega(k, \bar{y}, \bar{z}) \\
\begin{pmatrix} \boldsymbol{x}_\omega, \boldsymbol{y}_\omega, \\ \boldsymbol{d}_\omega, \boldsymbol{f}_\omega, \\ \boldsymbol{\Theta}_\omega \end{pmatrix} \in \operatorname{argmax}\left\{
\begin{array}{ll}
q_{\omega^{IV}}(\boldsymbol{y}_\omega, \boldsymbol{d}_\omega) - [q_\omega(y_\omega, d_\omega)] \\
\text{s.t. } (\boldsymbol{x}_\omega, \boldsymbol{y}_\omega, \boldsymbol{d}_\omega, \boldsymbol{f}_\omega, \boldsymbol{\Theta}_\omega) \in \\
\qquad \mathscr{F}^4_\omega(w, \bar{y}, \hat{z}, \check{z})
\end{array}
\right\} \forall \omega \in \Omega
\end{array}
\right\} \forall \omega \in \Omega
\end{array}
\right\}
\end{array}
\right\}.
\tag{B.21}
$$

In the formulation, $\mathscr{A}^{I}\left(\{q_\omega(\boldsymbol{y}_\omega, \boldsymbol{d}_\omega)\}_{\omega\in\Omega}\right)$ and $\mathscr{A}^{II}\left(\{q_\omega(y_\omega, d_\omega)\}_{\omega\in\Omega}\right)$ model the risk attitude of, respectively, the TSO (Stage I decision maker) and the firms (Stage II decision makers). The letter $\mathscr{A}$ stands for *attitude* as in "risk attitude" and, based on the risk attitude of the TSO and the firms, the two functions $\mathscr{A}^{I}$ and $\mathscr{A}^{II}$ coincide with either the expected

or the minimum value over Ω of, respectively, $q_\omega(\boldsymbol{y}_\omega, \boldsymbol{d}_\omega)$ (for the TSO) and $q_\omega(y_\omega, d_\omega)$ (for the firms).

In the formulation, the additive term $q_\omega(y_\omega, d_\omega)$ of Stage IV is reported in brackets as, due to it being constant w.r.t. the variables of this stage, it cannot affect the optimality of its solutions and, thus, it can be w.l.o.g. dropped.

B.5 Equilibrium-finding approaches

In this section, we show how to simplify the hierarchical nature of the proposed four-stage game into that of a two-stage game, and propose a bilevel-programming formulation for computing its equilibria. We will then recast the obtained bilevel problem into an equivalent (in terms of globally optimal solutions) single-level problem solvable to global optimality via a state-of-the-art spatial branch-and-bound method.

B.5.1 Understanding the internal relationships of the model

To better analyze the interplay between the different stages of the four-stage game, their decision variables, and the anticipation that is made at any stage of index i on the outcome of any stage of index $j > i$, we introduce the notion of a *Hierarchical Interaction Diagram* (HID). The HID of the proposed four-stage game is reported in Figure B.1. We compactly refer to the corresponding game as $[I \mid II \mid III \mid IV]$.

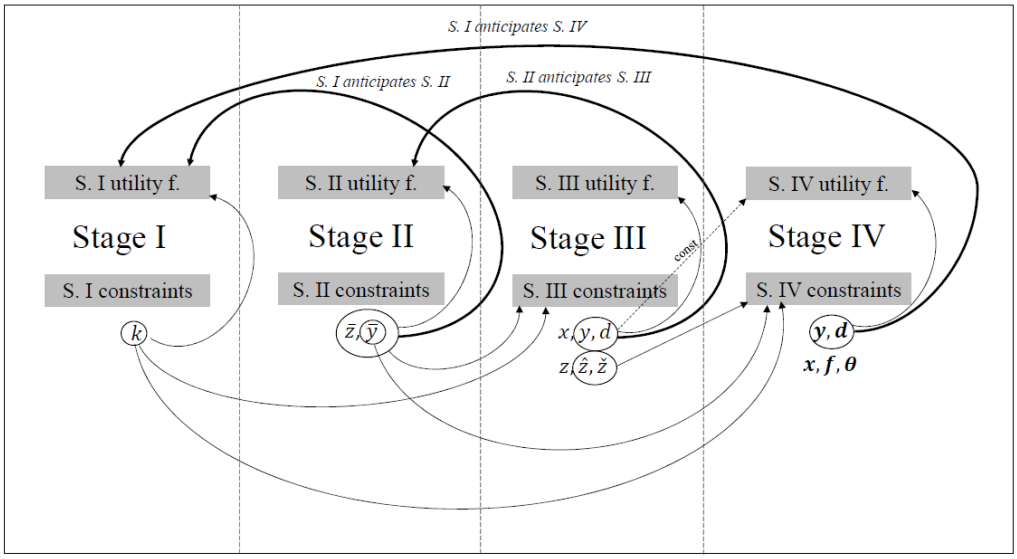

Figure B.1: HID of the proposed four-stage game $[I \mid II \mid III \mid IV]$.

The diagram displays the set of decision variables that are controlled at each stage of index i and what utility functions and constraint sets belonging to any stage of index j, with either $j > i$ or $j < i$, depend on them. The diagram is vertically split across stages. In each stage, the upper gray block represents the stage's utility (objective) function and the lower gray block its constraints set. The variables controlled at each stage are reported below the latter block.

In the diagram, a *forward arc* (i.e., left to right) between a variable of stage i and either the utility function or the constraint set of a stage of index $j > i$ indicates that stage j is parametric w.r.t. such a variable and that, in particular, stage j can observe the value that stage i assigns to such a variable before making its utility-maximizing decisions. A *backward arc* (i.e., an arc from right to left—we report it in a thicker line for greater readability) between a variable of a stage j and either the utility function or the constraint set of a stage of index $i < j$ indicates that the decisions at stage i are made in anticipation of the value that will be set at stage j for such a variable.

In the HID in Figure B.1, the forward arc between the (y, d) variables of Stage-III and the Stage-IV utility function is reported as a dashed line and labeled "const" as these variables only contribute to the Stage-IV utility function by an additive term which does not depend

on the Stage-IV variables. As such, the corresponding arc can (and will from now on) be dropped.

From the HID, we observe that there are no backward arcs from Stage IV to Stage III, which signifies that no Stage-III decisions are made in anticipation of the outcome of Stage IV. We also observe the lack of backward arcs not only from Stage IV to Stage III, but also from Stage IV to Stage II. Therefore, the only stage that anticipates the outcome of Stage IV is Stage I.

B.5.2 Equivalent two-stage game

In the following, we make the optimistic assumption that, if a stage admits several optimal solutions, the one that yields the best objective function value for the preceding stage(s) is chosen.

We start our analysis with the following proposition:

Proposition 1 *The four-stage game* $[I \mid II \mid III \mid IV]$ *reported in Figure B.1 can be transformed into the equivalent three-stage game* $[I \mid II + III \mid IV]$ *reported in Figure B.2, where Stages II and III are aggregated into the single Stage* $II + III$ *whose utility function coincides with the one of Stage II and whose constraint and variable set is the union of those of Stages II and III.*

Proof 1 *The result is proven by showing that any equilibrium sub-strategy* $(z^*, y^*, d^*, z^*, \hat{z}^*, \check{z}^*)$ *of the game* $[I \mid II + III \mid IV]$ *is optimal not only for its (combined) Stage* $II + III$*, but also for Stage III of the original game* $[I \mid II \mid III \mid IV]$ *(notice that, as Stage IV does not depend on Stage III, the Stage IV strategy is irrelevant and, hence, ignored here).*

Let us assume by contradiction that this is not the case and that there is a Stage-III equilibrium sub-strategy of the original game $[I \mid II \mid III \mid IV]$ *which satisfies* $\mathscr{A}^{II}\left(\{q_\omega(y_\omega^{**}, d_\omega^{**})\}_{\omega\in\Omega}\right) > \mathscr{A}^{II}\left(\{q_\omega(y_\omega^{*}, d_\omega^{*})\}_{\omega\in\Omega}\right)$*. If this is the case, the Stage-II utility function of the game* $[I \mid II + III \mid IV]$ *takes value* $\mathscr{A}^{II}\left(\{q_\omega(y_\omega^{**}, d_\omega^{**})\}_{\omega\in\Omega}\right) - g(\bar{y}^{**}, \bar{z}^{**}) > \mathscr{A}^{II}\left(\{q_\omega(y_\omega^{*}, d_\omega^{*})\}_{\omega\in\Omega}\right) - g(\bar{y}^{*}, \bar{z}^{*})$ *(notice that* g *is scenario-independent and, thus, it does not depend on the risk attitude of the players). This implies that* $(z^*, y^*, d^*, z^*, \hat{z}^*, \check{z}^*)$ *leads to a unilateral deviation and, as such, it does not belong to an equilibrium strategy of the three-stage game* $[I \mid II + III \mid IV]$*, leading to a contradiction.*

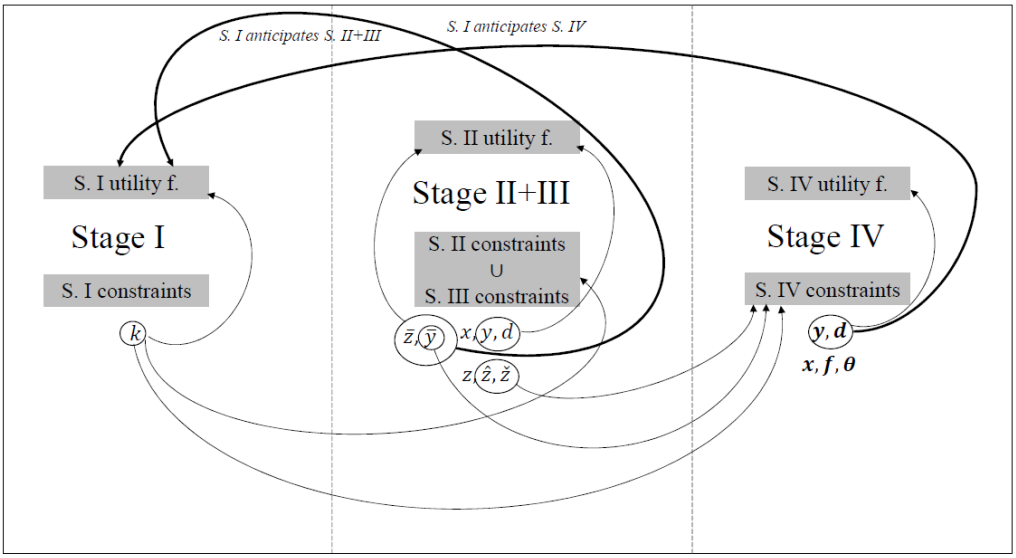

Figure B.2: HID of the three-stage game $[I \mid II + III \mid IV]$.

Next, we establish the following:

Proposition 2 *The three-stage game* $[I \mid II + III \mid IV]$ *reported in Figure B.2 can be transformed into the equivalent two-stage game* $[I + IV \mid II + III]$ *reported in Figure B.3, where Stages I and IV are aggregated into the single Stage* $I + IV$ *whose utility function coincides with the one of Stage I and whose constraint and variable set is the union of those of Stages I and IV.*

Proof 2 *First, we note that, as one can see from the diagram in Figure B.2, Stage* $II + III$ *does not anticipate Stage* IV*. This implies that, w.l.o.g., Stage* $II + III$ *of the game* $[I \mid II + III \mid IV]$ *can be further combined with Stage IV into the single Stage* $II + III - IV$*, where the dash* $-$ *signifies that the merged Stage* $II + III$ *and Stage* IV *take place simultaneously. This leads to the game* $[I \mid II + III - IV]$.

Next, we show that, in any equilibrium of the two-stage game $[I + IV \mid II + III]$ *of the claim, the sub-strategy* $(\boldsymbol{y}^*, \boldsymbol{d}^*, \boldsymbol{f}^*, \boldsymbol{\Theta}^*)$ *is optimal for Stage IV of the game* $[I \mid II + III - IV]$*. Let us assume by contradiction that this is not the case and that there is an equilibrium* $(k^*, \bar{y}^*, \bar{z}^*, z^*, y^*, d^*, z^*, \hat{z}^*, \check{z}^*, \boldsymbol{y}^{**}, \boldsymbol{d}^{**}, \boldsymbol{f}^{**}, \boldsymbol{\Theta}^{**})$ *of the game* $[I \mid II + III - IV]$ *where the Stage IV strategy* $(\boldsymbol{y}^{**}, \boldsymbol{d}^{**}, \boldsymbol{f}^{**}, \boldsymbol{\Theta}^{**})$ *satisfies* $\mathscr{A}^I\left(\{q_\omega(\boldsymbol{y}^{**}_\omega, \boldsymbol{d}^{**}_\omega)\}_{\omega\in\Omega}\right) > \mathscr{A}^I\left(\{q_\omega(\boldsymbol{y}^{*}_\omega, \boldsymbol{d}^{*}_\omega)\}_{\omega\in\Omega}\right)$*. If this is the case, the utility function of Stage* $I + IV$ *in the game* $[I +$

$IV \mid II+III]$ *takes value* $\mathscr{A}^I\left(\{q_\omega(\boldsymbol{y}^{**}_\omega, \boldsymbol{d}^{**}_\omega)\}_{\omega\in\Omega}\right) - h(k^*) - g(\bar{y}^*, \bar{z}^*) > \mathscr{A}^I\left(\{q_\omega(\boldsymbol{y}^{*}_\omega, \boldsymbol{d}^{*}_\omega)\}_{\omega\in\Omega}\right) - h(k^*) - g(\bar{y}^*, \bar{z}^*)$. *This implies that* $(\boldsymbol{y}^*, \boldsymbol{d}^*, \boldsymbol{f}^*, \boldsymbol{\Theta}^*)$ *does not belong to an equilibrium strategy of the game* $[I+IV \mid II+III]$*: a contradiction.*

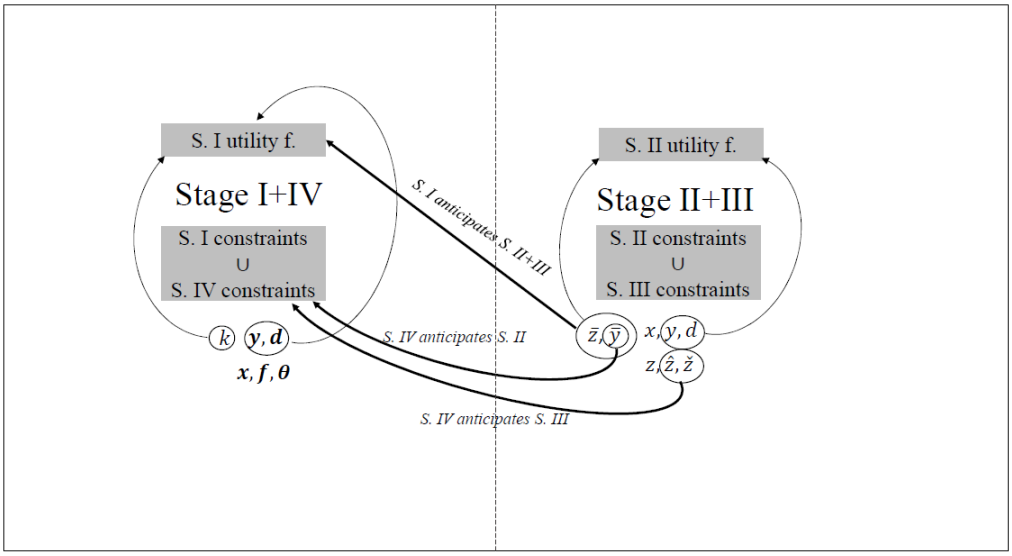

Figure B.3: Hierarchical interaction diagram of the two-stage game $[I+IV \mid II+III]$.

B.5.3 Equilibrium-finding bilevel problem and single-level reformulation

Thanks to the previous propositions, we obtain the following theorem:

Theorem 3 *The problem of computing an equilibrium in the proposed four-stage game can be cast as the following bilevel optimization problem:*

$$\left(\begin{array}{c} k, \\ \boldsymbol{y}_\Omega, \boldsymbol{d}_\Omega, \\ \boldsymbol{f}_\Omega, \boldsymbol{\Theta}_\Omega \end{array}\right) \in \operatorname{argmax} \left\{ \begin{array}{l} \mathscr{A}^I(\{q_\omega(\boldsymbol{y}_\omega, \boldsymbol{d}_\omega) - h(k) - g(\bar{y}, \bar{z})\}_{\omega\in\Omega}) \quad s.t. \\ k \in \mathscr{F}^1 \\ (\boldsymbol{y}_\Omega, \boldsymbol{d}_\Omega, \boldsymbol{f}_\Omega, \boldsymbol{\Theta}_\Omega) \in \bigtimes\limits_{\omega\in\Omega} \mathscr{F}^4_\omega(k, \bar{y}, \hat{z}_\omega, \check{z}_\omega) \\ \left(\begin{array}{c} \bar{y}, \bar{z}, \\ x_\Omega, y_\Omega, z_\Omega, \\ \hat{z}_\Omega, \check{z}_\Omega, d_\Omega \end{array}\right) \in \operatorname{argmax} \left\{ \begin{array}{l} \mathscr{A}^{II}(\{q_\omega(y_\omega, d_\omega)\}_{\omega\in\Omega}) - g(\bar{y}, \bar{z}) \quad s.t. \\ (\bar{y}, \bar{z}) \in \mathscr{F}^2 \\ (x_\Omega, y_\Omega, z_\Omega, \hat{z}_\Omega, \check{z}_\Omega, d_\Omega) \in \bigtimes\limits_{\omega\in\Omega} \mathscr{F}^3_\omega(k, \bar{y}, \bar{z}) \end{array} \right\} \end{array} \right\}. \tag{B.22}$$

The second-level problem in the bilevel problem (B.22) features a concave objective function (to be maximized), continuous variables, linear constraints, and linear or quadratic-convex constraints. Therefore, the lower-level problem is a convex optimization problem. This implies that its KKT conditions are both necessary and sufficient, and that every feasible solution of its KKT system is a global optimum of the problem.

Thanks to this, we can reformulate the bilevel problem as an equivalent single-level problem by substituting for the second-level problem its KKT system. For the sake of brevity, we do not report the whole KKT system here under the different choices of risk attitudes.

We, nevertheless, point out a peculiarity that occurs in the case where the Stage II players have a risk-averse attitude. In such a case, the equilibrium-finding problem features the following constraint:

$$\eta \leqslant \left(\sum_{t\in T} \left(\sum_{c\in C} \int_0^{d^{spot}_{ct\omega}} \pi_{ct\omega}(h)\mathrm{d}h - \sum_{g\in G} v_{gw} y^{spot}_{gt\omega} \right) + \right. \\ \left. - \sum_{g\in G^{\text{new}}} i_g \bar{y}_g - \sum_{s\in S^{\text{new}}} i_s \bar{z}_s \right) \quad \forall \omega \in \Omega, \tag{B.23}$$

where η is a new variable (being maximized) which is constrained to be no larger than the value taken by the welfare function under each scenario $\omega \in \Omega$. Letting ϖ_ω be the dual variable of such a constraint, the corresponding complementarity constraint featured in the KKT system of the lower-level problem reads:

$$0 \leqslant \left(\sum_{t\in T} \left(\sum_{c\in C} \int_0^{d^{spot}_{ct\omega}} \pi_{ct\omega}(h)\mathrm{d}h - \sum_{g\in G} v_{gw} y^{spot}_{gt\omega} \right) + \right. \\ \left. - \sum_{g\in G^{\text{new}}} i_g \bar{y}_g - \sum_{s\in S^{\text{new}}} i_s \bar{z}_s \right) - \eta \perp \varpi_\omega \geqslant 0 \quad \forall \omega \in \Omega. \tag{B.24}$$

Due to the worst-case nature of risk-aversion, Constraint (B.23) features among its terms what would otherwise be an objective function in the risk-neutral case (the welfare function under scenario $\omega \in \Omega$). Differently from the latter (risk-neutral) case, in which the KKT system contains the first derivative of such a function, in the risk-averse case the function shows up in its original (undifferentiated) form within Constraint (B.24). If the corresponding complementarity constraint is formulated as $\left(\sum_{t\in T} \left(\sum_{c\in C} \int_0^{d^{spot}_{ct\omega}} \pi_{ct\omega}(h)\mathrm{d}h - \right.\right.$

$\sum_{g\in G} \upsilon_{gw} y_{gt\omega}^{spot}\Big) - \sum_{g\in G^{\text{new}}} i_g \bar{y}_g - \sum_{s\in S^{\text{new}}} i_s \bar{z}_s - \eta\Big)\varpi_\omega = 0$ for all $\omega \in \Omega$, one obtains a (non-convex) constraint of degree 3, which will make solving the problem computationally much harder. We will discuss a way to circumvent such an issue in the next section.

B.6 Case study: Numerical results and discussion

Our model is coded in the Zimpl algebraic modeling language (Koch, 2001) and solved to global optimality with the spatial branch-and-bound method implemented in Gurobi 9.5. The experiments are run on an Intel(R) Core(TM) i7-6500U with 8 GB of RAM using 4 threads.

From a computational perspective, we formulate the complementarity conditions in the KKT system of the lower level problem as special ordered set of type 1 (SOS1) constraints. This allows for stating them without the need for introducing any further non-linearities to the formulation thanks to letting the (spatial) branch-and-bound solver branch on each pair of expressions involved in a complementary constraint without having to introduce binary variables to model their intrinsic disjunction and potentially incorrect big-M terms—for an in-depth discussion of this aspect, we refer the reader to Kleinert et al. (2020). This, in particular, circumvents the issue we mentioned at the end of the previous section related to the 3rd degree convex constraint.

B.6.1 Description of the six-node network of Chao and Peck (Chao and Peck, 1998)

Our case study is based on the widely adopted six-node network of Chao and Peck (1998), which has been established as a standard in many policy-related studies. Examples of such studies include, among others, Ehrenmann and Smeers (2005), Oggioni and Smeers (2013), Grimm et al. (2016), and Weibelzahl and Märtz (2020).

The six-node network is depicted in Figure B.4. As one can see from it, the network features six nodes linked by eight (pre-existing) transmission lines. Nodes 1, 2, and 3 are located in the North, while nodes 4, 5, and 6 are located in the South. The northern and southern subnetworks are connected by the two transmission lines $\ell = (1,6)$ and $\ell = (2,5)$, with a transmission capacity of 200 MWh and 250 MWh, respectively. The transmission capacity of the other lines is assumed to be infinite. The three nodes 3, 5, and 6 (highlighted in gray

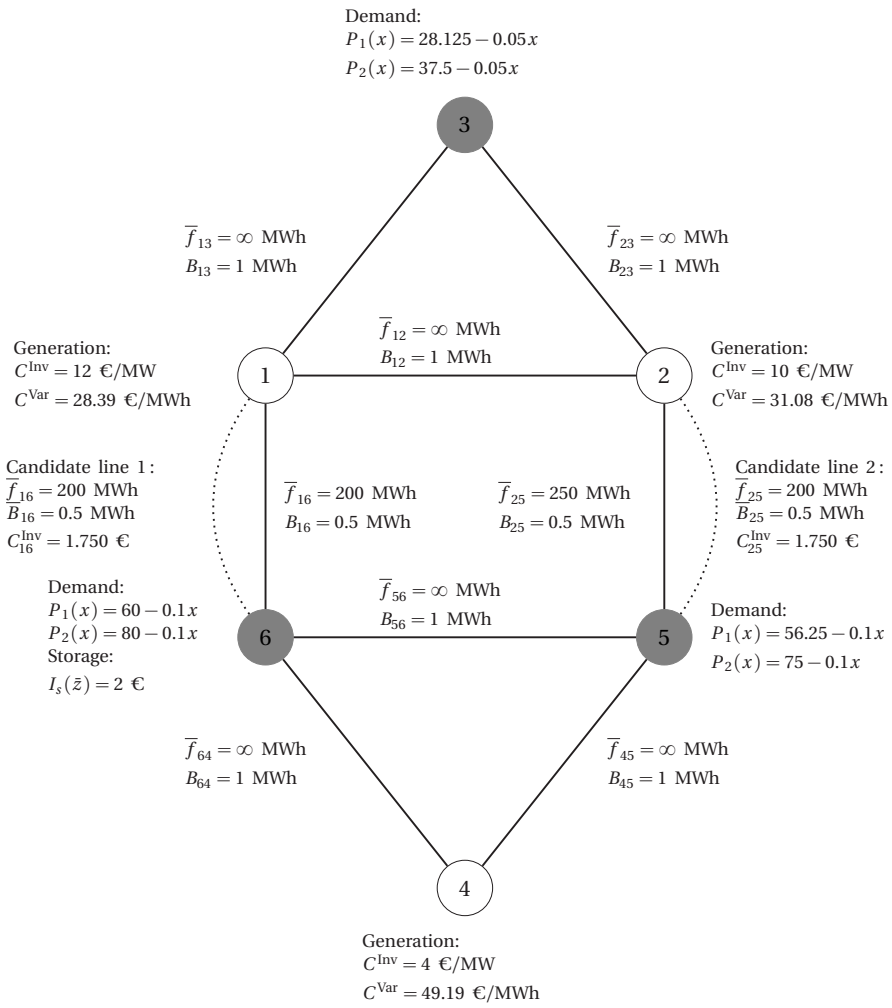

Figure B.4: Six-Node Network of Chao and Peck (1998) in the base scenario.

in the figure) are the three consumption centres of the network. Electricity generation can take place at the remaining nodes 1, 2, and 4.

To be able to analyze the flexibility puzzle described in this paper, we extend the original six-node network of Chao and Peck (1998) by several aspects, such as fluctuating demand as well as generation and grid investments, as described in the following.

In our case study, we consider $|T| = 2$ time periods, reflecting an on-peak and off-peak period. The demand functions of the on-peak time period ($t = 2$) are taken from the original six-node network, as described in Chao and Peck (1996). We create the demand functions of the off-peak time period ($t = 1$) from real-world demand data of the German electricity market, by adjusting the intercepts of the original demand functions by a factor 0.75 and in this way inducing the corresponding demand variation. Note that, in our setup, the total consumption at the two southern nodes 5 and 6 exceeds the consumption at the northern node 3. As a consequence, the southern subnetwork acts as a stylized version of the Southern-German demand centres consisting of Bavaria and Baden-Würtemberg.

With respect to the conventional generation side, in our case study we assume that there are no existing conventional generators, but we explicitly model conventional back-up generation investments. Similarly to the real-world German electricity system, in the six-node network the two northern generation nodes 1 and 2 are characterized by cheaper conventional generation technologies compared to the southern one (node 4). In line with Grimm et al. (2016), we assume that the three generators at nodes 1, 2, and 4 are candidate conventional generation facilities that can attract investments from private firms.

In contrast, renewable capacities are given as parameters at node 1, 2, and 4. The corresponding time-dependent, renewable generation availability (as a percentage of the given installed capacity), which is for instance driven by weather conditions, is modeled by the temporal availability factors. We use real-world data from the feed-in of renewables from the four German TSOs (50 Hertz, Amprion, TenneT, and TransnetBW). Overall, we assume that, out of a total installed renewable capacity of 100 MW, 44% takes place at node 1, 31% at node 2, and 25% at node 4.

We also assume that the private firms may decide to invest in new storage facilities at node 6 to inter-temporally balance volatile electricity feed-in across time periods.

Finally, we assume that two new transmission lines can be built in parallel to lines $l = (1,6)$ and $l = (2,5)$ to strengthen the north-south links. More detailed information on the demand, generation, storage, and transmission parameters is given in Figure B.4.

B.6.2 Uncertainties and related scenario definition

We consider five scenarios with a uniform probability distribution ($p_\omega = \frac{1}{5}$ for all $\omega \in \Omega$). Scenario $\omega = 1$ is taken as the base scenario. We assume three sources of long-run uncertainty (i.e., three *uncertainty dimensions*) that affect the investments in generation, storage, and transmission facilities, and construct Scenarios $\omega = 2$ to $\omega = 5$ along these three dimensions, as better described in the following.

The first uncertainty dimension refers to the exogenous development of installed capacity of renewable energy sources at nodes 1, 2 and 4. Driven by the goals defined in the Paris Agreement, many nations worldwide are increasing their investments in renewable energy sources. Therefore, in addition to our base scenario $\omega = 1$, we introduce a second scenario $\omega = 2$ featuring an increased overall installed capacity of 400 MW. Following the shares of renewable generation capacities across the individual nodes that we introduced before, this results in (increased) renewable capacities of 176 MW, 124 MW, and 100 MW for, respectively, nodes 1, 2, and 4.

The second uncertainty dimension that we model is an exogenous change in the demand at nodes 3, 5, and 6 caused by an increased electrification across different sectors such as, e.g., an increased penetration of electric vehicles and/or heat pumps. As such an electrification leads to a higher node-specific demand for electricity, in our third Scenario $\omega = 3$ we consider an overall demand increased by 50% in each of the three demand nodes, i.e., nodes 3, 5, and 6.

The third uncertainty dimension we consider is the exogenous development of CO_2 prices. Different policy makers make use of CO_2 prices in different ways. Currently, the German CO_2 price is 48 € per ton. However, research on the environmental costs of CO_2 indicates that, in general, the prices should/will be even higher in future than the German ones (Rennert et al., 2022). Therefore, our fourth scenario $\omega = 4$ features a higher CO_2 price compared to our base case of, namely 174 € per ton (Rennert et al., 2022), which has a direct impact on variable costs of production.

Finally, in scenario $\omega = 5$ we consider an increase in all three uncertainty dimensions.

Table B.1 summarizes the features of the five scenarios we consider across the three uncertainty dimensions.

Table B.1: Scenario definitions for the three uncertainty dimensions.

	Installed RES capacity	Level of Demand	CO_2 prices
Scenario $\omega = 1$	Base	Base	Base
Scenario $\omega = 2$	High	Base	Base
Scenario $\omega = 3$	Base	High	Base
Scenario $\omega = 4$	Base	Base	High
Scenario $\omega = 5$	High	High	High
Base	Node 1: 44 MW Node 2: 31 MW Node 4: 25 MW	100 %	48 € per ton
High	Node 1: 176 MW Node 2: 124 MW Node 4: 100 MW	150 %	174 € per ton

B.6.3 On the interplay between transmission, storage, and backup generation investments

In this section, we discuss the equilibrium outcomes considering two different spot market designs and four different settings of risk attitudes, as described below.

In particular, for the four different settings of risk attitudes we vary the public (Stage I) and the private (Stage II) risk attitude between a risk-neutral ("N") and a risk-averse ("A") decision maker. In this way, we arrive at four different cases of risk attitude, namely "NN", "NA", "AN", and "AA", where the first letter stands for the public investors' risk attitude and the second letter stands for the private investors' risk attitude.

Regarding the spot market designs, we analyze the impact of uniform and zonal spot market designs by applying both to our model.

The results obtained with the four variations of the model are reported in Tables B.2 and B.3.

B.6.3.1 On the effects of different risk attitudes

First, we analyze and discuss our results comparing the different cases of risk attitudes, i.e., "NN", "NA", "AN", and "AA".

Table B.2: Results for uniform spot market design.

Risk-attitudes	Objective Function	Generation Capacity Node 1	Generation Capacity Node 2	Generation Capacity Node 4	Storage Capacity	Line 1	Line 2
NN	69,612	471	229	0	228	1	1
NA	62,312	0	0	0	180	1	0
AN	23,035	0	285	1,150	0	0	0
AA	28,736	0	98	0	182	0	0

Table B.3: Results for zonal spot market design.

Risk-attitudes	Objective Function	Generation Capacity Node 1	Generation Capacity Node 2	Generation Capacity Node 4	Storage Capacity	Line 1	Line 2
NN	70,896	144	318	249	168	1	0
NA	65,362	0	98	0	182	1	0
AN	26,205	0	262	395	184	0	0
AA	28,736	0	98	0	182	0	0

Looking at the results from our case study reported in Tables B.2 and B.3, we see that, for the case of "NA" and applying uniform spot market pricing, there is no investment in back-up generation capacities. This suggests that the investments in line 1 are sufficient for allowing a sufficient amount of electricity to be charged and discharged to/from the storage facility, which have been subjected to a capacity investment, and for balancing the overall electricity system.

Assuming a uniform market design and comparing the ”AA” case to the ”NA” case, a neutral risk attitude at Stage I results in zero investments in transmission lines and in some (small) investments in generation capacity at node 2. The results indicate that a risk-avers attitude for both the private and the public investor seems to result in overall lower investments. However, when the risk attitude of the public investor changes and the ”NA” case is considered, the investments increase and so does welfare. With a further change in the risk attitude of the private investors to ”NN” case, we observe higher investments also from the public side.

Overall, risk-averse attitudes seem to hamper investments in both new transmission lines and private flexibility options. As an extreme case, risk aversity of private investors can yield no conventional backup generation investments.

B.6.3.2 On the effects between uniform and zonal prices

In general and as expected, our results indicate that welfare is higher (or at least not lower) under zonal pricing than under a uniform spot market design. This is in line but also extends previous results of the literature to the case where different levels of risk aversion are considered. The corresponding welfare effects are generally driven by a change in investments in generation and storage: For instance, the "NA" case results in slightly higher investments under a zonal market design as compared to the uniform market design, which leads to an increased welfare. However, we also see that, for both designs, an averse risk attitude on both stages I and II , i.e., the "AA" case, similarly results in low investments. Consequently, in the case of exclusively risk-averse decision makers on both stages, none of the two market designs can repair inefficiently-low flexibility investments.

For the "NN" case, our results also illustrate that a zonal market design (that considers inter-zonal transmission constraints) can lead to a generally lower need for expansion of the network.

B.7 Conclusion

With an increasing penetration of renewable energy sources, supply-side variability and its natural uncertainty pose new challenges for the balancing of demand and supply. In particular, the loss of production flexibility which is due to the growing predominance of renewable energy production leads to a so-called flexibility gap. In order to fill this gap, new forms of flexibility are required, ranging from new transmission flexibility to storage flexibility.

To solve the arising flexibility puzzle and answer the question of how to offer an adequate flexibility mix, we have proposed a multi-stage investment game under uncertainty. At Stage I of the game, the TSO invests in welfare-enhancing line extensions while forming rational expectations on the private investments in storage and conventional backup generation capacity that will take place at Stage II. In turn, these private flexibility investments depend on the anticipation of the zonal spot market outcomes taking place at Stage III, which are followed by a redispatch market at Stage IV.

Modeling and analyzing different types of risk attitudes and thanks to a widely adopted case

study, we have shown that a lower risk-aversion for a public investor results in increased investments and in an increased welfare even when the risk attitude of the private investor is still averse to risk. Comparing uniform and zonal market designs, our results indicate that, thanks to considering inter-zonal transmission lines, a zonal market design may exhibit a lower need for network expansion and consequently leads to an increase in regional investments in generation capacities as well as storage.

When discussing our first computational results, the case study also illustrates that, due to the urgent need for proper investments in flexibility, it is important to consider risk attitudes of different investors in addition to the market design itself. We find that, in the case study, different risk attitudes of private and public investors (such as firms and network operators) lead to different investments, which can be more or less welcome from a system perspective. Therefore, to purposefully incentivize (flexibility) investments, it is important to understand how policy makers can deal with different risk attitudes in order to support purposeful investments in flexibility.

Our work provides a basis for steering up an academic discussion on integrating risk attitudes into investment-decision making. In particular, it highlights that research and practice should reflect on the interplay of the risk attitude of public and private investors alike combination with different market designs when choosing the right mix of flexibility.

Our paper provides a range of future research. A future model extension could for example account for different types of demand flexibility (including, e.g., demand shifting), post-redispatch changes in storage values, or a market-based redispatch mechanism. This may further help policymakers to pave the way to a flexible, climate-neutral electricity system. As our work provides a basis for steering up an academic discussion on integrating risk-attitudes into decision making for investment incentives, further research might also extend our model with regard to, e.g., possibilities for investments at each node and the range of time periods. Finally, our paper notes that research and practice may reflect on the interplay of public and private investment risk-attitudes in combination with different market designs when choosing the right mix of flexibility within a flexibility puzzle.

Table B.4: Sets

Symbol	Description
$\mathscr{G}$	Electricity network
N	Set of network nodes
$C \subseteq N$	Set of consumer nodes
L	Set of transmission lines
$L^{\text{new}} \subseteq L$	Set of candidate transmission lines
$L^{\text{ex}} \subseteq L$	Set of existing transmission lines
T	Set of time periods
Ω	Scenario set
G	Set of generators
$G_n \subseteq G$	Set of generators located at node n
$G^{\text{new}} \subseteq G$	Set of new conventional generators
R	Set of renewable generators
$R_n \subseteq R$	Set of renewable generators located at n
S	Set of storage facilities
$S_n \subseteq S$	Set of storage facilities located at node n
$S^{\text{new}} \subseteq S$	Set of new storages

Table B.5: Parameters

Symbol	Description	Unit
$a_{c\,t\,\omega}$	Intercept of demand function c in period t under scenario ω	€/MWh
b_c	Slope of demand function c	€/MWh^2
v_g	Variable cost of generator g	€/MWh^2
i_g	Generation investment cost for g	€/MWh
$\bar{x}_{r\,t\,\omega}$	Maximum power output of r in period t under scenario ω	€/MWh^2
e_s	Storage efficiency of facility s	%
$\overline{z}_s^+$	Maximum percentage of capacity at s available to store energy in a period	%
$\overline{z}_s^-$	Maximum percentage of capacity at s available to discharge energy in a period	%
i_s	Storage investment cost for s	€/MWh
$\overline{f}_\ell$	Transmission capacity of line l	MWh
B_ℓ	Susceptance of line l	MWh
i_ℓ	Line investment cost for $l \in L^{\text{new}}$	€
p_ω	Probability for scenario ω	1

Table B.6: Variables and Derived Quantities

Symbol	Description	Unit
$d_{ct\omega}$	Electricity demand at c in period t under scenario ω	MWh
$y_{gt\omega}$	Electricity generation of g in period t under scenario ω	MWh
$\bar{y}_g$	Invested generation capacity of facility g	MWh
$z^+_{st\omega}$	Amount of electricity stored at s in period t under scenario ω	MWh
$z^-_{st\omega}$	Amount of electricity discharged at s in period t under scenario ω	MWh
$z_{st\omega}$	Amount of stored electricity at s in time period t under scenario ω	MWh
$\bar{z}_s$	Invested storage capacity of facility s	MWh
$f_{lt\omega}$	Power flow on line l in period t under scenario ω	MWh
$\Theta_{nt\omega}$	Phase angle value at node n in period t under scenario ω	rad
$\pi_{d,t,\omega}$	Electricity price at d in period t under scenario ω	€/MWh
W_ω	Welfare under scenario ω	€
W	Welfare aggregated over all scenarios minus line investment costs	€
$\boldsymbol{d}_{ct\omega}$	Final consumption of c in period t under scenario ω	MWh
$\boldsymbol{z}_{st\omega}$	Final amount of stored electricity at s in period t under scenario ω	MWh
$\boldsymbol{z}^+_{st\omega}$	Final amount of electricity stored in in period t under scenario ω	MWh
$\boldsymbol{z}^-_{st\omega}$	Final amount of electricity discharged in period t under scenario ω	MWh
$\boldsymbol{x}_{rt\omega}$	Final electricity generation of renewable r in period t under scenario ω	MWh
$\boldsymbol{y}_{gt\omega}$	Final electricity generation of g in period t under scenario ω	MWh
$\boldsymbol{f}_{l,t,\omega}$	Final power flow on line l in period t under scenario ω	MWh
$\boldsymbol{\Theta}_{nt\omega}$	Final phase angle value at node n in period t under scenario ω	rad

References

Ambrosius, M., J. Egerer, V. Grimm, and A. H. van der Weijde (2022). "Risk aversion in multi-level electricity market models with different congestion pricing regimes". In: *Energy Economics* 105, p. 105701.

Ambrosius, M., V. Grimm, T. Kleinert, F. Liers, M. Schmidt, and G. Zöttl (2020). "Endogenous price zones and investment incentives in electricity markets: An application of multilevel optimization with graph partitioning". In: *Energy Economics* 92, p. 104879.

Bjørndal, M. and K. Jørnsten (2001). "Zonal pricing in a deregulated electricity market". In: *The Energy Journal*, pp. 51–73.

Bjørndal, M. and K. Jørnsten (2007). "Benefits from coordinating congestion management: The Nordic power market". In: *Energy Policy* 35.3, pp. 1978–1991.

Bjørndal, M., K. Jørnsten, and V. Pignon (2003). "Congestion management in the Nordic power market: Counter purchasers and zonal pricing". In: *Journal of Network Industries* 4.3, pp. 271–292.

Bolusani, S., S. Coniglio, T. K. Ralphs, and S. Tahernejad (2020). "A unified framework for multistage mixed integer linear optimization". In: *Bilevel Optimization: Advances and Next Challenges*, pp. 513–560.

Boucher, J. and Y. Smeers (2001). "Alternative models of restructured electricity systems, part 1: No market power". In: *Operations Research* 49.6, pp. 821–838. ISSN: 0030364X. DOI: 10.1287/opre.49.6.821.10017.

Chao, H.-P. and S. Peck (1996). "A market mechanism for electric power transmission". In: *Journal of Regulatory Economics* 10.1, pp. 25–59.

Chao, H.-P. and S. Peck (1998). "Reliability management in competitive electricity markets". In: *Journal of Regulatory Economics* 14.2, pp. 189–200. DOI: 10.1023/A:1008061319181.

Daxhelet, O. and Y. Smeers (2007). "The EU regulation on cross-border trade of electricity: A two-stage equilibrium model". In: *European Journal of Operational Research* 181.3, pp. 1396–1412. ISSN: 0377-2217. DOI: 10.1016/j.ejor.2005.12.040.

Ehrenmann, A. and Y. Smeers (2005). "Inefficiencies in European congestion management proposals". In: *Utilities Policy* 13.2, pp. 135–152. DOI: 10.1016/j.jup.2004.12.007.

ENTSO-E (2023). “High-Level Report Ten Year Net Development Plan 2022 - Efficiencies and Regulatory Shortcuts”. In: *https://eepublicdownloads.blob.core.windows.net/public-cdn-container/tyndp-documents/TYNDP2022/public/high-level-report.pdf*.

Fridgen, G., L. Häfner, C. König, and T. Sachs (2016). “Providing utility to utilities: the value of information systems enabled flexibility in electricity consumption”. In: *Journal of the Association for Information Systems* 17.8, p. 1.

Fridgen, G., S. Halbrügge, M.-F. Körner, A. Michaelis, and M. Weibelzahl (2022). “Artificial intelligence in energy demand response: a taxonomy of input data requirements”. In: *Wirtschaftsinformatik 2022 Proceedings*.

German Transmission System Operators (2017). *Netzentwicklungspläne*. Accessed: April 2017. URL: https://www.netzentwicklungsplan.de/de/netzentwicklungs-plaene/netzentwicklungsplaene-2030.

Grimm, V., B. Rückel, C. Sölch, and G. Zöttl (2019). “Regionally differentiated network fees to affect incentives for generation investment”. In: *Energy* 177, pp. 487–502. ISSN: 03605442.

Grimm, V., A. Martin, M. Schmidt, M. Weibelzahl, and G. Zöttl (2016). “Transmission and generation investment in electricity markets: The effects of market splitting and network fee regimes”. In: *European Journal of Operational Research* 254.2, pp. 493–509.

Grimm, V., B. Rückel, C. Sölch, and G. Zöttl (2021). “The impact of market design on transmission and generation investment in electricity markets”. In: *Energy Economics* 93, p. 104934.

Hasan, E., F. D. Galiana, and A. J. Conejo (2008). “Electricity Markets Cleared by Merit Order—Part I: Finding the Market Outcomes Supported by Pure Strategy Nash Equilibria”. In: *IEEE Transactions on Power Systems* 23.2, pp. 361–371. DOI: 10.1109/TPWRS.2008.919238.

Heffron, R., M.-F. Körner, J. Wagner, M. Weibelzahl, and G. Fridgen (2020). “Industrial demand-side flexibility: A key element of a just energy transition and industrial development”. In: *Applied Energy* 269, p. 115026.

Jenabi, M., S. M. T. F. Ghomi, and Y. Smeers (2013). “Bi-level game approaches for coordination of generation and transmission expansion planning within a market environment”. In: *IEEE Transactions on Power Systems* 28.3, pp. 2639–2650. DOI: 10.1109/TPWRS.2012.2236110.

Keller, R., L. Häfner, T. Sachs, and G. Fridgen (2020). “Scheduling flexible demand in cloud computing spot markets: A real options approach”. In: *Business & Information Systems Engineering* 62, pp. 25–39.

Kleinert, T., M. Labbé, F. a. Plein, and M. Schmidt (2020). “There’s no free lunch: on the hardness of choosing a correct big-M in bilevel optimization”. In: *Operations Research* 68.6, pp. 1716–1721.

Koch, T. (2001). *Zimpl user guide*. Tech. rep.

Komendantova, N. and A. Battaglini (2016). “Beyond Decide-Announce-Defend (DAD) and Not-in-My-Backyard (NIMBY) models? Addressing the social and public acceptance of electric transmission lines in Germany”. In: *Energy Research & Social Science* 22, pp. 224–231.

Lund, P. D., J. Lindgren, J. Mikkola, and J. Salpakari (2015). “Review of energy system flexibility measures to enable high levels of variable renewable electricity”. In: *Renewable and Sustainable Energy Reviews* 45, pp. 785–807.

Ma, J., V. Silva, R. Belhomme, D. S. Kirschen, and L. F. Ochoa (2013). “Evaluating and planning flexibility in sustainable power systems”. In: *2013 IEEE Power & Energy Society General Meeting*. IEEE, pp. 1–11. ISBN: 978-1-4799-1303-9. DOI: 10.1109/PESMG.2013.6672221.

Oggioni, G. and Y. Smeers (2013). “Market failures of market coupling and counter-trading in Europe: An illustrative model based discussion”. In: *Energy Economics* 35, pp. 74–87. DOI: 10.1016/j.eneco.2011.11.018.

Pechan, A. (2017). “Where do all the windmills go? Influence of the institutional setting on the spatial distribution of renewable energy installation”. In: *Energy Economics* 65, pp. 75–86.

Rennert, K., F. Errickson, B. C. Prest, L. Rennels, R. G. Newell, W. Pizer, C. Kingdon, J. Wingenroth, R. Cooke, B. Parthum, et al. (2022). “Comprehensive evidence implies a higher social cost of CO2”. In: *Nature* 610.7933, pp. 687–692. DOI: 10.1038/s41586-022-05224-9.

Sensfuß, F., M. Ragwitz, and M. Genoese (2008). “The merit-order effect: A detailed analysis of the price effect of renewable electricity generation on spot market prices in Germany”. In: *Energy Policy* 36.8, pp. 3086–3094.

Shapiro, A., D. Dentcheva, and A. Ruszczynski (2021). *Lectures on stochastic programming: modeling and theory*. SIAM.

Stolten, D., B. Emonts, T. Grube, and M. Weber (2013). “Hydrogen as an enabler for renewable energies”. In: *Transition to Renewable Energy Systems*, pp. 195–216.

Weibelzahl, M. (2017). “Nodal, zonal, or uniform electricity pricing: how to deal with network congestion”. In: *Frontiers in Energy* 11, pp. 210–232.

Weibelzahl, M. and A. Märtz (2020). “Optimal storage and transmission investments in a bilevel electricity market model”. In: *Annals of Operations Research* 287, pp. 911–940. DOI: 10.1007/s10479-018-2815-1.

Weitemeyer, S., D. Kleinhans, L. Wienholt, T. Vogt, and C. Agert (2016). “A European perspective: potential of grid and storage for balancing renewable power systems”. In: *Energy Technology* 4.1, pp. 114–122.

Wogrin, S. and D. F. Gayme (2014). “Optimizing storage siting, sizing, and technology portfolios in transmission-constrained networks”. In: *IEEE Transactions on Power Systems* 30.6, pp. 3304–3313.

C Global perspective on CO_2 emissions of electric vehicles

Alexandra Märtz[a], Patrick Plötz[b], Patrick Jochem[c]

[a] Karlsruhe Institute of Technology (KIT), Institute for Industrial Production (IIP), Chair of Energy Economics, Hertzstraße 16, 76187 Karlsruhe, Germany.

[b] Fraunhofer Institute for Systems and Innovation Research ISI, Breslauer Strasse 48, 76139 Karlsruhe, Germany.

[c] German Aerospace Center (DLR), Institute of Networked Energy Systems, Energy Systems Analysis, Curiestrasse 4, 70563 Stuttgart, Germany.

Published in:
Environmental Research Letters (2021), 16 (5), Art. No.: 054043. doi:10.1088/1748-9326/abf8e1.

Abstract

Plug-in electric vehicles (PEVs) are a promising option for greenhouse gas (GHG) mitigation in the transport sector – especially when the fast decrease in carbon emissions from electricity provision is considered. The rapid uptake of renewable electricity generation worldwide implies an unprecedented change that affects the carbon content of electricity for battery production as well as charging and thus the GHG mitigation potential of PEV. However, most studies assume fixed carbon content of the electricity in the environmental assessment of PEV and the fast change of the generation mix has not been studied on a global scale yet. Furthermore, the inclusion of up-stream emissions remains an open policy problem. Here, we apply a reduced Life Cycle Assessment (LCA) approach including the well-to-wheel emissions of PEV and taking into account future changes in the electricity mix. We compare future global energy scenarios and combine them with PEV diffusion scenarios. Our results show that the remaining carbon budget is best used with a very early PEV market diffusion; waiting for cleaner PEV battery production cannot compensate for the lost carbon budget in combustion vehicle usage.

C.1 Introduction

Transport is responsible for about one quarter of global energy related greenhouse gas (GHG) emissions and transport is the only energy-related sector with emissions still growing compared to 1990 (International Energy Agency (IEA), 2018; European Comission, 2017). Road vehicles contribute the largest share to these emissions and current projections indicate a doubling of the passenger vehicle fleet until 2050 (Bunsen et al., 2018). Consequently, an increased market share of alternative fuel vehicles, such as plug-in electric vehicles (PEVs), including plug-in hybrid electric vehicles (PHEVs) and battery electric vehicles (BEVs), powered from renewable energy sources (RES) seems essential for significant GHG mitigation in passenger road transport. There are already many studies comparing GHG emissions of PEVs to internal combustion engine vehicles (ICEV) on a life-cycle basis (Bunsen et al., 2018; Cox et al., 2018; Creutzig, 2016).

Past studies have shown that life-cycle PEVs emissions depend heavily on the assumed electricity mix, driving patterns and ambient weather conditions (Yuksel et al., 2016; Tamayao et al., 2015; Nordelöf et al., 2014; Gómez Vilchez and Jochem, 2020). These factors vary regionally, so PEV emissions can also vary regionally.

Yuksel et al. (2016) consider regional differences due to marginal grid mix, ambient temperature, patterns of vehicles miles travelled, and driving conditions. They find that PEVs can have larger or smaller carbon footprints than gasoline vehicles, depending on these regional factors and the specific vehicle models being compared. However, Yuksel et al. (2016) use fixed historic carbon intensities and mention it as drawback in the discussion themselves. The exact results vary widely depending on the input assumptions and the source of electricity used for recharging. Nevertheless, the impacts can be highly uncertain. Cox et al. (2018) quantify parametric uncertainty and include changes to driving patterns due to the introduction of autonomous and connected vehicles. They perform a very comprehensive analysis of the uncertainty of many parameters with carbon intensity of the grid electricity in several scenarios. Yet, they use fixed intensity for the vehicle lifetime with 2017 or future 2040 values and neglect the changes in between. Likewise, Tamayao et al. (2015) study different charging patterns and local grid mixes, but neglect the future evolution of carbon intensity. Xu et al. (2020) considered the emissions from the whole PEV life cycle by a Life Cycle Assessment (LCA) and combined this with a sophisticated consideration of charging times in the European energy system. They concluded that on the European scale, a reasonable replacement of ICEVs by PEVs can lead to a substantial reduction in GHG emissions, but still depending on some uncertainties such as charging patterns. Kim et al. (2016) report the first cradle-to-gate emissions assessment for a mass-produced battery in a commercial BEV and compared the cradle-to-gate GHG emissions to an ICEV.

However, a major advantage of PEVs overlooked in most parts of the literature is the fast transformation of the energy system: A reduction in carbon intensity of electricity leads directly to lower upstream emissions and accordingly to lower emissions from the fuel perspective (i.e. well-to-wheel emissions) and lower emissions from vehicle and battery production (i.e. life-cycle perspective). For ICEVs this is only possible if low-carbon fuels, such as biofuels or synthetic renewable fuels are introduced in large quantities, which is highly uncertain (Brynolf et al., 2018).

Cox et al. (2018) show that it is imperative to consider changes to the electricity sector when calculating upstream impacts of PEVs, as without this, results could be overestimated. They included the impacts of changes to the electricity sector on the environmental burdens of producing and recharging future PEVs. Electricity used for charging is the largest source of variability in results. Woo et al. (2017) state that the reduction of greenhouse gas emissions by PEVs is strongly dependent on the country-specific electricity mix. In this regard,

Brynolf et al. (2018) focus on the reduced fossil carbon intensity by the introduction of low-fossil-carbon fuels. Accordingly, we do not consider low-carbon or carbon-free fuels in the following but focus on the indirect emissions from PEV and the changes with respect to the energy transition in electricity generation, i.e. lower GHG emissions for battery production and lower upstream emissions for electricity generation, which impacts the vehicle usage phase of all current PEVs (Cox et al., 2018; Kim et al., 2016).

The overall GHG emission reductions from PEVs are mainly driven by the development of vehicle stock and specific emissions from electricity generation. In the present study, we combine two PEV market scenarios with one electricity generation scenario, all scenarios are taken from the International Energy Agency (IEA) (2018). The first PEV market diffusion scenario is the IEA's EV30@30 market diffusion scenario (i.e. 30% sales share in 2030). This rather ambitious scenario is compared to a second PEV market scenario, the New Policy Scenario (NPS) that includes policies currently in action and policies that have been announced. The PEV sales shares according to these scenarios are translated to absolute sales in the most important markets globally and aggregated to a vehicle stock. Our vehicle stock model for PEVs differentiates between BEVs and PHEVs. Our analysis covers China, the US, Europe, India, and Japan. Jointly, these markets presently cover 80% of global passenger car sales and this share is expected to grow further in the future (Gómez Vilchez and Jochem, 2020).

The carbon intensity of the electricity is taken from the Sustainable Development Scenario (SDS) [1]. This scenario is consistent with the Paris Agreement, i.e. it respects the 'well-below 2 degrees' target. The carbon intensity of the grid declines in all major regions and is expected to be close to 0 g CO_2/kWh in 2050 (cf. Figure C.1). Please note that we have to choose an additional scenario for the carbon content of electricity, as the PEV diffusion scenarios alone do not make statements about the carbon content of the electricity.

[1] In the SDS only values for the whole EU are given. We, therefore consider country specific values from EU Reference Scenario (Capros et al., 2016) for European countries instead.

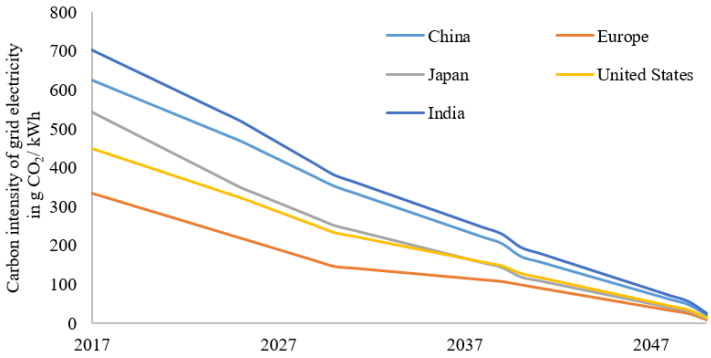

Figure C.1: Carbon intensity of grid electricity in g CO_2/kWh in major global economies according to the SDS of the IEA's World Energy Outlook (International Energy Agency (IEA), 2018).

Even without low-carbon fuels, ICEVs could improve their fuel efficiency further in the future but the reduction potential seems limited (Edenhofer, 2015). We assume that tailpipe emissions will decrease to 85 g CO_2/km but – even with mild hybridisation – no further (Fritz et al., 2019). Similar to PEVs, the upstream emissions from fuel production and transport are included in our well-to-wheel emissions of ICEVs.

C.2 Methods

We applied a reduced LCA approach including manufacturing emissions (for vehicle and battery) of PEVs (cf. Figure C.6). The focus lies on the usage phase, with additional consideration of emission factors from literature resulting from battery and vehicle production (International Energy Agency, 2017; Dunn et al., 2015; Egede et al., 2015; Hao et al., 2017). As the experience with PEV disposal is still limited we decided not to consider vehicle disposal in our analysis.

Our analysis focuses on the impact from GHG emissions in the electricity sector on the LCA (Yuksel et al., 2016). We investigate a future energy scenario for different global markets (China, Europe, Japan, United States and India) with high passenger car sales and link them to two different PEV market diffusion models (International Energy Agency (IEA), 2018; Gnann, 2015; Gnann et al., 2015; Wietschel et al., 2014). Because of the decarbonisation of

electricity generation, PEVs have the potential to emit less GHG than ICEVs with conventional fuels in all countries considered. Therefore, we assess the potential influence of the combined consideration of electricity generation mix and PEV market diffusion in Europe, China, Japan, US and India emphasizing the usage phase under consideration of battery and vehicle production.

C.2.1 Calculation of GHG emissions

C.2.1.1 GHG emissions from vehicle production

In a first step, the manufacturing GHG emissions for vehicle and battery production were calculated. All vehicles considered were assumed to be identical, with the exception of the addition of the batteries for PEVs. The associated assumptions are explained in the following and are also shown in Table C.1 in the appendix. The average battery capacity for BEV counts 25 kWh in 2017 and increases to 35 kWh (2030) (International Energy Agency (IEA), 2018; Ellingsen et al., 2016; Bunsen et al., 2018). Similarly, for PHEVs, the average battery capacity increases from 12 kWh in 2017 to 20 kWh in 2030 (Bunsen et al., 2018). The indirect battery emissions included decline from 140 kg CO_2 per kWh in 2017 to 75 kg CO_2 per kWh in 2030 (Kim et al., 2016). The GHG emissions for vehicle production are assumed 35 g CO_2/km in the period from 2017 to 2030. From 2030 on, they decrease linearly to 0 g CO_2/km in 2050 (Hawkins et al., 2012). Hence, only emissions from production of batteries and vehicles are covered. In addition, it is assumed that the vehicles have a lifetime of 12 years or 150,000 km of vehicle kilometres travelled for all countries until 2050 and that battery and vehicle production in 2050 will be completely carbon-free (Kawamoto et al., 2019). Due to the international production sites, the same emissions for production are assumed in the international comparison.

C.2.1.2 GHG emissions in the usage phase

In the vehicle usage phase, a distinction is made between emissions from fuel consumption for ICEVs and emissions from the supply of electricity for PEVs. Regarding the emissions from fuel consumption, a well-to-wheel GHG emission factor of 3.183 kg CO_2 per litre of gasoline (including upstream emissions) and a fuel economy of 0.07 litres per kilometre (7 litres/100km or 33.6 MPG) are assumed (International Energy Agency (IEA), 2017). Since the real fuel consumption of new ICEVs is on average about 40% higher than stated by the

vehicle manufacturer, a GHG emission factor of 297 g CO_2/km was assumed for 2017 (Fritz et al., 2019; The International Council on Clean Transportation (ICCT), 2017). From the year 2030, a GHG emission factor of 85 g CO_2/km is used (Fritz et al., 2019). This assumption remains valid until the year 2050. The relevant calculations of the country-specific emissions of the well-to-wheel phase for PEV are based on the emissions of electricity generation and derived from the SDS (International Energy Agency (IEA), 2018). Electricity production efficiency and GHG emissions per kWh electricity differ significantly among countries. This is also true for their development over time. The specific emissions from electricity generation for different countries are given in Figure C.1.

Including the emissions for each energy source (Turconi et al., 2013), the GHG emissions during the BEV usage phase are derived. Hence, BEV electricity efficiency was assumed to be 0.205 kWh/km, i.e. 20.5 kWh/100km (Jochem et al., 2015), and fixed over time. Multiplying the specific emissions from electricity generation by the BEV electricity efficiency results in the emissions for BEVs in the usage phase. For the PHEVs, the emissions from the usage phase are calculated using an utility factor, i.e. the share of kilometres driven on electricity. As the PHEV battery sizes increases from 12 to 20 kWh between 2017 and 2030, the utility factor is assumed to increase from 0.5 in 2017 to 0.75 in 2030 in line with existing studies (Plötz et al., 2020).

C.2.1.3 Overall GHG emissions

Taking into account the emissions from the vehicle production and the vehicle usage phase as well as the mileage of 150,000 km, the overall GHG emissions are obtained (cf. Figure C.2). Here, the emissions from the vehicle use phase are summed over a period of 12 years to take into account the change in emissions from electricity generation. The annual GHG emissions of PEVs in stock are reduced with every year of operation when the generation mix improves. This is fundamentally different from ICEVs – at least when not considering biofuels. This effect might even become stronger when disposal of PEVs is included in the analysis, because current disposal processes are still in an initial phase.

C.2.2 Market diffusion scenarios of PEVs

At the same time, the uncertainty of PEV market penetration is high. Consequently, we consider an ambitious scenario (EV30@30) and an alternative scenario with a decelerated market take-up of PEVs (NPS). The EV30@30 scenario pursues the ambitious goal of a market share of 30% for PEVs by 2030 (Bunsen et al., 2018). Current and future PEV market share and stock in 2017 up to 2050 for BEVs, PHEVs, and ICEVs are based on these scenarios (cf. Appendix Figures C.7 and C.8).

C.3 Results

We combine the scenarios for future PEV stock in the major car markets with values from literature on their life-cycle GHG balances and the impact from the decreasing carbon intensity of electricity over time. Consequently, the development of specific GHG emissions of PHEVs and BEVs in g CO_2/km shows a fast decrease until 2050 (cf. Figure C.2). While we assume that all newly registered PEVs show the same GHG footprint for a given year and for all regions (highly internationalized car market), the overall emissions are lower for those regions with low grid carbon intensities.

Today, these emissions of BEVs are in the range of 111 – 176 g CO_2/km (lowest for the European average and highest for India). For PHEVs, the emissions are slightly higher in the range of 183 – 216 g CO_2/km due to the additional part-time operation of the combustion engine. BEV life-cycle emissions can reach almost zero until 2050 whereas PHEVs are assumed to use conventional gasoline and thus their life-cycle emissions saturate at slightly higher levels in 2050.

Both, the future emissions of BEVs and PHEVs show a note-worthy change and clear decline due to the fast grid decarbonisation in many countries of the world.

Within the ranges of well-to-wheel emissions, the speed of GHG reduction varies among the countries. This becomes obvious even for European countries, where values may differ significantly from the European average (which is considered in Fig. C.2): E.g. while in Germany, current PHEVs and BEVs life-cycle emissions are closer to the European average, Polish emissions show higher values throughout the time-horizon considered.

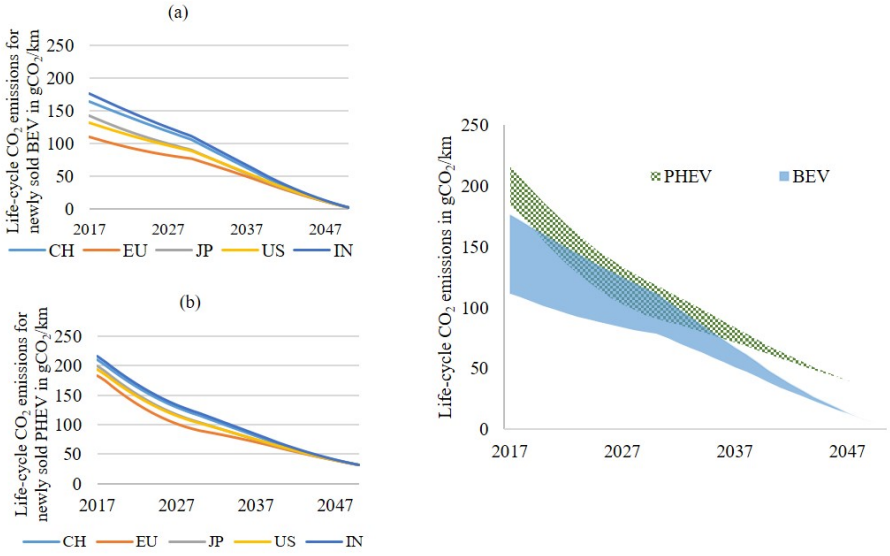

Figure C.2: Left: Overall GHG emissions for (a) BEVs and (b) PHEVs for different global markets. Right: Life-cycle CO_2 emissions in g CO_2/km for newly sold PEVs over time. The range indicates the range of emission values among major global markets (i.e. China, the United States, European average, India, and Japan).

The remaining emissions in 2050 stem from the usage phase only, which makes the carbon intensity of electricity to the dominant factor. Due to the assumptions from the SDS, the GHG emissions from battery production are close to zero by 2050. Near-zero GHG emissions from all passenger cars are in line with the ambition CO_2 mitigation required to limit global warming to well below 2°C (Axsen et al., 2020).

The results in Figure C.2 demonstrate that PEVs can lead to the required reduction. However, the full car stock needs to be near zero emission operation. Accordingly, policies have to make sure that full car stock is electric by 2050 or that the remaining fuel used to power ICEVs is carbon neutral. Thus, potential policies need to address the two aspects of (a) PEV diffusion and (b) low-carbon fuels simultaneously. Potential policies to address these topics are CO_2 fleet targets and PEV mandates for the first aspect and low-carbon fuel standards for the second aspect (Axsen et al., 2020).

The above-mentioned fast mitigation potentials by PEVs over time should, however, not be interpreted as an argument for postponing the PEV market penetration by hoping to

profit from the younger (i.e. less expensive and smaller carbon footprint) fleet in the future. For further investigation of this argument, we constructed two additional scenarios for China, as an example, based on the ambitious EV30@30 scenario. We assumed that the Chinese PEV market diffusion could deviate from the ambitious governmental market plans by postponing the market take-up by 10 years (i.e. the market share of the EV30@30 scenario in 2030 is achieved not before 2040).

After 2040, the market penetration may accelerate significantly to still achieve the same aggregated number of PEVs sold by 2050. We refer to this scenario as '$CHN_{lagged/ambitious}$'. In a second scenario, the market penetration may increase smoothly and similarly to the EV30@30 scenario, we refer to this as '$CHN_{lagged/realistic}$'. The resulting mitigation potentials compared to a pure ICEV fleet with conventional fuel are calculated and shown in Figure C.3.

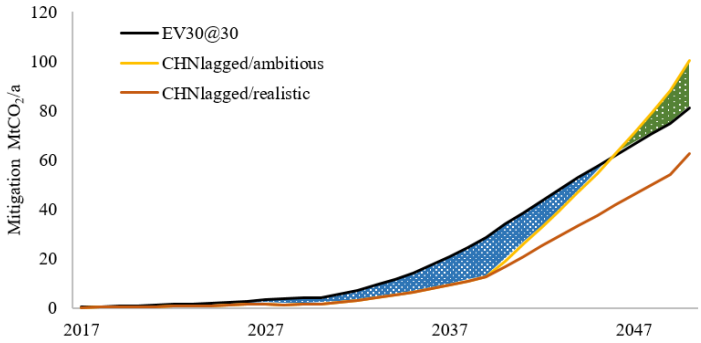

Figure C.3: Different mitigation potentials for China by PEV against conventional ICEV.

In comparison of the two additional scenarios to the original EVS30@30 scenario for China, it is clear that neither the '$CHN_{lagged/realistic}$' scenario nor the '$CHN_{lagged/ambitious}$' scenario achieve the same mitigation potential as the EV30@30 scenario until 2050. In terms of Figure C.3, the blue area (150 Mt CO2) exceeds the green area (46 Mt CO_2) significantly. Considering the annual mitigation potentials in Figure C.3, it seems more than challenging to overcompensate the missed mitigation even until 2060. Calculations for other markets show similar results. Hence, in our analysis the CO_2 budgets of accelerated PEV market scenarios always undercut those of lagged market scenarios.

C.4 Sensitivity analysis

We perform a sensitivity analysis to investigate how changes in electricity mix and battery capacity affect the LCA emissions from PEVs. First, we compare the results from the previous section to a model with constant GHG emissions from electricity generation over time by keeping the current electricity mix (2017) constant. The resulting LCA emissions are flat in the beginning and show a slight decrease after 2030 as the emissions from vehicle production are assumed to decrease linearly from 2030 onwards. This applies to both PHEVs and BEVs. Hence, assuming the constant electricity mix from 2017, the LCA emissions for BEVs results in poor values (between 121 g CO_2/km (EU) and 197 g CO_2/km (India) in 2030 and in a range of 69 – 144 g CO_2/km (lowest for the European average and highest for India) in 2050). For PHEVs, the emissions are higher in the range of 226 – 266 g CO_2/km for 2030 and between 183 g CO_2/km and 221 g CO_2/km in 2050 due to the additional partial operation of the combustion engine. Consequently, the difference to the scenarios considering rapid decarbonisation of the electricity system (see above) becomes obvious (cf. Figures C.4 and C.2).

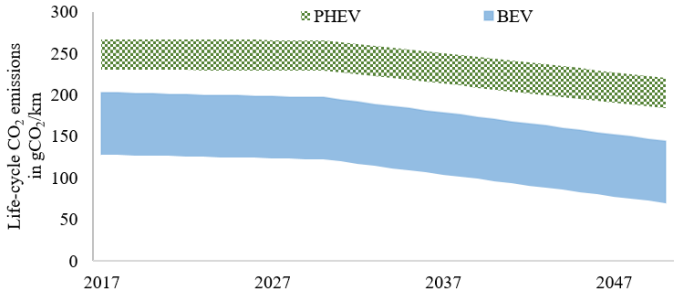

Figure C.4: Life-cycle CO_2 emissions in g CO_2/km for newly sold PEVs over time assuming constant GHG emissions from electricity generation over time. The range indicates the range of emission values among major global markets (i.e. China, the United States, European average, India, and Japan).

Second, the impact from battery capacity is analysed. From the current perspective it is unclear how the increasing habit with EV and further automatization of vehicles may have an influence on battery capacities. With increasing battery capacities (i.e. from 35 to 50 kWh), the resulting LCA emissions in the initial year increase, too. This can be explained by the increased manufacturing emissions of the higher battery capacity. However, due to the decarbonizing electricity mix over time, this effect becomes marginal until 2050 (cf. Figure C.5).

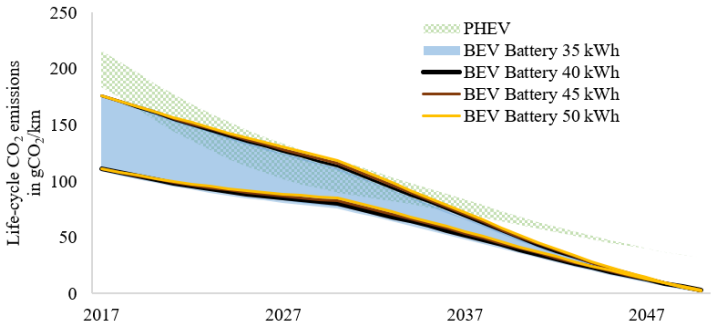

Figure C.5: Life-cycle CO_2 emissions in g CO_2/km for newly sold PEVs over time for different battery capacities for BEVs. The range between two lines of the same colour reflects the range of emission values among major global markets (i.e. China, the United States, European average, India, and Japan).

C.5 Discussion

Our findings come with a number of uncertainties and future parameters may evolve other than expected. First, the scenarios and GHG mitigation potentials rely on a set of assumptions, which we based on current literature. However, all relevant electricity scenarios assume a future decarbonisation of electricity generation, although at different speeds. Thus, the observed effect on carbon budget is robust against variation of the chosen scenario, yet the magnitude of the effect may vary. For example, current carbon content of battery production is about 75 kg CO_2/kWh. However, the future carbon content of the battery from production is expected to decline further (International Energy Agency (IEA), 2020) as the share of renewable electricity is growing in major battery producing countries and newer and larger factories have higher utilisation. For the long-term until 2050, several major battery-manufacturing countries (US, China, Japan and Europe) have declared to achieve climate neutrality by 2050 or 2060. Accordingly, carbon content of battery production will likely be very low in 2050. Interestingly, we identified that the share of emissions from production differs among countries – depending mainly on the national electricity mix. And there is again a dynamic effect: Over time the share of emissions during the production phase increases. However, the increase in battery capacities has only a marginal impact on the change in the life-cycle CO_2 emissions. This can be explained by the shares of the battery production emissions of the life-cycle CO_2 emissions. In 2030, these have a share of between 16% and 22% for a 35 kWh battery and rise to a share of between 21% and 29% for a 50 kWh battery. But there are still some uncertainties about future developments (Wu et al., 2018; Temporelli et al., 2020). Hence, while an improve in the national electricity mix

(where the car is used) seems more significant today, it might be desirable to focus more on emission reductions for vehicle production later, but far before 2050.

Second, there are other options apart from PEVs to reduce GHG emissions in transportation such as non-motorised or active modes as well as biofuels and synthetic fuels. Our results do not show that PEVs are preferable to these other measures but that if one chooses market diffusion of PEVs as a path for CO_2 reduction in passenger cars and expect the decarbonisation of electricity generation, one should not wait but increase market diffusion as soon as possible. Accordingly, any replaced conventional ICEV provides savings in the carbon budget if the energy transition in electricity generation proceeds as expected.

C.6 Conclusion

GHG emissions from PEVs exhibit a strong temporal change due to grid decarbonisation in many countries. The common assumption of fixed carbon intensity in the grid in many studies highly underestimates this change. Furthermore, if PEVs are chosen as a key option to reduce passenger car GHG emissions, then PEV market diffusion should not be postponed as improvements in electricity carbon intensity can immediately increase the remaining carbon budget. Our results demonstrate that a postponement of PEV market diffusion negatively influences the remaining carbon budgets.

Appendix

Table C.1: Vehicle characteristics (reference vehicle).

	ICEV (gasoline)	PHEV	BEV
Average battery capacity			
2017		12 kWh	25 kWh
2030		20 kWh	35 kWh
Indirect battery emissions			
2017		140 kg CO_2eq/kWh	
2030		75 kg CO_2eq/kWh	
2050		0 kg CO_2eq/kWh	
Vehicle manufacturing emissions			
2017		35 kg CO_2eq/kWh	
2030		35 kg CO_2eq/kWh	
2050		0 kg CO_2eq/kWh	
Fuel economy	7l/100km		
Emission factor gasoline			
2017	3.183 kg CO_2/L		
2030	1.214 kg CO_2/L		
2050	1.214 kg CO_2/L		
Utility factor			
2017		50%	
2030		75%	
Electricity efficiency			20.5 kWh/100 km
Annual mileage		12,500 km/a	

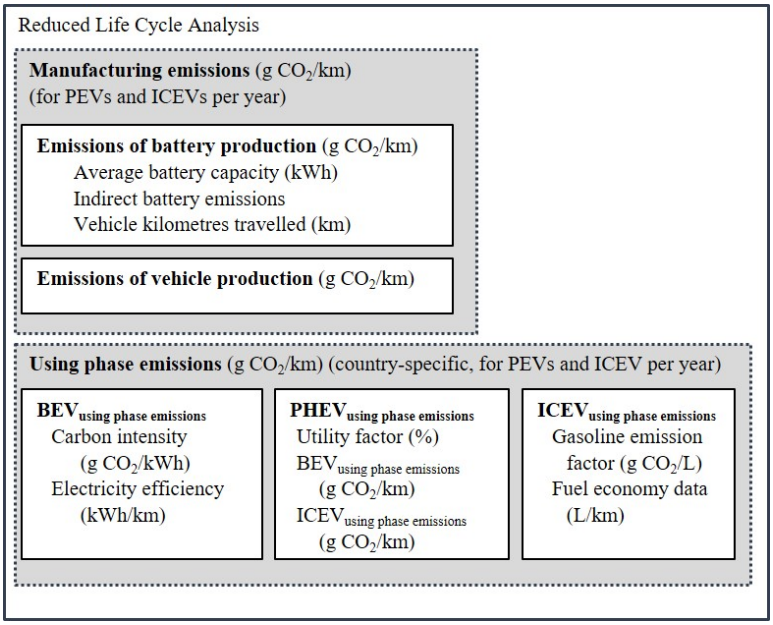

Figure C.6: Framework used in this contribution.

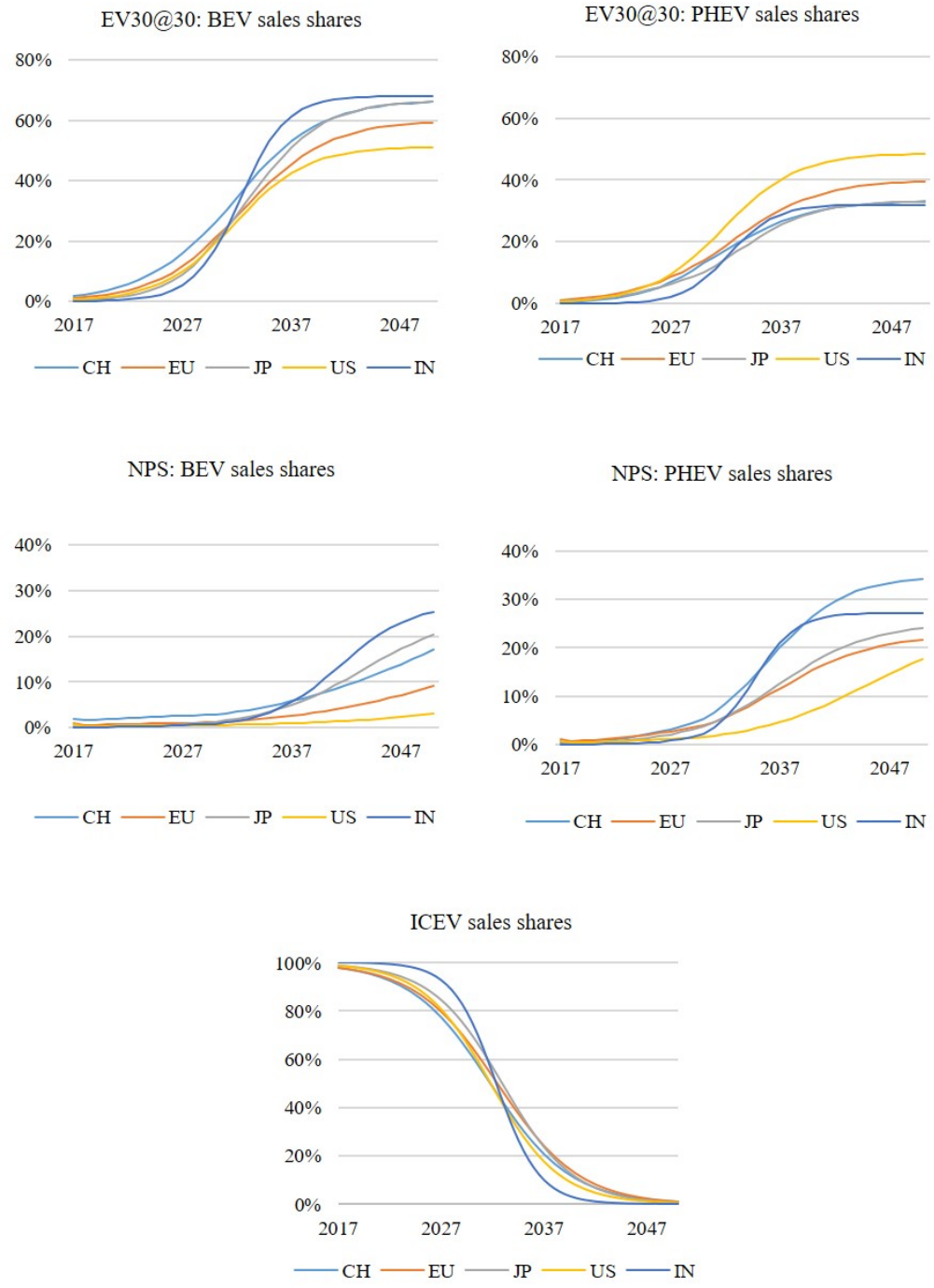

Figure C.7: Sales Shares for BEV, PHEV (EV30@30 and NPS scenario) and ICEV.

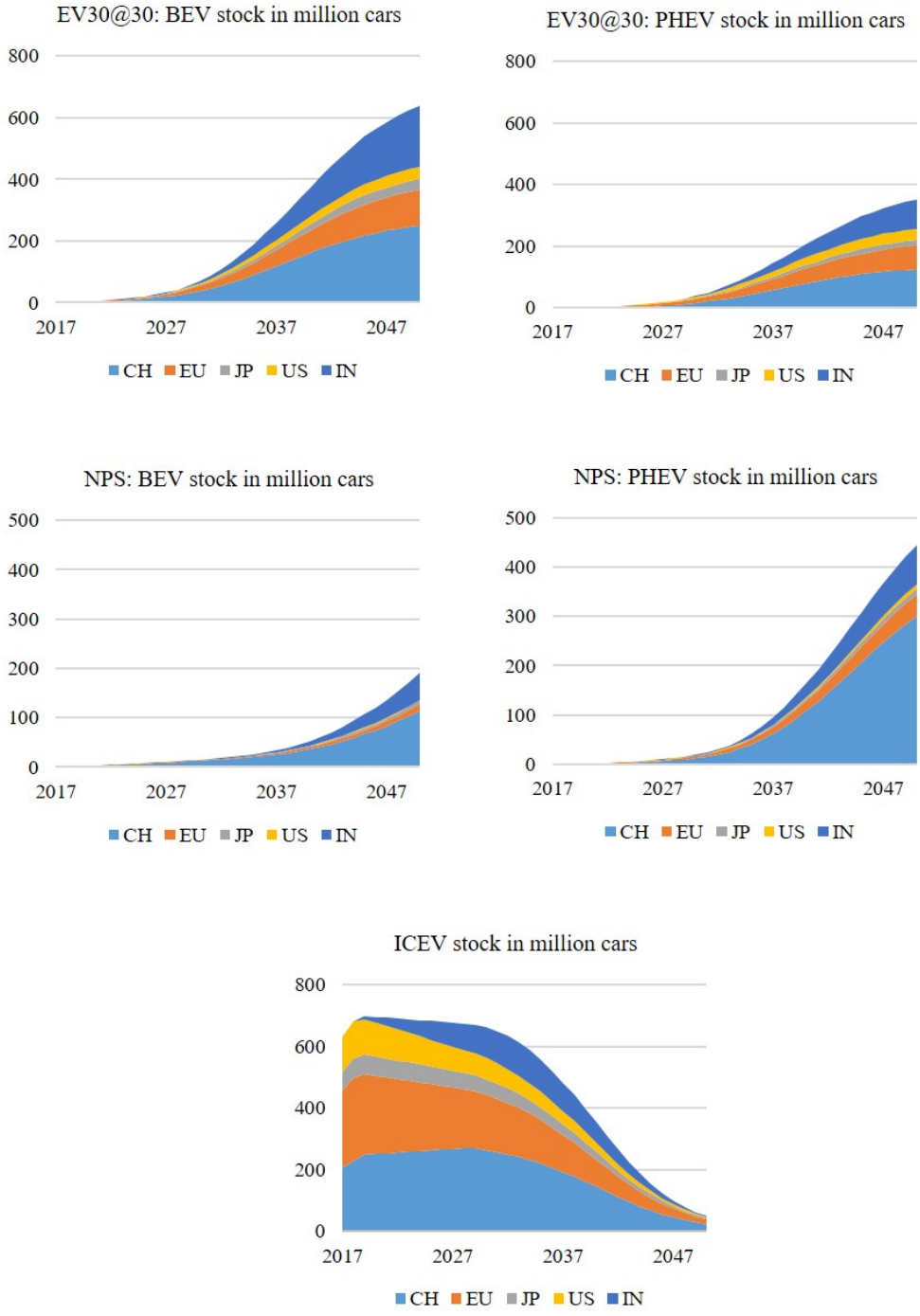

Figure C.8: Stock for BEV, PHEV (EV30@30 and NPS scenario) and ICEV.

References

Axsen, J., P. Plötz, and M. Wolinetz (2020). "Crafting strong, integrated policy mixes for deep CO_2 mitigation in road transport". In: *Nature Climate Change* 10.9, pp. 809–818.

Brynolf, S., M. Taljegard, M. Grahn, and J. Hansson (2018). "Electrofuels for the transport sector: A review of production costs". In: *Renewable and Sustainable Energy Reviews* 81, pp. 1887–1905.

Bunsen, T., P. Cazzola, M. Gorner, L. Paoli, S. Scheffer, R. Schuitmaker, J. Tattini, and J. Teter (2018). *Global EV Outlook 2018: Towards cross-modal electrification*. International Energy Agency.

Capros, P., A. De Vita, N. Tasios, P. Siskos, M. Kannavou, A. Petropoulos, S. Evangelopoulou, M. Zampara, D. Papadopoulos, C. Nakos, et al. (2016). *EU Reference Scenario 2016 - Energy, transport and GHG emissions: Trends to 2050*.

Cox, B., C. L. Mutel, C. Bauer, A. Mendoza Beltran, and D. P. van Vuuren (2018). "Uncertain environmental footprint of current and future battery electric vehicles". In: *Environmental Science & Technology* 52.8, pp. 4989–4995.

Creutzig, F. (2016). "Evolving narratives of low-carbon futures in transportation". In: *Transport Reviews* 36.3, pp. 341–360.

Dunn, J. B., L. Gaines, J. C. Kelly, C. James, and K. G. Gallagher (2015). "The significance of Li-ion batteries in electric vehicle life-cycle energy and emissions and recycling's role in its reduction". In: *Energy & Environmental Science* 8.1, pp. 158–168.

Edenhofer, O. (2015). *Climate change 2014: mitigation of climate change*. Vol. 3. Cambridge University Press.

Egede, P., T. Dettmer, C. Herrmann, and S. Kara (2015). "Life cycle assessment of electric vehicles - a framework to consider influencing factors". In: *Procedia Cirp* 29, pp. 233–238.

Ellingsen, L. A.-W., B. Singh, and A. H. Strømman (2016). "The size and range effect: lifecycle greenhouse gas emissions of electric vehicles". In: *Environmental Research Letters* 11.5, p. 054010.

European Comission (2017). *Statistical pocketbook transport and figures*. URL: https://ec.europa.eu/transport/%20facts-fundings/statistics/pocketbook-2017_en (Retrieved 09/01/2020).

Fritz, M., P. Plötz, and S. A. Funke (2019). "The impact of ambitious fuel economy standards on the market uptake of electric vehicles and specific CO_2 emissions". In: *Energy Policy* 135, p. 111006.

Gnann, T. (2015). *Market diffusion of plug-in electric vehicles and their charging infrastructure*. Fraunhofer Verlag Stuttgart, Germany.

Gnann, T., P. Plötz, A. Kühn, and M. Wietschel (2015). "Modelling market diffusion of electric vehicles with real world driving data - German market and policy options". In: *Transportation Research Part A: Policy and Practice* 77, pp. 95–112.

Gómez Vilchez, J. J. and P. Jochem (2020). "Powertrain technologies and their impact on greenhouse gas emissions in key car markets". In: *Transportation Research Part D: Transport and Environment* 80, p. 102214.

Hao, H., Z. Mu, S. Jiang, Z. Liu, and F. Zhao (2017). "GHG emissions from the production of lithium-ion batteries for electric vehicles in China". In: *Sustainability* 9.4, p. 504.

Hawkins, T. R., O. M. Gausen, and A. H. Strømman (2012). "Environmental impacts of hybrid and electric vehicles — a review". In: *The International Journal of Life Cycle Assessment* 17, pp. 997–1014.

International Energy Agency (2017). *Electricity Information*.

International Energy Agency (IEA) (2017). *CO_2 emissions from fuel combustion*. URL: `https://www.iea.org/reports/%20co2-emissions-from-fuel-combustion-overview` (Retrieved 11/10/2020).

International Energy Agency (IEA) (2018). *World Energy Outlook 2018*. Paris, France.

Jochem, P., S. Babrowski, and W. Fichtner (2015). "Assessing CO_2 emissions of electric vehicles in Germany in 2030". In: *Transportation Research Part A: Policy and Practice* 78, pp. 68–83.

Kawamoto, R., H. Mochizuki, Y. Moriguchi, T. Nakano, M. Motohashi, Y. Sakai, and A. Inaba (2019). "Estimation of CO_2 emissions of internal combustion engine vehicle and battery electric vehicle using LCA". In: *Sustainability* 11.9, p. 2690.

Kim, H. C., T. J. Wallington, R. Arsenault, C. Bae, S. Ahn, and J. Lee (2016). "Cradle-to-gate emissions from a commercial electric vehicle Li-ion battery: a comparative analysis". In: *Environmental science & technology* 50.14, pp. 7715–7722.

Nordelöf, A., M. Messagie, A.-M. Tillman, M. Ljunggren Söderman, and J. Van Mierlo (2014). "Environmental impacts of hybrid, plug-in hybrid, and battery electric vehicles—what

can we learn from life cycle assessment?" In: *The International Journal of Life Cycle Assessment* 19, pp. 1866–1890.

Plötz, P., C. Moll, G. Bieker, P. Mock, and Y. Li (2020). "Real-world usage of plug-in hybrid electric vehicles". In: *communications* 49.30, pp. 847129–102.

Tamayao, M.-A. M., J. J. Michalek, C. Hendrickson, and I. M. Azevedo (2015). "Regional variability and uncertainty of electric vehicle life cycle CO_2 emissions across the United States". In: *Environmental Science & Technology* 49.14, pp. 8844–8855.

Temporelli, A., M. L. Carvalho, and P. Girardi (2020). "Life cycle assessment of electric vehicle batteries: an overview of recent literature". In: *Energies* 13.11, p. 2864.

The International Council on Clean Transportation (ICCT) (2017). *Annual report*.

Turconi, R., A. Boldrin, and T. Astrup (2013). "Life cycle assessment (LCA) of electricity generation technologies: Overview, comparability and limitations". In: *Renewable and Sustainable Energy Reviews* 28, pp. 555–565.

Wietschel, M., P. Plötz, A. Kühn, and T. Gnann (2014). "Market evolution scenarios for electric vehicles - Summary". In: *Commissioned by acatech-German National Academy of Science and Engineering and Working Group* 7.

Woo, J., H. Choi, and J. Ahn (2017). "Well-to-wheel analysis of greenhouse gas emissions for electric vehicles based on electricity generation mix: A global perspective". In: *Transportation Research Part D: Transport and Environment* 51, pp. 340–350.

Wu, Z., M. Wang, J. Zheng, X. Sun, M. Zhao, and X. Wang (2018). "Life cycle greenhouse gas emission reduction potential of battery electric vehicle". In: *Journal of Cleaner Production* 190, pp. 462–470.

Xu, L., H. Ü. Yilmaz, Z. Wang, W.-R. Poganietz, and P. Jochem (2020). "Greenhouse gas emissions of electric vehicles in Europe considering different charging strategies". In: *Transportation Research Part D: Transport and Environment* 87, p. 102534.

Yuksel, T., M.-A. M. Tamayao, C. Hendrickson, I. M. Azevedo, and J. J. Michalek (2016). "Effect of regional grid mix, driving patterns and climate on the comparative carbon footprint of gasoline and plug-in electric vehicles in the United States". In: *Environmental Research Letters* 11.4, p. 044007.

D Charging behavior of electric vehicles: Temporal clustering based on real-world data

Alexandra Märtz[a], Uwe Langenmayr[a], Sabrina Ried[a], Katrin Seddig[a], Patrick Jochem[b]

[a] Karlsruhe Institute of Technology (KIT), Institute for Industrial Production (IIP), Chair of Energy Economics, Hertzstraße 16, 76187 Karlsruhe, Germany.

[b] German Aerospace Center (DLR), Institute of Networked Energy Systems, Energy Systems Analysis, Curiestrasse 4, 70563 Stuttgart, Germany.

Published in:
Energies (2022), 15 (18), Art. No.: 6575. doi:10.3390/en15186575.

Abstract

The increasing adoption of battery electric vehicles (BEVs) is leading to rising demand for electricity and, thus, leading to new challenges for the energy system and, particularly, the electricity grid. However, there is a broad consensus that the critical factor is not the additional energy demand, but the possible load peaks occurring from many simultaneous charging processes. Hence, sound knowledge about the charging behavior of BEVs and the resulting load profiles is required for a successful and smart integration of BEVs into the energy system. This requires a large amount of empirical data on charging processes and plug-in times, which is still lacking in literature. This paper is based on a comprehensive data set of 2.6 million empirical charging processes and investigates the possibility of identifying different groups of charging processes. For this, a Gaussian mixture model, as well as a k-means clustering approach, are applied and the results validated against synthetic load profiles and the original data. The identified load profiles, the flexibility potential and the charging locations of the clusters are of high relevance for energy system modelers, grid operators, utilities and many more. We identified, in this early market phase of BEVs, a surprisingly high number of opportunity chargers during daytime, as well as switching of users between charging clusters.

D.1 Introduction

On the one hand, the increasing adoption of battery electric vehicles (BEVs) may pose challenges for the power grid, especially for the low-voltage distribution grid where charging infrastructure for BEVs is typically located (Jochem et al., 2018). On the other hand, the batteries of BEVs represent a flexibility potential that might become more and more valuable to the energy system in the face of the rollout of renewable energy sources (RES), and the concomitant phase-out of coal and nuclear energy sources (Xu et al., 2020). On average, passenger cars are typically parked 23 h a day (Ecke et al., 2020). Thus, BEVs' idle times often exceed the charging duration. The resulting flexibility could be used, for example, for postponing or interrupting charging processes, or even feeding back into the grid (Ried, 2021). By applying controlled charging strategies, charging costs can be reduced or RES usage increased (Seddig et al., 2019).

In order to address future challenges and opportunities associated with BEV adoption from

an energy system perspective, distribution system operators (DSOs) need to quantify impacts on grid infrastructure and necessities for grid reinforcement. Therefore, sound forecasts of new load by BEV charging are required. Moreover, new market players of the energy system, such as aggregators, need insights into BEVs' flexibility potential for determining smart charging or load shifting strategies. Consequently, meaningful data is required for energy systems analyses.

As is today's best practice, synthetic load profiles or empirical data from field tests are used as input data to energy system models (Heinz, 2018; Schäuble et al., 2017). However, with the growing application of BEVs, it is of great significance to have a deep understanding of BEV users' driving and charging patterns for forecasting both their charging processes and the associated flexibility potential. A detailed insight into the complexity of spatial and temporal charging behavior has enormous significance for the future dimensioning and flexibility assessment of local grids and charging infrastructure or for the use of the flexibility potential of BEVs for the integration of RES.

For this reason, our contribution is twofold. Firstly, we provide insights into real-world charging behavior, based on a comprehensive real-world data set of 2.6 million charging processes in 2019. We particularly focus on the charging process, especially the charging patterns and charging power used, and the plug-in times, i.e., the corresponding charging flexibility potential. The aim is to investigate what insights can be gained using the temporal individual charging behavior of BEVs' users. For this purpose, we used a two-stage cluster algorithm procedure to identify charging user groups and to derive a standard charging pattern for each user group. We subsequently validated and mapped the BEVs user groups to charging locations, such as at home, at work and in public, supported by synthetic load profiles. In addition, this paper also provides the statistic parameters to replicate and reuse the underlying real-world data set. Thus, on the one hand, the paper allows the drawing of conclusions about real charging behavior and, at the same time, reduces the lack of data, by providing the possibility to replicate the underlying data set, which supports current energy system modelers to consider the load flexibilities of BEVs in much more detail.

To address the above-mentioned research contribution, this work is divided into five parts. Section D.2 provides a short overview of the existing literature. Section D.3.1 describes the characteristics of the analyzed real-world data set as the basis for the subsequent analyses, as well as describing the necessary data adjustments. Section D.3.2 presents the applied methodology of the two cluster algorithms (Gaussian Mixture Model clustering, k-Means

clustering). Section D.4 describes the results, particularly the assignment of the single charging events to temporal charging clusters and the investigation of the homogeneity of these temporal charging clusters. Based on these temporal charging clusters, we derive user groups and address the associated charging behavior. For validation, we use results from a synthetic load profile generator for BEVs. Section D.5 discusses the findings of this work and Section D.6 provides the conclusion.

D.2 Literature review

The individual charging pattern of BEVs represents a large uncertainty in many analyses due to lack of real-world data (ElNozahy and Salama, 2013; Kong and Karagiannidis, 2016), while individual charging behavior has an influence on numerous aspects. In order to provide grid stability, even with a high penetration of BEVs, DSOs are particularly interested in the individual charging behavior and the resulting load peaks to quantify impacts on grid infrastructure and necessities for grid reinforcement (Knezović et al., 2017). Ge et al. (2020) determine a random based spatial-temporal prediction of BEV charging to obtain more precise insights. Crozier et al. (2021) apply a stochastic model based on two different data sources (travel survey data as well as vehicle usage data) to evaluate the BEV charging load and the impacts on the electricity network. One of their key findings is that peak charging demand varies strongly among regions and that representative data is required. Individual charging behavior of BEVs also plays a key role in determining the need for charging infrastructure (Chakraborty et al., 2019; Kavianipour et al., 2021). There is a substantial amount of literature on the prediction of individual charging behavior. One commonly used method is the application of machine learning algorithms to predict charging behavior (Chung et al., 2019; Huber et al., 2020). An alternative method to machine learning algorithms is simulation (Pagani et al., 2019; Zhang et al., 2020). Zhang et al. (2020) investigated charging profiles of electric vehicles presenting a sophisticated simulation method that takes people's demographic and social characteristics into account. Pagani et al. (2019) developed and applied a novel agent-based simulation framework, which takes the charging behavior of individual electric vehicle users as well as the spatial distribution of electric vehicles into account. Knowing the individual charging behavior and the resulting flexibility potential is also crucial for aggregators for defining load shifting strategies. Others, like Sohnen et al. (2015), use BEVs' flexibility potential to evaluate greenhouse gas emissions of BEV charging processes on a dispatch model, based on temporal and spatial effects. Flath et al. (2014) analyzed the importance of BEV charging and underlined the possibility of area pricing. This

possibility is particularly relevant for real world application if the load flexibilities of EVs are offered and used by energy providers. Deng et al. (2020) found that the flexibility provided by BEVs could be used for power reserves and accordingly modeled an BEV aggregator to elaborate this potential of BEVs. Gunkel et al. (2020) consider EV flexibility in detail and with respect to the transmission system development. The review paper of Venegas et al. (2021) goes one-step further and identifies the services which can be provided through BEVs along the value chain. Thereby, possible barriers are classified for active BEV integration. Consequently, meaningful data based on real-world data is required for a successful integration of EVs into the energy power system (Das et al., 2020).

Cluster analysis is increasingly applied to smart meter electricity demand data to identify patterns in electricity consumption. The aim is to improve load forecasting, to increase the alignment of demand response programs or to improve the performance in distribution grids (Ma et al., 2017; Xiang et al., 2020). Clearly, the scope of the focus in the literature is not only on load profiles for BEVs. In Ma et al. (2017) different cluster analysis strategies are examined to identify typical daily heating energy usage profiles. With respect to BEVs, the cluster algorithm is often applied to the charging power profiles. A dataset of hourly load profiles was investigated in Satre-Meloy et al. (2020) and clustering applied to cumulative load profiles to model power consumption during evening peak hours. In Yang et al. (2018) the driving and charging behavior of BEVs' drivers in Shanghai were investigated. They used a machine learning approach as a classifier to analyze the related habitual driver behavior. It is worth emphasizing that clustering is often applied to charging profiles, but not exclusively to the temporal charging behavior. This is the reason why the focus of this contribution is exclusively on the latter.

Up to now, only a few papers have considered empirical data from BEVs to generate BEV load profiles. Among them one is by Schäuble et al. (2017), who gained empirical EV load profiles based on three electric mobility studies. The derived charging load profiles gave a realistic understanding of the BEV energy demand. Another data source are the charging stations, where the dataset from Elaad (elaad.nl) is used in literature (Amara-Ouali et al., 2021; Helmus et al., 2018). In the absence of real data, one approach is to use synthetic load profiles derived from the driving behavior of conventional vehicle users, like in Heinz (2018) In this case, real-world data from BEVs' charging and mobility behavior are lacking. As an alternative, previous studies often rely on numerous assumptions for uncontrolled individual charging behavior (Kong and Karagiannidis, 2016; Gadea et al., 2018; Li and Lenzen, 2020; Fernandez et al., 2010; Plagowski et al., 2021; Shafiee et al., 2012; Shahidinejad et al., 2011).

Thus, the individual charging behavior of BEVs plays an important factor in numerous research aspects. Due to the frequent lack of representative real-world data, this paper aims to contribute data and provide insights into the charging behavior based on temporal data of a real-world charging data set of BEV users. At the same time, the possibility of reproducing the underlying dataset is given.

D.3 Materials and methods

D.3.1 Materials

D.3.1.1 Data characteristics

The analyzed dataset includes real BEV mobility and charging data from the German vehicle manufacturer BMW. All charging events are associated with the i3 model. The dataset comprises about 2.6 million charging processes, each giving information on the location (approximate GPS coordinates), plug-in time, plug-out time, the time of the end of the charging process, starting state-of-charge (SoC) of the battery, ending SoC, and charged energy. The data for our analysis was collected from 1 January 2019 until 31 December 2019 and covers all of Germany and approximately 21,000 BEVs. The identifiers of the individual vehicles are pseudonymized identification numbers so matching the charging activity to the vehicle is possible. The dataset is the largest dataset on charging patterns from a BEV perspective known in literature.

D.3.1.2 Charging behavior

The following subchapter presents and discusses the evaluation of the data and the 2.6 million charging processes. Figure D.1 shows the distribution of plug-in and plug-out times within a day. It is visible that a larger share of BEVs were connected to the grid in the afternoon and evening hours and the majority of BEVs were unplugged in the morning. It is also noticeable that the frequency of plug-out times was higher than the frequency of plug-in times.

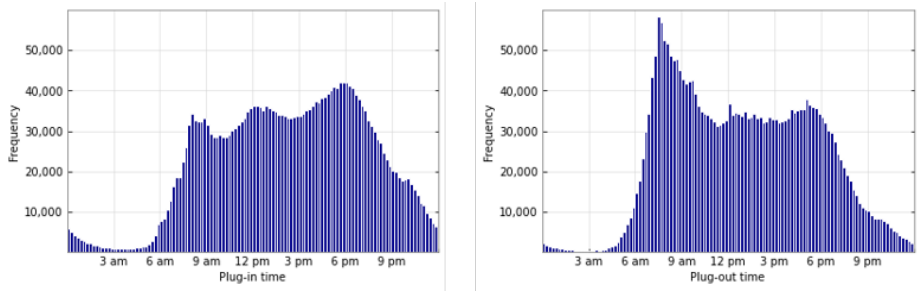

Figure D.1: (a) Distribution of plug-in times over all Germany; (b) Distribution of plug-out times over all Germany.

The average distance driven between two charging processes amounted to 67 km. The remaining battery's SoC at the beginning of a charging process was 53% on average. The average charging frequency was 96 charging events per BEV over the registration period in the year 2019. Adjusted for the number of weeks in which the vehicle was charged, this corresponded to an average of 3.11 charging processes per week. Therefore, a BMW i3 was charged approximately every two days on average. Compared to Schäuble et al. (2017), the charging frequency per BEV in the i3 dataset was higher.

During each charging process, an average of 9.24 kWh of electricity was charged. This meant that, in total, all i3 generated an additional energy demand of 24,595 MWh over one year. The distribution of the additional energy demand of all i3 BEVs for all of Germany in hourly resolution is shown in Figure D.2.

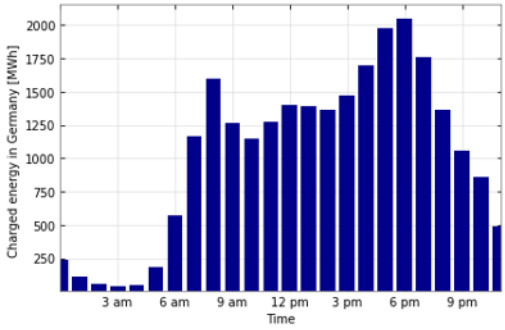

Figure D.2: Charged energy of all i3 BEV for all of Germany in hourly resolution.

For all BEVs, the cumulative average charged energy represents a typical pattern. In order to consider spatial aspects, the plug-in and plug-out times of the different federal states in

Germany are shown in Appendix D.7.1 (cf. Figure D.9). The main trend was very similar, but there were differences in the number of BEVs and the related spatial charged energy (cf. Figure D.10).

In general, the challenge of integrating BEVs into the power grid lies mainly in the potential load peaks, rather than in the provision of the additional energy. These load peaks depend, in particular, on the individual charging behavior, the charging power used and, thus, the associated simultaneity of the charging processes (Jochem et al., 2018; Märtz et al., 2019).

Therefore, we analyzed the real charging behavior and real charging load profiles of today's BEV users. Based on the entire i3 dataset, a cumulative, as well as an average (per BEV), charging load profile were generated. The resulting power curves for both all considered charging processes over all of Germany and the per vehicle average are presented in a weekly average in Figure D.3(a). A classic average load curve could be seen over the period of a week with load peaks in the morning and evening hours. In general, more charging processes took place during the week than on weekends. On average, the load peak for one vehicle was 0.19 kW on weekdays and 0.15 kW on weekends. It is noticeable that there was also a basic charging load during the night hours.

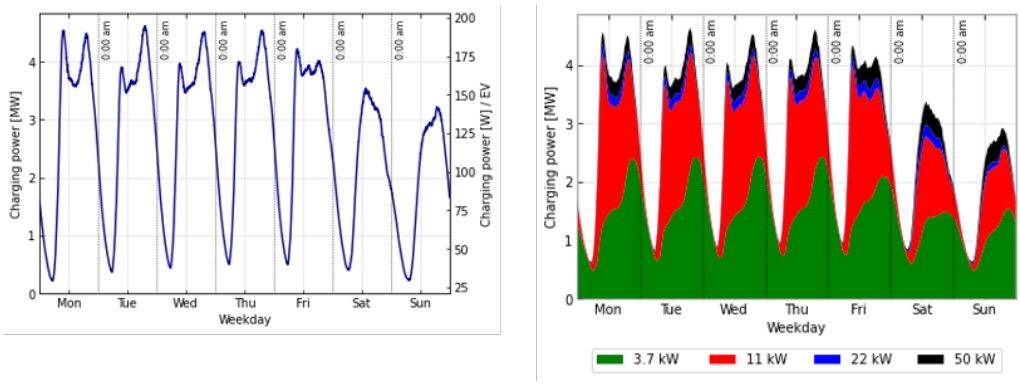

Figure D.3: (a) Average power profile, aggregated (left axis) and proportional (right axis); (b) Average charging profile differentiated by the charging power used.

Since the used charging rate also has an influence on the charging patterns, we considered the used charging power as well. Figure D.3(b) shows the average charging power used

over time. Here, the assumption was made that the identification of the used charging rate is possible based on the average charging power of each charging process, calculated by:

$$\text{average charging power}_i[\text{MW}] = \frac{\text{charged energy}_i\ [\text{MWh}]}{\text{charging duration}_i\ [\text{h}]} \tag{D.1}$$

for each charging process i. It was noticeable that especially lower charging power rates (3.7 kW and 11 kW) were used for the majority of charging processes.

D.3.1.3 Flexibility potential

The flexibility potential of charging processes is of high interest for energy system modelers. Whenever the plug-in time is longer than the charging time a flexibility can be assumed. There are different definitions of load flexibilities of BEVs. In the following we took a conservative approach and defined the shiftable load as follows: If the plug-in duration exceeds the charging time (i.e., there is a temporal flexibility), it is assumed that the load during the temporal flexibility can be increased by the average charging power (cf. Equation (D.1)) of the charging process. However, if the temporal flexibility is shorter than the charging time only the corresponding fraction is considered and for temporal flexibility this fraction is set to 1. The energy demand during the plug-in period remains the same and the necessary reduced charging at another time is not considered. Hence, other approaches for considering load flexibilities of BEVs, e.g., considering also load shifting potentials between charging events might show significant higher load shifting potentials. Consequently, according to our approach the flexible load is always below the overall load. The average flexibility potential considering the temporal aspects is shown in Figure D.4(a).

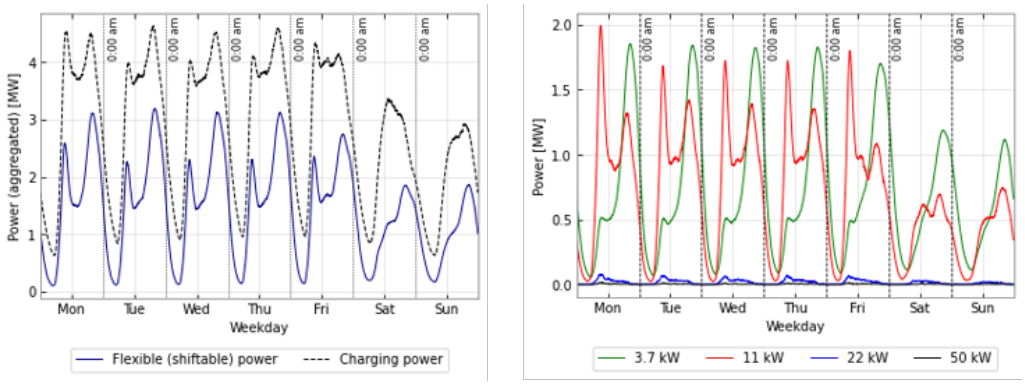

Figure D.4: (a) Average power profile and flexible (shiftable) power; (b) Flexible (shiftable) power per charging power used.

The absolute flexible, shiftable load that could potentially be offered to the grid was quite homogeneous on weekdays and reduced on weekends. The potential flexibility is, of course, always below the load curve, since there are also load processes that do not offer the possibility of shifting the load over time. In the analyzed dataset, about 63% of the charging processes had a flexibility potential. In the remaining charging processes, the vehicles were either not fully charged, i.e., the plug disconnected earlier, or the BEV user terminated the charging process exactly when a SoC of 100% was reached. The temporal flexibility was 8 h on average. It could be seen that there was a comparatively high flexible, shiftable load share, particularly in the morning hours and during the night. BEVs being charged either at the workplace or at home during the night might explain this. Figure D.4(b) shows the flexible, shiftable load in relation to the average charging power used. It was obvious that there was a correlation: the higher the charging power used, the lower the flexible (shiftable) load. This could lead to the conclusion that for numerous charging processes that are associated with a high idle time, lower charging rates are more likely to be used. In addition, the temporal pattern of the shiftable power (which is strongly dependent on the charging power used) can also give an indication of the charging location. In particular, home charging or workplace charging is most likely to be associated with a high idle time and a lower charging rate. This could also be an explanation for the related load peaks.

D.3.1.4 Data adjustment

The data involves the date and time of both BEV plug-in and plug-out. These continuous values are difficult to cluster as they do not concentrate on one single day and, therefore, are

spread across the whole year. Hence, the dataset was adjusted to enable useful clustering. The first step was based on the assumption that all charging activities started at the same day. The plug-in time was implemented as plug-in time at minute of the day. This approach had the shortcoming that the considered period started at 12 am and ended at 11:59 pm. Early and late plug-in times might not be clustered into one cluster because they lost their spatial proximity. The distribution of the plug-in times is shown in Figure D.5. It is visible that the charging activities decreased in early morning hours and increased again later; forming a turning point at around 3 am (red dashed line). To restore the spatial proximity, all charging activities with a plug-in time below this minimum (purple bars) were moved to the right side (blue bars) to continue the time after 12 pm (green dashed line). The data covered by the purple bars was removed to avoid repetition. The second feature used for the clustering

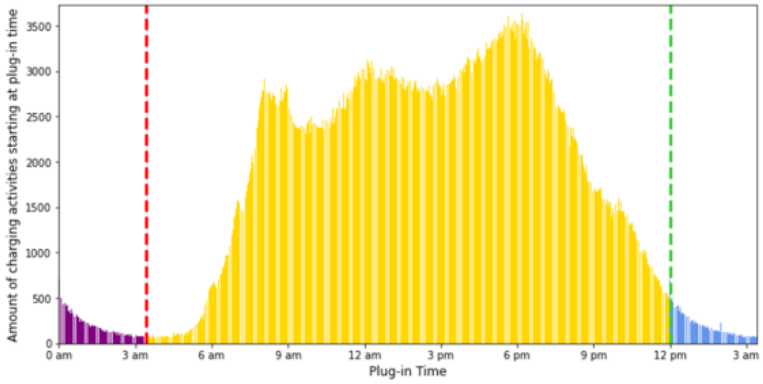

Figure D.5: Distribution of the plug-in times (taking into account data adjustment).

approach was the plug-in duration. However, the plug-in duration of the different charging activities differs significantly. Some BEVs are plugged-out after a few minutes, while others are plugged-in for several days. Such a dataset repeats itself, creating a cloud of data points for each day (one cloud for the BEVs disconnecting on the same day, one cloud for BEVs disconnecting on the second day, one for the third day, and so on) and making it impossible to gain meaningful clustering results because the clustering might only concentrate on the daily clouds instead of intraday activities. Therefore, we adjusted the data in such a way that all charging activities, which neither ended on the same day nor the next day, ended on the next day, but kept the original plug-out time. This way, two clouds occurred: one for the same day charging activities and one for the overnight charging activities. In addition, the plug-in duration was comparable. The final adjusted data is depicted in Figure D.6. The y-axis covers the plug-in duration and, therefore, added dashed lines depict the plug-out

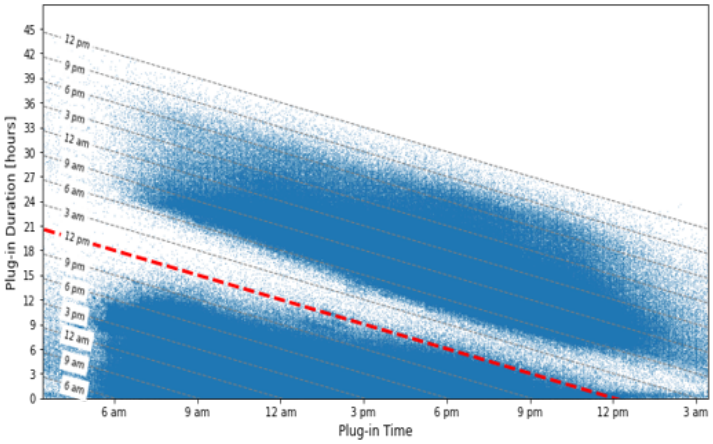

Figure D.6: Final adjusted data depending on plug-in time and plug-in duration, red dashed line represents midnight.

time. Two clouds can be observed. All data points above the midnight line (red dashed line) represented charging activities, which ended on another day; all below represented same-day charging activities.

D.3.2 Methods

In a first step, we examined the temporal charging behavior and investigated whether a homogeneous charging behavior could be derived and whether conclusions could be drawn about the charging location and charging type. The aim was to examine if BEV user groups, having similar plug-in time and plug-in duration switch, existed, as they would therefore, have similar temporal charging patterns.

D.3.2.1 Gaussian Mixture Model clustering

Due to the sheer amount of data points, it was difficult to recognize clusters immediately, making it difficult to choose the clustering approach right away. Therefore, in a first step the distribution of the data was analyzed, shown in Figure D.7. The high concentration of the data is a common indicator for the application of density-based approaches. In addition, the clustering approach needs to perform well with large datasets regarding computation time and memory limitations (Patel and Kushwaha, 2020). Based on these limiting factors,

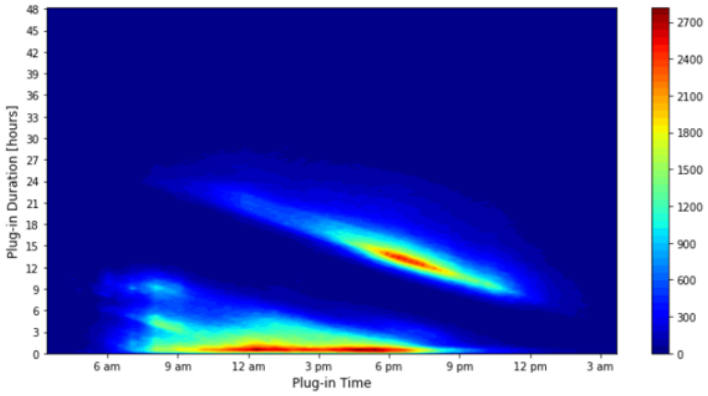

Figure D.7: Density distribution of the final dataset.

the Gaussian Mixture Model (GMM) clustering was applied. The GMM clustering is an unsupervised approach, which decomposes complex distribution of a database $p(x)$ into K Gaussian distributions $\mathcal{N}(x|\mu_k, Cov_k)$, so called components, with a mean μ_k, covariance Cov_k and weight π_k each (Bishop and Nasrabadi, 2006); each distribution represents a cluster:

$$p(x) = \sum_{k=1}^{K} (\pi_k \mathcal{N}(x|\mu_k, Cov_k)) \tag{D.2}$$

Before choosing the final number of clusters, the clustering approach was conducted with several different numbers of clusters and the Aikaki Information Criterion (deLeeuw, 1992) and the Bayesian Information Criterion (Schwarz, 1978) were calculated. Both criteria helped to assess the fit of the developed model, and to avoid overfitting of the data. Based on the analysis of these two criteria, the GMM clustering was conducted with seven clusters.

D.3.2.2 K-Means Clustering

To analyze the charging behavior, only BEV users with more than 20 charging activities were chosen for the second clustering approach. The number of total charging activities and the charging activities during each of the above-derived temporal charging clusters were counted, and the share of charging activities for each cluster for the user was calculated. These shares for each user built the base for the next clustering step.

The unsupervised k-means clustering approach was used to derive the different temporal

behavior clusters (Lloyd, 1982). K-Means is a simple and commonly used clustering approach for behavior analysis. Some examples where k-means is applied for driving pattern analysis are Fugiglando et al. (2018) and Dardas et al. (2020). The aim of k-means clustering is to find K cluster centers μ_k and assign each data point x_n of the data set N to a cluster center. The assignment of data point x_n to a cluster center is conducted via binary variable $b_{n,k}$. Each data point can be assigned to only one cluster center. The k-means approach finds values for μ_k and $b_{n,k}$ to minimize the sum of all distances between the data points and their cluster centers. This function is sometimes called distortion measure:

$$J = \sum_{n=1}^{N} \sum_{k=1}^{K} b_{n,k} \parallel x_n - \mu_k \parallel^2 \tag{D.3}$$

Due to the seven clusters in the GMM clustering, the dataset of the k-means clustering has seven dimensions. To examine if all these dimensions are necessary for the k-means clustering, the dimensions were normalized and the number of dimensions reduced by a subsequent principal component analysis. The final number of clusters was chosen by applying the elbow technique for different numbers of clusters (Syakur et al., 2018). Based on this analysis, five clusters were chosen.

D.4 Results

Based on the methodological approach described in the previous Section D.3.2.1, seven temporal charging clusters were identified. In the following, we examine the seven clusters (cf. Figure D.8) in more detail and validate them with the aim of trying to categorize them. The already high number of seven clusters showed that the data was too complex to be described by a few Gaussian distributions. Moreover, the following two main agglomerations of charging incidents, identified in Figure D.7, were somewhat surprising: there were many overnight chargers, who plugged-in between 6 pm and 9 pm, and another hot spot seemed to be a huge group of opportunity chargers during the day, who stood out because of the short charging times during the daytime. This latter group has not been considered in most energy systems models. Besides these two hot spots, there was still a broad range of other charging incidents. Consequently, the GMM clustering split the overnight (Clusters 2, 3, and 4), as well as the daytime (Clusters 1, 5, 6, and 7), chargers into different groups. The mean, weight, and covariance of each cluster and the total number of samples in each cluster are depicted in Table D.2 in the Appendix D.7.2. The evaluation of the identified charging

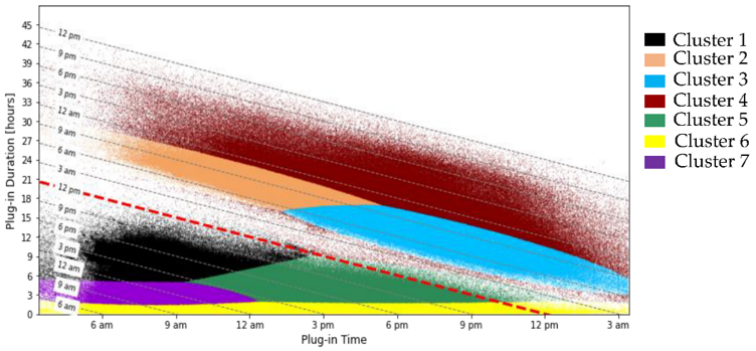

Figure D.8: Related Clusters to the GMM-Clustering, red dashed line represents midnight.

clusters is shown in Table D.1. The associated graphs can be found in Appendix D.7.2 (Figures D.11–D.17). There, the distribution of the plug-in times, the plug-out times and the distribution of the plug-in durations, as well as the average load profile (considering the charging powers used), are shown.

As shown in Table D.2 and in Figures (Figures D.11–D.17) (in Appendix D.7.2), the temporal charging clusters differed with regard to the temporal charging characteristics, such as plug-in time, plug-out time and plug-in duration. Differences could also be identified with regard to the charging power used, as well as the load peaks and the temporal flexibility potential. It should be noted that the effective flexibility potential was higher due to the data adjustment, since the charging processes with more than 48 h were not included. The number of charging processes within a cluster also influenced the peak load.

Cluster 1 and Cluster 7 were characterized by plugging-in during the morning and plugging-out after a medium plug-in duration. The charging events included in Cluster 5 were charging processes that began in the afternoon and had a medium plug-in duration. Cluster 6 contained the charging processes that took place during the day and had a rather short plug-in duration. Clusters 1, 5, 6, and 7 were united by the fact that they were plugged-in and plugged-out on the same day. Clusters 2 to 4 did not have plug-in and plug-out times on the same day (represented by the red dashed line in Figure D.8) and, therefore, had a significantly longer plug-in duration. The temporal flexibility potential and the charging power used also varied significantly per temporal charging cluster (see Table D.1). Interestingly, while temporal charging clusters with low flexibility potential tended to be associated with charging processes that had used high charging power (cf. Cluster 6), high temporal flexibilities were mainly associated with charging processes with low charging power (cf. Clusters 2, 3, and 4).

Table D.1: Characteristics of the temporal charging clusters.

	Cluster 1	Cluster 2	Cluster 3	Cluster 4
Mean Plug-In Time	8.28 a.m.	12.57 a.m.	7.26 p.m.	5.44 p.m.
Mean Plug-Out Time	4.30 p.m.	8.52 a.m.	7.55 a.m.	1.43 p.m.
Mean Plug-In Duration	8h 8min	19h 55min	12h 28min	19h 57min
Charging Power [%]	3.7 kW: 60.21%	3.7 kW: 71.64%	3.7 kW: 77.71%	3.7 kW: 76.54%
	11 kW: 39.29%	11 kW: 28.13%	11 kW: 22.21%	11 kW: 23.30%
	22 kW: 4.45%	22 kW: 0.21%	22 kW: 0.07%	22 kW: 0.15%
	50 kW: 0.04%	50 kW: 0.02%	50 kW: 0.01%	50 kW: 0.01%
Temporal Flexibility	3h 58min	15h 25min	6h 45min	14h 18min
Description of Charging Behavior	Morning to afternoon / Evening charging	Noon to next morning charging	Evening to next morning charging	Overnight rest charging

	Cluster 5	Cluster 6	Cluster 7
Mean Plug-In Time	2.37 p.m.	2.01 p.m.	9.03 a.m.
Mean Plug-Out Time	5.53 p.m.	2.39 p.m.	12.03 a.m.
Mean Plug-In Duration	3h 41min	48min	2h 59min
Charging Power [%]	3.7 kW: 62.25%	3.7 kW: 38.36%	3.7 kW: 53.65%
	11 kW: 36.96%	11 kW: 35.97%	11 kW: 45.00%
	22 kW: 0.71%	22 kW: 9.33%	22 kW: 1.22%
	50 kw: 0.09%	50 kw: 16.34%	50 kW: 0.13%
Temporal Flexibility	56min	2min	44min
Description of Charging Behavior	Afternoon medium-term charging	Short-term charging	Morning medium-term charging

Based on the clustering results, we analyzed how homogeneous the charging behavior of BEV users was. The results of this assessment showed that BEV users did not behave homogeneously by charging their BEVs during similar hours and for similar durations. This finding contradicted the classification of BEV users into fixed user groups.

D.5 Discussion

The identified temporal charging clusters are not very useful for energy system modelers as the characteristics of users and charging locations are missing. With this additional information the modelers would be able to allocate the right charging patterns to the observed users or charging. We, therefore, added two further analyses: first, we tried to identify whether users switch between clusters and, second, we compared our empirically based findings with currently applied load curves, which are usually based on empirical data from conventional vehicles. If these two load curves coincide, current load curves can be further applied in energy systems modeling.

For identifying switching car users between clusters, we applied a k-means clustering with the original user IDs (cf. Appendix D.7.3). Surprisingly, there was quite frequent change between charging clusters. This might come from the free charging opportunities at attractive parking places. The k-means clustering came up with 5 user groups which did not seem as homogenous than expected. Nevertheless, they were analyzed in further detail (cf. Appendix D.7.3).

For comparing our load patterns with existing approaches in literature, which base their charging patterns on plug-in assumptions and empirical mobility data from conventional car usage, we applied the MobiFlex tool (Heinz, 2018) for generating synthetic load patterns (cf. Appendix D.7.4). The comparison between the two charging curves were surprisingly similar. Only the frequent opportunity charging during the daytime was underrepresented in the synthetic load profiles by the MobiFlex tool. Furthermore, the switching between the different charging incidents could not be found in the synthetic load profiles. However, in our analyses we found that the resulting charging load patterns at the different charging locations, such as home, workplace, public or fast charging, showed surprising similar results. As these results are of high interest for all energy system modelers, we plotted the resulting load curves from the MobiFlex tool (cf. Figures D.24 - D.27) and provide the underlying csv

files in the Supplementary Materials.

Even though our dataset was very comprehensive compared to other current available data from BEVs, our approach relied only on the technical data, and user data was not available. Furthermore, all data came from only one specific BEV, the i3 by BMW, and all charging was undertaken in an early market phase of BEVs. Nevertheless, the dataset delivers significant insights to current literature.

D.6 Conclusion

Within the scope of the analysis, the charging behavior of an empirical dataset of real-world charging data, containing approximately 21,000 battery-electric vehicles and about 2.6 million charging processes over a period of one year, was investigated.

In summary, our results show that, based on the exclusive consideration of individual temporal charging data, conclusions could be drawn about battery-electric vehicle user groups and related charging patterns and flexible (shiftable) load. Two main findings could be highlighted: in this early market phase, a surprisingly high number of opportunity chargers during the day, as well as switching users between charging clusters, were identified. Moreover, an estimation of the charging location is possible. We provided resulting load curves, which can be used in energy system models to consider the load shifting potential of battery electric vehicles in more detail.

For future research, further factors of the charging process should be considered in addition to the temporal aspects. For example, the charging power, the amount of energy charged and the charging frequency also play a decisive role. The spatial distribution should also be taken into account in future studies. It should also be emphasized that the underlying real-world data set can be reproduced, based on our analysis, and can, thus, be used for further scientific studies, such as investigating numerous research questions with regard to battery-electric vehicles and to support the successful sustainable integration of electric vehicles into the energy system.

D.7 Appendix

D.7.1 Charging behavioral data

a) Plug-in and plug-out times per Federal State

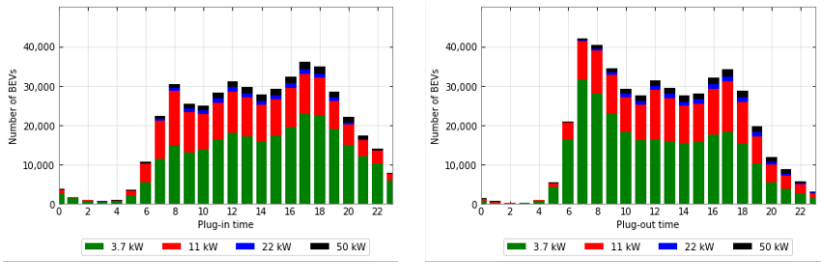

(a) Baden-Wurttemberg

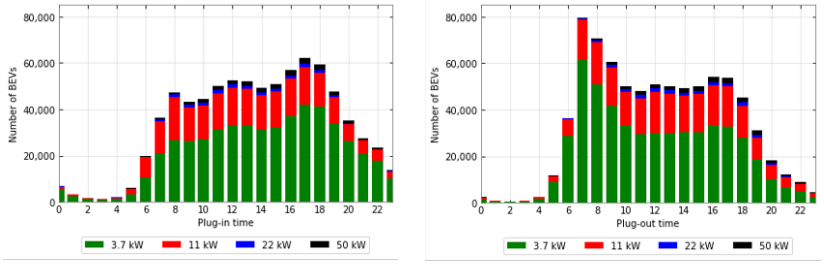

(b) Bavaria

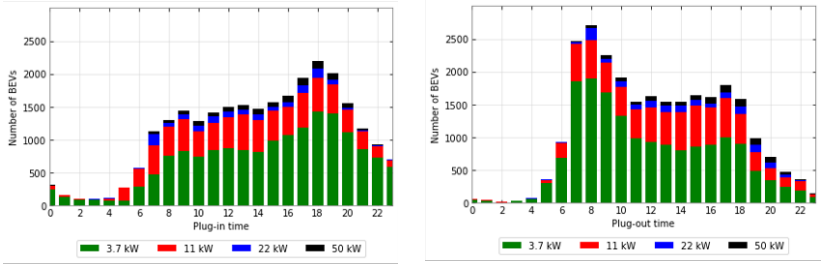

(c) Berlin

Fig. D.9. Cont.

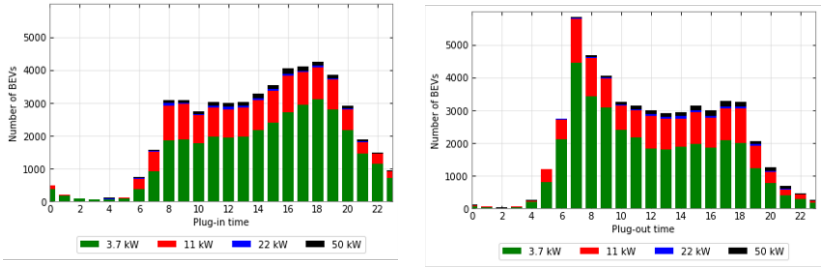

(d) Brandenburg

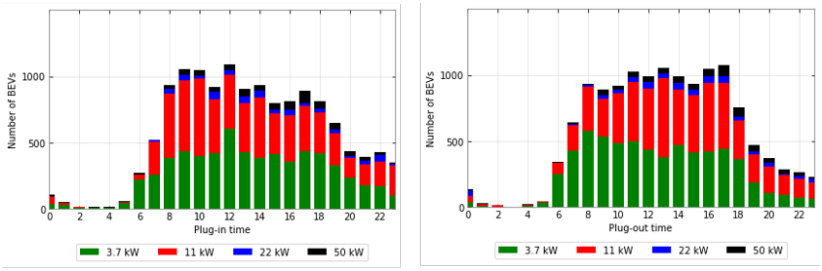

(e) Bremen

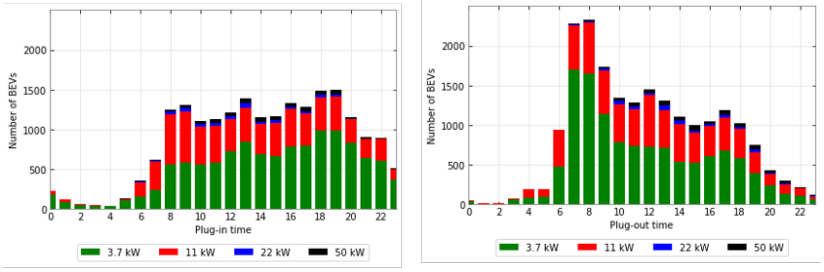

(f) Hamburg

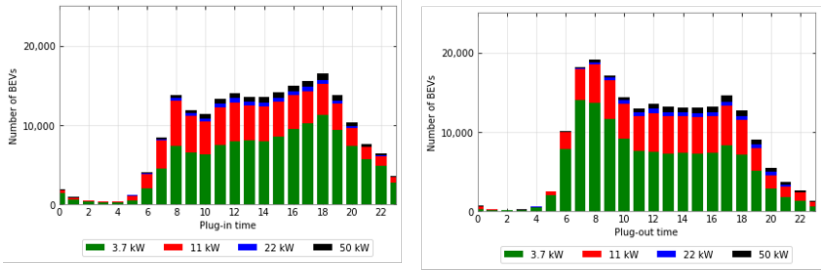

(g) Hesse

Fig. D.9. Cont.

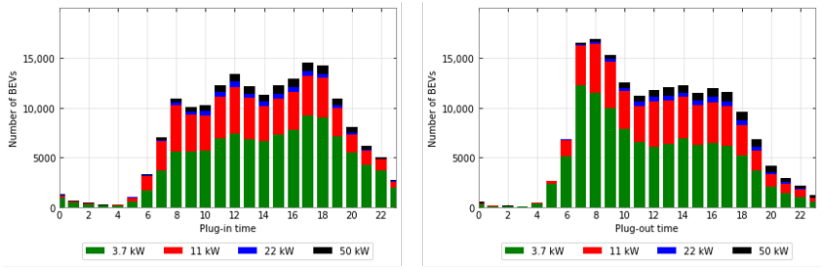

(h) Lower Saxony

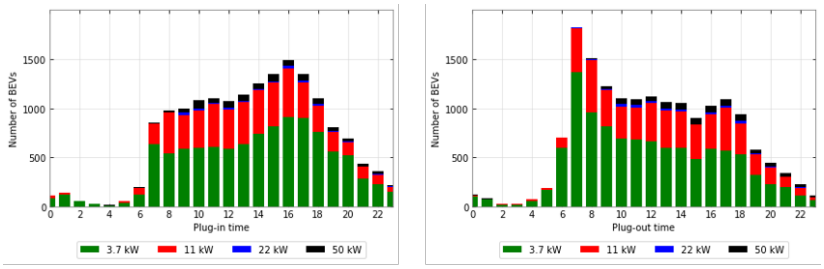

(i) Mecklenburg Pomerania

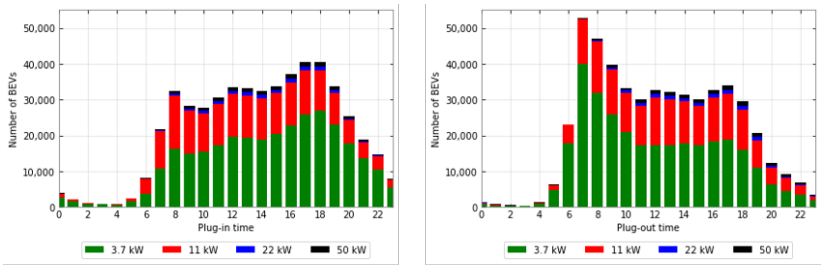

(j) North Rhine-Westphalia

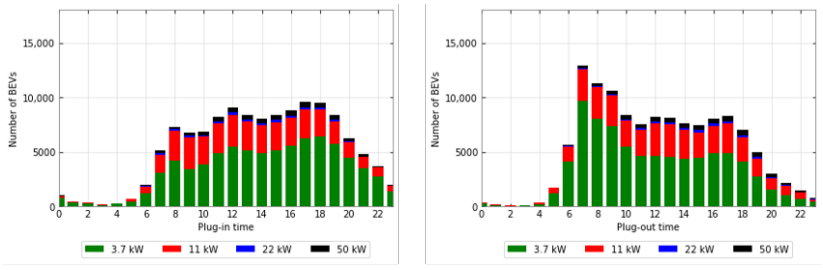

(k) Rhineland-Palatinate

Fig. D.9. Cont.

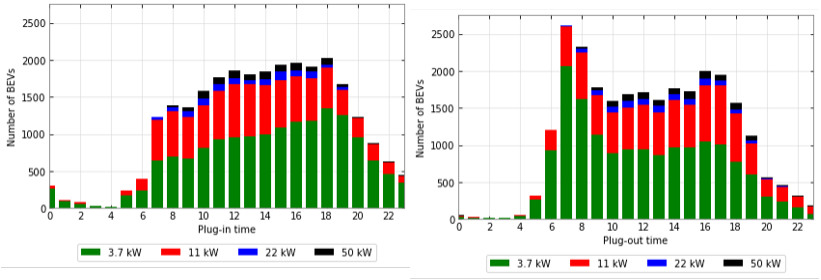

(l) Saarland

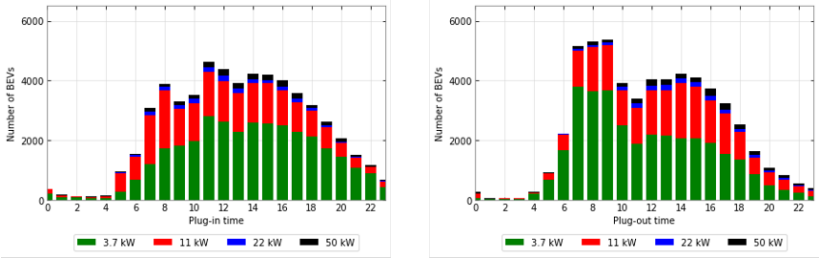

(m) Saxony

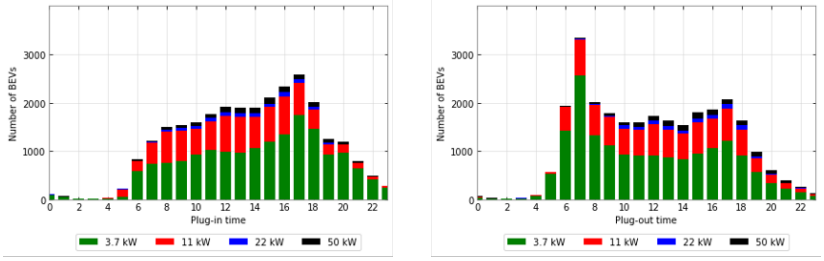

(n) Saxony-Anhalt

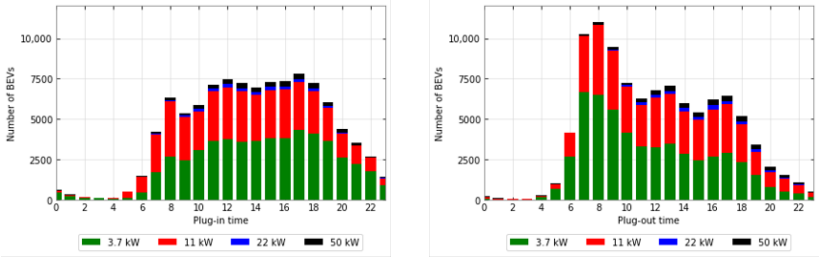

(o) Schleswig-Holstein

Fig. D.9. Cont.

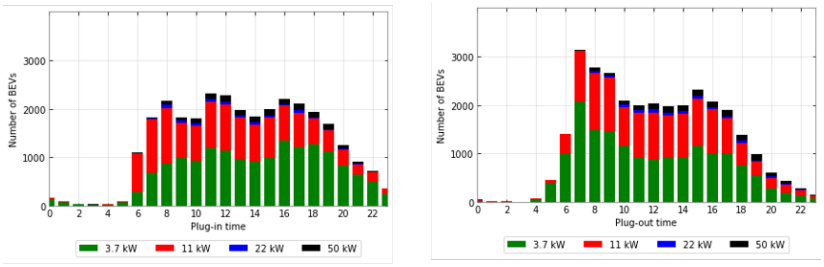

(p) Thuringia

Figure D.9: (a-p) Plug-in and plug-out times taking into account the charging power used per state.

b) Charged energy per Federal State [MWh]

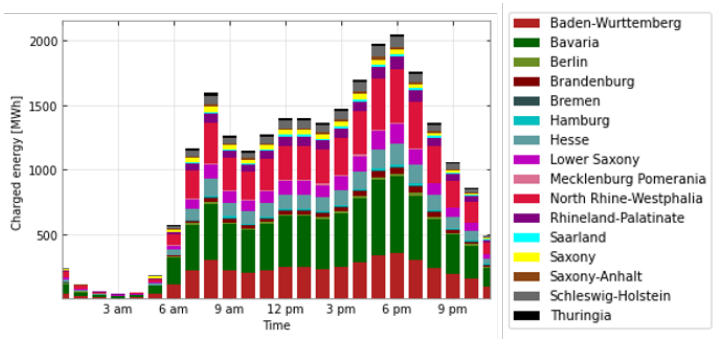

Figure D.10: Charged energy of all i3 BEVs per Federal State.

D.7.2 Further descriptive statistical indicators

a) The mean, weight and covariance of each cluster an the total number of samples in each cluster.

Table D.2: The mean, weight and covariance of each cluster and the total number of samples in each temporal charging cluster.

	Mean μ	Covariance Matrix $\sum$
Cluster 1	$\mu = \begin{pmatrix} 535.8582 \\ 451.0746 \end{pmatrix}$	$\sum = \begin{pmatrix} 14,186.4869 & -4976.5643 \\ -4976,5643 & 19,795.8058 \end{pmatrix}$
Cluster 2	$\mu = \begin{pmatrix} 845.9111 \\ 1132.1117 \end{pmatrix}$	$\sum = \begin{pmatrix} 34,623.8945 & -32,903.1621 \\ -32,903.1621 & 36,569.0678 \end{pmatrix}$
Cluster 3	$\mu = \begin{pmatrix} 1163.0563 \\ 757.6981 \end{pmatrix}$	$\sum = \begin{pmatrix} 23,110.7883 & -21,835.7093 \\ -21,835.7093 & 27,697.1618 \end{pmatrix}$
Cluster 4	$\mu = \begin{pmatrix} 1058.0706 \\ 1176.7476 \end{pmatrix}$	$\sum = \begin{pmatrix} 62,463.0494 & -62,508.4638 \\ -62,508.4638 & 103,104.9956 \end{pmatrix}$
Cluster 5	$\mu = \begin{pmatrix} 875.8100 \\ 193.8779 \end{pmatrix}$	$\sum = \begin{pmatrix} 29,305.3776 & -4100.6763 \\ -4100.6763 & 8072.3007 \end{pmatrix}$
Cluster 6	$\mu = \begin{pmatrix} 848.3180 \\ 49.5780 \end{pmatrix}$	$\sum = \begin{pmatrix} 54,307.5902 & -699.9006 \\ -699.9006 & 982.6405 \end{pmatrix}$
Cluster 7	$\mu = \begin{pmatrix} 559.3524 \\ 167.3003 \end{pmatrix}$	$\sum = \begin{pmatrix} 12,351.5615 & -847.9476 \\ -847.9476 & 6524.9913 \end{pmatrix}$

	Weight π	Number of Samples in Cluster
Cluster 1	0.1000	252,370
Cluster 2	0.0902	215,767
Cluster 3	0.2229	660,084
Cluster 4	0.1184	272,415
Cluster 5	0.2071	396,360
Cluster 6	0.2071	617,763
Cluster 7	0.0995	247,508

b) Charging characteristics for the identified temporal charging clusters

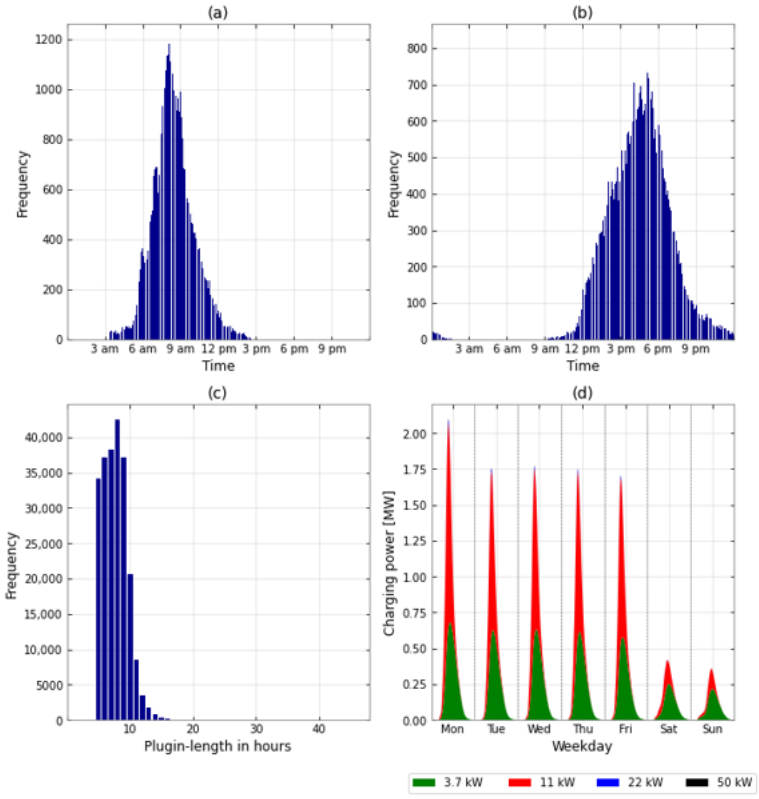

Figure D.11: Charging characteristics of temporal charging cluster 1: (a) Frequency of different plug-in times; (b) Frequency of different plug-out times; (c) Frequency of different plug-in lengths; (d) Charging power used.

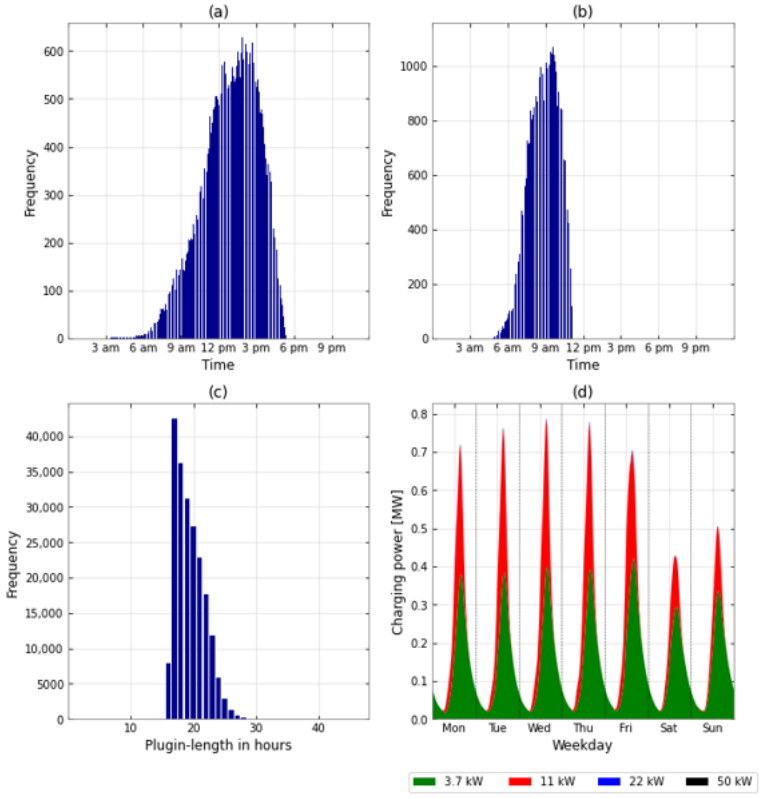

Figure D.12: Charging characteristics of temporal charging cluster 2: (a) Frequency of different plug-in times; (b) Frequency of different plug-out times; (c) Frequency of different plug-in lengths; (d) Charging power used.

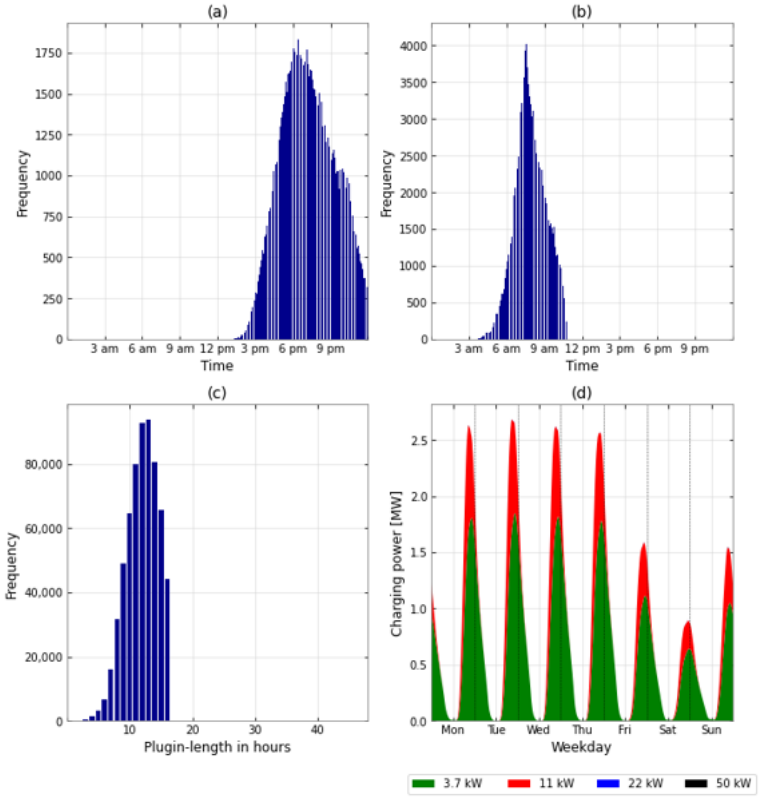

Figure D.13: Charging characteristics of temporal charging cluster 3: (a) Frequency of different plug-in times; (b) Frequency of different plug-out times; (c) Frequency of different plug-in lengths; (d) Charging power used.

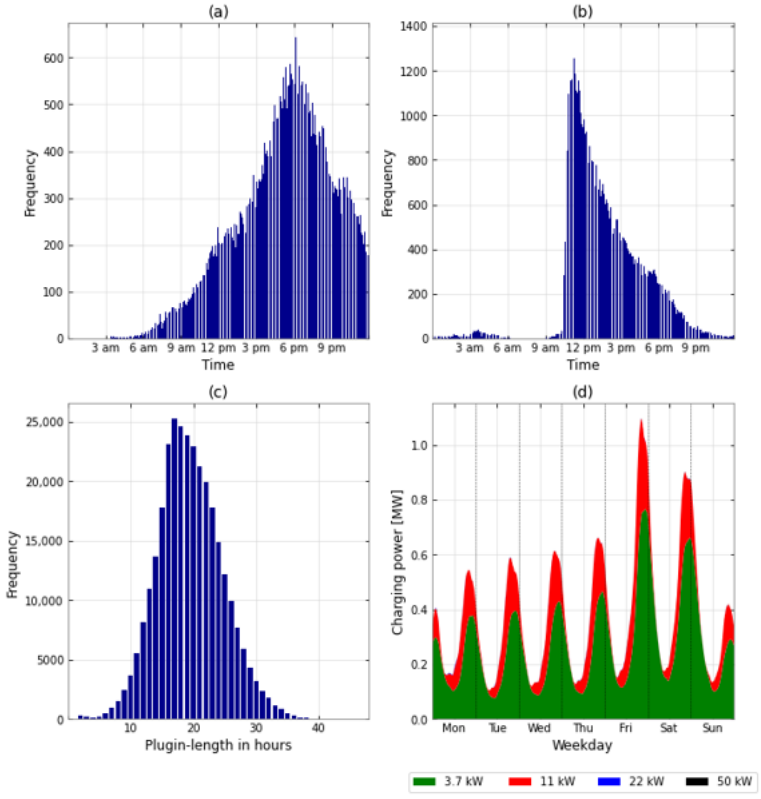

Figure D.14: Charging characteristics of temporal charging cluster 4: (a) Frequency of different plug-in times; (b) Frequency of different plug-out times; (c) Frequency of different plug-in lengths; (d) Charging power used.

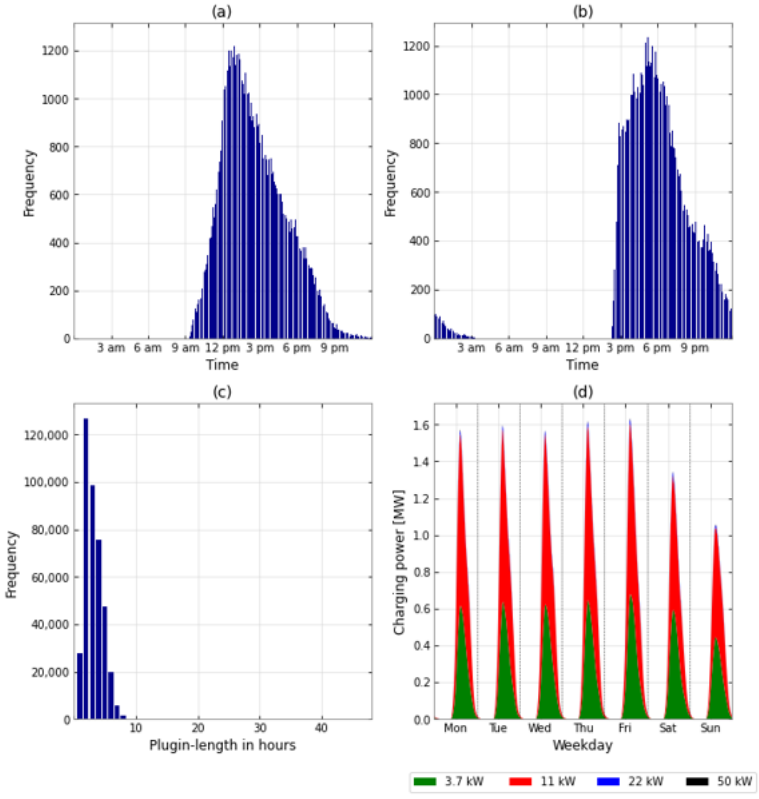

Figure D.15: Charging characteristics of temporal charging cluster 5: (a) Frequency of different plug-in times; (b) Frequency of different plug-out times; (c) Frequency of different plug-in lengths; (d) Charging power used.

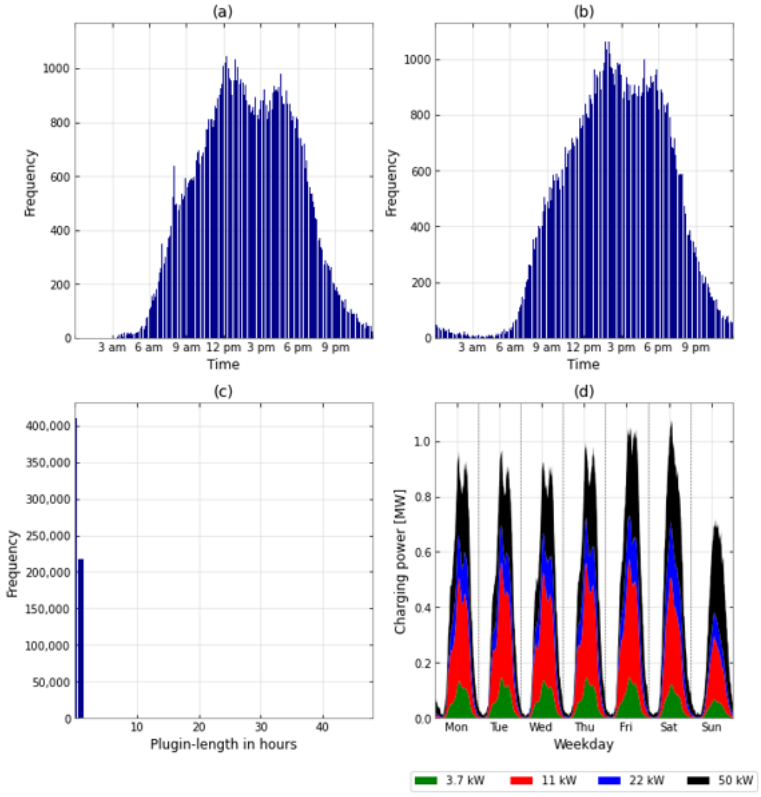

Figure D.16: Charging characteristics of temporal charging cluster 6: (a) Frequency of different plug-in times; (b) Frequency of different plug-out times; (c) Frequency of different plug-in lengths; (d) Charging power used.

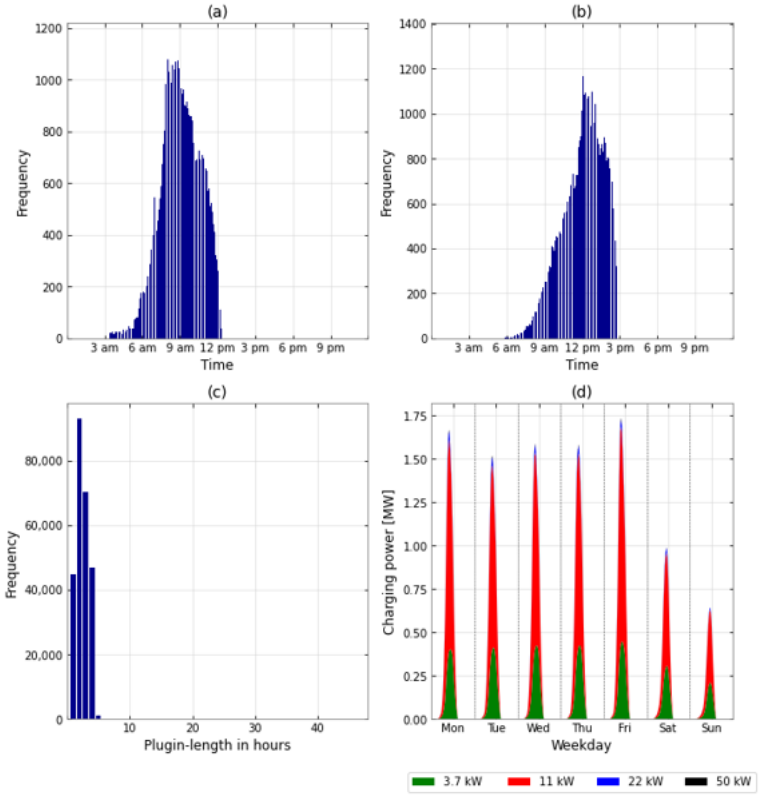

Figure D.17: Charging characteristics of temporal charging cluster 7: (a) Frequency of different plug-in times; (b) Frequency of different plug-out times; (c) Frequency of different plug-in lengths; (d) Charging power used.

D.7.3 Clustering of user groups

To cluster users into charging groups, we applied the k-Means clustering approach (Section D.3.2.2). The resulting five user groups are composed of the shares of the differently used temporal charging clusters (cf. Figure D.8) and are shown in Figure D.18.

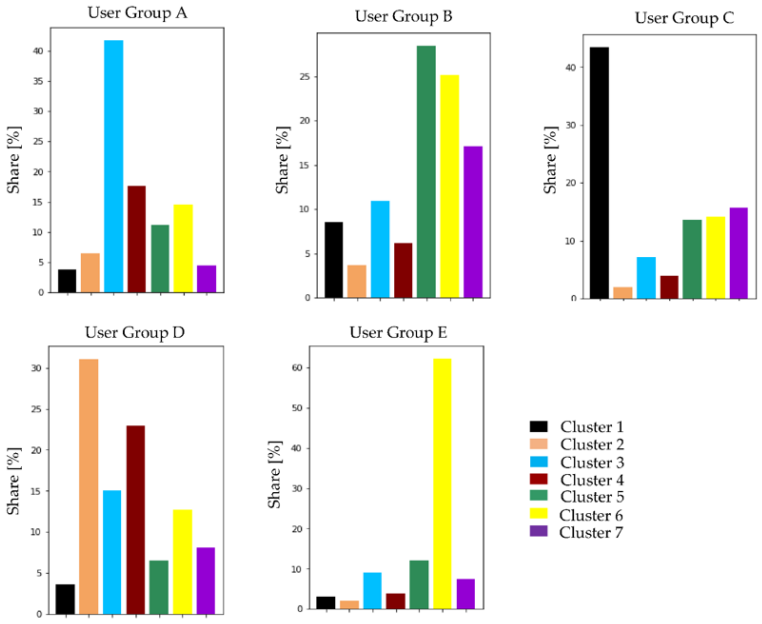

Figure D.18: Related Clusters to the k-Means Clustering.

In the following, the five identified user groups were analyzed taking into account the load pattern, and the charging power used, as well as the flexible (shiftable) power. User Group A included 7830 BEV users and 1,056,623 charging activities. This user group was characterized by the fact that the main charging activities took place mainly at night, with a strong focus on the afternoon/evening plug-in times and the morning unplugging times. In addition, there were short- and medium-term activities. The load pattern, as well as the associated charging power and the flexible shiftable power, are shown in Figure D.19. The afternoon/evening plug-in times can also be seen in the load pattern, which were particularly evident in the afternoon/evening hours. The charging activities mainly took place with smaller charging powers (3.7 kW and 11 kW). Occasionally, charging powers of 22 kW or 50 kW were also in use and could be assigned to short- or medium-term charging activities.

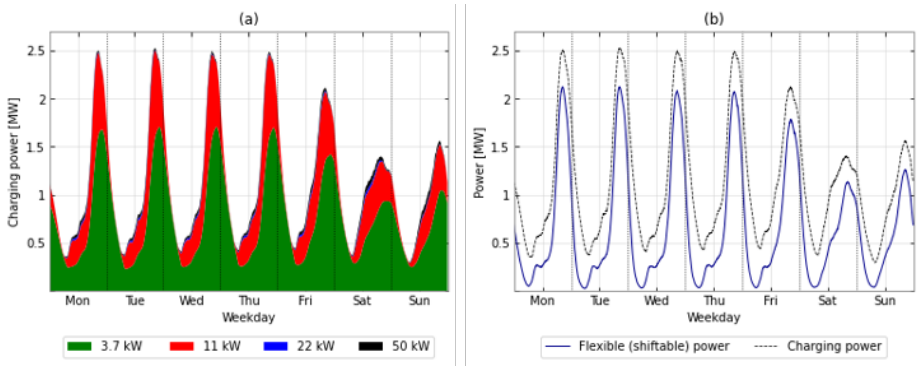

Figure D.19: (a) User Group A: Charging power profile as a function of the assumed charging power used; (b) User Group A: Relation between the charging power profile and the associated flexible (shiftable) power.

User Group B consisted of 5232 BEV users and 661,683 charging activities with a strong focus on short- and medium-term charging activities. The load pattern and the flexible (shiftable) load are pictured in Figure D20. The peak tended to be in the morning hours and the most used charging power in this user group was 11 kW. User Group B had a medium flexible power shifting potential.

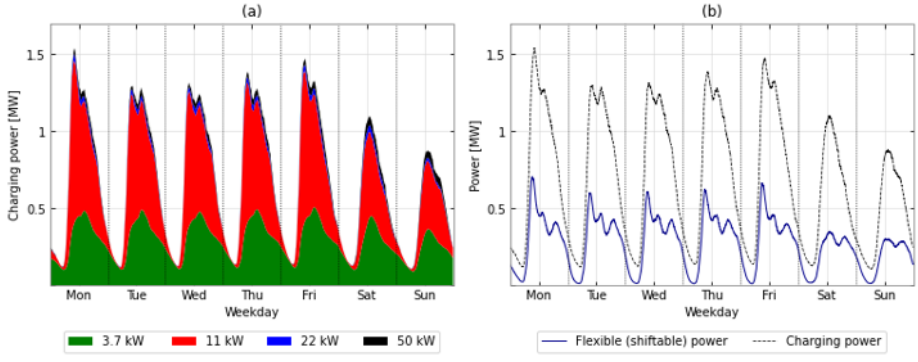

Figure D.20: (a) User Group B: Charging power profile as a function of the assumed charging power used; (b) User Group A: Relation between the charging power profile and the associated flexible (shiftable) power.

User Group C had 1900 BEV users and 240,897 charging activities, which were typified by a high share of medium-term charging activities, which mainly started in the morning hours (cf. Figure D.21). Other short- and medium-term activities also occurred in this charging type. This composition of the temporal charging clusters was also reflected in the load pattern. In this user group, the load peaks were found in the morning hours and had a high

temporal density. Interestingly, the extreme load peaks were only observed on weekdays. The most frequently used charging power in this user group was 3.7 kW and 11 kW during the week; charging processes with higher charging powers could also be assigned at the weekend. In general, this user group had a high potential for flexible power, which was particularly concentrated in the morning hours.

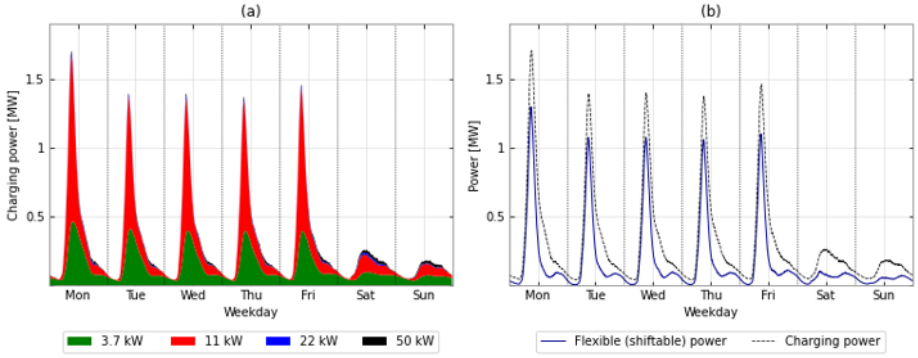

Figure D.21: (a) User Group C: Charging power profile as a function of the assumed charging power used; (b) User Group A: Relation between the charging power profile and the associated flexible (shiftable) power.

2994 BEV users and 328,562 charging activities characterized User Group D. A high share of the charging activities took place over the night but without concentration on evening plug-ins and morning plug-outs. Furthermore, some short-term activities took place. Nevertheless, the occurrence of the charging process was more widely distributed throughout the day. In Figure D.22, it can be seen that here, too, the focus was on the lower charging powers (3.7 kW and 11 kW) and that there were decisive differences between weekday and weekend. In general, there was a very high flexible (shiftable) load in this user group.

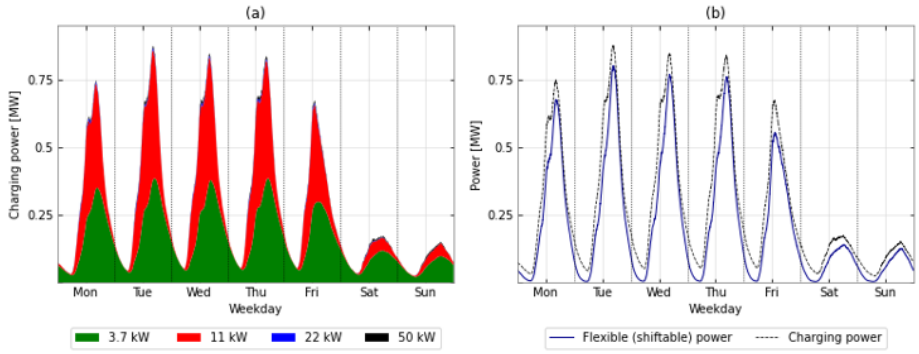

Figure D.22: (a) User Group D: Charging power profile as a function of the assumed charging power used; (b) User Group A: Relation between the charging power profile and the associated flexible (shiftable) power.

User Group E included 2683 BEV users and 329,998 charging activities. The users charged, in particular, by means of short-term charging processes during the daytime hours. What was remarkable here was the share of charging processes that were carried out with a high charging power of 11 kW, 22 kW and 50 kW (cf. Figure D.23). The charging behavior of this user group was quite uniform over the course of a week; only on Sundays were there slightly fewer charging processes on average. This user group had only a very low flexible power shifting potential.

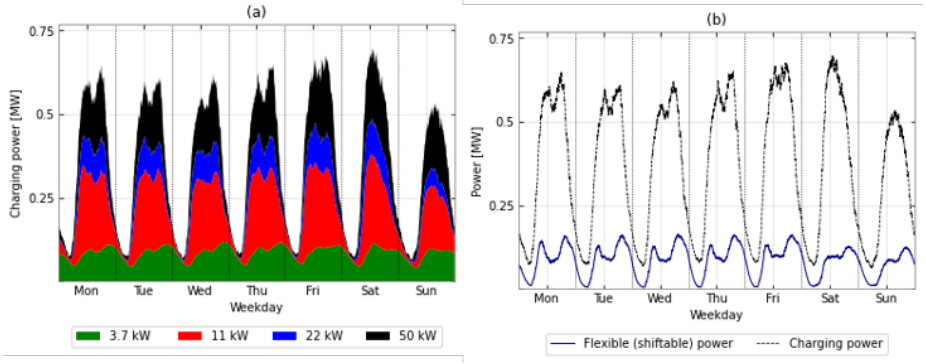

Figure D.23: (a) User Group E: Charging power profile as a function of the assumed charging power used; (b) User Group A: Relation between the charging power profile and the associated flexible (shiftable) power.

The five user groups described in detail above were compared to each other. The user groups differed in terms of their average load profile and the load peak, as well as the most frequently used charging power with regard to the flexible (shiftable) load.

The load profiles resulted from the composition of the temporal charging cluster shares (cf. Figure D.8) and, therefore, led to very different load profiles of the different user groups. The flexibility resulting from the idle time when the BEV was connected to the grid, but the charging process was already completed, also showed differences. Obviously, the number of BEVs and charging processes also had a decisive influence. In particular, user group A had the highest load peaks, which were higher on weekdays than on weekends. User Group C showed a peak especially on weekday mornings and User Group E showed a constant load curve over a week, in average. The charging pattern could be explained by the shares of charging processes in the temporal charging clusters. While User Groups A and D offered a high temporal flexibility potential, a significantly higher load could be shifted in User Group A. The focus of the shiftable load in User Group D was also mainly on weekdays. In terms of temporal flexibility, User Groups B and C were similar, but they differed in terms of the shiftable load. While User Group B also had a share of shiftable loads at the weekend, the share of shiftable loads in User Group C was particularly during the week. User Group E generally had a very low flexibility potential in terms of time and quantity.

D.7.4 Comparison with synthetically generated charging profiles

In this section, we analyze the hypothesis that the identified temporal charging clusters and, thus, the identified user groups could be associated to charging locations. Therefore, the MobiFlex simulation model that generates synthetic BEV charging profiles based on empirical and representative driving data of conventional passenger vehicles, was applied. For further details, please refer to Ried (2021), Ecke et al. (2020), and Heinz (2018).

The following assumptions were made for the generation of the synthetic load profiles. These assumptions were based on the obtained temporal charging clusters (Figure D.8 and Table D.1). Further input data of the MobiFlex model can be found in Table D.3.

- Temporal chargings in Clusters 2 and 3 represented home charging activities because of overnight charging events, relatively long charging durations and a peak in plug-out-time during the morning hours (commuters).
- Temporal chargings in Clusters 1 and 7 represented workplace charging, because they covered charging events with plug-in time in the morning and the plug-out occurring on the same day.

- Temporal chargings in Cluster 6 represented public charging, because of short plug-in durations.

Table D.3: Further input data for the MobiFlex model.

Parameter	Value
Average battery capacity (calculated using the analyzed dataset)	23.4 kWh
Average energy consumption	17 kWh/100 km
Charging efficiency	90%
Probability of charging power at home	
3.7 kW	76.2%
11 kW	23.7%
22 kW	0.1%
50 kW	0.0%
Probability of charging power at work	
3.7 kW	57.0%
11 kW	42.1%
22 kW	0.8%
50 kW	0.1%
Probability of charging power at public	
3.7 kW	38.4%
11 kW	36.0%
22 kW	9.3%
50 kW	16.3%

The probabilities of charging power at the different locations were calculated based on charging power per charging event in the respective charging location. In the following analysis, four model configurations were carried out: (1) Home charging only, (2) Public charging only, (3) Workplace charging only, (4) Both home and workplace charging. Different user groups were not pre-determined in advance. Instead, the MobiFlex model was applied to the full dataset of all approximately 2300 passenger cars. Those vehicles that could be replaced by BEVs under the given assumptions then determined the total charging power. For comparability reasons, the load profiles are shown on a per vehicle basis. The

charging profiles generated are shown below (Figures D.24 - D.27). These reflect the load profile on the one hand and the charging power used on the other. In order to draw conclusions about the charging location, they were compared with the user groups obtained by the k-means clustering.

In the first model configuration, only the possibility of home charging was considered. The probabilities for the charging power used can be taken from Table D.3. The resulting charging pattern is shown in Figure D.24.

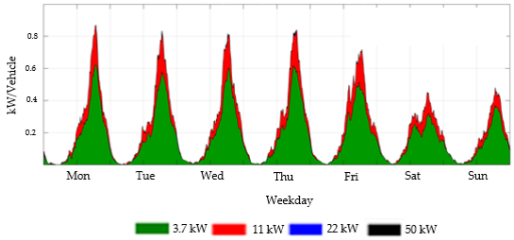

Figure D.24: Charging patterns for uncontrolled charging for "home charging".

The charging pattern of this configuration, the load peaks in the evening and the used charging power showed a congruence with User Group A (cf. Figure D.19(a)). The second configuration examined the case where only public charging was possible. The resulting charging pattern (Figure D.25) showed similarities with User Group E (Figure D.23(a)). There were two peaks on weekdays and one main peak on Saturday morning. However, the MobiFlex model did not show any overnight charging.

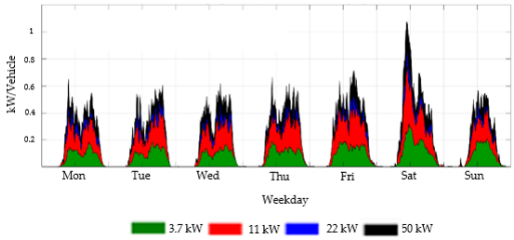

Figure D.25: Charging patterns for uncontrolled charging for "public charging".

When charging is only possible at the workplace, MobiFlex generated the charging pattern shown in Figure D.26, which had similarities to User Group C (cf. Figure D.21(a)). Here, the load peak in the morning hours was particularly characteristic.

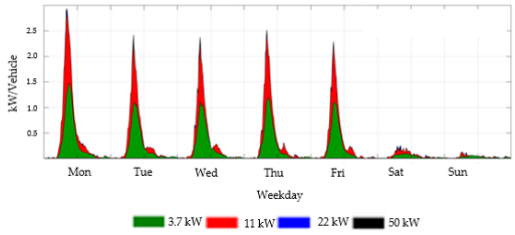

Figure D.26: Charging patterns for uncontrolled charging for "workplace charging".

If both home charging and workplace charging were included in the charging processes, it resulted in the load profile illustrated in Figure D.27. However, this charging pattern did not resemble any of the above user groups.

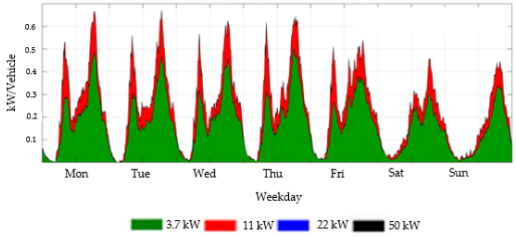

Figure D.27: Charging patterns for uncontrolled charging for "home and workplace charging".

This might lead to the hypothesis that the temporal charging in Clusters 2 and 3 mainly covered home charging, temporal charging in Clusters 1 and 7 mainly workplace charging, and in Cluster 6 public charging. Since the user groups were composed of the shares of the temporal charging clusters (see Figure D.18), User Group A might be rather home chargers, User Group C workplace chargers, and User Group E mostly public short-term chargers. Thus, possible charging locations could be assigned to the three user groups.

References

Amara-Ouali, Y., Y. Goude, P. Massart, J.-M. Poggi, and H. Yan (2021). “A review of electric vehicle load open data and models”. In: *Energies* 14.8, p. 2233.

Bishop, C. M. and N. M. Nasrabadi (2006). *Pattern recognition and machine learning*. Vol. 4. 4. Springer.

Chakraborty, D., D. S. Bunch, J. H. Lee, and G. Tal (2019). “Demand drivers for charging infrastructure-charging behavior of plug-in electric vehicle commuters”. In: *Transportation Research Part D: Transport and Environment* 76, pp. 255–272.

Chung, Y.-W., B. Khaki, T. Li, C. Chu, and R. Gadh (2019). “Ensemble machine learning-based algorithm for electric vehicle user behavior prediction”. In: *Applied Energy* 254, p. 113732.

Crozier, C., T. Morstyn, and M. McCulloch (2021). “Capturing diversity in electric vehicle charging behaviour for network capacity estimation”. In: *Transportation Research Part D: Transport and Environment* 93, p. 102762.

Dardas, A. Z., A. Williams, and D. Scott (2020). “Carer-employees’ travel behaviour: Assisted-transport in time and space”. In: *Journal of Transport Geography* 82, p. 102558.

Das, H. S., M. M. Rahman, S. Li, and C. Tan (2020). “Electric vehicles standards, charging infrastructure, and impact on grid integration: A technological review”. In: *Renewable and Sustainable Energy Reviews* 120, p. 109618.

deLeeuw, J. (1992). “Introduction to Akaike (1973) information theory and an extension of the maximum likelihood principle”. In: *Breakthroughs in statistics: foundations and basic theory*. Springer, pp. 599–609.

Deng, R., Y. Xiang, D. Huo, Y. Liu, Y. Huang, C. Huang, and J. Liu (2020). “Exploring flexibility of electric vehicle aggregators as energy reserve”. In: *Electric Power Systems Research* 184, p. 106305.

Ecke, L., B. Chlond, M. Magdolen, and P. Vortisch (2020). *Deutsches Mobilitätspanel (MOP) - Wissenschaftliche Begleitung und Auswertungen Bericht 2019/2020: Alltagsmobilität und Fahrleistung*.

ElNozahy, M. S. and M. M. Salama (2013). “A comprehensive study of the impacts of PHEVs on residential distribution networks”. In: *IEEE Transactions on Sustainable Energy* 5.1, pp. 332–342.

Fernandez, L. P., T. G. San Román, R. Cossent, C. M. Domingo, and P. Frias (2010). "Assessment of the impact of plug-in electric vehicles on distribution networks". In: *IEEE Transactions on Power Systems* 26.1, pp. 206–213.

Flath, C. M., J. P. Ilg, S. Gottwalt, H. Schmeck, and C. Weinhardt (2014). "Improving electric vehicle charging coordination through area pricing". In: *Transportation Science* 48.4, pp. 619–634.

Fugiglando, U., E. Massaro, P. Santi, S. Milardo, K. Abida, R. Stahlmann, F. Netter, and C. Ratti (2018). "Driving behavior analysis through CAN bus data in an uncontrolled environment". In: *IEEE Transactions on Intelligent Transportation Systems* 20.2, pp. 737–748.

Gadea, A., M. Marinelli, and A. Zecchino (2018). "A market framework for enabling electric vehicles flexibility procurement at the distribution level considering grid constraints". In: *2018 Power Systems Computation Conference (PSCC)*. IEEE, pp. 1–7.

Ge, X., L. Shi, Y. Fu, S. Muyeen, Z. Zhang, and H. He (2020). "Data-driven spatial-temporal prediction of electric vehicle load profile considering charging behavior". In: *Electric Power Systems Research* 187, p. 106469.

Gunkel, P. A., C. Bergaentzlé, I. G. Jensen, and F. Scheller (2020). "From passive to active: Flexibility from electric vehicles in the context of transmission system development". In: *Applied Energy* 277, p. 115526.

Heinz, D. (2018). *Erstellung und Auswertung repräsentativer Mobilitäts-und Ladeprofile für Elektrofahrzeuge in Deutschland*. Tech. rep. Working Paper Series in Production and Energy.

Helmus, J., J. Spoelstra, N. Refa, M. Lees, and R. van den Hoed (2018). "Assessment of public charging infrastructure push and pull rollout strategies: The case of the Netherlands". In: *Energy Policy* 121, pp. 35–47.

Huber, J., D. Dann, and C. Weinhardt (2020). "Probabilistic forecasts of time and energy flexibility in battery electric vehicle charging". In: *Applied Energy* 262, p. 114525.

Jochem, P., A. Märtz, and Z. Wang (2018). "How might the German distribution grid cope with 100% market share of PEV". In: *Proceedings of the 31th International Electric Vehicle Symposium, EVS31, Kobe, Japan*. Vol. 30.

Kavianipour, M., F. Fakhrmoosavi, H. Singh, M. Ghamami, A. Zockaie, Y. Ouyang, and R. Jackson (2021). "Electric vehicle fast charging infrastructure planning in urban networks considering daily travel and charging behavior". In: *Transportation Research Part D: Transport and Environment* 93, p. 102769.

Knezović, K., M. Marinelli, A. Zecchino, P. B. Andersen, and C. Traeholt (2017). “Supporting involvement of electric vehicles in distribution grids: Lowering the barriers for a proactive integration”. In: *Energy* 134, pp. 458–468.

Kong, P.-Y. and G. K. Karagiannidis (2016). “Charging schemes for plug-in hybrid electric vehicles in smart grid: A survey”. In: *IEEE Access* 4, pp. 6846–6875.

Li, M. and M. Lenzen (2020). “How many electric vehicles can the current Australian electricity grid support?” In: *International Journal of Electrical Power & Energy Systems* 117, p. 105586.

Lloyd, S. (1982). “Least squares quantization in PCM”. In: *IEEE Transactions on Information Theory* 28.2, pp. 129–137.

Ma, Z., R. Yan, and N. Nord (2017). “A variation focused cluster analysis strategy to identify typical daily heating load profiles of higher education buildings”. In: *Energy* 134, pp. 90–102.

Märtz, A., L. Held, P. Jochem, W. Fichtner, M. Suriyah, and T. Leibfried (2019). “Development of a Tool for the Determination of Simultaneity Factors in PEV Charging Processes”. In: *Proceedings of the E-Mobility Integration Symposium, Dublin, Ireland*. Vol. 14.

Pagani, M., W. Korosec, N. Chokani, and R. S. Abhari (2019). “User behaviour and electric vehicle charging infrastructure: An agent-based model assessment”. In: *Applied Energy* 254, p. 113680.

Patel, E. and D. S. Kushwaha (2020). “Clustering cloud workloads: K-means vs gaussian mixture model”. In: *Procedia Computer Science* 171, pp. 158–167.

Plagowski, P., A. Saprykin, N. Chokani, and R. Shokrollah-Abhari (2021). “Impact of electric vehicle charging - An agent-based approach”. In: *IET Generation, Transmission & Distribution* 15.18, pp. 2605–2617.

Ried, S. (2021). “Gesteuertes Laden von Elektrofahrzeugen in Verteilnetzen mit hoher Einspeisung Erneuerbarer Energien - Ein Beitrag zur Kopplung von Elektrizitäts-und Verkehrssektor”. PhD thesis. Karlsruhe Institute for Technology (KIT), Karlsruhe.

Satre-Meloy, A., M. Diakonova, and P. Grünewald (2020). “Cluster analysis and prediction of residential peak demand profiles using occupant activity data”. In: *Applied Energy* 260, p. 114246.

Schäuble, J., T. Kaschub, A. Ensslen, P. Jochem, and W. Fichtner (2017). “Generating electric vehicle load profiles from empirical data of three EV fleets in Southwest Germany”. In: *Journal of Cleaner Production* 150, pp. 253–266.

Schwarz, G. (1978). “Estimating the dimension of a model”. In: *The Annals of Statistics*, pp. 461–464.

Seddig, K., P. Jochem, and W. Fichtner (2019). “Two-stage stochastic optimization for cost-minimal charging of electric vehicles at public charging stations with photovoltaics”. In: *Applied Energy* 242, pp. 769–781.

Shafiee, S., M. Fotuhi-Firuzabad, and M. Rastegar (2012). “Impacts of controlled and uncontrolled PHEV charging on distribution systems”. In: *9th IET International Conference on Advances in Power System Control, Operation and Management (APSCOM 2012)*. IET, pp. 1–6.

Shahidinejad, S., S. Filizadeh, and E. Bibeau (2011). “Profile of charging load on the grid due to plug-in vehicles”. In: *IEEE Transactions on Smart Grid* 3.1, pp. 135–141.

Sohnen, J., Y. Fan, J. Ogden, and C. Yang (2015). “A network-based dispatch model for evaluating the spatial and temporal effects of plug-in electric vehicle charging on GHG emissions”. In: *Transportation Research Part D: Transport and Environment* 38, pp. 80–93.

Syakur, M., B. Khotimah, E. Rochman, and B. D. Satoto (2018). “Integration k-means clustering method and elbow method for identification of the best customer profile cluster”. In: *IOP conference series: materials science and engineering*. Vol. 336. IOP Publishing, p. 012017.

Venegas, F. G., M. Petit, and Y. Perez (2021). “Active integration of electric vehicles into distribution grids: Barriers and frameworks for flexibility services”. In: *Renewable and Sustainable Energy Reviews* 145, p. 111060.

Xiang, Y., J. Hong, Z. Yang, Y. Wang, Y. Huang, X. Zhang, Y. Chai, and H. Yao (2020). “Slope-based shape cluster method for smart metering load profiles”. In: *IEEE Transactions on Smart Grid* 11.2, pp. 1809–1811.

Xu, L., H. Ü. Yilmaz, Z. Wang, W.-R. Poganietz, and P. Jochem (2020). “Greenhouse gas emissions of electric vehicles in Europe considering different charging strategies”. In: *Transportation Research Part D: Transport and Environment* 87, p. 102534.

Yang, J., J. Dong, Q. Zhang, Z. Liu, and W. Wang (2018). “An investigation of battery electric vehicle driving and charging behaviors using vehicle usage data collected in Shanghai, China”. In: *Transportation Research Record* 2672.24, pp. 20–30.

Zhang, J., J. Yan, Y. Liu, H. Zhang, and G. Lv (2020). “Daily electric vehicle charging load profiles considering demographics of vehicle users”. In: *Applied Energy* 274, p. 115063.

E Development of a tool for the determination of simultaneity factors in PEV charging processes

Alexandra Märtz[a], Lukas Held[b], Patrick Jochem[a], Wolf Fichtner[a], Michael Suriyah[b], Thomas Leibfried[b]

[a] Karlsruhe Institute of Technology (KIT), Institute for Industrial Production (IIP), Chair of Energy Economics, Hertzstraße 16, 76187 Karlsruhe, Germany.

[b] Karlsruhe Institute of Technology (KIT), Institute for Electric Energy Systems and High-Voltage Technology (IEH), Engesserstrasse 11, 76131 Karlsruhe, Germany.

This paper was presented at the 3rd E-Mobility Integration Symposium and published in the Symposium's proceedings.

Abstract

In this paper, an open-source tool for the calculation of simultaneity factors of electric vehicles (i.e. battery electric vehicles and plug-in hybrid electric vehicles) charging processes is presented. In addition, the peak loads of EV and households can also be displayed, taking into account the EV and household specific simultaneities. In the following, the underlying input parameters and calculations of the tool are explained. Based on this, different results are generated and discussed in detail.

E.1 Introduction

One challenge of electric vehicles (EV) is the relatively high additional load compared to other domestic appliances and the resulting effects on the power grid. This effect of EV (i.e. battery electric vehicles (BEV) and plug-in hybrid electric vehicles (PHEV)) have already been analysed and discussed in numerous studies (Jochem et al., 2018; Rolink, 2013; Stöckl, 2014; Probst, 2014). One factor that has been often neglected in previous analyses is the simultaneity of charging processes (Vennegeerts et al., 2018). It is often assumed that all EV are charged simultaneously at a constant charging rate throughout the entire charging process. However, this reflects an empirically unrealistic simultaneity factor for EV. In other studies, the simultaneity factor is based on current mobility behaviour or is limited to selected applications (e.g. EV can only charge with a charging rate of 3.7 kW), see for instance Rolink (2013) and Heinz (2018).

If the simultaneity of the charging processes is analysed, a distinction must be made between two different simultaneity factors. Firstly, there is the simultaneity factor which describes the percentage of EV charged at the same day. This considers the fact that not each EV is charged on a daily basis. On the other hand, the simultaneity of the charging processes taking place within one day must also be taken into account.

With regard to the simultaneity of the charging processes taking place within one day, a tool is developed which will be offered as an open-source tool to download from a public website (https://doi.org/10.5281/zenodo.3364366). The tool calculates the simultaneity of the charging processes within one day taking into account the number of EV, arrival and departure time, vehicle class (small, medium, or large), various charging rates (3.7 kW, 7.4 kW,

11 kW, 22 kW and 44 kW), battery capacity, and State of Charge (SoC) at arrival as well as desired SoC at departure. The percentage of EV charging on the same day might be included, too. The user of the tool can chose to either use the included data or individual adjusted data. Thus, it is also possible to consider future trends. Especially for analysing the resulting grid impacts (e.g. transformer or cables), household loads with the specific simultaneities in combination with the associated simultaneities of EV charging play a decisive role and are therefore incorporated in the tool. Hence, using the tool, different simultaneity factors (i.e., EV alone or EV plus household) can be easily displayed.

The paper is structured as follows. Chapter E.2 gives an overview of the default input data on which the tool is based. Chapter E.3 presents the calculations of the tool in detail. The results generated by the tool are analysed and discussed in Chapter E.4. Chapter E.5 concludes our contribution.

E.2 Input data

The default data set is based on different sources (e.g. Stöckl (2014), Probst (2014), and Zimmer et al. (2011)) and each value can be modified by the user. Most values can be changed directly in the user interface. Specific input data (e.g. average charging durations) can only be changed in the program code.

All input profiles in this paper have time intervals of 15 minutes as the household load profiles used are only available in 15 min intervals. This can be changed in the code, but makes the according adjustment of the time resolution of input load profiles necessary.

One input parameter is the number of simulated days. The tool calculates the maximum simultaneity factor on a daily basis. This calculation is then repeated to determine the probability of the occurrence of a specific simultaneity factor. Consequently, a higher amount of simulated days increases the accuracy of the results, but also increases the simulation time. The influence of the number of repetitions on the results is examined in Chapter E.4.

E.2.1 Households

For the households in the regarded power grid, only the number of households and the yearly energy consumption per household in kWh have to be entered as input data. To represent the load of a household, a profile is chosen randomly out of a database with 365,000 profiles. This database was generated using Uhlig, M. (2019). All profiles in the database have a yearly energy consumption of 1000 kWh. Hence, the chosen profile is scaled according to the yearly energy consumption per household. The preset value is 3216 kWh, which was the average yearly energy consumption of a two-person household in Germany in 2017 according to Statistisches Bundesamt (2019) and in the basic settings 10 households are considered.

E.2.2 Electric vehicles

Regarding the EV many different parameters influence the calculations. One main parameter is the number of EV considered. The tool differentiates between PHEV and BEV and three vehicle classes (small, medium, big). The share of the individual vehicle classes was calculated from Zimmer et al. (2011). The battery capacity data for BEV and PHEV for the underlying setting are taken from EVBox (2019). The default data is presented in Tab. E.1.

Table E.1: Default values for EV.

	BEV		
	small	medium	big
Share EV class [%]	7	3	5
Battery capacity [kWh]	30.46	37.9	75
	PHEV		
	small	medium	big
Share EV class [%]	5	40	40
Battery capacity [kWh]	8.4	12.26	8.4

As already mentioned, the tool distinguishes between two simultaneity factors. The simultaneity factor, which describes the percentage of EV charged at the same day is set to 78%. This value is based on Figenbaum and Kolbenstvedt (2016) and is preset for the basic setting.

The arrival time is randomly assigned to the EV according to the distribution of Stöckl (2014).

It was assumed, that every used EV is charged as soon as it arrives at home. During the charging process, a distinction is to be made between 2 variants. Either the SoC limits (SoC at the beginning and SoC at the end of the charging process) are set individually or the SoC at the beginning of the charging process is determined according to the distribution of Leou et al. (2013). For the latter, the final SoC is always set to 100%.

Since different charging rates occur simultaneously in reality, an additional aspect covered in the tool is the possibility taking into account simultaneously different charging rates. The default charging power distribution follows Probst (2014) and the calculations are performed on the average charging rate. In the presettings, the tool differentiates between 3.7 kW, 7.4 kW, 11 kW, 22 kW and 44 kW with a share of 73.7%, 0%, 21.5%, 3.5% and 1.3%, respectively.

E.3 Calculations in the tool

E.3.1 Start

The number of vehicles per vehicle class i is calculated by multiplying the given share of each vehicle class i $S_{\text{Veh,i}}$ with the total number of EV $N_{\text{EV,Total}}$ (see Equation (E.1)).

$$N_{\text{EV,i}} = N_{\text{EV,Total}} \cdot S_{\text{Veh,i}} \tag{E.1}$$

The main part of the tool is the calculation of the different maximum simultaneity factors and peak powers on a daily level. For example, the calculation of the simultaneity factor of EV for one day k $SF_{\text{EV,k}}$ is repeated accordingly to the entered number of simulated days N_{Days}.

E.3.2 Daily simultaneity factor for electric vehicles

First, an arrival time $\text{T}_{\text{Arrival}}$ is assigned to each EV randomly accordingly to the distribution in Chapter E.2. As the accuracy of the distribution is one hour, we assume a uniform distribution in each hour. Next, the charging duration $\text{T}_{\text{Charging}}$ for each EV is calculated. If the EV is charging on the considered day, the SoC before $\text{SoC}_{\text{Char.,Start}}$ and after $\text{SoC}_{\text{Char.,End}}$

the charging process are determined. The formula for the calculation of the average energy capacity of all EV's batteries is given in Equation (E.2).

$$E_{\text{EV,Avg.}} = \sum_{i=1}^{6} E_{\text{EV,i}} \cdot S_{\text{EV,i}} \tag{E.2}$$

In Equation (E.2), $E_{EV,i}$ is the average energy capacity of vehicle class i. $E_{EV,i}$ and $S_{EV,i}$ are input parameters. The necessary charging energy $E_{Charging}$ is calculated as given in Equation (E.3).

$$E_{\text{Charging}} = (SoC_{\text{Char.,End}} - SoC_{\text{Char.,Start}}) \cdot E_{\text{EV,Avg.}} \tag{E.3}$$

The charging time $T_{Charging}$ is calculated by multiplying the necessary charging energy $E_{Charging}$ and the average charging duration per kWh $T_{Char.,Avg.}$ (see Equation (E.4)).

$$T_{\text{Charging}} = E_{\text{Charging}} \cdot T_{\text{Char.,Avg.}} \tag{E.4}$$

$T_{Char.,Avg.}$ is defined as given by

$$T_{\text{Char.,Avg.}} = \sum_{j=1}^{5} S_{\text{Char.Power,j}} \cdot T_{\text{Char.,j}} \tag{E.5}$$

$S_{Char.Power,j}$ is the share of charging power j on the total amount of EV and $T_{Char.,j}$ is the corresponding average charging duration per kWh for charging power j. Using the charging duration $T_{Charging}$, the end time of the charging process can then be calculated using

$$T_{\text{End}} = T_{\text{Arrival}} + T_{\text{Charging}} \tag{E.6}$$

Finally, the charging profile of each EV is defined. The profile contains the information whether the EV is charging or not for each time step of the day (e.g. 96 time steps per day for a 15 min resolution).

In order to obtain the collective profile $N_{EV,Collective}$, the profiles of all individual vehicles are summarised. This delivers the number of maximum simultaneously charging EV $N_{EV,Simul.}$. $N_{EV,Simul.}$ is then used to calculated the maximum daily simultaneity factor $SF_{EV,k}$ (see Equation (E.7)).

$$SF_{\text{EV,k}} = N_{\text{EV.,Simul.}} / N_{\text{EV,Total}} \tag{E.7}$$

The arrival time $T_{Arrival}$ and the SoC (depending on the option chosen) are assigned randomly (see Chapter E.2 for more information). In contrast to that, for the energy capacity of the EV

$E_{EV,Avg.}$ as well as the charging duration per kWh $T_{Char.,Avg.}$ average values are used and the values are not assigned randomly. The reason for that is that these values are EV dependend and should be constant for all simulated days.

E.3.3 Unbalanced charging

If the option that considers unbalanced charging is chosen, the calculation for the daily simultaneity factor is equal until Equation (E.6). Here, the profiles are not added to get the collective profile $N_{EV,Collective}$, but divided between the different phases. If the charging power is 3.7 kW one-phase charging is assumed, for 7.4 kW two-phase charging and for all additional charging powers three-phase charging (which is provided by the German electricity grid). If less than three phases are used, the selection of the phases is uniformly distributed. Now, the profiles for each phase ($N_{EV,Ph1}$, $N_{EV,Ph2}$, and $N_{EV,Ph3}$) are generated by adding up the profiles of the EV charging for each phase individually. The profiles are multiplied with a weighting factor (1 for one-phase charging, 1/2 for two-phase charging, 1/3 for three-phase charging) before adding up the profiles.

Out of the profiles $N_{EV,Ph1}$, $N_{EV,Ph2}$, and $N_{EV,Ph3}$ the maximum number of simultanously charging vehicles for each phase $N_{EV,Simul.,Ph1}$, $N_{EV,Simul.,Ph2}$, and $N_{EV,Simul.,Ph3}$ are determined. These results are then used to calculate the maximum daily simultaneity factor $SF_{EV,k,PhO}$ for each phase O (see Equation (E.8)).

$$SF_{EV,k,PhO} = N_{EV.,Simul.,Ph0}/N_{EV,Total} \tag{E.8}$$

E.3.4 Load profile of the households

For each household l, a randomly chosen energy consumption profile $E_{Household,1000,l,k}$ is applied. This profile is scaled to an annual electricity consumption of 1000 kWh. Accordingly, the profile has to be scaled according to the average annual electricity consumption of households considered E_{Con} (cf. Equation (E.9)).

$$E_{Household,l,k} = E_{Household,1000,l,k} \cdot \frac{E_{Con}}{1000} \tag{E.9}$$

Finally, the profiles of all households are added to a collective profile $E_{Household,Collective}$. For this profile, the peak power is determined and saved in $P_{Household,k}$.

E.3.5 Total peak power on daily level

To determine the total peak power, a collective profile E_{Total} including the EV and households is calculated using Equation (E.10).

$$E_{\text{Total}} = E_{\text{Household,Collective}} + E_{\text{EV,Collective}} \tag{E.10}$$

with

$$E_{\text{EV,Collective}} = N_{\text{EV,Collective}} \cdot P_{\text{Char.,Avg.}} \tag{E.11}$$

and

$$P_{\text{Char.,Avg.}} = \sum_{j=1}^{5} S_{\text{Char.Power,j}} \cdot P_{\text{Char.,j}} \tag{E.12}$$

With $E_{EV,Collective}$, the collective profile of EV, $P_{Char.,Avg.}$, the average charging power, and $P_{Char.,j}$ the individual charging power j. The maximum power of the collective profile E_{Total} is the total peak power $P_{Total,k}$. Finally, the daily maximum values for $SF_{EV,k}$, $P_{Household,k}$, and $P_{Total,k}$ are determined for day k.

E.3.6 Calculation of the final results

As the last step, the result on a daily level ($SF_{EV,k}$, $P_{Household,k}$, and $P_{Total,k}$) for each of the N_{Days} days are sorted in order to determine the maximum value as well as the quantiles. Additionally, the result plots are generated.

E.4 Results

In the following exemplary results for the default data are provided (see Chapter E.2). It is assumed that each of the 10 households (with an annual energy consumption of 3216 kWh/a) is endowed with an EV. The probability that a car is charged on the selected day amounts 78% and the simulation considers 1000 days. The distribution of the charging power, the share of EV classes, and the energy capacity can be found in Chapter E.2. The following results assume that $SoC_{\text{Char.,Start}} = 0\%$ and $SoC_{\text{Char.,End}} = 100\%$. This represents an extreme scenario and explains the (possibly) higher simultaneity factors. Based on the default data and especially caused by the high share of PHEV, the average battery capacity per EV amounts to

15.7 kWh. The average charging power based on the preset charging rates is 6.43 kW. These values are used for further calculations.

E.4.1 Simultaneity factor of EV

The main objective of the tool is to calculate the simultaneity of EV charging processes. In Fig. E.1, an exemplary distribution of the simultaneity factor of EV is presented.

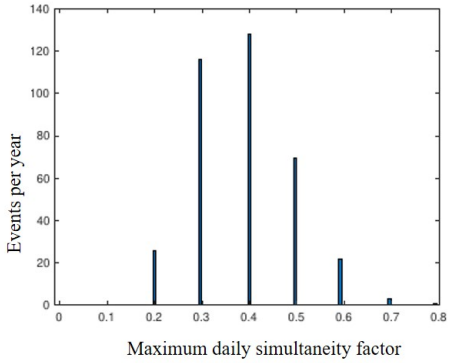

Figure E.1: Distribution of the simultaneity factor of EV.

The x-axis describes the simultaneity factor of EV and the y-axis the number of simultaneities occurred per year. In addition to the simultaneity factor for EV, various percentiles are also mapped, see Tab. E.2.

Table E.2: Results of simultaneity factor of EV.

	Tool results
Max. simultaneity factor	0.8
Prob. max. simult. factor [%]	0.2
99.9th percentile	0.8
99th percentile	0.7
95th percentile	0.6
90th percentile	0.5
50th percentile	0.4

In the exemplary results, the maximum simultaneity factor amounts 0.8. Since 10 vehicles were assumed in the example, in maximum 8 EV charge in parallel. However, this case only occurs with a probability of 0.2%. Considering the different percentiles, it can be seen that the 50th percentile is already at 0.4 and thus significantly below the maximum simultaneity factor.

E.4.2 Peak power of EV and household

In addition to the EV specific simultaneity factor, the EV peak power and the household peak load are calculated within the tool, see Fig. E.2 and Fig. E.3. Since EV loads are affected by different simultaneities than household loads, these different simultaneities are explicitly taken into account.

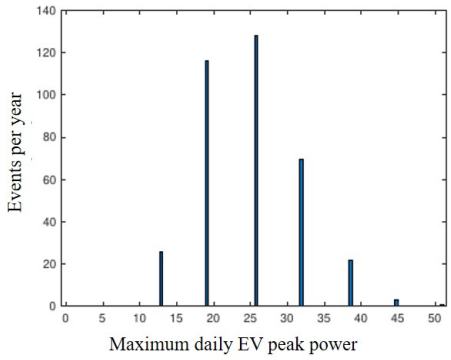

Figure E.2: Distribution of EV peak power.

The EV peak load in this exemplary calculation is 51.44 kW. This is calculated by the maximum simultaneity factor, the number of EV and the average charging power. The household peak power results from the summation of the individual load profiles and amounts for the default values to 30.95 kW. In addition to the calculations of the household peak power, the 99th, the 90th and the 50th percentile are also calculated.

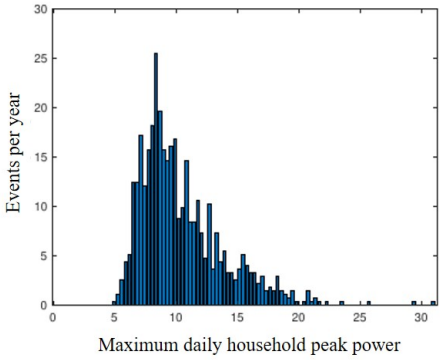

Figure E.3: Distribution of household peak power.

E.4.3 Total peak power

For grid analyses, it is important to consider the total peak load, i.e. both the EV and household loads. In order to calculate the total peak load, the individual household and EV loads are summated. It must be mentioned, that for both load curves the specific simultaneities are included. Therefore, total peak load is calculated from the sum of these two load curves. The distribution of the exemplary total peak load is presented in Fig. E.4.

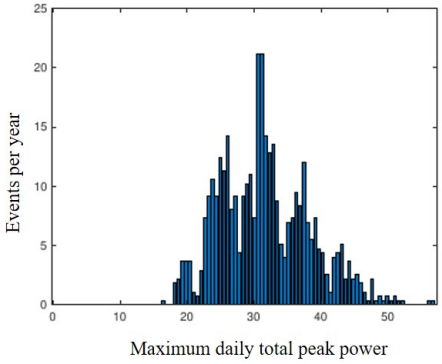

Figure E.4: Distribution of total peak power.

Tab. E.3 shows the different peak loads. As the peak load times of EV and households diverge, the total peak load is lower than the sum of the individual peak loads.

Table E.3: Peak Loads.

	EV	Household	Total
Peak Power [kW]	51.44	30.95	56.70

E.4.4 Sensitivity analysis

Within the framework of this subchapter E.4.4, the number of simulated days, the number of EV, and the distribution of the charging rate is varied and the corresponding results analysed.

In Tab. E.4 the results for a different number of simulated days is presented. A differentiation is made between 1000, 10,000, and 100,000 days. As it can be seen in Tab. E.4, the maximum simultaneity factor and the relative percentiles are quite similar. However, the probability of the maximum simultaneity factor decreases significantly. The household peak load is 30.95 kW, 31.97 kW, and 36.07 kW, respectively. The associated total load peak differ between 56.70 kW, 60.06 kW, and 66.73 kW.

Table E.4: Tool results for various numbers of simulated days.

Simulated days	1,000	10,000	100,000
Max. simultaneity factor	0.8	0.8	0.9
Prob. max simult. factor [%]	0.2	0.09	0.007
99.9th percentile	0.8	0.7	0.8
99th percentile	0.7	0.6	0.7
95th percentile	0.6	0.6	0.6
90th percentile	0.5	0.5	0.5
50th percentile	0.4	0.4	0.4
EV peak load [kW]	51.44	51.44	57.87
Household peak load [kW]	30.95	31.97	36.72
Total peak load [kW]	56.70	60.06	66.73

Second, the number of EV is varied. Fig. E.5 shows the simultaneity factor if just one EV is considered. In this case, the simultaneity of the charging processes is either 1 or 0.

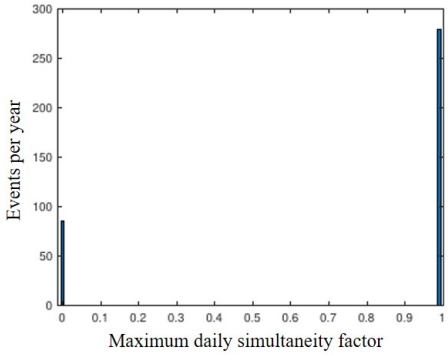

Figure E.5: Distribution of the simultaneity factor for one EV.

By increasing the number of EV, the simultaneity factor decreases, but the total load increases, see Tab. E.5.

Table E.5: Results for different number of EV.

Number of EV	1	10	20
Max. simultaneity factor	1	0.8	0.6
Prob. max simult. factor [%]	78	0.2	0.1
EV peak load [kW]	6.43	51.44	77.16
Household peak load [kW]	24.40	30.95	25.59
Total peak load [kW]	30.83	56.70	85.71

Third, since the limitation of the charging power is seen as a possibility to reduce the network loads, the simultaneity factors at different charging rates are shown in the following. Fig. E.6 shows the corresponding simultaneities if EV can only be charged with a charging power of 3.7 kW.

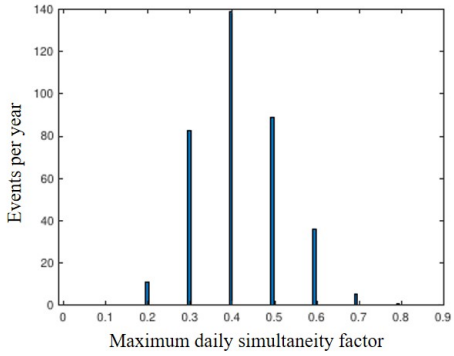

Figure E.6: Distribution of simultaneity factor of EV if EV can only be charged with 3.7 kW.

In comparison, Fig. E.7 shows the simultaneities when all EV are charged with 11 kW. It can be seen that due to the shorter charging duration at 11 kW, the maximum simultaneities decrease.

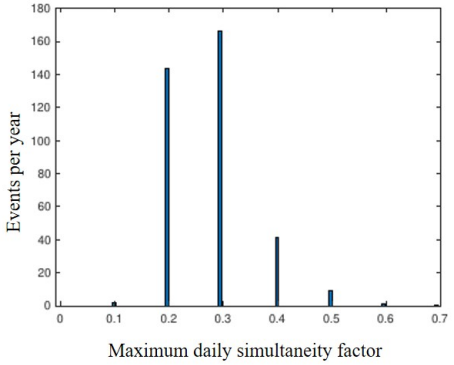

Figure E.7: Distribution of simultaneity factor of EV if EV can only be charged with 11 kW.

However, the change in average charging power also influences the EV peak load. Compared to the default charging rate distribution (see E.2.2) the EV peak load decreases from 51.44 kW to 33.30 kW at a charging rate of 3.7 kW and increases to 77 kW at a charging rate of 11 kW. Consequently, the charging power is a very decisive parameter for the grid impact, which can be seen also on the level of total peak load (see Tab. E.6).

Table E.6: Results for different distributions of charging rates.

Charging rate [kW] (100%)	3.7	11
Max. simultaneity factor	0.9	0.7
Prob. max simult. factor [%]	0.1	0.1
EV peak load [kW]	33.30	77
Household peak load [kW]	29.28	27.32
Total peak load [kW]	40.38	82.18

E.4.5 Unbalanced charging

An additional feature of the Tool is the differentiation between balanced and unbalanced charging of EV. At previous results it was assumed, EV are charged symmetric at all phases. Now, we assume a three-phase system like it exists in Germany and other countries. In order to represent the more realistic case that the individual EV are distributed unbalanced over the three phases, this can be explicitly taken into account in the tool. However, due to the lack of data, the household loads remains symmetrically spread over the three phases.

If the unbalanced charging setting is selected, the simultaneity factors for the individual phases are calculated (cf. Fig. E.8).

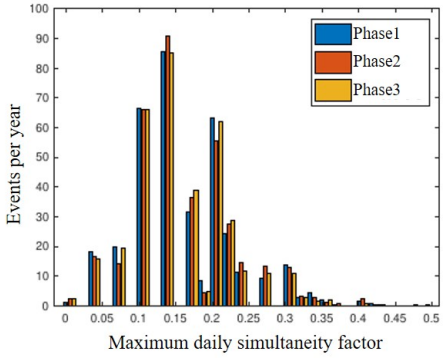

Figure E.8: Distribution of simultaneity factor in a three-phase system (unbalanced charging).

As can be seen in Fig. E.8, the simultaneities for each of the three phases are now shown (see Tab. E.7). Due to the unbalanced distribution of the EV between the three phases, the load

on the individual phases is different. This is also reflected in Fig. E.9, which represents the EV peak power per phase.

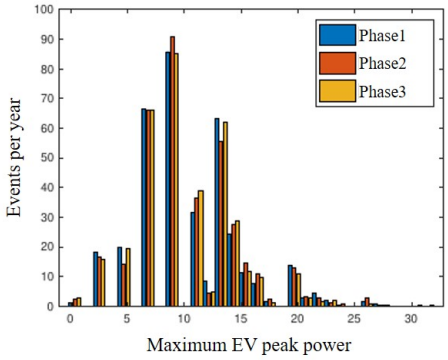

Figure E.9: Distribution of EV peak power in a three-phase system (unbalanced charging).

If one compares the results between unbalanced and balanced charging (cf. Tab. E.7), considerable differences can be identified. If the maximum simultaneity factor of the individual phases are summed up (0.43/ 0.43/ 0.5), they rise above the maximum value for balanced loading (0.8).

Table E.7: Balanced vs. unbalanced charging.

Charging	Unbalanced	Balanced
Max. simultaneity factor	0.43 / 0.43 / 0.5	0.8
Prob. max sim. factor [%]	0.1 / 0.1 / 0.1	0.2
99.9th percentile	0.43 / 0.4 / 0.47	0.8
99th percentile	0.37 / 0.37 / 0.33	0.6
95th percentile	0.3 / 0.3 / 0.3	0.6
90th percentile	0.23 / 0.27 / 0.23	0.5
50th percentile	0.13 / 0.13 / 0.13	0.4

The consideration of the unbalanced distribution is particularly important for the network analyses with regard to grid voltage and cable limitations.

E.5 Conclusion

In summary, the simultaneity of charging processes plays a significant role in the analysis of the network effects of EV. However, it is important to consider whether the EV are distributed balanced or unbalanced between the three phases. In general, it can be said that the simultaneity of the charging processes is in any case below the empirically unrealistic but frequently assumed simultaneity factor of 1. As can be seen in the results, concurrences of 0.8 occur sporadically, but with a very low probability for 10 EV. Since the total peak load is important for grid analyses, the household loads should also be included in the analysis in addition to the EV loads. However, since the times of household peak loads and EV peak loads fall apart, this should also be taken into account in the calculation of the total peak load. Due to the time difference between EV peak loads and household peak loads, this peak load is lower than the sum of the individual peaks. As shown, in particular the charging power and the number of EV taken into account have a strong influence on the simultaneity factors. However, when using the tool and the resulting simultaneities or peak loads, it should be noted that extreme values can occur empirically by accident.

References

EVBox (2019). *Check charging specifications.* URL: https://evbox.com/en/electric-cars/ (Retrieved 08/12/2019).

Figenbaum, E. and M. Kolbenstvedt (2016). *Learning from Norwegian battery electric and plug-in hybrid vehicle users - Results from a survey of vehicle owners,* URL: https://www.toi.no/getfile.php?mmfileid=43161 (Retrieved 08/12/2019).

Heinz, D. (2018). *Erstellung und Auswertung repräsentativer Mobilitäts-und Ladeprofile für Elektrofahrzeuge in Deutschland.* Tech. rep. Working Paper Series in Production and Energy.

Jochem, P., A. Märtz, and Z. Wang (2018). "How might the German distribution grid cope with 100% market share of PEV". In: *Proceedings of the 31th International Electric Vehicle Symposium, EVS31, Kobe, Japan.* Vol. 30.

Leou, R.-C., C.-L. Su, and C.-N. Lu (2013). "Stochastic analyses of electric vehicle charging impacts on distribution network". In: *IEEE Transactions on Power Systems* 29.3, pp. 1055–1063.

Probst, A. (2014). "Auswirkungen von Elektromobilität auf Energieversorgungsnetze analysiert auf Basis probabilistischer Netzplanung". PhD thesis. Stuttgart.

Rolink, J. (2013). "Modellierung und Sysemintegration von Elektrofahrzeugen aus Sicht der elektrischen Energieversorgung". PhD thesis. Dortmund.

Statistisches Bundesamt (2019). *Energy consumption.* URL: https://www.destatis.de/EN/Themes/Society-Environment/Environment/Material-Energy-Flows/Tables/electricity-consumption-households.html (Retrieved 08/12/2019).

Stöckl, G. (2014). "Integration der Elektromobilität in das Energieversorgungsnetz". PhD thesis. Munich.

Uhlig, M. (2019). *Lastprofilgenerator zur Modellierung von Wirkleistungsprofilen privater Haushalte.* URL: http://doi.org/10.5281/zenodo.803261 (Retrieved 08/12/2019).

Vennegeerts, H., J. Tran, F. Rudolph, and P. Pfeifer (2018). "Metastudie Forschungsüberblick Netzintegration Elektromobilität". In: *Study Commissioned by Forum Network Technology/Network Operation in the VDE and the German Association of Energy and Water Industries*, pp. 17–21.

Zimmer, W., M. Buchert, S. Dittrich, F. Hacker, R. Harthan, H. Hermann, W. Jenseits, P. Kasten, C. Loreck, K. Götz, et al. (2011). “OPTUM: Optimierung der Umweltentlastungspotenziale von Elektrofahrzeugen”. In: *Integrierte Betrachtung von Fahrzeugnutzung und Energiewirtschaft. Schlussbericht.*